Multi-objective optimization of the electrocoagulation process for removal of fluoride from drinking water and subsequent control of residual aluminium.

This thesis is submitted as a partial fulfilment of the PhD programme in Engineering

by

RICHA SINHA

ID: 2012RCE9022

under the supervision of

Dr. SANJAY MATHUR

Associate Professor

MNIT, Jaipur

DEPARTMENT OF CIVIL ENGINEERING

MALAVIYA NATIONAL INSTITUTE OF TECHNOLOGY, JAIPUR

NOVEMBER, 2015

DECLARATION

I hereby certify that the work which is presented in the thesis entitled **"Multi-objective optimization of the electrocoagulation process for removal of fluoride from drinking water and subsequent control of residual aluminium"** in partial fulfilment of the requirements for the award of Doctor of Philosophy, in the Department of Civil Engineering, Malaviya National Institute of Technology, Jaipur, is an authentic record of my own work unless otherwise referenced or acknowledged. The thesis was completed under the supervision of Dr. Sanjay Mathur, Associate professor, Department of Civil Engineering, Malaviya National Institute of Technology, Jaipur. The results presented in this thesis have not been submitted in part or full, to any other University or Institute for award of any degree. The content of the thesis has been checked using online software "Turnitin".

Richa Sinha
2012RCE9022
Department of Civil Engineering
MNIT, Jaipur

CERTIFICATE

This is to certify that the work reported in this thesis entitled **"Multi-objective optimization of the electrocoagulation process for removal of fluoride from drinking water and subsequent control of residual aluminium"** has been carried out by Ms. Richa Sinha and submitted to Malaviya National Institute of Technology, Jaipur for the award of Doctor of Philosophy. It is a bonafide record of research work carried out by her under my supervision. The thesis work has reached the requisite standard, fulfilling the requirements for the degree of Doctor of Philosophy. The thesis embodies the original work done by her and has not been carried out earlier to the best of my knowledge and belief.

Dr. Sanjay Mathur
Associate Professor
Department of Civil Engineering
MNIT, Jaipur

Acknowledgement

First and foremost, praises and thanks to God, the Almighty, for His showers of blessings throughout my research work to complete the research successfully.

The completion of my dissertation and subsequent Ph.D. has been a long journey and this thesis is the end of my journey in obtaining my Ph.D. At the end of my thesis, it is a pleasant task to express my thanks to all those who contributed in many ways to the success of this study and made it an unforgettable experience for me.

I express my sincere gratitude to my advisor Dr. Sanjay Mathur, Department of Civil Engineering, MNIT, Jaipur. This work would not have been possible without his guidance, support and encouragement. Under his guidance I successfully overcame many difficulties and learned a lot. I appreciate all his contributions of time, ideas, and funding to make my Ph.D. experience productive and stimulating. The joy and enthusiasm he has for this research was motivational for me, even during tough times in the Ph.D. pursuit. During the most difficult time of writing this thesis, he gave me the moral support and freedom I needed to move on. He always knew where to look for the answers to obstacles while leading me to the right source, theory and perspective. His patience, flexibility, genuine concern, and faith in me during the dissertation process enabled me to attend to life while also earning my Ph.D.

My thesis committee guided me through all these years. Thank you to Prof A.B. Gupta, Dr. U. Brighu and Dr. N. Kaul for being my major advisors. Their valuable advice, constructive criticism and extensive discussions around my work were a great help. During this work, I have used the expertise of Prof. Y.P. Mathur, Dr. Amar Patnaik and Dr. Amit Singh. I found them more than willing to share their treasure of knowledge with me. I wish to express my profound gratitude to them for their tender care and guidance. Their enthusiasm, encouragement and faith in me throughout have been extremely helpful. They were always available for my questions and generously gave their time and knowledge. I would also like to thank Prof. M.K. Banerjee and Prof. S.K. Biswas for their help and support. I am also thankful to the Head of Department (Civil), Prof. Gunwant Sharma for being a support. I extend my sincere thanks to Mr. Rajesh Saxena and Mr. S. Ansari for their motivation and support for completing the work. Their personal cheering is greatly appreciated.

I take this opportunity to sincerely acknowledge, Malaviya National Institute of Technology, Jaipur, for providing financial assistance which buttressed me to perform my work comfortably. I am grateful to Prof. I.K. Bhat, Director, MNIT, Jaipur, for his supportive gesture. I would also like to thank the team at the Materials Research Centre, MNIT, Jaipur for their help and support in testing various samples.

I am indebted to my colleagues for providing a stimulating and fun filled environment. I am ever indebted to Kavita Verma and Priya for their care and moral support. They have helped me survive all the stress and not letting me give up. I am also

thankful to Aditya, Priyesh, Sunder and Ashish, who made the working environment worthwhile. I would also like to extend huge thanks to my hostelmates, Shuchi, Poonam, Vatsala, Tanuja and Niketa for their valuable support. They have re-energized and given me a much-needed reprieve from work.

Finally, I would like to thank my family whom I owe a great deal. To my late father, thank you for having faith in me. Hope, I made you proud. To my fiancee Mahesh, for his unconditional support during my good and bad times. I couldn't have completed all the required paperwork and delivered it to the correct place without him. I finish with acknowledging, where the most basic source of my life energy resides: my MOTHER. Her support has been unconditional all these years. She has cherished with me every great moment and supported me whenever I needed it. Hence, great appreciation and enormous thanks are due to her, for without her understanding, I am sure this thesis would never have been completed.

I thank you all.

(Richa Sinha)

Dedicated to my Parents and Fiancee

List of Publications

In Journals

1. Sinha, R., Mathur, S. (2015) "Use of activated silica sol as a coagulant aid to remove aluminium from water defluoridated by electrocoagulation", Desalination and water treatment DOI: 10.1080/19443994.2015.1084536.

2. Sinha, R., Mathur, S. (2015) "Control of aluminium in treated water after defluoridation by electrocoagulation and modelling of adsorption isotherms", Desalination and water treatment DOI: 10.1080/19443994.2015.1060538.

3. Sinha, R., Mathur, S., Brighu, U. (2015) "Aluminium removal from water after defluoridation with electrocoagulation process", Environmental technology DOI:10.1080/09593330.2015.1043958.

4. Sinha, R., Singh, A., Mathur, S. (2014) "Multiobjective Optimization for minimum residual fluoride and specific energy in electrocoagulation process", Desalination and water Treatment DOI:10.1080/19443994.2014.990929.

5. Sinha, R and Mathur, S. (2014), "Development of regression equation for defluoridation by continuous flow electrocoagulation "International Journal of Applied Engineering Research, 9(2), 201-206.

6. Sinha, R., Khazanchi, I. and Mathur, S. (2012) "Fluoride removal by a continuous flow electrocoagulation reactor from groundwater of Shivdaspura", International Journal of Engineering Research and Application, 2(5), 1336-1341.

In Conferences

1. Sinha, R., and Mathur, S. (2013), "Perspectives of electrocoagulation as a treatment technology for Defluoridation of Water: A Critical Review", International Conference on Water, Desalination, Treatment and Management (InDACON-2013),21-22 Feb, Jaipur

2. Sinha, R., and Mathur, S. (2013), "Evaluation of continuous flow electrocoagulation system for defluoridation", 7th International conference on Water Management (WATMAN 2013), 7-9 Feb, Chennai.

3. Sinha, R., and Mathur, S. (2013), "Study of laboratory scale electrocoagulation for defluoridation of water", International Conference- India Water Week, 8-12 April, New Delhi

4. Sinha, R., Khazanchi, I. and Mathur, S. (2012), "Performance of continuous flow electrocoagulation system in removing fluoride from groundwater of Shivdaspura", National Conference on Water Quality Management (NCWQM-2012), 20-22 Dec, Jaipur.

Abstract

Water is an essential part of life. Water, fit for human consumption is available in limited quantity. This demands for new treatment technologies to treat huge amount of groundwater, which is not fit for human consumption. Presence of inorganic constituents in water is a major public health problem and fluoride is one such problem. Fluoride is known to occur in high concentrations in many parts of the world and can have adverse effects on human health and well being. Drinking water is the major source of fluoride uptake. Several defluoridation processes are being practised such as adsorption, chemical precipitation, electrodialysis and electrochemical method.

The removal of fluoride from drinking water using aluminium compounds is more prevalent than other defluoridation techniques due to the strong affinity between aluminium and fluoride. Electrocoagulation (EC) with aluminium electrodes is one such technique which is successfully used for defluoridation of water. But various monomeric and polymeric hydroxyl species of aluminium and fluoride complexes are formed in the process which may lead to high aluminium concentrations in drinking water. In the recent past, the adverse effects of aluminium have been recognized. Aluminium is found to be a potential neuro-toxicant. Therefore, it is imperative to control the residual aluminium in the water.

The present study was proposed in view of the synergistic effects of the aluminium/ fluoride compounds and the induced toxicity in drinking water due to their high concentrations. The main objective of the present study was to optimize the EC process to control fluoride in treating water with minimum energy input and then control residual aluminium in subsequent steps. For optimization of energy input, a program was developed in FORTRAN to minimize energy used for target fluoride removal. It helps in controlling aluminium dissolution and only amount necessary for desired fluoride removal was introduced in the solution. In next step, flocculation and settling followed by filtration was attempted. It appreciably reduces the aluminium concentration but not below the permissible limit. Performing this step, gave a clear insight that the aluminium concentration was mostly due to the flocs present in the water and efficient settling of these flocs was required for aluminium control. Therefore, coagulants aids (bentonite clay and activated silica sol) were used to improve settling efficiency Both coagulant aids brought down the aluminium content below permissible limits. With optimised dose of bentonite, residual aluminium was brought down to a range of $0.03 - 0.08\, mg/L$. With optimised dose of activated silica sol, residual aluminium was brought down to a much lower range of $0.003 - 0.034\, mg/L$.

Contents

List of Figures

List of Tables

Nomenclature

List of symbols

A Cross sectional area of electrodes

$AandB$ Redlich peterson constant

Al_r Residual aluminium

Al_{th} Theoretical aluminium liberated from anode

C_0 Initial fluoride concentration

C_c Current concentration

C_e Fluoride concentration at equilibrium

F F-value

F Faraday's constant

F_r Residual fluoride

F_t Total fluoride

Fi Initial fluoride concentration

i Applied current

J Current density

k_{dif} Rate constant of intraparticle diffusion

K_f Freundlich constant

K_l Langmuir constant

k_1 Rate constant of first order adsorption

k_2 Rate constant of second order adsorption

M Molecular mass of aluminium

n empirical constant

p p-value

Q Charge loading

q_e Amount of fluoride adsorbed at equilibrium

q Amount of fluoride adsorbed at time t

q_{max} Maximum adsorption capacity

R^2 Coefficient of determination

t Electrolysis time

USD U.S. Dollar

V Volume of the reactor

W Mass of dissolved anode

x unit price of energy

y unit price of aluminium

z unit price of coagulant aid

χ^2 Chi square

List of abbrevations

AA Activated alumina

AAS Atomic absorption spectrophotometer

ANOVA Analysis of variance

BIS Bureau of Indian standards

D.C. Direct current

DF Degree of freedom

DOE Design of experiments

EC Electrocoagulation

ECF Electrocoagulation-flotation

EDX Energy dispersive X-ray spectrometry

FE-SEM Field emission scanning electron microscopy

FTIR Fourier transform infrared spectroscopy

FUC Fluoride uptake capacity

ICMR Indian council of medical research

MS Mean of squares

NTU Nephelometric turbidity unit

OA Orthogonal array

OFAT One factor at the time

RMSE Root mean square error

RSM Response surface methodology

SDWR secondary drinking water regulation

SEEC Specific electrical energy consumption

S/N Signal to noise ratio

SS Sum of squares

SSV Settled sludge volume

TISAB Total ionic strength adjustor buffer

USEPA United States Environmental Protection Agency

WHO World health organization

XRD X-ray diffraction

CHAPTER 1

Chapter 1

Introduction

This Chapter includes a brief introduction to the research problem and the tasks to be performed in the research work. It also outlines the framework of the thesis. In a nutshell this chapter unveils the research work presented in the thesis.

1.1 Background of the problem

Water is an essential part of life. It is not only a resource, but instead it is a life source. Due to increase in the world's population and contamination of available water sources, there is a rising increase in demand for new water treatment technologies. The expected increase of human population is about 9 billion by 2050 [1]. With limited water resources, providing drinking water to the consumers will be a problem in the near future. Access to safe drinking water is the basic right and providing it to the consumer is a challenge to water treatment engineering. Wide varieties of treatment processes are available for water treatment. The amount and type of treatment applied depends on the source type and quality of water. A major public health problem is the presence of inorganic constituents in water and fluoride is one of them.

Fluorides occur naturally in the earth's crust where they are found in rocks, coal, clay, and soil. They are released into the environment through various natural processes like: weathering of rocks, dissolution of minerals and volcanic emissions. Various anthropogenic processes like: coal combustion, waste from various industrial processes, including steel manufacture, primary aluminium, copper and nickel production, phosphate ore processing, phosphate fertilizer production, glass, brick and ceramic manufacturing, and adhesive production also contribute to fluorides in water [2]. The main health concern regarding fluoride is likely to be from excessive oral exposure in drinking water. Fluoride levels in surface water vary according to geographical location and proximity to emission sources. Surface water concentrations generally range from $0.001 - 0.3\,mg/L$ [3]. Sea water contains more fluoride than fresh water,

with concentrations ranging between $1.2 - 1.5\,mg/L$. Higher levels of fluoride are found in areas where the natural rock content is rich in fluoride and near industrial outfalls.

1.1.1 Status of groundwater fluoride

Fluoride is known to occur in high concentrations in many parts of the world and can have adverse effects on human health and well being. An approximate view of the fluoride concentration scenario 'in the World' and 'in India' has been presented here.

IN WORLD: Brindha and Elango [4] reported the prevalence of fluorosis in Arizona, Arkansas, California, Colorado, Idaho, Illinois, Iowa, Kansas, Minnesota, Nevada, New Mexico, North Carolina, North Dakota, Oklahoma, Oregon, South Carolina, South Dakota, Texas, Utah and Virginia. Figure 1.1 shows the occurrence of fluoride in various parts of the world and its approximate range found in the literature.

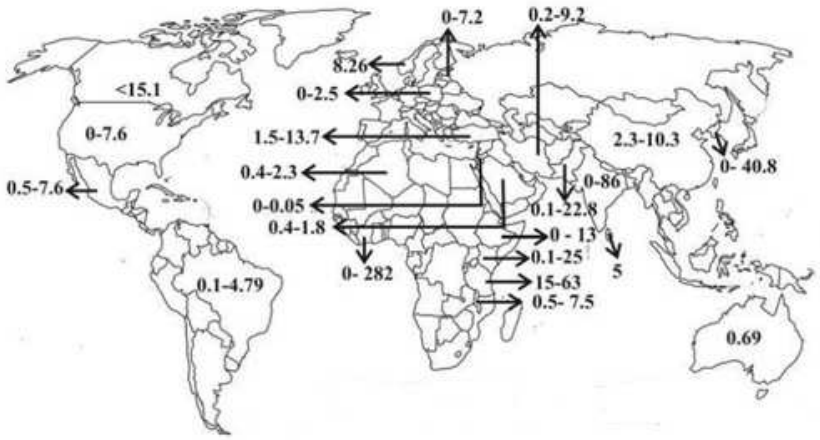

Figure 1.1: Fluoride concentration in various parts of the world [4].

IN INDIA: Twelve million tons of fluoride are deposited in India out of the eighty-five million present in the earth's crust [5]. Thus, it is obvious that fluoride contamination in India is widespread. According to Susheela [6], sixty-six million of the total population is consuming fluoride rich water. Figure 1.2 shows different parts of India where high concentrations of fluoride is present in groundwater. A detailed list of concentrations of fluoride in groundwater and their sources is given in Table 1.1. It can be clearly observed from Figure 1.2 that $2 - 8\,mg/L$ range of fluoride is prevalent and there are only four regions in which the fluoride contamination is beyond this range.

Table 1.1: Fluoride distribution in India, enlisted from literature [4].

State	***Source***	***Fluoride Range***	***References***
Andhra Pradesh, Kurmapalli watershed	Fluoride rich rocks	Up to 21 mg/L	[7]
Andhra Pradesh, Nalgonda	Fluoride rich grantic rocks	$0.4-20\,mg/L$	[8]
Andhra Pradesh, Visakhapatnam	Granitic rocks	$0.6-2.1\,mg/L$	[9]
Andhra Pradesh and Jharkhand	Coal ash	$0.1-4\,mg/L$	[10]
Assam, Guwahati	Granite Rocks	$0.18-6.88\,mg/L$	[11]
Delhi	Irrigation water and brick industries	$0.1-16.5\,mg/L$	[12]
Gujarat, Mehsana	Granite, gneiss and pegmatite	$0.94-2.81\ mg/L$	[13]
Haryana, Bhiwani	Rocks	$0.14-86\,mg/L$	[14]
Karnataka, Bellary	Apatite, hornblende and biotite	$0.33-7.8\,mg/L$	[15]
Kerala, Palghat	Hornblende and biotite gneiss	$0.2-5.75\,mg/L$	[16]
Maharashtra, Yavatmal	Amphibole, biotite & fluoroapatite	$0.3-13.41\ mg/L$	[17]
Rajasthan, Hanumangarh	Rocks	$1.01-4.42\,mg/L$	[18]
Tamil Nadu, Erode	Host rocks and weathering of fluorite	$0.5-8.2\,mg/L$	[19]
Uttar Pradesh, Kanpur	——-	$0.14-5.34\,mg/L$	[20]
West Bengal, Hooghly	Super phosphate fertilizer	$0.01-1.18\,mg/L$	[21]

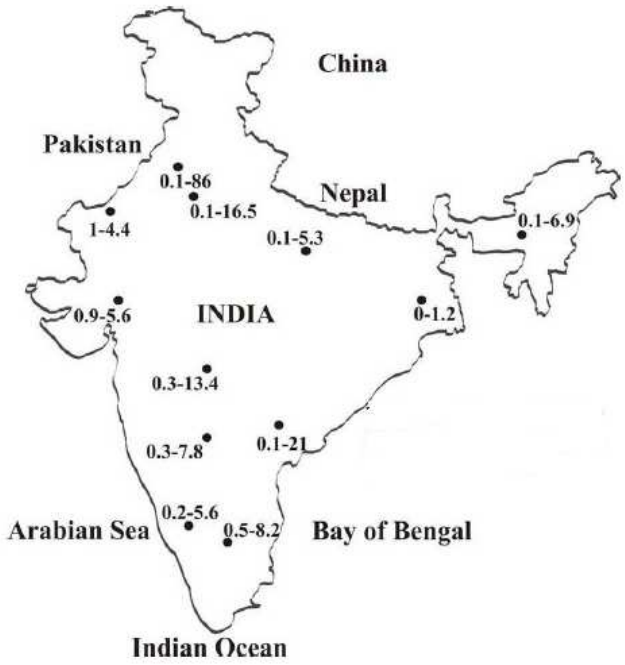

Figure 1.2: Fluoride concentration in various parts of India [4].

1.1.2 Health implications

Excessive ingestion of fluorides has adverse implications on human health. It causes a disease known as fluorosis. Fluorosis is mainly of two types: dental and skeletal fluorosis. Dental fluorosis is the loss of lustre and shine of the dental enamel. This condition is termed as hypomineralization of dental enamel [22] and starts due to incorporation of fluoride in the teeth during the time of tooth development. In more severe cases of dental fluorosis the teeth are discoloured and pitted. Figure 1.3 shows various levels of dental fluorosis.

Figure 1.3: Levels of dental fluorosis [23].

Skeletal fluorosis refers to the problem in bone due to excessive exposure of fluorides. Fluoride changes the physicochemical properties of bone by replacing the hydroxyl ion in hydroxyapatite to form fluorapatite. This might cause the bones to become brittle and reduce their tensile strength [24]. Poisoning of fluoride leads to

Figure 1.4: Depiction of skeletal fluorosis.

severe pain associated with rigidity and restricted movements of cervical and lumbar spine, knee and pelvic joints as well as shoulder joints. Figure 1.4 depicts some deformations of bones due to skeletal fluorosis.

1.1.3 Limits of fluoride in drinking water

Various regulating bodies have enforced the fluoride limit in drinking water. Table 1.2 enlists permissible levels of fluoride in drinking water as prescribed by different agencies. For present study permissible limit of fluoride in drinking water has been used as $1.0\,mg/L$ as prescribed by various regulating authorities.

Table 1.2: Drinking water standards for fluoride as prescribed by various authorities.

Authority	***Permissible Limit*** (mg/L)	***Reference***
Bureau of indian standards BIS (IS-10500 : 2012)	1.0	[25]
Indian Council of Medical Research	1.0	[26]
The Committe on Public Health Engineering Manual and Code of Practice, Government of India	1.0	[26]
World Health Organisation (WHO)	1.5	[27]

1.2 Defluoridation Processes

Several defluoridation processes are existing such as adsorption [28], chemical precipitation [29]-[31], electrodialysis [32] and electrochemical method [33] [34]. The two widely used techniques in India for defluoridation are Nalgonda process and Activated Alumina (AA) process [35]. Generation of large volumes of sludge, the hazardous waste categorization of metal hydroxides, and high costs associated with chemical treatments have made the conventional chemical coagulation techniques for defluoridation less acceptable [36]. The present scenario demands for a process

which addresses the above mentioned problems. A new process is required which solves the problems of existing coagulation processes. Electrocoagulation (EC) is a promising alternative to the conventional coagulation techniques [37]. It has been applied successfully to treat various wastewater and potable water [38].

1.2.1 Electrocoagulation process

EC is an electrochemical technique which removes pollutants from water. This process involves applying electric current to the electrodes. The anode undergoes oxidation and produce metal hydroxides which serve as coagulating agents. The generation of coagulant in this process is in-situ. The removal mechanism of pollutant can be considered similar to the chemical coagulation processes. EC is emerging as a promising process that can be retrofitted to existing methods of defluoridation. EC has been suggested as an alternative to conventional coagulation [39] [40]. Reduced sludge production, no requirement for chemical handling and ease of operation are some of the advantages of this process [41]. It has also been reported that the EC process for fluoride removal does not require a big investment [33].

In the present work EC with aluminium electrodes has been used for defluoridation of water. To understand the working of the EC process, it is important to understand electrolytic reactions, fluoride removal mechanism and other fundamentals. These all concepts have been discussed in the next chapter.

1.3 Role of aluminium in fluoride removal

Aluminium compounds are widely used for treatment of water, especially for removal of fluoride owing to the high affinity of fluoride towards aluminium. But recently, aluminium compounds have come under scrutiny due to the concerns about metal residuals in the public water supply. In response, various regulations have been promulgated for aluminium which have been presented in Table 1.3

Table 1.3: Drinking water standards for aluminium, prescribed by various authorities.

Authority	***Permissible Limit*** (mg/L)	***Reference***
BIS (IS-10500 : 2012)	0.2	[25]
WHO	0.2	[27]
(USEPA SDWR)	$0.05-0.2$	[42]
Canadian operational guidance	$0.1-0.2$	[43]

Aluminium sulphate $Al_2(SO_4)_3$ (better known as alum) or Polyaluminium chloride

(PACl) are commonly used coagulants in drinking water treatment. They enhance the removal of particulate, colloidal and dissolved substances via coagulation processes. The treatment of surface water with alum has been used for centuries in all parts of the world. The use of alum as a coagulant for water treatment often leads to higher concentrations of aluminium in the treated water than in the raw water [44]. There is considerable concern throughout the world over the levels of aluminium found in drinking water sources (raw water) and treated water. Acid rain has also increased the aluminium level in many freshwater sources [45]. A high $(3.6-6\,mg/L)$ concentration of aluminium in treated water gives rise to turbidity, reduces disinfection efficiency, and may precipitate as $Al(OH)_3$ during the course of distribution [46]. Aluminium is not a routine monitoring parameter in finished water, in most of the water treatment plants. Furthermore, relatively lesser attention has been paid to the speciation of aluminium in raw, treated and distributed waters [47].

1.3.1 Aluminium and fluoride toxicity

Aluminium was earlier regarded as a relatively innocuous element, but researchers have found that its various bound forms with the hydroxide ion and inorganic ions are toxic in nature. Aluminium is found to be a potential neuro-toxicant and medical research and epidemiological surveys suggest that dissolved aluminium entering the bloodstream may cause Alzheimer's disease, Lou Gehrig's disease and other forms of senile dementia, encephalopathy, bone mineralization disorders, etc [48]. Aluminium -fluoride complexes also increase the risk of developing Alzheimer's disease. It causes disruption of brain's aerobic metabolism, reduction of effectiveness of acetylcholine as a transmitter, and increase in free radicals. Strunecka and Patocka [49] studied the nature of Aluminium- fluoro complexes and found that they act as phosphate analogs in the G-protein. They become signal disruptors in the cellular regulatory mechanism and are found to be a potential danger for all living organisms. The excerpts from the Abridged Final Report on the Review of Toxicological Literature on Aluminium Compounds prepared by Scott Masten [48], also elaborate on the toxicity of aluminium.

In a study of more than $3,500$ French men and women above the age of 65, a significant decrease in cognitive abilities was found when their drinking water contained calcium, aluminium, and fluorine [50]. Their results confirm the importance of estimation of aluminium speciation and assessment of the association between aluminium exposure and Alzheimer's disease. Researchers [51] hypothesized a possible synergistic role of aluminium with fluoride in aggravation of skeletal fluorosis by conducting studies on people in Sanganer area in Jaipur having high fluoride $(1.19-11.3\,mg/L)$ and aluminium$(0.017-0.125\,mg/L)$ concentrations in their drinking water sources. Health studies of the affected people by Jajoo [52] and Sayal [53] also revealed

toxic effects of aluminium fluoride complexes in fluorosis endemic areas and report some appearances of neuro-symptoms in patients affected with fluorosis. It mostly affected the older generation, due to the consumption of contaminated water over a longer period of time. All these studies indicate the synergistic associations of both aluminium and fluorides in the drinking water supply and therefore suggest that it might be prudent to make sure that residual aluminium was minimized in the defluoridated drinking water supplies.

1.4 Research objectives

Ingestion of excess fluorides and aluminium by humans is found to cause many neurological, skeletal, gastrointestinal and clinical toxic effects. The present study was proposed in view of the synergistic effects of the aluminium/ fluoride compounds and the induced toxicity in drinking water due to residual fluoride and aluminium concentrations. The main objective of the present study was to optimize the EC process to control fluoride in treating water with minimum energy input and then control residual aluminium in subsequent steps. The present research has following subsidiary objectives:

- Parametric study of the EC process for defluoridation to select operational parameters and their operating range for design of experiments (DOE).
- Development of a model and assessment of the effect of selected input (operating) parameters: initial fluoride, applied current and electrolysis time on three responses (residual fluoride, residual aluminium and specific electrical energy consumption (SEEC) for fluoride removal on the EC process.
- Development of regression equation for the responses and its experimental verification.
- Optimization of the EC process using the grid search method programmed in FORTRAN for minimum energy input to achieve target fluoride removal.
- Control of aluminium through flocculation, settling and filtration.
- Control of aluminium through the use of coagulant aid (bentonite and activated silica sol), followed by flocculation, settling and filtration.
- Development of a model and assessment of the effect of operating parameters: aluminium after EC and coagulant aid dose on the response (aluminium after coagulant aid dosing).

- Development of regression equation for the responses and its experimental verification.
- Study of adsorption isotherms for both fluoride and aluminium removal.
- Sludge characterization.

1.5 Outline of the work

The present work has been broadly classified in two parts; fluoride removal and aluminium removal. A description of present work is outlined in the Figure 1.5 and the text following it gives an elaborate view.

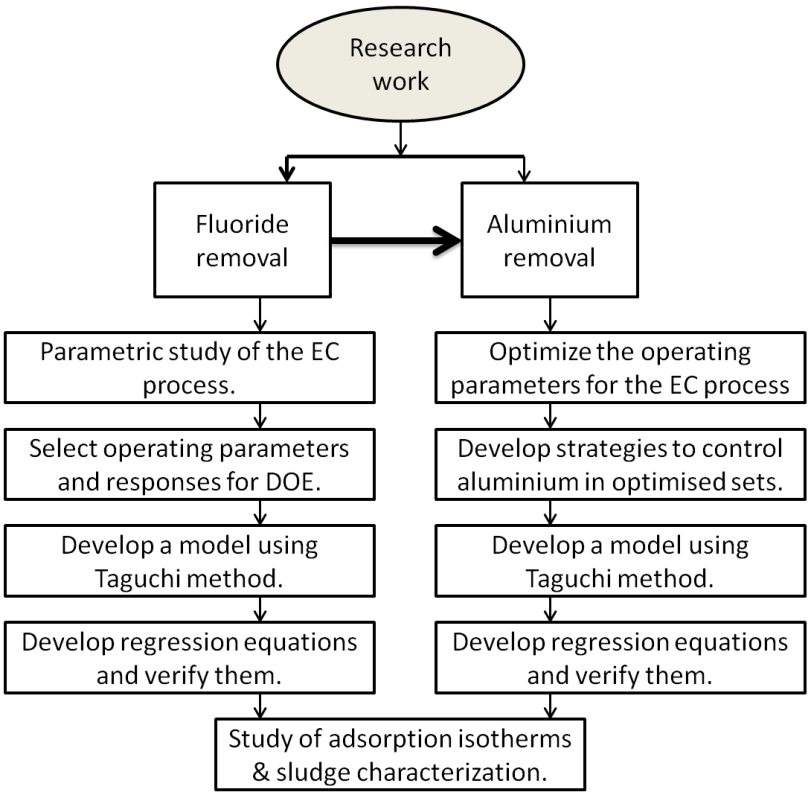

Figure 1.5: Outline of the research work.

Fluoride removal: The EC process has been used for removal of fluoride. As a first step, parametric study for fluoride removal was performed. The samples were prepared in the laboratory using tap water, so it was necessary to investigate the effect of operational parameters like initial fluoride concentration, applied current, electrolysis time, pH, inter-electrode distance, etc. on efficiency of the EC process. These findings help us to select operational parameters and their ranges for development of statistical model. The parametric investigations lead to selection of three operating parameters (initial fluoride concentration, applied current and electrolysis time) and three responses

(residual fluoride, residual aluminium and SEEC) for development of statistical model. Taguchi method was used to develop a statistical model and find the effects of input parameters on the selected responses. The model was validated by ANOVA and residual plots. Regression equations were developed for selected responses and its experimental verification was done.

Aluminium removal: Regression equations were used to optimize the operating parameters of the EC process. A program was developed in FORTRAN to optimize the parameters for minimum energy input which leads to required dissolution of aluminium in the EC reactor. The further work for aluminium removal was carried out on the optimized sets. In subsequent steps, strategies to control aluminium were developed. Two strategies were used to remove aluminium from the water treated after the EC process. In the first strategy after optimizing the energy input; flocculation, settling and filtration was done. In the second strategy, after optimizing energy input; coagulant aid was added in the water, followed by flocculation, settling and filtration. Taguchi method was used to design the experiments and develop a model for aluminium removal. Regression equations were developed for the response and its experimental verification was done.

1.6 Organisation of the thesis

The entire thesis is summed up in eight chapters. Presented below are the highlights of the chapters.

Chapter 1 presents an overview of the problem statement and outline of the tasks performed in the present research.

Chapter 2 includes a literature review designed to provide a summary of the base knowledge already available involving the issues of interest. First section includes a list of various defluoridation processes used for treatment. Second section presents the basics of coagulation and flocculation. The third section gives a detailed insight into the fundamentals of the EC process and review of proposed mechanisms for fluoride removal by the EC process.

Chapter 3 gives the detailed description of methodology used for the research. It also introduces the analytical techniques and softwares used for completion of the research.

Chapter 4 discusses the various parameters affecting the EC process for fluoride removal, which forms a baseline data for further research.

Chapter 5 illustrates all the findings related to the development of a model for fluoride removal. In this Taguchi design is implemented and investigation of the effects of input variables (operational parameters) on an output variable (response) is done. It also describes about the EC kinetics and identifies the reaction order for EC process.

Reaction kinetics and adsorption isotherm study for fluoride removal is also included in this chapter.

Chapter 6 includes the strategies used for controlling aluminium concentration in the treated water and discusses about the development of a model for aluminium removal. It also includes study of adsorption isotherms for aluminium removal.

Chapter 7 includes the characterization of sludge and cost analysis.

Chapter 8 is the concluding chapter, which includes the main findings of the present study.

Chapter Summary

Fluoride contamination is a major health problem and poses problem like dental fluorosis and skeletal fluorosis. Several fluoride treatment techniques are used for defluoridation of water. But owing to the high affinity of fluoride with aluminium, the techniques using aluminium for treatment purposes are popular. Initially, aluminium was considered to be an innocuous element, but researches have proven aluminium to be a potent neurotransmitter. Therefore, it is necessary to control the aluminium in drinking water treated for high fluoride. A wide variety of treatment techniques are available for removal of fluoride. But EC has emerged as an efficient technique owing to a few of its advantages like low operating cost, lesser sludge production, no chemical handling, etc.

The present study has focussed on treating fluoride contaminated water by the EC process using aluminium electrodes. Also, as a subsequent step it delineates measures for controlling the aluminium concentration in water treated by the EC process. The next chapter gives an overview of the various defluoridation processes which are being practised. It also explains the concepts of coagulation and the EC process.

CHAPTER 2

Chapter 2

Defluoridation processes, coagulation and electrocoagulation

The chapter begins with the summary of various defluoridation processes. It further provides insight into the basic concepts and theory of coagulation, flocculation and EC. Also several investigations that have been carried out in the recent past for fluoride removal by the EC process have been reported. The next part of the chapter includes the introduction to the DOE and adsorption isotherms; as they also form an integral part of the present study.

2.1 Defluoridation processes

Defluoridation refers to methods of water treatment that reduce the concentration of fluoride in the water, in order to make it safe for consumption. Fluoride has been a matter of controversy for human consumption, since long. Initially, it was of the opinion that a minimum concentration of fluoride is needed for good strength of bones and teeth, but subsequent evidences stated that there is no requirement of extra fluoride for human consumption. Many methods have been investigated to remove fluoride from water. A list of techniques with a brief description has been presented in the Table 2.1.

Table 2.1: Summary of defluoridation processes being practised.

S.No	***Flouride Removal Method***	***Process***	***Remarks***
1	Alum+Lime (Nalgonda)	Alum and lime are added and stirred well. $Al(OH)_3$ flocs develop on which fluoride adsorbs and is removed [54].	Established Process, high volume of sludge. Careful pH control of treated water is required [55]. High residual aluminium is reported in treated water [56].
2	Activated Alumina(AA)	AA is granular and highly porous substance used for adsorption of fluoride.	90% removal achived [57]. Requires regeneration and disposal of regeneration waste. Pre & post pH adjustment required [58]. Residual Al exceeds limit of $0.2\,mg/L$ [59].
3	Lime	Fluoride is precipitated in the form of CaF_2.	Quantity of sludge and poor settling characteristics of precipitate [60] are few problems.
4	Bone Charcoal	This is an ion exchange process in which carbonate radical of the apatite comprising bone is replaced by fluoride to form an insoluble fluorapatite.	Defluoridation capacity $2-4\,mgF/g$ [60]. Efficient process, high removal, local availability. Capacity reduces drastically after successive regenerations. Use constrained by the religious beliefs.

5	Montmorillonite	The mechanism for fluoride removal was due to the interaction between the metal oxides at the surface of montmorillonite and fluoride ions [55]	Significant concentration of Al^{3+}, Fe^{3+} and silica are released from acidified montmorillonite lattice (pH ~ 2; 1 : 10w/v) which will eventually be coming into treated water [55]. Sufficient time for adsorption equilibrium of fluoride ions is 180 min and, the maximum removal of fluoride ion was obtained at pH 6 [61][62].
6	Red Mud	Possibility of removal of fluoride ion is explained on the basis of the chemical nature and specific interaction with metal oxide surfaces [63].	Low adsorption capacity Needs pre treatment. Requirement of regeneration.
7	Natural Adsorbents Seeds of the Drumstick tree, roots of Vetiver grass and Tamarind seeds	Drumstick seeds act as a adsorbent 70% removal from roots of Vetiver grass [64].	No reproducible results were obtained from drumstick seeds [64]. Quantity of Vetiver grass required is huge.

8	Ion exchange membranes	Cation exchange resins impregnable with alum solution have been found to act as defluoridating agents. Polystyrene anion exchange resins in general and strongly basic quaternary ammonium type resins in particular are known to remove fluorides from water along with other anions [57].	They have low capacity of fluoride removal. They are not very economical.
9	Electrodialysis	The separation is accomplished by alternately placing cation- and anion-selective membranes in a parallel fashion across the current path [60]. The membranes were prepared from interpolymeric films based on high-density polyethylene (HDPE)–linear lowdensity polyethylene (LLDPE)–styrene–divinylbenzene, which had a ratio of HDPE to LLDPE kept at 80 : 20 [65].	Excellent technique for simultaneous defluoridation and desalination. Commercially established. Requires high degree of pre-treatment. Ineffective in removing low-molecular-mass, non-charged compounds. Membrane scaling is a problem.
10	Zirconium-impregnated fibrous protein (ZrFP)	High sorption capacity up to 12.6 mgF/g at equilibrium fluoride concentration of 1 mg/L [66]	Promising application in the defluoridation of drinking water. No known toxicity. Still in developing stage

2.2 Coagulation -Flocculation

To remove colloidal impurities from water, number of methods are used and among all the methods, coagulation/flocculation is an important method for this purpose [67]. Coagulation and flocculation phenomena have been practiced from earliest times in water and wastewater treatment, using a variety of substances. The process of withdrawing the forces, which stabilizes colloidal particles and cause aggregation of colloidal particles is called coagulation/flocculation.

A colloid is a microscopic particle, typically having dimension in the range of 10 nm to 100 μm, which is dispersed throughout the other substance [68]. These particles cannot settle or be removed by ordinary filtration. Colloids can be defined as substances that apparently go into solution but, in fact, remain dispersed as discrete particles. The like charge of colloids causes repulsion in adjacent particles and hence prevents effective agglomeration and flocculation. As a result, charged colloids tend to remain dispersed. In coagulation the attachment of small particle to surface and one another is promoted, thus the repulsive potential of electrical double layer of colloids is reduced and micro flocs are produced. When microflocs aggregate they form larger structures, generally stated as flocs. Inorganic coagulants like aluminium or iron salts are added to promote coagulation. This process is necessary to remove particulate matter which is too small in size and cannot be settled by gravity in sufficient time frame.

Colloidal suspensions are stable due to electrostatic charge. Usually, the net charge on the colloids is negative. Ions present in the water will be affected by the charged surface of the colloid. Negatively charge surface attracts the ions of opposite charge (counter ions) towards itself, thereby forming a fixed layer. This layer displaces with the colloid. Other ions present in the solution arrange themselves accordingly, with greater concentration of counter ions being closer to the colloid. This arrangement produces a net charge which is stronger at the fixed layer and decreases exponentially as the distance from the colloid increases. Structure of colloid particle and arrangement of charge around it is shown in Figure 2.1.

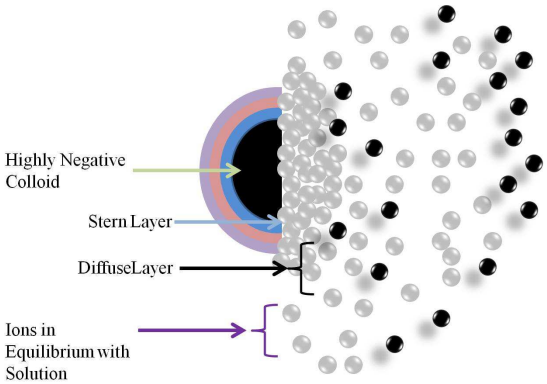

Figure 2.1: Colloid particle and the arrangement of charge around it.

When colloids come in close proximity, two forces act on them. The electrostatic potential created by counter ions surrounding the colloid, which prevents the contact and the vanderwaal's force which is force of attraction. Vanderwaal force is the strongest force at close distances but decreases exponentially with distance. After a maximum net repulsive force known as the energy barrier, is passed the contact between the particles is possible. Overcome of energy barrier is important for agglomeration of particles. Brownian movement, random movement of smaller colloids because of molecular bombardment, might produce enough momentum to overcome the barrier and collide. But these processes are too slow to be efficient for water purification.

Main mechanisms that take place in the process of coagulation and flocculation, are listed to be colloidal destabilization, precipitation and co-precipitation, where colloidal destabilization stands for coagulation and occur through addition of coagulants. Two distinct steps must occur for coagulation to take place; repulsion forces must be reduced and contact between the destabilized particles must be achieved with the help of particle transport [69]. This can be achieved by three mechanisms [70]. These methods may take place individually or collectively to destabilize colloidal particles, facilitating their removal from suspension [71]-[73].

- ***Compression of electrical double layer:*** This is achieved through the addition of a coagulant into a suspension of colloids. Ions possessing a net charge opposite to the net charge of the colloidal material are attracted to the area surrounding outside the particle, referred to as the diffuse layer. As more counter-ions are added to the suspension they are attracted towards the suspended particles causing the diffuse layer to become compressed. This, in turn, reduces the amount of energy required to move the two colloidal particles of like surface charge together. Sufficient compression of the ionized layer causes the Vanderwaal's forces to dominate and remove the energy barriers.

- ***Surface charge neutralization:*** This process involves the addition of a coagulating agent with a net charge which is opposite to that of the net surface charge of the suspended particles. These ions become part of ions already surrounding the colloid. The added ions have greater affinity for the surface of colloid so they are adsorbed and neutralize the surface charge of the colloid. As the charge is neutralized the electrostatic potential present in the solution which was preventing contact of particles, vanishes. Care has to be taken to prevent overdosing of coagulant, as it can result in restabilizing the suspension.

- ***Inter-particle bridging:*** This occurs when high-molecular-weight polymers branch out and adsorb to multiple particles. Also the process may occur when polymer chemically reacts with other polymer or share ions directly to form ionic bridges. The resulting aggregated particles may have reactive polymer branches

extending into the suspension. The branched polymer that facilitates this process must extend past the diffuse layer to avoid repulsion tendencies of similarly charged particles. The polymer branches which are created, causes particle destabilization and may cause re-stabilization. During interparticle bridging, particles come together to form a mesh-like matrix consisting of destabilized colloids and polymer branches. As the floc begins to settle, it may entrap smaller particles. This process is referred to as sweep floc, flocs are generated by the hydrolysis of coagulant. These flocs settle under gravity and as it settles the colloids are swept away from the suspension. Most conventional surface water treatment plants operate in the region where sweep floc is the predominant mechanism of coagulation [73].

2.2.1 Flocculation

Flocculation is a stage that is rapidly followed by coagulation and relies on providing turbulence to promote collisions. In coagulation the particles come together, while flocculation is a phase in which the flocs begin to form larger aggregates. Flocculation is a slow mixing stage. The particles are encouraged to form large aggregates while the water is gently mixed. Rough mixing can cause the flocs to break and lead to restablization. When the contacts are produced by Brownian motion, the process is termed as perikinetic flocculation and when it is produced by stirring it is known as orthokinetic flocculation. Collisions of the microfloc particles cause them to produce larger, visible flocs called pinflocs. The floc size continues to build through additional collisions and interaction with inorganic polymers formed by the coagulant or with organic polymers added, thus forming macroflocs. High molecular weight polymers, called coagulant aids, may be added during this step to help bridge, bind, and strengthen the floc, add weight, and increase the settling rate. Once the optimum size and strength of the floc has reached, the water is ready for the sedimentation process.

2.2.2 Coagulation chemistry

The chemistry of coagulants in solution is quite multifaceted. Coagulants (e.g. metal coagulants Al or Fe) in solution complex with water to from aqua-metal complexes $[M-(H_2O)_6]^{3-}$. In the present study the coagulation with aluminium is done so coagulation details of aluminium are discussed.

Aluminium has a high tendency to hydrolyze in aqueous solutions [74]. When Al(III) is added in water it will dissociate to yield trivalent Al^{+3} ions, which hydrate to form aquometal complexes $[Al(H_2O)_6]^{3+}$. These complexes pass through a series of hydrolytic reactions in which a water molecule in the hydration shell is replaced by

the OH^- ions. This gives rise to the formation of a variety of species. The hydrolysis scheme of Al (III) as suggested by [75] and [76] is shown in Equation 2.1−2.7.

$$Al^{3+} + H_2O \rightarrow AlOH^{2+} + H^+ \tag{2.1}$$

$$AlOH^{2+} + H_2O \rightarrow Al(OH)_2^+ + H^+ \tag{2.2}$$

$$Al(OH)_2^+ + H_2O \rightarrow Al(OH)_3 + H^+ \tag{2.3}$$

$$Al(OH)_3 + H_2O \rightarrow Al(OH)_4^- + H^+ \tag{2.4}$$

$$2Al^{3+} + 2H_2O \rightarrow Al_2(OH)_2^{4+} + 2H^+ \tag{2.5}$$

$$3Al^{3+} + 4H_2O \rightarrow Al_3(OH)_4^{5+} + 4H^+ \tag{2.6}$$

$$13Al^{3+} + 28H_2O \rightarrow Al_{13}O_4(OH)_{24}^{7+} + 32H^+ \tag{2.7}$$

In the basic and acidic solution, Al ion will be found in anionic $\left(Al(OH)_4^-\right)$and cationic $\left(Al(OH)_2^+\right)$ forms, respectively [36]. In the absence of significant concentrations of other anions, the aqueous Al will form various hydroxyl complexes, the relative amounts of which will depend on both pH and initial concentration of the Al in solution [77]. However, the hydrated ion $Al(H_2O)_x^{3+}$ exists in the solution at $pH < 4$ but the hydroxide complexes are formed at $pH > 4$ [78]. The solubility of aluminium in equilibrium with solid phase $Al(OH)_3$ depends on the surrounding pH. At pH between 5 and 6, the predominant hydrolysis products are found to be $Al(OH)^{2+}$ and $Al(OH)_2^+$. The solid $Al(OH)_3$ is most prevalent in pH range of 5–8. The soluble species $Al(OH)_4^-$is the predominant species at pH values more than 9. Solubility of Gibbsite at different pH is shown by $MINEQL^+$ software in Figure 2.2. Solid $Al(OH)_3$ precipitates at pH of 5 when it predominates over soluble complexes in the pH range of 5–9. At higher pH (pH >10), the dominating species present is the soluble aluminates, $Al(OH)_4^-$.

Thermodynamic calculations show that aluminium fluoride complexes are generally the dominant inorganic aluminium species [79][80]. Changes are produced in the progress of aluminium in water, when fluoride is present. Fluoride ion forms strong complexes with aluminium due to which there is a considerable increase in the solubility of Al [81]. It is reported that the fluoride complexes AlF^{2+}, AlF_2^+, AlF_3 and AlF_4^- predominate in acid solution in the presence of $1 \times 10^{-5}M$ fluoride, until $Al(OH)_3$ precipitates [36]. Aluminium complexes are not precipitated until the solution pH has

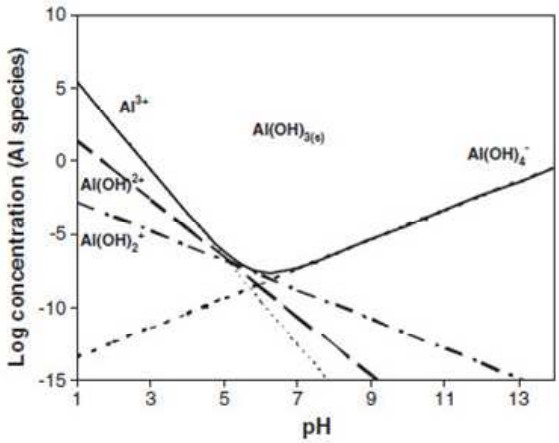

Figure 2.2: Solubility of aluminium hydroxide at different pH values by using $MINEQL^{+}$ software [36].

reached to 6. The complex of $Al(OH)_4^-$ is formed in alkaline solution. The charge on hydrolysis products and the precipitation of metal hydroxides are both controlled by pH. The hydrolysis products possess a positive charge at pH values below the isoelectric point of the metal hydroxide [82]. These positively charged species can cause destabilization of negatively charged colloids by adsorption and charge neutralization. Negatively charged species, predominate above the isoelectric point and are ineffective for the destabilization of negatively charged colloids.

According to Stumm and O'melia [69], $Al(III)$ accomplish destabilization by two mechanisms: adsorption & charge neutralization and enmeshment in a sweep floc. If aluminium salt is added to water in concentrations less than the solubility limit of the metal hydroxide, the hydrolysis products will form and adsorb onto the particles, causing destabilization by charge neutralization. When the amount of aluminium (III) added to water is sufficient to exceed the solubility of the metal hydroxide, the hydrolysis products will form as kinetic intermediates in the formation of metal hydroxide precipitate. In this situation charge neutralization and enmeshment in the precipitate both contribute to coagulation [83]. Interrelations between pH, coagulant dosage, and colloid concentration determine the mechanism responsible for coagulation. Precipitation of amorphous metal hydroxide is necessary for sweep floc coagulation. The solubility of $Al(OH)_3(s)$ is minimal at particular pH and increases as the pH increases or decreases from that value.

2.3 Electrocoagulation process

EC has a long history and the first plant was built in London in 1889 for treating sewage [84][85]. Though the EC process has shown promising results but its success has been limited. However, there has been renewed interest in this technology due to demand

of water treatment technologies. According to Rajeshwar *et al* [86], benefits from using electrochemical techniques include: environmental interests, versatility, energy efficiency, amenable to automation and cost effectiveness. In addition to the mentioned advantages electrochemical based systems also allow controlled and rapid reactions, viability due to compact systems and instead of using chemicals they employ electrons which facilitate water treatment.

EC is an in situ generation of active coagulant by electrically oxidizing anode material. This is an effective technology for treating polluted water. To understand EC; knowledge of electrochemistry, coagulation and flotation is required.

2.3.1 Electrocoagulation as a treatment technology for fluoride removal

EC system comprises of electrodes: anode and cathode both of which are made of aluminium. There are multiple electrochemical reactions which occur simultaneously at the anode and the cathode. The schematic diagram of EC reactor is shown in Figure 2.3.

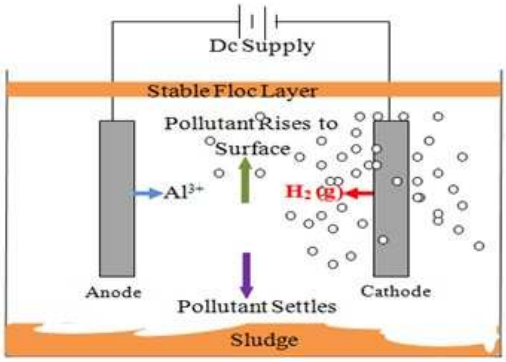

Figure 2.3: Schematic diagram of the EC process.

As the current is passed through the electrodes the anode undergoes electrolytic oxidation and forms metal ions which act as coagulants. The electrolytic dissolution of Al anodes by oxidation produces aqueous Al^{3+} species [87]. The Al^{3+} ions further react to form $Al(OH)_3$ flocs. These flocs are believed to adsorb fluoride [88]. Freshly formed amorphous $Al(OH)_3$ precipitates, that are required for sweep coagulation have large surface areas. These precipitates (flocs) are beneficial for rapid adsorption of soluble compounds and entrapping of colloidal particles. The formed flocs polymerize usually at high aluminium concentrations. The reactions at anodes are summarized below in Equation 2.8 $-$2.11.

$$Dissolution\,of\,metal: Al \rightarrow Al^{3+}(aq) + 3e^{-} \tag{2.8}$$

$$Hydrolysation: Al^{3+}(aq) + 3H_2O \rightarrow Al(OH)_3 + 3H^+(aq) \tag{2.9}$$

$$Polymerization: nAl(OH)_3 \rightarrow Al_n(OH)_{3n}(s) \tag{2.10}$$

$$Main\,removal\,reaction: Al(OH)_{3n}(s) + mF^-(aq) \rightarrow Al_nF_m(OH)_{3n-m}(s) + mOH^-(aq) \tag{2.11}$$

The water is electrolysed and formation of hydrogen gas takes place. These bubbles float to the top of the tank, colliding with particles suspended in the water on the way up, adhering to them and floating them to the surface of the water. They form a stable floc layer at the top surface of the reactor. The reactions at cathodes are summarized below in Equation 2.12 and 2.13.

$$Reduction\,of\,metal: Al^{3+}(aq) + 3e^- \rightarrow Al(s) \tag{2.12}$$

$$Hydrogen\,and\,hydroxide\,formation: 2H_2O(l) + 2e^- \rightarrow H_2(g) + 2OH^- \tag{2.13}$$

2.3.1.1 Cell arrangement

EC cell is made up of two cells cathode and anode. The electrodes are generally made up of aluminium in case of fluoride removal. Cathode could be made of iron or stainless steel since coagulants are released from the anode. The electrodes are connected to an external power source; anode will corrode and generate coagulant while cathode will be subjected to passivation. The electrodes can be connected by using monopolar or bipolar connections. In monopolar connection- series, a pair of electrodes placed between the two outer electrodes. The outer electrodes are connected to the negative and positive terminal, while the inner electrodes are interconnected (Figure 2.4a). In monopolar connection- parallel, some electrodes are connected to the positive terminal and some are connected to the negative terminal (Figure 2.4b). In bipolar connections only the electrodes at the end are connected to the power source and the rest of the electrodes are placed in-between them. These electrodes induce a charge in them when current is applied to the outer electrodes (Figure 2.5).

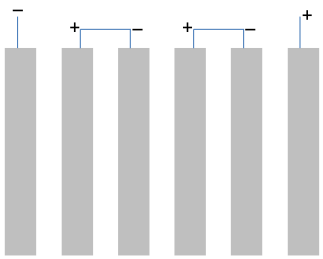

(a) series connection

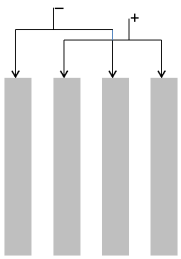

(b) parallel connection

Figure 2.4: Monopolar electrode connection.

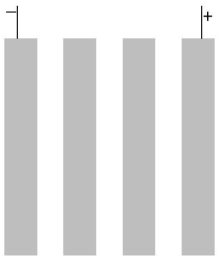

Figure 2.5: Bipolar electrodes in parallel connection.

2.3.1.2 Treatment parameters

- ***Electrode material:*** This defines the type of electrochemical reaction occurring in an EC system. Aluminium and iron both have been successfully used for the EC process. Inert electrodes, such as metal oxide coated titanium are used as cathodes in some reactors. When water to be treated has significant amounts of calcium or magnesium ions, the inert cathode is recommended [89]. There are some studies where combinations of aluminium and iron electrodes have been used [90][91]. Optimal material selection depends on the pollutants to be removed and the chemical properties of electrolyte. For removal of fluoride aluminium electrodes are used as fluoride has more affinity for aluminium.

- ***pH of the solution:*** The EC process is highly dependent on the pH of the solution [33][92]. pH has an effect on the conductivity of the solution, dissolution of the electrodes, hydroxide speciation and zeta potential of colloidal particles. During the EC treatment process pH increases constantly, making it a constantly changing parameter and therefore mechanistic studies are difficult to conduct. The increase in pH is due to the formation of hydroxyl ions during the EC process, which are formed by electrolysis of water. In the present study aluminium electrodes were used and during the EC process aluminium hydroxide was formed. Aluminium hydroxide is an amphoteric hydroxide. In the basic and acidic solution, Al ion

will be found in anionic $Al(OH)_4^-$ and cationic $Al(OH)^{2+}$ forms, respectively. The solid $Al(OH)_3$ is most prevalent between pH 6 and 8, but above pH 9 the soluble species predominate [34]. To avoid the dissolution of aluminium in the water, maintaining the pH is of prime importance.

- ***Co-existing ions:*** Hu and co-workers [93] , have reported the effect of co-existing ions (SO_4^{2-},Cl^-,Ca^{2+}) on the process of fluoride removal. They reported that SO_4^{2-} has a negative impact on the process of fluoride removal as it inhibits local corrosion of electrodes which in turn reduces the efficiency of applied current. Also, there is ion exchange competition between $SO_4^{2-}$and F^-. Chloride ions have a positive impact as it is found that they rupture the passive layer on electrodes, thereby increasing the efficiency of current [94]. Also Ca^{2+} has a positive impact due to the known fact of formation of calcium fluoride precipitate.

- ***Applied current and treatment time:*** Current is directly proportional to the rate of electrochemical reactions taking place on the electrode surface and it also has an influence on the electrode potential, which defines the reactions taking place on the electrode surface. Coagulant produced by electrolysis can usually be calculated according to Faraday's law when current and treatment time is known. Coagulant concentration produced by electrolysis on anodes is directly proportional to the electric charge added per volume (coulombs per litre).

2.3.2 Benefits and drawbacks of EC treatment

EC has been thought of as a distinct economical and environmental friendly choice for treatment of water. This technique is very efficient as adsorption of hydroxides is several times greater on in situ rather than on pre precipitated hydroxides. EC requires simple equipments and can be designed for any size. The operation is simple and cost-effective. The start-up, maintenance and operating costs are low. Practically no chemical is added to the solution so chances of secondary pollution also reduces. Low current is required for operation and so can be run by green processes like solar, windmills and fuel cells. The production of sludge by the process is also minimized. Flotation is self induced by the production of gas bubbles in the process. It efficiently removes the colloidal particles as compared to conventional chemical and biological techniques [95].

There are a few shortcomings of the process which are; periodical replacement of sacrificial anodes and requirement of minimum conductivity without which the current would not pass. Therefore, in the water with low TDS, conductivity has to be introduced. Also an impermeable oxide layer may be formed on the cathode that may interfere with the performance of the EC cell. However, if polarity is changed this interference can be overcome.

2.4 Research findings in the recent past

Due to increase in the problem of fluorides, extensive research techniques have been practised for defluoridation. Among all the techniques, EC is emerging as a promising technique and a lot of research work is being carried out in this area. A brief outline of the work reported by various researchers about fluoride removal by EC has been presented here.

Mameri et al. (2001) [81], studied the performance of pilot scale electrochemical reactor equipped with aluminium bipolar electrodes. They concluded that water defluoridation in a small plant by EC appeared very promising for in depth development studies.

Hu et al. (2003) [93], have carried out batch experiments with bipolar electrodes to investigate the effect of type and concentration of co-existing ions on defluoridation in EC. They concluded that defluoridation efficiency is 100% in absence of co-existing ions. In the system with co-existing anions, the defluoridation reaction takes place in bulk solution and the residual fluoride concentration is controlled by Al(III) dosage. The presence of sulphate ions decreases the defluoridation efficiency, whereas the chlorides and nitrates prevent this inhibition.

Emamjomeh & Sivakumar (2006) [96], conducted batch experiments with monopolar aluminium electrodes for fluoride removal. They developed an empirical model using critical parameters such as current concentration, electrode distance, and initial fluoride concentration. Fluoride ions were removed electrochemically from solution by ECF process. The fluoride removal efficiency increases steadily with increasing current values from 1 to $2.5\,A$. In the batch monopolar ECF process, the optimal detention time was found to be $55\,min$ when the operational parameters including initial F^-concentration, current value, and inter electrode distance were respectively kept at $10\,mg/L$, $1.5\,A$, and $5\,mm$. The experimental results reported that the rate constant for defluoridation by monopolar ECF process depends on the current concentration (I/V), electrode distance and initial fluoride concentration. The Al^{3+}/F^-mass ratio is found to be not significantly different between monopolar and bipolar ECF systems. Overall, the results showed that the EC technology is an effective process for defluoridation of water.

Hu et al. (2007) [39], derived a variable order kinetic (VOK) model from the Langmuir equation to simulate the kinetics of the defluoridation of EC using bipolar aluminium electrodes. The results reported good agreement between the predictive equation and the experimental data. The critical parameters, 'I_{max}' and 'k' for VOK model are constants when the initial fluoride concentration and current vary. Another critical parameter, current efficiency, is independent upon initial fluoride concentration, but varies with current density and needed to be obtained by experiment. The model

cannot successfully simulate the defluoridation in the EC process if the pH changes too violently.

Zhu et al. (2007) [40], investigated a new approach to study fluoride distribution in the EC defluoridation process, which has divided the fluoride into three parts: remained in water, removed by electrodes, and adsorbed on hydroxide aluminium flocs. Several critical parameters such as pH, charge loading, current density and initial fluoride concentration were investigated for fluoride removal. It was reported that the removal by the electrodes was primarily responsible for the high defluoridation efficiency, and the adsorption by hydroxide aluminium flocs gave a secondary effect. The parameters affected the efficiencies of defluoridation in a way of changing the fluoride distribution in the EC process. A chemical complex of $Al_n(OH)_mF_k^{3n-m-k}$ was formulated to explain the mechanism inside the EC defluoridation process. The new approach provides a detailed insight of the electrocondensation effect, which helps to gain more scientific comprehension about the cooperation between electrochemical and chemical ways occurring inside the EC process.

Zuo et al. (2008) [94], conducted experiments using combined EC and EF process to remove fluoride from drinking water. Its efficacy was investigated by varying parameters like initial pH, initial fluoride, charge loading and co-existing ions. The total hydraulic retention time required was only $30\,min$. After treatment, the fluoride concentration was reduced from initial $4.0-6.0\,mg/L$ to lower than $1\,mg/L$. It was found that influent pH is an important variable that affected fluoride removal significantly. Effective defluoridation was achieved at the influent pH range of 6.0–7.0, also no pH readjustment was needed after treatment. In addition, it was found that $SO4^{2-}$ had negative effect, Ca^{2+} had positive effect, while Cl^{-} had little effect on the fluoride removal.

Hu et al. (2008) [97], have treated high fluoride synthetic wastewater by EC process and considered the parameters like dose of SDS, charge loading and flow rate for their investigations. They also reported a comparison between a batch reactor and continuous flow reactor. The removal of suspended solids (SS) in the continuous system was less than that in the batch system because the scum was disturbed by the flow of wastewater in the flotation tank. It decreased with the increase in flow rate when the flow rate reaches higher than $800\,mL/min$, yet it increased with the increase in flow rate when the flow rate falls below $200\ mL/min$.

Ghosh et al. (2008) [98], investigated the process of EC for effective removal of fluoride from water. Different initial fluoride concentrations and both monopolar and bipolar electrode connections were studied. The final recommendable limit of fluoride ($1\,mg/L$) was obtained in $30\,min$ at $625\,A/m^2$ using bipolar connection. By-products obtained from the EC bath were analyzed using SEM, EDAX, FTIR and XRD and explained. Comparative cost estimation for both electrode connections was also

presented in the study. Total operating costs for monopolar and bipolar connections were 0.38 and 0.62 $US\$/m^3$, respectively, for the initial fluoride concentration of $10\,mg/L$. These findings might be useful in order to treat the fluoride contaminated water for drinking.

Emamjomeh & Sivakumar (2009) [34], investigated the effects of the different parameters such as: current density $12.5-50\,A/m^2$, flow rate $150-400\,mL/min$, initial pH (4–8), and initial fluoride concentration $(5-25\,mg/L)$, using continuous flow experiments with monopolar aluminium electrodes for fluoride removal. The highest treatment efficiency was obtained for the largest current. The removal efficiency was found to be dependent on the current density, the flow rate and the initial fluoride concentration when the final pH ranged between 6 and 8. The composition of the sludge produced was analyzed using the XRD spectrum. The presence of the aluminium hydroxide $[Al(OH)_3]$ in the above pH range, which maximizes the formation of aluminium fluoride hydroxide complex $[Al_nF_m(OH)_{3n-m}]$, is the main reason for defluoridation by EC.

Drouiche et al. (2009) [99], studied the treatment of synthetic fluoride containing solution by EC method. Parameters which were investigated are: applied potential, electrolysis time and electrolyte concentration. They reported that with increase in applied potential and electrolysis time the Al^{+3} dose increases, which in turn favours the removal of fluoride ions. Analysis of solid products formed by aluminium electrodes was done using SEM, EDAX, FTIR and XRD. It was also reported that the formation of cryolite and sodium aluminium fluorite was the main reason of defluoridation by the EC process.

Emamjomeh et al. (2011) [36], have investigated in detail the mechanism of fluoride removal in EC process. A monopolar batch ECF reactor was used for understanding of the mechanism of fluoride removal. The experimental results elucidated that the EC/F process is highly dependent on the pH of the solution. Solid $Al(OH)_3$ is most prevalent at a pH range of 5–8. The soluble species $Al(OH)_4^-$ is the predominant species when the final pH increases to 10. The removal efficiency decreased when the final pH was increased from 8 to 10. The mechanism for the fluoride removal was confirmed to be not only the competitive adsorption between OH^- and F^- but also the formation of solid cryolite in the final pH range of 5–8. It could be observed that the defluoridation process is more efficient for the final pH ranging between 6 and 8.

Drouiche et al. (2011) [100], conducted EC experiments with bipolar aluminium electrodes to determine the optimum conditions for fluoride removal from synthetic high fluoride water. A full factorial 2^3 design of experiments was used to obtain the best conditions for fluoride removal. Initial fluoride concentration, applied potential and supporting electrolyte are the factors which were taken into consideration. Mathematical equation showing the relation between residual fluoride condition and

investigated factors was also developed.

Behbahani et al. (2011) [101], applied response surface methodology (RSM) to evaluate the effect of main operational variables, including initial pH, initial fluoride concentration, current density and reaction time for the removal of fluoride and its relative operating costs by EC. It was reported that the effect of initial pH was negligible on fluoride removal efficiency and operating costs. With the decrease of initial fluoride concentration, fluoride removal efficiency, improved; however, it had no effect on operating costs. On the other hand, the increase of current density and reaction time severely influenced process performance and increase fluoride removal efficiency and operating costs. According to the ANOVA results, the models presented the high R^2 values of 96.5% and 97.3% for fluoride removal efficiency and operating costs, respectively. The optimum initial pH, initial fluoride concentration, current density and reaction time were found to be 7, 25 mg/L, 0.0167 A/cm^2, 25 min, respectively, for the removal of fluoride.

Drouiche et al. (2012) [102], have successfully applied the EC process to remove fluoride from pretreated photovoltaic aqueous solution. The defluoridation was found to be dependent on the initial pH, distance between electrodes and the applied potential. The most effective conditions to achieve standard discharge for fluoride by EC was obtained with typical operating conditions; 30 V applied potential, 40 min operating time and pH 6.

Takdastan et al. (2014) [103], proposed EC by iron and aluminium electrodes for removing fluoride from drinking water. Effects of different operating conditions such as treatment time, initial pH, applied voltage, type and number of electrodes, the spaces between aluminum and iron electrodes, and energy consumption during EC were investigated in the batch reactor. It was reported that the energy consumption with aluminum electrodes was less than iron electrodes; thus, EC with aluminum electrodes can be more effective compared with iron electrodes for fluoride removal.

Naim et al. (2015) [104], studied the effect of different variables on the defluoridation by the EC process. The investigated parameters are different fluoride concentrations, pH of the solution, temperature, speed of agitation, electrode spacing, type of comprising water, electrolyte additives and mono and bipolar configurations. The type of comprised water was the only variable that did not pose observable effect. A multivariate study was applied to get a set of predictive multiple regression equations. It was advised that due to the high economic value, the low applicable energy, as well as the saving of time; the predictive equations for the EC defluoridation must be used.

2.5 Research gap

The work done in this area in the recent past has been cited in the section 2.4. The information presented in the section 2.4 leads to identification of research gap in the study of fluoride removal by EC. A list of parameters and their corresponding investigators have been tabulated in Table 2.2.

Table 2.2: Summary of investigations done on EC process.

S.No	***Parameters***	***Batch reactor***		***Continuous reactor***	
		Investigators	***Range***	***Investigator***	***Range***
1	Initial F- conc (mg/L)	Hu *et al.*, 2007 [39]	15,20,25	Emamjomeh & Sivakumar, 2009 [34]	5,10,15
		Zhu *et al.*, 2007 [40]	$3-15$		
		Ghosh *et al.*, 2008 [98]	8, 10		
		Drouiche *et al.*, 2011 [100]	20, 25		
		Naim *et al.*, 2015 [104]	$4-6$		
			$6.44-57.90$		
2	Initial pH	Zhu *et al.*, 2007 [40]	$5.5-8$	Zuo *et al.*, 2008 [94] Emamjomeh & Sivakumar, 2009 [34]	$3-9$
		Zuo *et al.*, 2008 [94]	$3-9$		$4-8$
		Emamjomeh *et al.*, 2011 [36]	$2-10$		
		Drouiche *et al.*, 2012 [102]	$4-9$		
		Takdastan *et al.*, 2014 [103]	4,7.5,10		
			$4-8$		
3	Current (A)/ Current density(A/m^2)	Zhu *et al.*, 2007 [40]	$4.63-92.59$	Emamjomeh & Sivakumar, 2009 [34]	$12.5-50$
		Hu *et al.*, 2007[39]	$0.1-0.4$		
			$0.15-0.75$		
4	Charge loading (F/m^3, C/L)	Zhu *et al.*,2007 [40]	$0.52-4.15$	Hu *et al.*, 2008 [97]	$250-1500$
		Zuo *et al.*, 2008 [94]	$1-3.5$		

5	Inter-electrode distance (*mm*)	Emamjomeh & Sivakumar, 2006 [96]	$5-15$		
			$10-20$		
		Drouiche *et al.*, 2012 [102]	$20-40$		
		Takdastan *et al.*, 2014 [103]	$20-40$		
6	Conductivity	Ghosh *et al.*, 2008 [98]	$0.4-0.9$ mmohs		
		Drouiche *et al.*, 2009 [99]	$0-100\,mg/L$		
		Drouiche *et al.*, 2011 [100]	(NaCl conc)		
7	Co-existing ions	Hu *et al.*, 2003 [93]	Cl^-, NO_3^{2-}	Zuo *et al.*, 2008	Ca^{2+}, Cl^-
			SO_4^{2-}		SO_4^{2-}
8	Applied potential (*V*)	Drouiche *et al.*, 2009 [99]	$10-30$		
		Drouiche *et al.*, 2011[100],	$10-30$		
		2012 [102]	$5-20$		
		Takdastan *et al.*, 2014 [103]			
9	HRT (*min*)	Emamjomeh & Sivakumar,	$0-60$	Zuo *et al.*, 2008	$20-60$
		2006 [96]	$0-9$		
		Hu *et al*, 2007 [39]	$20-60$		
		Zuo *et al*, 2008 [94]	$10-80$		
		Drouiche *et al.*, 2009 [99]	$10-40$		
		Takdastan *et al.*, 2014 [103]			

10	Flow rate (mL/min)	N.A.		Hu *et al.*, 2008 [97] Emamjomeh and Sivakumar, 2009 [34]	$200-800$ $150-400$
11	Electrode configurations	Hu *et al.*, 2003 [93] Ghosh *et al.*, 2008 [98] Takdastan *et al.*, 2014[103] Naim *et al.*, 2015 [104]		Mameri *et al.*, 2001[81]	
12	Sludge characterization	Ghosh *et al.*, 2008 [98] Drouiche *et al.*, 2009 [99] Emamjomeh *et al.*, 2011 [36]		Emamjomeh & Sivakumar, 2009 [34]	
13	Specific Energy	Zuo *et al.*, 2008 [94] Takdastan *et al.*, 2014 [103]			
14	Cost	Behbahani *et al.*, 2011 [101]		Emamjomeh & Sivakumar, 2009 [34]	
15	Optimization	Drouiche *et al.*, 2011 [100] Behbahani *et al.*, 2011[101]			
16	Residual aluminium				

17	Adsorption isotherms				

The Table 2.2 clearly shows that not much literature is available on areas like: development of regression equations for fluoride removal, specific energy consumed in the process, adsorption isotherms and residual aluminium in the treated water. Therefore in the present work apart from focussing on the main problem of controlling aluminium in treated water, work has also been done on the mentioned areas.

Chapter Summary

A wide variety of treatment techniques are available for removal of fluoride which are listed in this chapter. This chapter informs that coagulation-flocculation is frequently used for water treatment and explain its mechanism. In the next part, the chapter discusses the process of EC and its basic concepts. Aluminium electrodes were used to generate the coagulant, so a detailed discussion about the coagulation chemistry of aluminium has been reviewed.

In the end, the investigations carried out in the recent past about fluoride removal by EC have been reported. A summarised table of researchers and their work has been developed to identify the research gap. Thus, it was identified that residual aluminium in treated water was the prime focus of research. Other areas like optimization of the process, and adsorption isotherm study also needs attention.

The next chapter marks the formal beginning of the thesis and discusses the materials and methodology used for conducting the present study.

CHAPTER 3

Chapter 3

Materials and Methods

This Chapter describes the research methodology used in detail for the present study. It gives an insight into the experimental setup of the reactor and analysis done in collecting the data. The entire work was carried out in the PHE laboratory of Department of Civil Engineering in Malaviya National Institute of Technology, Jaipur. The experiments have been divided into two parts: fluoride removal and aluminium removal. EC process has been used to remove fluoride from the water; the samples were then tested for aluminium concentration. The aluminium concentration was not within the permissible limits, so a further level of treatment has been done to control it.

3.1 Fluoride removal

This section includes the description of the materials and the process used for defluoridation.

3.1.1 Experimental Setup

The batch EC cell of 2 L effective volume has been used for the experimental study. The electrode arrangement consists of two aluminium electrodes connected in a monopolar mode. The electrode with dimensions: 84 mm width, 71 mm height, 2.5 mm thickness; were placed 10 mm apart in the fluoride containing solution. No regular approach has been suggested in the literature about the reactor design for EC. However, details about the surface area of electrode to volume ratio is present in the literature as shown in Table 3.1. It ranges from 6 to 41 m^2/m^3. In the present work this ratio is kept to be 12 m^2/m^3, which is in agreement with the cited range from the literature. The electrodes were connected to a D.C. power supply. The solution was stirred using a magnetic stirrer to ensure complete mixing. A pictorial representation of the experimental setup is shown in Figure 3.1.

Table 3.1: Electrode surface area to reactor volume (A/V) ratio and current density employed [105]

Reference	***A/V*** (m^2/m^3)	***Current density*** (A/m^2)	***Pollutant removed***
Emamjomeh *et al.* (2006)	22	12.5 – 31.25	Fluoride water
Holt *et al.* (2005)	10.5	3.4 – 2.7	Turbidity from clay solution
Hu *et al.* (2003)	40.9	55	Fluoride water
Can *et al.* (2003)	16.78	25 – 250	Color from dye solution
Chen *et al.* (2000)	18.6	30 – 80	Oil from restaurant wastewater
Mameri *et al.* (1998)	6.4 – 34.6	3.12 – 289	Fluoride water
Ming *et al.* (1983)	6 – 8	14	Fluoride water

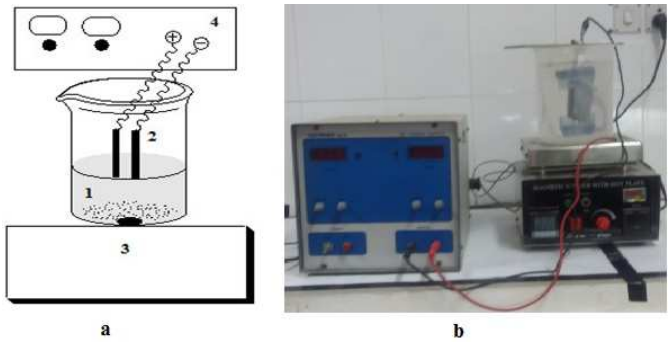

Figure 3.1: Experimental set-up for fluoride removal. (a) Schematic diagram experimental setup 1: EC reactor, 2: Al electrodes, 3: magnetic stirrer and 4: DC power supply, (b) Image of the experimental set-up of batch EC process.

3.1.2 Water samples and chemicals

The influence of the operating parameters on the defluoridation process was investigated using synthetic sample (tap water and sodium fluoride (NaF)). The properties of the tap water are listed in Table 3.2. Conductivity of the samples was promoted by adding 2 mM sodium chloride (NaCl). The conductivity value has been set to $0.97 \pm 0.02\, mS/cm$ for all prepared samples. With the use of 1 : 1 HCl, the pH of the solution was adjusted to 6.

Table 3.2: Water quality of sample

Chemical Parameters	***Concentration***	***Units***
Total Alkalinity	$200-208$	mg/L as $CaCO_3$
Hardness	$164-168$	mg/L as $CaCO_3$
Total dissolved solid	$250-255$	mg/L
Chloride	$23-26$	mg/L
Conductivity	$0.48-0.51$	mS/cm
pH	$7.2-7.5$	

3.1.3 Methodology

EC experiments were performed in the batch reactor and samples were collected at the end of each run from the reactor to measure fluoride, aluminium and pH. All experiments were conducted at room temperature of about 25 ± 2^oC. Before each EC run, the electrodes were washed with acetone to remove surface grease, and impurities on the aluminum electrode surfaces were removed by means of dipping electrodes in dilute HCl solution. Anode was weighed before and after each run. The initial fluoride was varied between the range of $2-8\,mg/L$ and the applied current was varied over the range of $0.15-0.75\,A$, however, it was held constant for each run. All experiments have been performed in duplicate sets and the average readings have been reported.

3.2 Aluminium removal

This section includes the description of the materials and the process used for control of aluminium.

3.2.1 Experimental set-up

The set-up consists of the EC reactor and an overhead stirrer as shown in Figure 3.2. The conventional coagulation technique was employed to control the aluminium in the water treated for fluoride after the EC process. The speed of the stirrer was controlled by a tachometer and it was varied accordingly for the rapid mix and slow-mix (flocculation) phase.

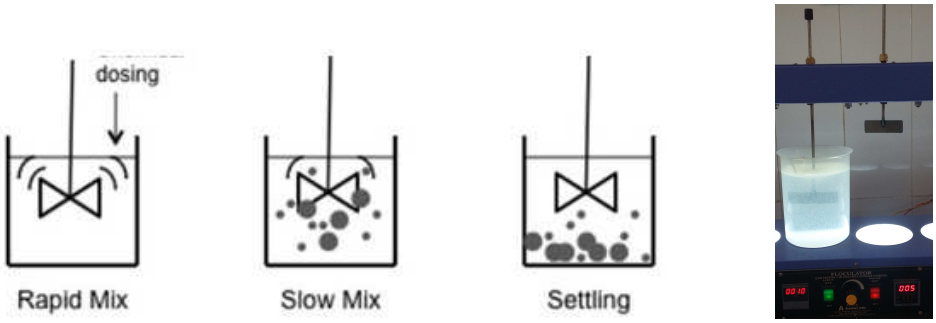

(a) (b)

Figure 3.2: Experimental set-up for aluminium removal. (a) Schematic diagram of flocculation and settling.(b) Image of EC reactor and overhead stirrer.

3.2.2 Water samples and chemicals

Water after each EC run was used for the coagulation-flocculation experiments. In the present study two coagulant aids were used; bentonite and activated silica sol. Bentonite used in the experiments was of SRL (Sisco Research Laboratries, Pvt. Ltd) make. Colloidal or activated silica sol was prepared in the laboratory by the following method; a 3% of sodium silicate solution was prepared and mixed with equal volume of 0.33N sulfuric acid. This results into a 1.5% silica suspension. The prepared suspension was used for dosing in the experiments.

3.2.3 Methodology

Two strategies have been employed for control of aluminium. In the first strategy, after the EC run, an overhead stirrer was placed in the reactor. Flocculation and settling was done. The supernatant was collected and filtered by 2.2 μm filter (Whatman Grade 42) and analyzed for residual aluminium. In the second strategy, coagulant aid (bentonite/ activated silica sol) was added after EC process, and mixed thoroughly for 1 min at 40 rpm. Flocculation, settling and filtration followed this process.

After the treatment process the sludge was collected and dried at a temperature of $110-120^oC$ for about 12 to 18 hours. Then it was ground to a fine powder to use for analysis.

3.3 Analytical procedures

Based on the Standard Methods [106] various analytical techniques were used for the accumulation of data. Brief description of the techniques is mentioned below:

- ***Fluoride measurement:*** Samples were collected after the EC process and after settling for analysis of fluoride. Fluoride was determined by using the ionometric

standard method [106]; using selective fluoride electrode (Thermo Scientific, 9609BNWP combination electrode), see Figure 3.3. A three point calibration was done daily using standard fluoride solutions of $0.1\,mg/L$, $1\,mg/L$ and $10\,mg/L$. The electrode slope was kept between $-54\,mV$ to $-64\,mV$. Fluoride ions can complex with aluminium, silicon, iron and other polyvalent cations even with hydrogen, therefore; total ionic strength adjustor buffer (TISAB) was added in all the standards and samples so that fluoride ions are decomplexed. TISAB was prepared by adding $4\,gm$ CDTA (1, 2-Diaminocyclohexane tetra-acetic Acid), with $57\,mL$ glacial acetic acid and $58\,gm$ NaCl in about $500\,mL$ distilled water. pH of the solution was adjusted to $5-5.5$ using $5\,M$ NaOH and the volume of the final solution was made to$1\,L$.

Figure 3.3: Fluoride ion meter

- ***pH measurement:*** The pH of a solution is a measure of the molar concentration of hydrogen ions in the solution and as such is a measure of the acidity or basicity of the solution. pH of the synthetic sample was adjusted to 6 using $1+1$ HCl . pH of the solution was measured before and after the EC process. pH of the samples was also measured after settling and filtration. It was determined by using the Haana HI-98128, with an accuracy of ± 0.02 pH (see Figure 3.4). Electrodes were thoroughly rinsed with distilled water before being immersed in the sample solution and then it was reimmersed after washing with distilled water to confirm the reading.

Figure 3.4: pH meter

- ***Conductivity meter:*** Electrical conductivity is a numerical expression of the ability of an aqueous solution to carry an electric current. To ensure minimum

conductivity for the EC process, conductivity of the samples was set by addition of sodium chloride. A conductivity meter manufactured by Lutron of model CD-4302 shown in Figure 3.5, was used for analyzing conductivity. The range of this instrument is $2-20\,mS$. Conductivity of the tap water used for EC experiments was $0.48\pm0.02\,mS/cm$ and after addition of NaCl it rises to $0.97\pm0.02\,mS/cm$.

Figure 3.5: Conductivity meter

- ***Atomic Absorption Spectrophotometer:*** Atomic absorption spectroscopy (AAS) is a spectroanalytical procedure for the quantitative determination of chemical elements using the absorption of optical radiation (light) by free atoms in the gaseous state. Atomic absorption utilizes the principle that each atom absorbs light at a specific wavelength. Therefore, at a specific wavelength, the quantity of the absorbing element can be quantified and is proportional to its concentration. For determination of aluminium the wavelength is $309.3\,cm$. It requires standards with known analyte content to establish the relation between the measured absorbance and the analyte concentration and relies therefore on the Beer-Lambert Law. AAS was used for determination of residual aluminium in the water sample. The aluminium concentration was measured after the EC process and after flocculation, settling and filtration. This measurement was done using Thermo Scientific AAS (iCE 3000 series) with graphite furnace as shown in Figure 3.6. The aluminium content after EC and direct filtration was measured using the flame technique. Nitrous oxide-acetylene flame was used for detection of aluminium by flame technique. Sample is aspirated, aerosolized, and mixed with combustible gases. During combustion, atoms of the element of interest in the sample are reduced to free, unexcited ground state atoms, which absorb light at characteristic wavelengths. The samples after settling and filtration were measured using the graphite furnace technique. Sample is placed in a graphite tube which is in the path of light with a wavelength of $309.3\,cm$ (Al absorption band). The sample then undergoes temperature programming which dries, ashes and atomizes the sample. In the present study total aluminium was analyzed, all samples tested for aluminium were acid digested by adding dil HNO_3.

Figure 3.6: Atomic-Absorption spectrophotometer

- ***Nephelometer:*** Turbidity is a measure of water clarity how much the material suspended in water decreases the passage of light through the water. Turbidity of the samples was measured after the EC process and after settling and filtration. Turbidity was measured using Digital Nephelometer (Model 341 E, Electronics India) (Figure 3.7) with an accuracy of 2% F.S. ± 1 digit. The range of the instrument was 0 to 19.9 NTU and 0 to 199.9 NTU.

Figure 3.7: Nephelometer

- ***Particle size analyzer:*** Particle size analysis was done to determine the size range of particles in the suspension obtained after EC. Particle size measurements were taken using Malvern Mastersizer-2000 (Figure 3.8. The instrument operates between $0.02 - 2000\,\mu m$. Laser diffraction is used for particle sizing. Laser diffraction measures particle size distributions by measuring the angular variation in intensity of light scattered as a laser beam passes through a dispersed particulate sample. Large particles scatter light at small angles relative to the laser beam and small particles scatter light at large angles. The angular scattering intensity data is analyzed to calculate the size of the particles responsible for creating the scattering pattern.

Figure 3.8: Particle size analyzer

- ***Fourier- Transform infrared (FTIR) spectrometer***: is used to identify the presence of certain functional groups in a molecule. In infrared spectroscopy, IR radiation is passed through a sample. Some of these radiations are absorbed by the sample and some of it is transmitted through it. The resulting spectrum represents the molecular absorption and transmission, creating a molecular fingerprint of the sample. The dried sludge, bentonite and activated silica sol was analyzed using Perkin Elmer Spectrum Two FTIR spectroscopy, (Figure 3.9).

Figure 3.9: Fourier transform infrared spectrometer

- ***Field Emission Scanning Electron Microscope (FE-SEM) and Energy Dispersive X-ray Spectrometry (EDX):*** SEM is one of the most versatile and well known analytical techniques. Compared to the conventional optical microscope, an electron microscope offers advantages, including high magnification, large depth of focus, great resolution and ease of sample preparation and observation. Electrons generated from an electron gun enter a surface of a sample and generate many low energy secondary electrons. The intensity of these secondary electrons is governed by the surface topography of the sample. An image of the sample surface is therefore constructed by measuring secondary electron intensity as a function of the position of the scanning primary electron beam. EDX analysis is widely used for chemical analysis. The characteristic X-rays emitted from the sample serve as fingerprints and give elemental information of the samples To know the external morphology of sludge and electrodes, SEM was used. SEM was performed using Nova Nano FE-SEM 450. It gives a resolution of $1.4\,kV$ (TLD-SE) and $1\,nm$ at $15\,kV$ (TLD-SE). The samples were coated with

Platinum to ensure conductivity. The SEM uses a focused beam of high-energy electrons to generate a variety of signals at the surface of solid specimens. The signals that derive from electron-sample interactions reveal information about the sample including external morphology (texture), chemical composition, crystalline structure and orientation of materials making up the sample. The FE-SEM is coupled to an EDX detector for measuring the elemental chemical composition (Figure 3.10). EDX analysis usually involves the generation of an X-ray spectrum from the entire scan area of the SEM. The Y-axis shows the counts (number of X-rays received and processed by the detector) and the X-axis shows the energy level of those counts.

Figure 3.10: FE-SEM-EDX

- ***X-ray diffraction (XRD):*** XRD analysis is based on constructive interference of monochromatic X-rays and a crystalline sample. The X-rays are generated by a cathode ray tube, filtered to produce monochromatic radiation, collimated to concentrate, and directed towards the sample. The interaction of the incident rays with the sample produces constructive interference (and a diffracted ray) when conditions satisfy Bragg's Law ($n\lambda=2d \sin \theta$). This law relates the wavelength of electromagnetic radiation to the diffraction angle and the lattice spacing in a crystalline sample. These diffracted X-rays are then detected, processed and counted. By scanning the sample through a range of 2θ angles, all possible diffraction directions of the lattice should be attained due to the random orientation of the powdered material. Conversion of the diffraction peaks to d-spacings allows identification of the mineral because each mineral has a set of unique d-spacings. Typically, this is achieved by comparison of d-spacings with standard reference patterns. The composition of sludge produced after the EC process was analyzed by XRD technique. The XRD measurements were carried out by PANanalytical Xpert powder (Figure 3.11).

Figure 3.11: XRD

3.4 Statistical Methods

DOE and statistical models were used to study the effect of input parameters and their interaction terms. DOE is a tool that assists in the planning, conducting, analyzing and interpreting controlled tests to evaluate the optimal factors. DOE helps to investigate the effects of input variables (operational parameters) on an output variable (response) at the same time. These experiments consist of a series of runs in which purposeful changes are made to the input variables. Data are collected at each run. Literature survey and parametric investigations suggested that applied current, electrolysis time and initial fluoride concentration are important operational parameters of concern for fluoride removal using the EC process.

3.4.1 Taguchi design

Genichi Taguchi, a Japanese engineer, proposed several approaches to experimental designs that are sometimes called "Taguchi Methods." Taguchi has envisaged a new method of conducting the design of experiments which are based on well defined guidelines. This method uses a special set of arrays called orthogonal arrays. These standard arrays stipulate the way of conducting the minimal number of experiments which could give the full information of all the input parameters that affect the performance of the response. The crux of the orthogonal array method lies in choosing the level combinations of the input design variables for each experiment. The design of an experiment involves the following steps:

- ***Selection of the independent variables:*** The knowledge of the process under investigation is of prime importance before conducting the experiment. Factors that are likely to influence the outcome have to be identified. In order to compile the list of input factors for the present study; extensive literature review and parametric investigations were done.

- ***Deciding the number of levels:*** Once the input parameters are decided, the number of levels for each parameter is decided. The selection of the number of levels depends on how the performance parameter is affected due to different level settings. If the performance parameter is a linear function of the independent variable, then the number of level setting shall be two. However, if the independent variable is not linearly related, then three, four or higher level settings can be selected depending on whether the relationship is quadratic, cubic or higher order. In the absence of exact nature of the relationship between the independent variable and the performance parameter, one could choose two level settings. After analyzing the experimental data, one can decide whether the assumption of level setting is right or not based on the percent contribution and the error calculations.

- ***Selection of an orthogonal array:*** Before selecting the orthogonal array, the minimum number of experiments to be conducted shall be fixed. Once the minimum number of experiments is decided, the further selection of orthogonal array is based on the number of input parameters and number of levels for each parameter.

- ***Conducting the experiment:*** Once the orthogonal array is selected, the experiments are conducted as per the level combinations. It is necessary that all the experiments are conducted.

- ***Analysis of the data:*** The analysis of the data is done to fulfil three objectives: to establish the optimum condition of a process, to estimate the contribution of individual factors and to estimate the response under the optimum condition.

- ***Inference:*** From the above experimental analysis, it is clear that the higher the value of sum of squares of an independent variable, the more it has influence on the performance parameter. The ratio of individual sum of square of a particular independent variable to the total sum of squares of all the variables can be calculated. This ratio gives the percent contribution of the independent variable on the performance parameter. In addition to the above, near optimal solution to the problem could be found. This near optimum value may not be the global optimal solution. However, the solution can be used as an initial/starting value for the standard optimization technique.

Taguchi design of experiments includes four phases. All the phases are depicted in Figure 3.12.

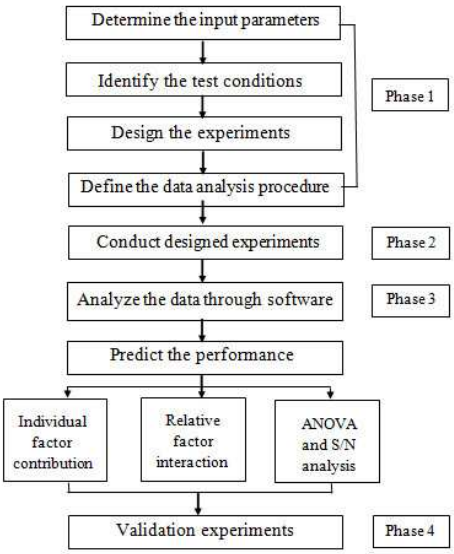

Figure 3.12: Flowchart depicting phases of Taguchi design.

3.5 Softwares used

3.5.1 MINITAB:

Minitab software is developed at the Pennsylvania State University by researchers Barbara F. Ryan, Thomas A. Ryan, Jr., and Brian L. Joiner in 1972. It is a general-purpose statistical software package designed for easy interactive use. It provides a simple, effective way to input statistical data, manipulate that data, identify trends and patterns, and then extrapolate answers to the problem at hand. Minitab DOE commands include the following features: catalogs of designed experiments to create a design, automatic creation and storage of design after specification of its properties, display and storage of diagnostic statistics to interpret the results and graphs to interpret and present the results.

In the present study MINITAB 14 has been used for implementation of Taguchi design. The study for fluoride removal was conducted using Taguchi method of design of experiments (MINITAB 14). The operating parameters studied were initial fluoride concentration (2, 5 and 8 mg/L), applied current (0.31, 0.53 and 0.75 A) and electrolysis time (10, 30 and 50 min) for three responses: residual fluoride, residual aluminium and SEEC. The performance of the target was chosen to be of minimization type. The main effect and interaction plots were generated by the software. Also ANOVA analysis was done using the same software.

3.5.2 SYSTAT

SYSTAT 7 is also a statistical software package, developed by Leland Wilkinson in the late 1970s, who was at the time an assistant professor of psychology at the

University of Illinois at Chicago. SYSTAT provides a powerful statistical and graphical analysis system in a new graphical user interface environment using descriptive menus, toolbars and dialog boxes. It offers numerous statistical features from simple descriptive statistics to highly sophisticated statistical algorithms.

In the present study SYSTAT 7 has been used to find the relation between the responses and operational parameters. The relationship between residual fluoride, residual aluminium and SEEC with combination of control factors is obtained using non-linear regression analysis.

3.5.3 FORCE 2.0

Force 2.0 is a full-featured programming environment for FORTRAN 77 (the engineering programming language).

In the present study FORCE 2.0 was used to develop a program in FORTRAN. The program was written to optimize the values of applied current (i) and electrolysis time (t) for target value of residual fluoride as 0.7 mg/L after the EC process. The minimum values of "i" and "t" for target value of residual fluoride, were determined for each initial fluoride concentration using the grid search method, programmed in FORTRAN. This method was implemented because on increasing the values of "i" and "t", energy consumption also increases which in turn increases the dissolution of aluminium. So, to control the aluminium introduced in the EC reactor, the product of "i" and "i" were minimized.

Chapter Summary

This Chapter has provided the description of materials and methodology used for performing the experiments. It has the details of experimental setup and solutions prepared for the study. The detailed procedure of experiments is given which explains the technique used for fluoride removal and aluminium removal. An explanation of the use of software for the research is also mentioned.

The next chapter marks the beginning of results and discussions.

CHAPTER 4

Chapter 4

Parametric investigations for fluoride removal

The present Chapter as the name signifies elucidates the effect of operational parameters like pH, inter-electrode distance, initial fluoride concentration, applied current and electrolysis time which governs the EC process for fluoride removal. Other parameters like SEEC, charge loading, anode consumption, fluoride uptake capacity (FUC) were also studied. The findings in this Chapter form the baseline data for the present study and also explains the motive of using selected range of operational parameters for the design of experiments in the later part of the study.

4.1 Effect of operating parameters on fluoride removal

It is well known that the efficiency of the EC process for fluoride removal depends on operating parameters like initial pH of water sample, inter-electrode distance, initial fluoride concentration, applied current, electrolysis time, etc.

For the present work, synthetic samples of fluoride water were prepared in the laboratory using tap water. Thus, it was necessary to investigate effects of these parameters on fluoride removal from such synthetic samples. The present parametric study was conducted to determine the performance of EC process for synthetic sample prepared in the laboratory. The findings from this study were also used to determine the effective range of operational parameters for treatment of synthetic water samples.

DOE was implemented using Taguchi method to develop statistical model for fluoride removal through the EC process. These parametric investigations serve as a baseline study to identify major operational parameters and their respective ranges for design of experiments in later part of the study. The effects of operational parameters like pH, inter-electrode distance, initial fluoride concentration, applied current, electrolysis time, SEEC, charge loading, anode consumption, and FUC have

been discussed below.

4.2 Effect of pH

pH of the solution plays an important role in electrochemical and chemical coagulation process [107]. The efficiency of the EC process is highly dependent on the pH of the solution [33] [107]. pH affects the speciation of aluminium which in turn has a significant influence on the defluoridation mechanism. Since aluminium hydroxide is an amphoteric hydroxide, pH is a sensitive factor for the formation of $Al(OH)_3$ flocs. The solubility of aluminium in equilibrium with solid phase $Al(OH)_3$ depends on the surrounding pH, as the solid $Al(OH)_3$ is most prevalent between pH 6 and 8, and above pH 9, the soluble species $Al(OH)_4^-$ is the predominant species [34]. It was studied by Emamjomeh and Sivakumar [34] that increase of pH beyond 8 leads to decrement of fluoride removal efficiency. They reported that on increasing pH from 6 to 8, residual fluoride increased from 0.74 to $1.05\,mg/L$ and the final pH reached to 9. Hence it was clear that fluoride removal efficiency decreases from 90 to 75% when final pH is more than 8. The above decrease was found to be due to the formation of soluble AlO_2 in high pH, which is not useful in defluoridation. The results obtained, show that the defluoridation process is more efficient for the final pH ranging between 6 and8 [36]. Similar conclusions were also made by Zuo *et al.* [94]. Zuo *et al.* [94] also reported that when the influent pH is in the range of $6-7$, the effluent pH is in the range of $7-8$. Hence, no pH readjustment is needed after the treatment.

Acquiring knowledge from the literature, a study was conducted in the laboratory for studying the effect of initial pH on defluoridation process. The experiments were conducted to find the value of initial pH, for which maximum efficiency of fluoride removal can be attained. Therefore, experiments were performed varying the initial pH in the range of $5.00-8.00$; keeping the initial fluoride concentration, applied current and electrolysis time constant for all runs. Each experiment was repeated twice and the average values for defluoridation efficiency and effluent pH were reported in the Figure 4.1.

It can be observed from the Figure 4.1 that defluoridation efficiency increases from 70 to 86% when initial pH is increased from 5.00 to 6.00. The maximum efficiency of 86% was achieved at initial pH of 6.00. On further increase in pH beyond 6.00 the efficiency of the process tends to decrease. At initial pH of 8.00, the efficiency of the process was found to be 75%. Figure 4.1 also shows the variation of effluent pH with influent pH. It can be observed that pH of the effluent increases after the treatment. This increase is mainly attributed to CO_2 transfer [107]. In acidic medium oversaturation of CO_2 is caused, and it is released from water due to disturbance of H_2 and O_2 bubbles produced at electrodes [94]; thereby increasing the pH. In addition partial exchange of

fluoride ions with OH^- ions in $Al(OH)_3$ occurs, which causes a pH increase [88].

When the influent pH was in the range of $5.00-8.00$ the effluent pH was observed to be in the range of $6.53-9.01$. A decrement is observed in fluoride removal efficiency when initial pH was 5.00 and 5.50. This is because the effective working pH range of $6.00-8.00$ is attained towards the end of treatment and hence not much of solid phase $Al(OH)_3$ is formed to assist in removal of fluoride. The results reported in the literature corroborates with the results obtained in the present study.

The initial pH of 6 gave maximum fluoride removal efficiency and the final pH attained was close to 7 (suitable for drinking purposes). No readjustment of pH was required during or after the treatment. Therefore, the pH value of the influent was kept constant $(pH = 6)$ for all the experiments conducted for the development of statistical modelling in later part of the study.

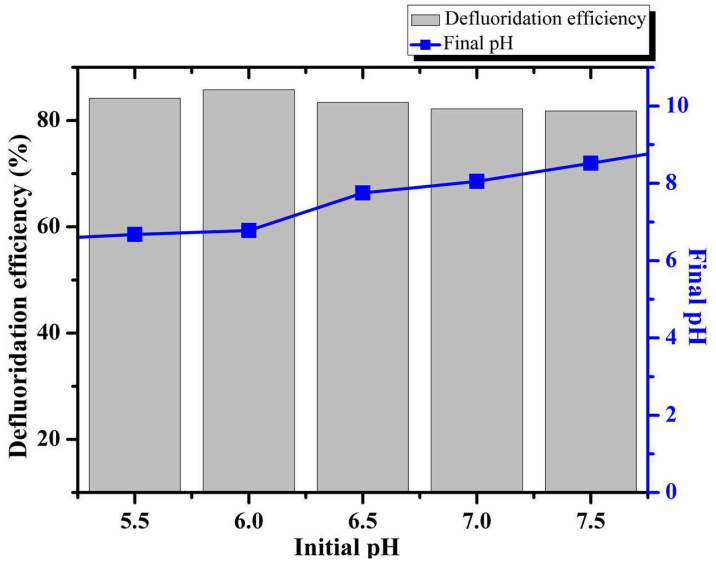

Figure 4.1: Defluoridation efficiency and effluent pH at varying initial pH (F_i=5 mg/L, i=0.30 A, t=30 min, d=10 mm).

4.3 Inter-electrode distance

Inter-electrode distance is the distance between the electrode plates in the reactor and change in this distance affects the efficiency of EC process. It has been reported by Emamjomeh & Sivakumar [105], that as the inter-electrode distance increases, resistance between electrodes also increases and efficiency of the process decreases. The same conclusion is also mentioned by Zhang *et al* [108]. Drouiche *et al* [102], have also mentioned in their study that lesser inter electrode distance gives better treatment efficiency and reported that optimum inter-electrode distance in their work was found to be 10 mm.

The experiments were conducted to investigate effect of inter electrode distance on

fluoride removal through EC with aluminium electrodes. The study was conducted for four electrode distances; 5 *mm*, 10 *mm*, 15 *mm*, and 20 *mm*; keeping the initial fluoride concentration, applied current and electrolysis time constant for all runs.

Each experiment was repeated twice and the average was calculated and reported in the Figure 4.2. It can be observed from the Figure 4.2 that defluoridation efficiency increases from 83% to 86%, when inter electrode distance is increased from 5 *mm* to 10 *mm*. But a decrement of efficiency from 71 to 62% was observed, when inter electrode distance is increased from 10 *mm* to 20 *mm*. When the inter-electrode plate distance is small, the bubbles generated at the cathode cause a powerful air flotation effect. As a result, the formed aluminium -fluoride flocs float upwards and are easily removed. However, if the electrode plate distance is too small, chances of short circuiting increase [108]. The results reported in the literature corroborates with the results obtained in the present study.

Based on the above discussions, the inter electrode distance was kept constant (10 *mm*) for all the experiments conducted for the development of statistical modelling in later part of the study.

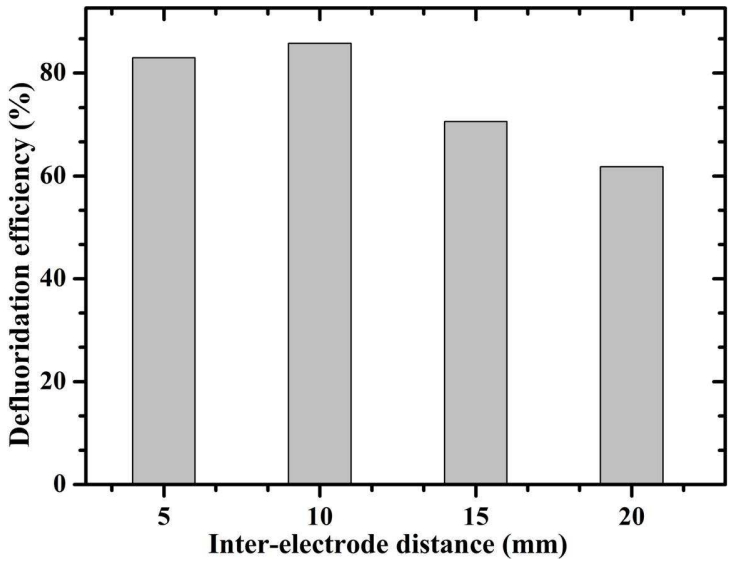

Figure 4.2: Defluoridation efficiency at varying inter-electrode distance (F_i=5 mg/L, i=0.30 A, t=30 min, pH=6).

4.4 Effect of initial fluoride concentration

Almost 90% of the fluoride contaminated regions in India have fluoride concentrations between $2-8\,mg/L$ (Refer Chapter 1). This range was found to be the most prevalent range and hence the present study was restricted to the range of $2-8\,mg/L$. To understand the effect of initial fluoride concentration on fluoride removal, the experiments were performed for two initial fluoride concentrations; minimum and

maximum of the mentioned range i.e. 2 and 8 mg/L at the applied current of $0.15 - 0.75\,A$.

It can be observed from the Figure 4.3 that when the initial fluoride concentration was increased from 2 mg/L to 8 mg/L at a constant electrolysis time of 20 min and constant applied current of $0.30\,A$, the values for residual fluoride concentration increases from 0.57 mg/L to 2.18 mg/L. This is possibly due to formation of insufficient aluminium hydroxide complexes. It was also observed that the higher initial fluoride concentration requires a higher value of applied current or longer electrolysis time for bringing down the residual fluoride below the permissible limit of 1 mg/L (IS:10500:2012 [25]). A similar conclusion was made by Zhu *et al.* [40]. It can also be seen from Figure 4.3 that high initial fluoride concentration of 8 mg/L cannot be reduced to the desirable residual fluoride concentration of 1 mg/L in 60 min at low value of $0.15\,A$ of applied current. So a higher current or higher electrolysis time is required to achieve the desired residual fluoride concentration.

It was also observed that when the initial fluoride concentration was increased from 2 mg/L to 8 mg/L, at applied current of $0.30\,A$ and 10 min of electrolysis time; the total fluoride removed was increased from 1.76 mg to 9.2 mg. It is because more fluoride is readily available to be removed by the produced aluminium hydroxide flocs. This means at same energy input, increase in initial fluoride concentration causes the defluoridation capacity to increase.

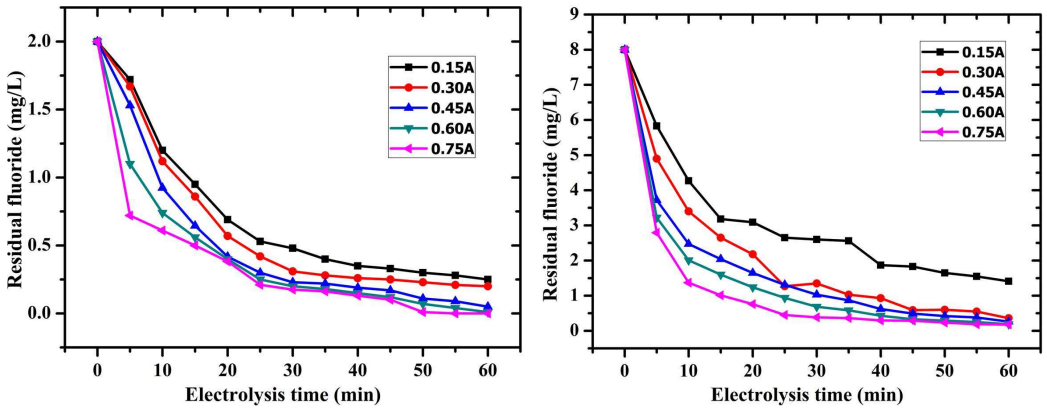

Figure 4.3: Effect of electrolysis time on residual fluoride at varying applied current (a) F_i=2 mg/L (b) F_i=8 mg/L (pH=6, d=10 mm).

4.5 Effect of electrolysis time

Electrolysis time also referred as treatment time is one of the important parameters governing the EC process. The time dependence of fluoride removal by EC process was studied at varying applied current ($0.15 - 0.75\,A$) and initial fluoride concentration of 2

and $8\,mg/L$. The results are shown in Figure 4.3 and detailed results are presented in appendix A. It can be observed from the Figure 4.3 that up to $60-70\%$ of the initial concentration decreases within $10\,min$ from the start of the process. At the beginning of the process the fluoride removal is rapid and later it decreases gradually over almost the entire process examined. Fluoride ions are more abundant in the beginning of the EC process. The generated aluminium hydroxide due to corrosion of the anode at that time will form complexes with fluoride and therefore rapid removal of fluoride was observed. However, as the experiment proceeds the aqueous phase fluoride concentration goes on reducing and aluminium hydroxide concentration keeps on increasing. This attributes to the reason that all the curves are nearly same at the end of treatment.

The results in Figure 4.3 indicate that the residual fluoride concentration is decreased from 2 to $0.57\,mg/L$ when the electrolysis time is increased to $20\,min$ at a constant applied current of $0.30\,A$. Drouiche *et al.* [99], have also illustrated that the increase in electrolysis time decreases the residual fluoride content. Zuo *et al.* [94] have explained that when the treatment time is less, fluoride removal efficiency is low. For initial fluoride concentration of $2\,mg/L$ at $0.30\,A$, the residual fluoride after $10\,min$ of electrolysis time is $1.12\,mg/L$. The reason is attributed to the relatively low mass transfer rate. The formation of $Al(OH)_{3-x}F_x$ flocs is a multi-step process; including formation of direct complex of Al^{3+} with F^- during the initial time phase, hydrolysis of the aluminium species, mass transfer of F^- from the bulk solution to the $Al(OH)_3$ flocs, and ion exchange. However, due to short time limited number of $Al(OH)_3$ flocs are formed and hence mass transfer of F^- from the bulk solution is relatively low.

4.6 Effect of applied current

Applied current and electrolysis time are important parameters of concern in EC process. They both together determine the coagulant produced and the bubble generation rate. The applied current and electrolysis time go hand in hand. If the applied current is less, more electrolysis time is required for removal of fluoride and vice versa. In the present study, applied current was varied from a considerable low value of $0.15\,A$ to upper value of $0.75\,A$. The time of electrolysis was kept constant at $60\,min$. The samples were collected at an interval of $5\,min$ and residual fluoride was measured. Residual fluoride decreases with increasing applied current because applied current determines the dissolution of aluminium. Lower the applied current, lower is the aluminium generated and hence fluoride reduction is low. The results suggest that higher value of applied current removes fluoride the quicker due to the abundance of aluminium ions for coagulation.

It may be noted that for the higher concentration of initial fluoride ($8\,mg/L$), the lowest current ($0.15\,A$), was not able to bring down the residual fluoride concentration

below 1 mg/L in 60 min of electrolysis time. Further increase in electrolysis time might reduce the fluoride content further, but it is not advisable to run the EC process for longer run times, as the pH in the process increases continuously. As already mentioned that aluminium speciation depends on the solution pH and with an increase in pH the efficiency of the process decreases. Moreover, the soluble species of aluminium will start forming which will eventually contribute to the residual aluminium of the process. From the Figure 4.3 it can be easily observed that for minimum value of initial fluoride concentration (2 mg/L) and minimum value of applied current (0.30A), 15 min of electrolysis time was sufficient to bring down the fluoride within acceptable limits (IS:10500:2012 less than 1 mg/L [25]). Similarly for maximum value of initial fluoride concentration (8 mg/L) at minimum value of applied current (0.30 A), 40 min was sufficient to lower the residual fluoride to the prescribed limit.

Therefore, the applied current range was selected as $0.30 - 0.75\,A$ and the electrolysis time was selected as $10 - 50\,min$ (allowing sufficient margin for desired fluoride removal) for development of statistical model.

4.6.1 Derived forms of applied current

Different investigators have used different forms of applied current like current density, charge loading and current concentration to explain their results.

Current density is the measure of flow of current across a given area and is calculated by the Equation 4.1

$$J = i/A \tag{4.1}$$

Where,

J is the current density in A/m^2,

i is the applied current in A and

A is the cross- sectional area of the electrodes in m^2.

Current density is inversely proportional to the surface area of the electrodes, more is the surface area lesser will be the current density. Effect of current density has been explained by Zhu *et al.* [40], and Emamjomeh and Sivakumar [34] in their investigations. Zhu *et al.* [40] have concluded that higher current density is required to achieve higher defluoridation efficiency.

Current concentration is the ratio between the current flowing through a compartment of EC cell and the volume of that compartment. It is calculated by using the formula given in Equation 4.2

$$C_c = i/V \tag{4.2}$$

Where

C_c is the current concentration in A/m^3,

i is the applied current in A and

V is the volume of the reactor in m^3.

Current concentration is inversely proportional to the volume of the reactor; more the volume of reactor lesser will be the current concentration. Its effect on fluoride removal has been investigated by Emamjomeh and Sivakumar [96]. They reported that current concentration (i/V) is an important parameter that determines aluminium dissolution in water. They have also reported that considering the Faraday's formula, it is clear that electrolysis time and current concentration are two parameters that determine the aluminium dissolution. Emamjomeh and Sivakumar [96] also reported that lower the current concentration, lower is the aluminium dissolution and hence fluoride reduction is low.

Current density and current concentration used in the experimental study have been explained presented in Table 4.1.

Table 4.1: Values of applied current and their corresponding current density and current concentration.

S.No	Applied current (A)	Current density (A/m^2)	Current concentration (A/m^3)
1	0.15	5.76	75
2	0.30	11.54	150
3	0.45	17.31	225
4	0.60	23.07	300
5	0.75	28.85	375

Referring Table 4.1, it can be easily understood that current density and current concentration increases with the increase in applied current, if surface area of the electrodes and volume of the reactor was kept constant respectively.

In the present study the surface area of the electrodes was $0.026\,m^2$ and the volume of the batch reactor was $0.002\,m^3$. Therefore, the A/V ratio was $13\,m^2/m^3$. A study was conducted to investigate the effect of A/V ratio on fluoride removal by varying surface area of the electrode. The EC run was stopped when the fluoride level was close to $1\,mg/L$. The time to reach $1\,mg/L$ (t_1) was recorded. This study was carried out by varying the A/V ratio (increasing the electrode area) and keeping the current density constant. All the results have been presented in the Table 4.2

Table 4.2: Effect of A/V ratio on the time (t_1) v/s current density.

Current density (A/m^2)	A/V (m^2/m^3)		
	13	17.5	20
11.54	40 *min*	35 *min*	32 *min*
17.31	30 *min*	20 *min*	17 *min*
23.07	25 *min*	10 *min*	05 *min*
28.85	15 *min*	05 *min*	05 *min*

From the results in the Table 4.2, it can be clearly observed that the increase of the electrode area, i.e. increase of the (A/V) parameter, induces a decrease of the necessary time t_1 for a given current density. So it can be concluded that for a particular A/V ratio, increase in current density up to a certain extent can decrease the time, crossing which the decrement of time will be insignificant. Similar conclusions have been made by Mameri *et al.* [33]. But here also the importance is of applied current. To achieve constant current density with change in surface area, applied current needs to be regulated. This means when A/V is increased, applied current needs to be increased in order to keep the current density constant. The decrease in t_1 is due to increase in aluminium dose caused by increase of applied current.

4.6.2 Charge loading

Charge loading has also been used by some researchers (Zuo *et al.* [94], Hu *et al.* [97]) to assess the removal of fluoride from water. Charge loading is defined as the charge transferred in electrochemical reaction for a given amount of water treated and is calculated by using Equation 4.3.

$$Q = \frac{ixt}{V} \tag{4.3}$$

Where,

Q is the charge loading in C/L,

i is the applied current in A,

t is the treatment time in *sec*, and

V is the volume of water treated in L.

Effect of different charge loading on fluoride removal was investigated for two initial fluoride concentration (2 and 8 mg/L) and two applied current values (0.30 and 0.75 A). The results are illustrated in the Figure 4.4. These results can be explained by Faraday's law which states that the amount of metal dissolved electrochemically is proportional to the charge loading [85]. When the charge loading is low, dosing of aluminium is not sufficient. As a result small amount of $Al(OH)_3$ flocs are formed which does not remove the fluoride effectively. It can be observed from Figure 4.4a that as we increase

the charge loading from 46.5 to 139.5 C/L, the residual fluoride decreases from 1.67 to 0.86 mg/L at applied current of 0.30 A and initial fluoride concentration of 2 mg/L. With increase in charge loading the dosage of aluminium increases, thereby increasing the floc formation. Hence more fluoride can be adsorbed onto the flocs and fluoride removal increases. Significant increase in fluoride removal can be observed in initial stages. Increase in charge loading beyond a critical point, does not reflect as increase in removal efficiency. It can be seen from Figure 4.4a that at initial fluoride concentration of 2 mg/L and applied current of 0.30 A, significant decrement of residual fluoride can be observed till 279 C/L after which not much lowering of fluoride can be observed. Similarly at initial fluoride concentration of 8 mg/L and applied current of 0.30 A, significant decrement was observed till 325.5 C/L, crossing which no considerable enhancement in fluoride removal can be seen. Similar trends were obtained by Zhu *et al.* [40] and Chen *et al.* [107]. The results indicates that a critical charge loading is required and once that value is reached, no significant enhancement in fluoride removal can be observed.

Though all the derived forms have their own significance in study of fluoride removal; it is clear from all the above discussions that it is actually applied current which is the basic unit for all. Current density is defined as a function of applied current and surface area of electrodes. Current concentration is defined as a function of applied current and volume of the reactor. Charge loading is defined as a function of applied current, electrolysis time and volume of reactor. In the present study the volume of the reactor and the surface area of electrodes were fixed. So the only variable parameter was applied current. Also all the derived forms of current affect the aluminium dissolution which in turn affect the fluoride removal. But considering the Faraday's law it is the applied current and electrolysis time which determines the coagulant dosage. Therefore applied current and electrolysis time were selected as two of the major operational parameters to develop a statistical model.

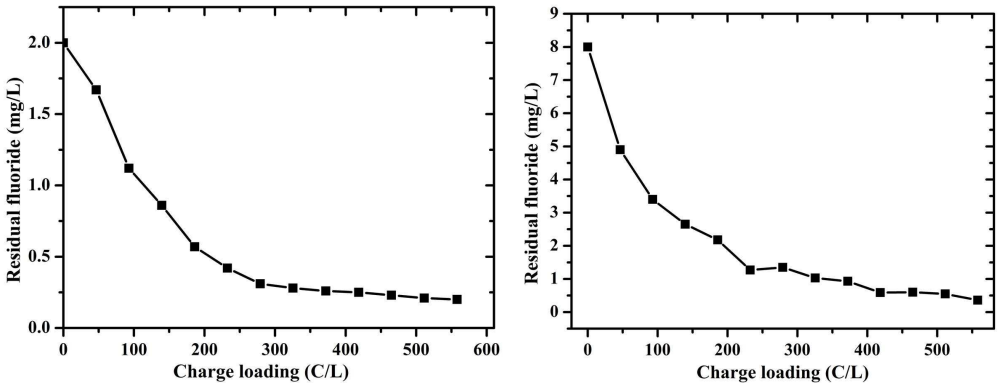

Figure 4.4: Effect of charge loading on residual fluoride (a) F_i=2 mg/L i=0.30 A (b) F_i=8 mg/L i=0.30 A.

4.7 Effect of fluoride uptake capacity (FUC)

FUC is defined as the capacity in *mg* of removed fluoride per gram of the used aluminium coagulant in a batch experiment. In the present study FUC was calculated for initial fluoride concentration of $2\,mg/L$ and $8\,mg/L$ and applied current of $0.30\,A$ and $0.75\,A$. The results are shown in Figure 4.5. It can be clearly observed that FUC decreases with increase in electrolysis time and then tends to stabilise. It is because of this fact, that treatment time should be carefully decided to minimize the wastage of energy and dissolution of aluminium in water. For initial fluoride concentration of $2\,mg/L$ and applied current of $0.30\,A$, the FUC decreases from $104.84\,mg/g$ to $36.73\,mg/g$ when the time is increased from $10\,min$ to $60\,min$. Similarly, for initial fluoride concentration of $8\,mg/L$ and applied current of $0.30\,A$, the FUC decreases from $548.02\,mg/g$ to $151.70\,mg/g$ when the time is increased from $10\,min$ to $60\,min$. FUC per unit aluminium consumed in EC process is very high as compared to Activated alumina process. Researchers (Karthikeyan *et al.* [109], Leela [110]) have reported the capacity of AA to be between $3\,mg/g$ in alkaline water and $20\,mg/g$ in acidic water. In present study the achieved values of FUC in EC process are as high as $369.32\,mg/g$. This may be suggested, that high FUC in EC process indicates towards efficient use of aluminium in EC process, which might result in low residual aluminium in treated water. AA process results in high residual aluminium in output water ranging from $0.1\,mg/L$ to $0.3\,mg/L$ [23].

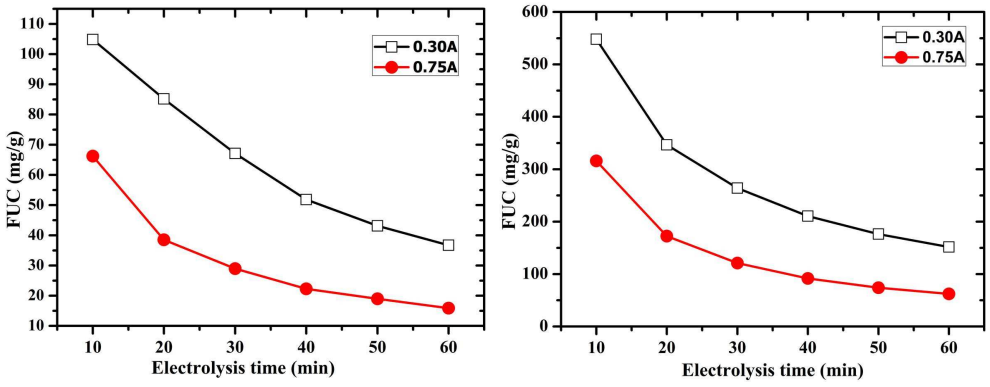

Figure 4.5: FUC at varying electrolysis time and applied current (a) F_i=2 mg/L (b) F_i=8 mg/L.

4.8 Specific electrical energy consumption (SEEC)

SEEC controls energy input and aluminium dissolution in EC process and hence it is an important parameter of concern. SEEC is defined as energy per unit mass of fluoride removed and calculated by Equation 4.5.

$$SEEC = \frac{Energy\,consumed}{Fluoride\,removed} \tag{4.4}$$

$$SEEC(\frac{J}{mg}) = \frac{V \times i \times t}{F_t - F_r} \tag{4.5}$$

Where,

V is the voltage in V

i is the applied current in A

t is the electrolysis time in min

F_t is the total fluoride present in the solution in mg/L

F_r is the fluoride removed from the solution after EC treatment in mg/L

In the present study SEEC was calculated for initial fluoride concentration of 2 and $8\,mg/L$ and applied current of 0.30 and $0.75\,A$. The results are shown in Figure 4.6. It can be observed that SEEC increases with increase in time for a constant current and a constant initial fluoride concentration. It can be seen in Figure 4.6a, that SEEC increases from $605.90\,J/mg$ to $1333\,J/mg$ when the time is increased from $5\,min$ to $60\,min$; at a constant initial fluoride concentration of $2\,mg/L$ and applied current of $0.30\,A$. It can also be observed from Figure 4.6a and 4.6b that for a constant initial fluoride concentration and constant electrolysis time, the SEEC increases with increase in applied current value. At initial fluoride concentration of $2\,mg/L$ and $30\,min$ of electrolysis time, SEEC increases from 709.88 to $3182.56\,J/mg$ when applied current was increased from $0.30\,A$ to $0.75\,A$. SEEC decreases with increase in initial fluoride concentration, keeping the current value same. When initial fluoride concentration was increased from 2 to $8\,mg/L$, SEEC decreases from $559.30\,J/mg$ to $137.42\,J/mg$ at applied current of $0.30\,A$ and electrolysis time of $20\,min$. This is because the per unit fluoride removal is more when initial fluoride loading is increased as more fluoride is available for removal per joule of energy spent. Similar results have been reported by Sinha *et al.* [111]. With the increase in the SEEC the fluoride removal also increases but after a certain value of energy consumed the fluoride removal is insignificant and most of the energy consumed is wasted. The above inferences can be clearly seen in Figure 4.7. For maintaining the economics of the process, energy input (i and t) should be minimized for bringing fluoride within permissible limit.

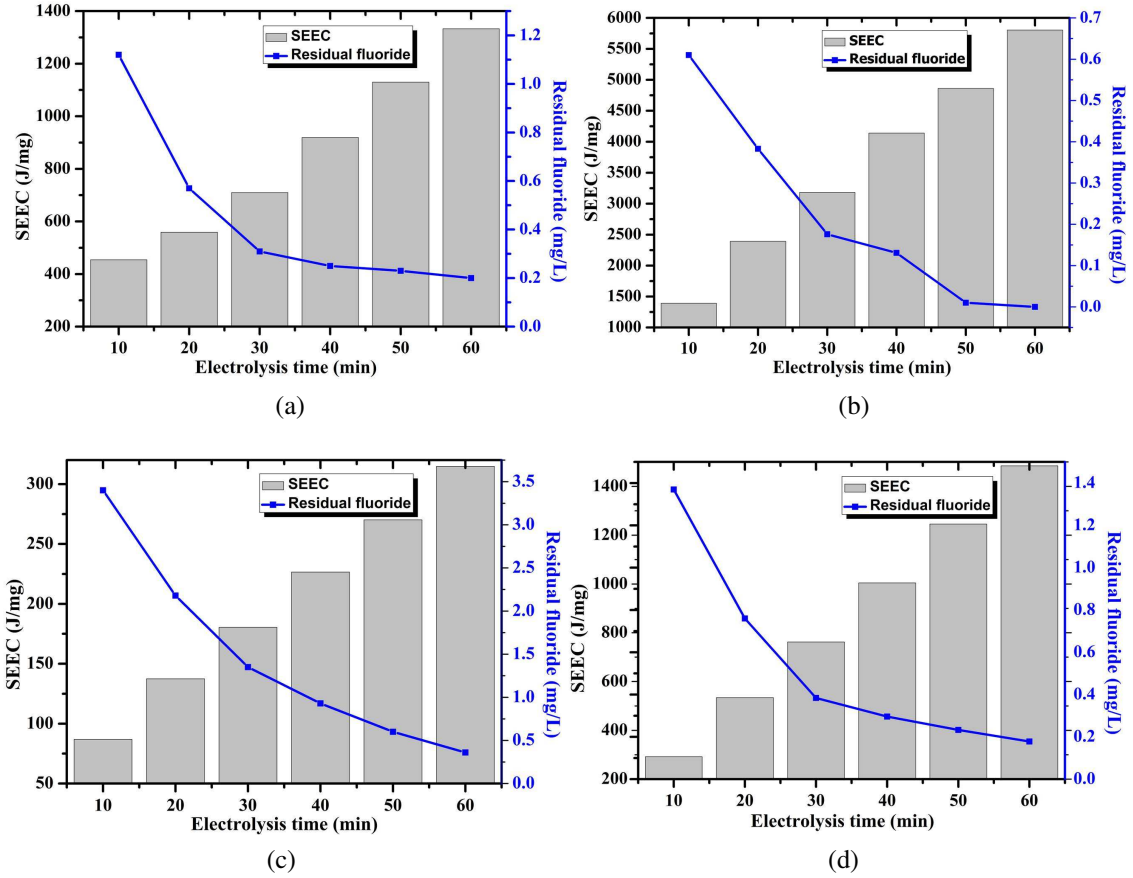

Figure 4.6: Effect of electrolysis time and applied current on SEEC for different initial fluoride concentration (a) F_i=2 mg/L, i=0.30 A (b) F_i=2 mg/L, i=0.75 A (c) F_i=8 mg/L, i=0.30 A (d) F_i=8 mg/L, i=0.75 A.

4.9 Anode consumption

Applied current and electrolysis time are the two major operating parameters in EC process which determines the dissolution of aluminium in the reactor. Aluminium dissolution can be calculated using Faraday's Law. Faraday's Law of Electrolysis states that for a given quantity of D.C electricity (electric charge), the mass of an elemental material altered at an electrode is directly proportional to the element's equivalent weight. In context of the present study Faraday's Law determines the aluminium dissolution from the electrode [85]. The coagulant generation is described by Equation 4.6:

$$Al_{th} = \frac{i \times t \times M}{Z \times F} \tag{4.6}$$

Where,

Al_{th} is theoretical concentration of Al^{3+} liberated from anode (g),

i is applied current in A,

M is molecular mass of aluminium (27 g/mol),

t is electrolysis time (sec)

Z is valencey number (Z=3 for aluminium)

F is Faraday's constant (96485 C/mol)

The anode dissolution generates the aluminium coagulant for the treatment. In Figure 4.7, relation between theoretical aluminium dissolution, residual fluoride and electrolysis time has been shown. It can be observed that as the dose increases the removal efficiency increases up to a certain extent, after which the change in efficiency is marginal. Therefore, only required extent of treatment must be given so as to restrict the unnecessary coagulant to enter the reactor.

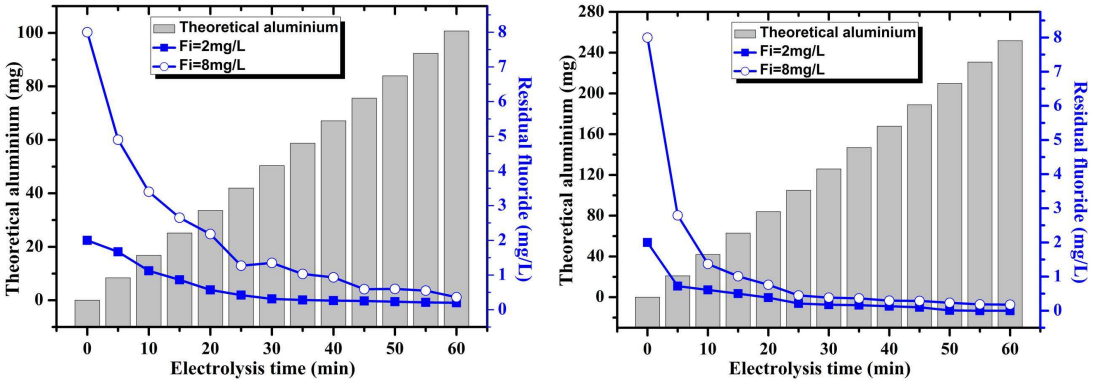

Figure 4.7: Effect of electrolysis time and applied current on theoretical aluminium and residual fluoride (a) i=0.30 A (b) i=0.75 A.

In next part, the anode consumption was observed for applied current $0.15 - 0.75\,A$ and time duration of 60 min. The actual and theoretical value of anode consumption is presented in the Table 4.3. The current efficiency was more than 100% in all the observed readings. Mameri *et al.* [81] and Hu *et al.* [93] also observed the current efficiency to be greater than 100%. This result could be attributed to the phenomenon of pitting corrosion. This is a localized kind of corrosion caused by presence of high concentrations of chloride and is erroneously considered as aluminium dissolved by electrochemical process. There are four steps suggested by Foley [112] in the localized corrosion of aluminium: (1) adsorption of reactive anions on the oxide film; (2) chemical reactions of adsorbed anions with Al(III) in the oxide film; (3) thinning of the film by dissolution of the metal; and (4) direct attack of the exposed metal by water or anions. The SEM images of unused electrode, anode and cathode are shown in Figure 4.8. The images also show sign of pitting corrosion. The unused electrode is smooth and has no signs of corrosion; anode shows the signs of pitting corrosion while the cathode shown is smoother.

Table 4.3: Anode consumption for different applied current (t=60 min).

Applied current (A)	***Theoretical anode consumption*** *(mg)*	***Experimental anode consumption*** *(mg)*	***Current Efficency (%)***
0.15	50.36	51.11	101.5
0.30	104.16	110.56	105.76
0.45	151.08	157.43	104.2
0.60	201.45	211.32	104.9
0.75	252.00	265.36	105.15

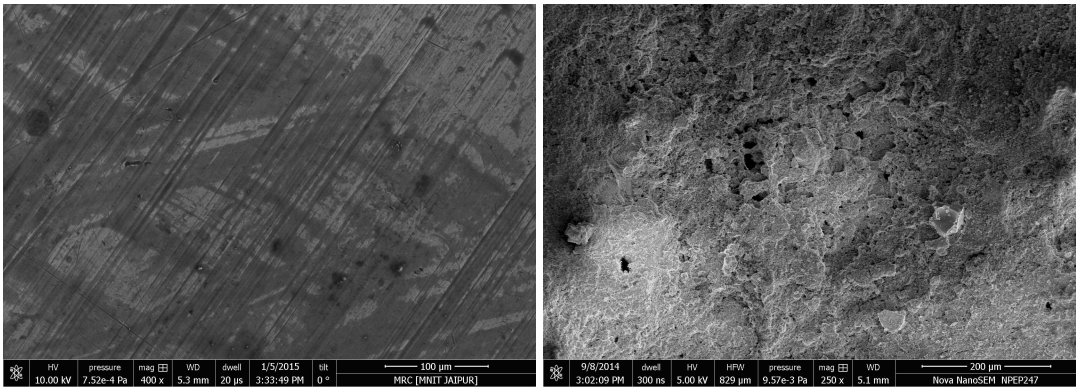

(a) (b)

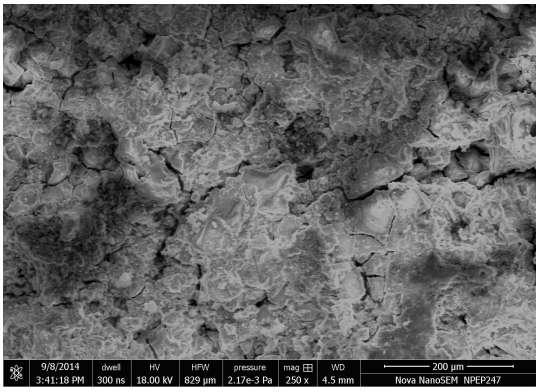

(c)

Figure 4.8: SEM images of electrodes (a) unused electrode (b) cathode (c) anode.

To understand the variation in SEEC and theoretical aluminium, with change in applied current and electrolysis time, the results have been presented in Table 4.4.

Table 4.4: Relation between residual fluoride, SEEC and theoretical aluminium with change in applied current, electrolysis time and initial fluoride concentration.

$F_i(mg/L)$	$i(A)$	$t(min)$	$F_r(mg/L)$	SEEC (J/mg)	$Al_{th}(mg)$
2	0.30	45	0.22	1028.31	75.54
2	0.75	25	0.21	2704.02	104.92
8	0.30	35	1.03	200.81	58.75
8	0.75	15	1.01	415.23	62.95

For achieving residual fluoride concentration of $0.22\,mg/L$ for initial fluoride concentration of $2\,mg/L$; two combinations for running EC are available. First is to go for a low applied current high electrolysis time, another is to go for high applied current low electrolysis time. It can be clearly observed from Table 4.4 that when low current high time ($0.30\,A$ and $45\,min$) was applied, then the values of SEEC and theoretical aluminium were $1298.4\,J/mg$ and $75.54\,mg$ respectively. But when high applied current and low electrolysis time ($0.75\,A$ and $25\,min$) was applied, then the values of SEEC and theoretical aluminium were increased to $2704.2\,J/mg$ and $104.92\,mg$ respectively. Hence, this observation suggests that high electrolysis time and low applied current is advisable for restricting the unnecessary aluminium dissolution and minimizing energy wastage.

Based on discussion in above sections, it is clear that excess electrolysis time or applied current; both have their own limitations. Increase in treatment time leads to increase in pH and hence decreases the efficiency of fluoride removal. Increase in applied current leads to increased energy consumption and increased aluminium dissolution, which affect the economics of the process and might also end up in more residual aluminium at the end of the treatment process. Therefore, while running the EC process, selection of these two parameters requires attention and a trade off has to be made between them.

These parametric investigations and there corroboration with literature gave us an insight that initial fluoride concentration, applied current and electrolysis time are the three major parameters which governs the EC process. These three parameters were used to develop statistical model in the later part of study. This study also helped to resolve the ranges for the chosen parameters. The range of initial fluoride concentration was kept between $2-8\,mg/L$; as this is the most prevalent range of fluoride contamination found in India. The applied current range studied is between $0.15-0.75\,A$. But from the results it can be observed that for the maximum range of $8\,mg/L$ and applied current of $0.15\,A$, even $60\,min$ were not sufficient to bring down the residual fluoride within permissible range. More treatment time can bring it down, but it can also be observed that with increase in electrolysis time the FUC decreases. This suggests that the fluoride removal capacity decreases, and in turn the energy consumed is also wasted. Moreover, with increase in treatment time the pH also increases and

increase in pH will lead to more dissolution of aluminium in water. Keeping the above findings in mind the applied current range selected was $0.30 - 0.75\,A$. It was earlier concluded that for minimum value of initial fluoride concentration ($2\,mg/L$) and minimum value of applied current ($0.30\,A$), $15\,min$ of electrolysis time was sufficient to bring down the fluoride within acceptable limits (IS:10500:2012 less than $1\,mg/L$). Similarly, for maximum value of initial fluoride concentration ($8\,mg/L$) at minimum value of applied current ($0.30\,A$), $40\,min$ was sufficient to lower the residual fluoride to prescribed limit. Therefore, the electrolysis time range set for the study was $10 - 50\,min$ (allowing sufficient margin for desired fluoride removal) for development of statistical model.

Chapter Summary

This Chapter presents a study of various parameters which are affecting the EC process. Investigations and inferences made on the parameters are reported in the Chapter. This study was conducted to select the parameters of concern to be used in designing of experiments. Preliminary investigations were carried out for studying the effect of initial pH and inter-electrode distance. The results showed that initial pH 6 and inter-electrode distance 10 *mm* gave the best results for defluoridation efficiency. So these parameters were fixed to the above values for all further investigations.

Three main operational parameters of concern (initial fluoride concentration, applied current and electrolysis time) were used on the basis of literature review and experimental investigations to design the experiments. The investigations made in this Chapter helped to select the range of these three parameters. SEEC was considered as a response parameter, along with residual fluoride and residual aluminium. Other parameters like charge loading, anode consumption and FUC were reported for general information about the details of EC process.

The next chapter marks the beginning of development of model for fluoride removal using the operational parameters and their ranges selected in this chapter.

CHAPTER 5

Chapter 5

Development of model for fluoride removal

This Chapter implements the design of experiments for the development of statistical model for fluoride removal. Taguchi design has been used to develop the statistical model. The choice and range of operational parameters were on the basis of literature review and investigations made in Chapter 4. The model for fluoride removal was developed to understand the interaction between operating parameters and responses. The model analyses the data to describe dependence of responses on the operating parameters. It allows us to predict the change in behaviour of responses against change in operating parameters. The equations developed through statistical model development were used to optimize the operational parameters for better economy of treatment and efficiency of the process.

The parametric study was conducted to select the operating parameters and their working ranges for design of experiments. The choice and range of operational parameters have been made on the basis of literature review and investigations made in Chapter 4. Out of five control factors, namely, pH of water, inter electrode distance, applied current, electrolysis time, and initial fluoride concentration, first two were kept constant for the present study and the remaining three were used as operational parameters for the experimental investigations. These three operational parameters were investigated for three responses, namely, residual fluoride, residual aluminium and SEEC.

This Chapter implements the design of experiments which helps in development of a statistical model for fluoride removal. A statistical model is a probability distribution, constructed to draw inferences from the available data [113]. The model for fluoride removal was developed to understand the process in a better way. The model analyses the data and describes that how response values are dependent on the operating parameters. It gives us information about the behaviour of the system and allows us to predict the change in behaviour by changing the operating parameters. It has also been

used to optimize the operational parameters and improve the economics and efficiency of the process.

DOE was used to develop statistical model. DOE is an experimental method which is used to statistically signify the relationship between input parameters to output responses. It constitutes a systematic way of planning of experiments, collection and analysis of data [114]. OFAT (one factor at the time) and factorial designs can possibly be used for DOE. OFAT aimed at running an experiment at one particular condition and repeating the experiment by changing any other factor till the effect of all factors are recorded and analyzed [115]. Thus it involves carrying many experiments, which is time consuming and laborious [116]. Also in this process, interactions between factors are not taken in account [115]. In factorial design a large number of experiments are to be carried out if input parameters increases.

Taguchi suggested a specially designed method called the use of orthogonal array to study the entire parameter space with limited number of experiments to be conducted [117]. It employs signal to noise (S/N) ratio instead of responses itself to determine the optimum settings of the operating parameters, neglecting the variations caused by the uncontrollable factors [118]. Additionally, Taguchi's method for experimental design is straightforward and easy to apply to many processes, making it a powerful yet simple tool [114]. In the present study, Taguchi design was used to develop a statistical model for fluoride removal.

5.1 Implementation of Taguchi Design

Taguchi's orthogonal method has been used by several investigators for the optimal design of experiments and to study the effects of multiple parameters [119]. The steps included in the Taguchi parameter design are: selecting the proper Orthogonal Array (OA) according to the number of controllable factors (operating parameters); running experiments based on the OA; analyzing data; identifying the optimum condition; and conducting confirmation runs with optimal levels of all the parameters [114]. In the present study, Taguchi design was employed for the development of statistical model using MINITAB 14.0 software.

For implementation of Taguchi design the first step is to decide the operating parameters and their ranges. The operating parameters and their ranges, which were used for the implementation of Taguchi design have been presented in Table 5.1. Operating parameters; applied current, electrolysis time and initial fluoride concentration, were used for the study of defluoridation by EC. Three responses were considered, namely, residual fluoride, residual aluminium and SEEC. In the next step, level of Taguchi design is decided. Since there are three parameters which have to be used in the design and parametric investigations have shown that operating parameters

are not linearly related. The selected OA in this study was $L27$ (3^{13}) orthogonal design. Twenty-seven experiments were carried out for three levels (minimum, maximum and mid value) of three operating parameters.

Table 5.1: Levels used for operational parameters

Parameters	***Notation***	***Units***	***Level 1***	***Level 2***	***Level 3***
Initial fluoride concentration	F_i	mg/L	2	5	8
Applied current	i	A	0.31	0.53	0.75
Electrolysis time	t	min	10	30	50

The parameters and their respective ranges were used to design the Taguchi matrix. Table 5.2 presents the operational settings of twenty seven experiments which were performed to gather the required data. The second, third and fourth columns (Table 5.2) show the operational parameter settings given by Taguchi DOE matrix. The experiments were performed in duplicates and average value of each response has been presented in Table 5.2. The residual aluminium presented in Table 5.2 includes both dissolved and bind forms of aluminium. It can be observed from the residual aluminium response column that after the treatment, aluminium is introduced in the water. The aluminium concentration in all the sets was more than the IS:10500:2012 permissible limit ($0.2\,mg/L$) [25]. The response values are transformed into S/N ratios. The term "signal" represents the desirable value and the "noise" represents the undesirable value. The formulae for S/N are designed such that, always the larger factor level settings can be selected to optimize the performance characteristics of an experiment. Therefore, the method of calculating the S/N ratio depends on whether the performance characteristic has smaller-the-best, larger the- better or nominal-the-better formulation [120]. In this study performance characteristic has “smaller the better” formulation. It is so because the process efficiency will increase if all the three responses are minimized. The formula to calculate S/N ratio is given in Equation 5.1 [120].

$$\frac{S}{N} = -10log\frac{1}{n}\left(\sum_{i=1}^{n} y_i^2\right) \tag{5.1}$$

Where,

n is the number of tests and

y_i is the value of experimental result of the ith test.

In MINITAB, higher values of S/N ratio identify operational parameter settings with significant response.

Table 5.2: Orthogonal array for L27 3^3 Taguchi Design and their respective response.

Set No.	***Operating parameters***			***Response***		
	F_i (mg/L)	i (A)	t (min)	F_r (mg/L)	Al_r (mg/L)	$SEEC$ (J/mg)
1	2	0.31	10	1.12	9.40	454.43
2	2	0.31	30	0.31	19.48	709.88
3	2	0.31	50	0.23	28.12	1129.66
4	2	0.53	10	0.71	10.60	776.51
5	2	0.53	30	0.36	26.12	1832.37
6	2	0.53	50	0.09	47.04	2622.25
7	2	0.75	10	0.61	14.90	1392.08
8	2	0.75	30	0.18	33.48	3182.56
9	2	0.75	50	0.01	48.50	4861.81
10	5	0.31	10	1.56	6.20	116.25
11	5	0.31	30	0.71	12.10	279.39
12	5	0.31	50	0.29	18.05	424.52
13	5	0.53	10	1.42	7.81	279.80
14	5	0.53	30	0.25	17.50	632.65
15	5	0.53	50	0.19	27.60	1041.27
16	5	0.75	10	1.27	9.25	518.76
17	5	0.75	30	0.14	25.80	1194.44
18	5	0.75	50	0.11	39.45	1978.52
19	8	0.31	10	3.40	6.07	86.93
20	8	0.31	30	1.35	10.53	180.41
21	8	0.31	50	0.60	17.50	270.20
22	8	0.53	10	2.30	6.53	175.74
23	8	0.53	30	0.56	15.79	403.91
24	8	0.53	50	0.30	25.75	650.45
25	8	0.75	10	1.37	10.00	291.85
26	8	0.75	30	0.38	23.68	762.21
27	8	0.75	50	0.23	40.42	1245.65

5.1.1 Validation of the model

5.1.1.1 Analysis of variance (ANOVA)

The adequacy of the model was assessed through ANOVA. ANOVA is a statistical technique that subdivides the total variation in a set of data into component parts associated with specific sources of variation for the purpose of testing hypotheses on the parameter of the model [121]. In order to find out statistical significance of various factors like initial fluoride (F_i), applied current (i), and electrolysis time (t) on residual fluoride, residual aluminium and SEEC; ANOVA is performed on experimental data. Tables 5.3, 5.4 and 5.5 shows the results of the ANOVA on mentioned responses: residual fluoride, residual aluminium and SEEC respectively.

The frequency test (F-test) is utilized in statistics to analyze the significant effects of the parameters, which form the performance characteristics. F value has been calculated by the software and displayed. For respective F-value, corresponding p-value has been given. This analysis was carried out for a level of significance of 5%, i.e., for 95% level of confidence. The last column of the ANOVA table presents the p-value. The p-value informs us, for every tested factor, whether its effect is significant or whether stated tendencies in the data are merely due to chance. Generally a value of $p<0.05$ denotes a significant contribution of that parameter while the higher value suggest that the respective parameter has no influence. Often p values less than 0.1 are also considered to be still of relevance, as values between 0.05 and 0.1 are said to have marginal significance [122].

The p-values in the Table 5.3-5.5 indicate that all main effects are highly significant since they have very small p-values when compared with interaction factors. In case of residual fluoride as a response (Table 5.3); all the three parameters initial fluoride, applied current and electrolysis time have p-values of 0.003, 0.005 and 0.000 respectively. This is less than 0.05 and hence accounts for the significance of these factors, electrolysis time being the most significant of them. Interaction effects have p value>0.1 so they are not significant. In case of residual aluminium as a response (Table 5.4), initial fluoride, current, time and interaction effect (i xt) are significant parameters while (F_i x t) are marginally significant. This gives an indication that the combined effect of the factors "i" and "t" plays an important role in the dissolution of aluminium anode. Therefore, to minimize the introduction of aluminium in the solution the settings for "i" and "t" have to be carefully made. In case of SEEC as a response (Table 5.5), only main parameters are significant rest all are insignificant.

Another statistical parameter R^2 also referred to as the goodness of fit is also used for validating the model. R^2 is the fraction of the overall variance. It determines how closely a certain function fits a particular set of experimental data. R^2 values range from 0 to 1, with 1 representing a perfect fit between the data and the line drawn through them, and 0 representing no statistical correlation between the data and the line. High R^2 values obtained from ANOVA of the three responses validates the model. R^2 value for residual fluoride, residual aluminium and SEEC is 0.9468, 0.9959 and 0.9985 respectively .

Table 5.3: ANOVA table for residual fluoride

Source	*DF*	*Seq SS*	*Adj SS*	*Adj MS*	*F*	*p*
F_i	2	512.29	512.29	256.15	13.30	0.003
i	2	438.51	438.51	219.26	11.39	0.005
t	2	1604.71	1604.71	802.35	41.67	0.000
$F_i \times i$	4	31.27	31.27	7.82	0.41	0.800
$i \times t$	4	73.55	73.55	18.39	0.95	0.481
$F_i \times t$	4	80.68	80.68	20.17	1.05	0.440
Error	8	154.03	154.03	19.25		
Total	26	2895.04				
S = 4.38 R^2 = 0.9468						

Table 5.4: ANOVA table for residual aluminium

Source	*DF*	*Seq SS*	*Adj SS*	*Adj MS*	*F*	*p*
F_i	2	81.075	81.075	40.538	100.14	0.000
i	2	133.004	133.004	66.502	164.28	0.000
t	2	555.758	555.758	277.879	686.45	0.000
$F_i \times i$	4	3.512	3.512	0.878	2.17	0.163
$i \times t$	4	7.169	7.169	1.792	4.43	0.035
$F_i \times t$	4	0.504	0.504	0.126	0.31	0.863
Error	8	3.238	3.238	0.405		
Total	26	784.261				
S = 0.636 R^2 = 0.9959						

Table 5.5: ANOVA table for SEEC

Source	*DF*	*Seq SS*	*Adj SS*	*Adj MS*	*F*	*p*
F_i	2	766.57	766.57	383.29	1013.63	0.000
i	2	685.96	685.96	342.98	907.04	0.000
t	2	541.44	541.44	270.72	715.94	0.000
$F_i \times i$	4	1.17	1.17	0.29	0.78	0.570
$i \times t$	4	3.77	3.77	0.94	2.49	0.126
$F_i \times t$	4	2.66	2.66	0.66	1.76	0.231
Error	8	3.03	3.03	0.38		
Total	26	2004.59				
S = 0.614 R^2 = 0.9985						

5.1.1.2 Residuals

The adequacy of the model was also evaluated by the residuals. Residuals are actually the difference between the actual and the predicted response value. Normal probability plots are a suitable graphical method for judging the normality of the residuals [123]. The data are plotted against a theoretical normal distribution in such a way that the

points should form an approximate straight line. Departures from this straight line indicate departures from normality.

Residuals versus fits plot is the most frequently created plot, when conducting a residual analysis. It is a scatter plot of residuals on the y axis and fitted values (estimated responses) on the x axis. The model is adequate if constant variance is observed in the vertical direction and the scatter is symmetric vertically about zero [124]. The normal probability plots and plots of residuals versus fitted values for residual fluoride, residual aluminium and SEEC are illustrated in Figure 5.1-5.2. All the plots fulfil the mentioned criterions and suggest towards the adequacy of the model.

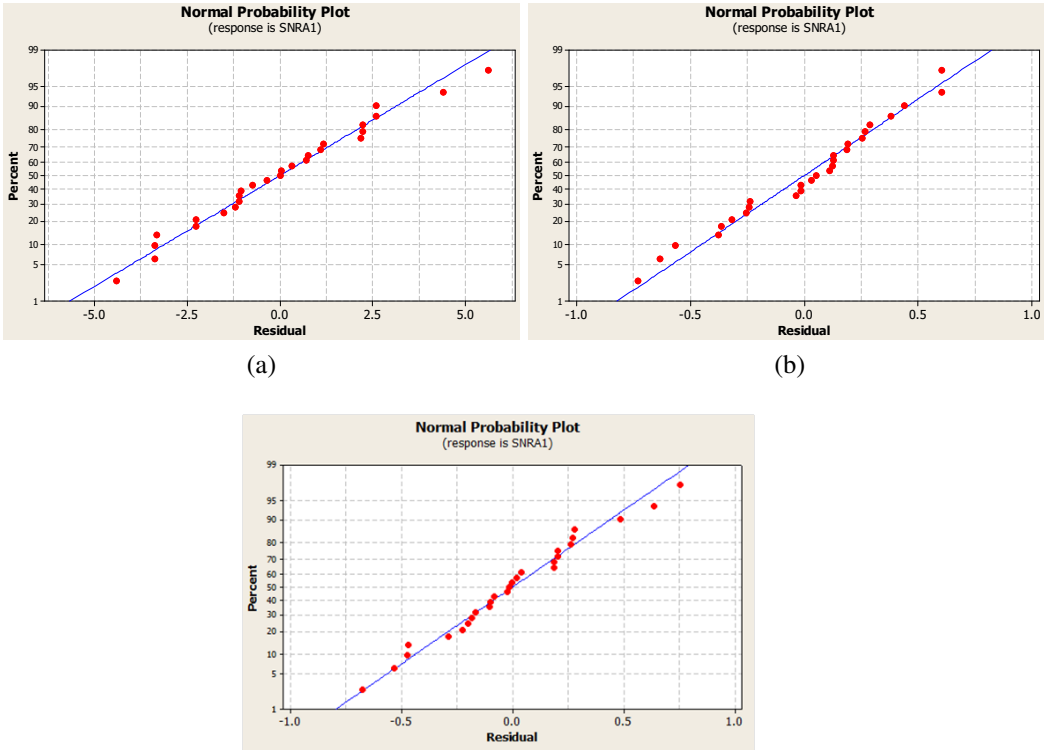

Figure 5.1: Normal probability plot (a) residual fluoride (b) residual aluminium (c) SEEC

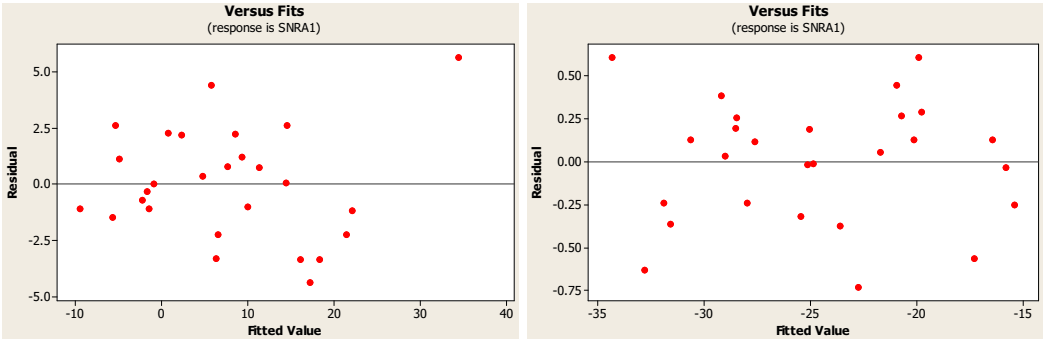

(a)

(b)

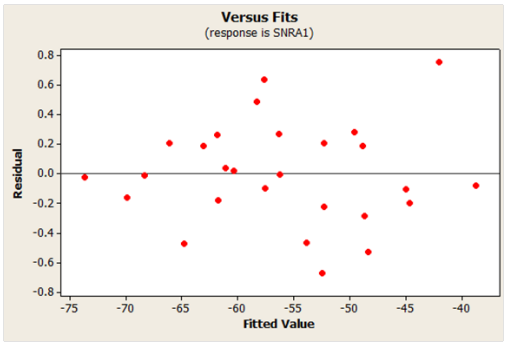

(c)

Figure 5.2: Residual plots (a) residual fluoride (b) residual aluminium (c) SEEC.

5.1.2 Main effect and interaction effects

The main effect and interaction plots help us to understand the change in response with change in operational parameter. There is a main effect when different levels of a factor affect the response differently. A main effect plot, graphs the response mean for each factor level connected by a line. When the line is horizontal (parallel to the x-axis), then there is no main effect. Each level of the factor affects the response in the same way, and the response mean is the same across all factor levels. When the line is not horizontal, then there is a main effect. Different levels of the factor affect the response differently. The steeper is the slope of the line, the greater the magnitude of the main effect. The main effect graphs are shown in Figure 5.3.

Interaction plots are studied when the effect of one factor depends on the level of the other factor. Parallel lines in an interaction plot indicates no interaction. The greater is the difference in slope between the lines, the higher is the degree of interaction. However, the interaction plot does not inform about the statistically significant interactions. But it is known from the section 5.1.1 that, except for "*ixt*" interaction for residual aluminium all others are marginally significant. Interaction plots are shown in Figure 5.4.

Figure 5.3a shows the main effect plot for residual fluoride as a response. It can be clearly observed that with increase in initial fluoride the residual fluoride increases (S/N

decreases). It is also observed that with increase in applied current and electrolysis time, the residual fluoride decreases.

Figure 5.3b shows the effect of operational parameters on residual aluminium. With increase in initial fluoride, residual aluminium decreases. It can be observed that as the initial fluoride increases from 2 to 8 mg/L, more fluoride is available to bind with aluminium and hence lesser aluminium is present in the solution. But with increase in time and current the residual aluminium increases. With more applied current and electrolysis time, more aluminium is released as a coagulant and hence the residual aluminium increases.

Figure 5.3c shows the effect of operational parameters on SEEC. With increase in initial fluoride, SEEC decreases; as there is availability of more fluoride so per unit removal is increased. With more current and time, SEEC increases as it is directly proportional to applied current and time.

The interesting fact is that the main effect plots for SEEC and residual aluminium are almost similar (Compare Figure 5.3b and 5.3c). This gives an indication that residual aluminium is related with SEEC. This also suggests that with increase in energy consumption, residual aluminium increases; keeping the initial fluoride concentration constant. Therefore minimization of energy will lead to lesser introduction of aluminium in the solution. Energy consumption is calculated by product of applied current, electrolysis time and voltage. Voltage remains constant for a specific applied current. So, it is the product of current and time which needs to be minimized for restricting the aluminium in the water.

The inferences obtained from these plots are similar to the parametric investigations discussed in Chapter 4. This also explains that the developed model is adequate to understand the effect of operational parameters on the responses.

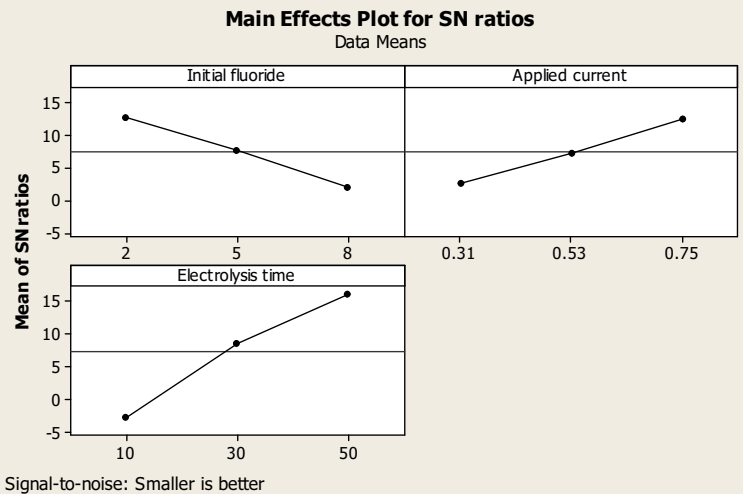

(a)

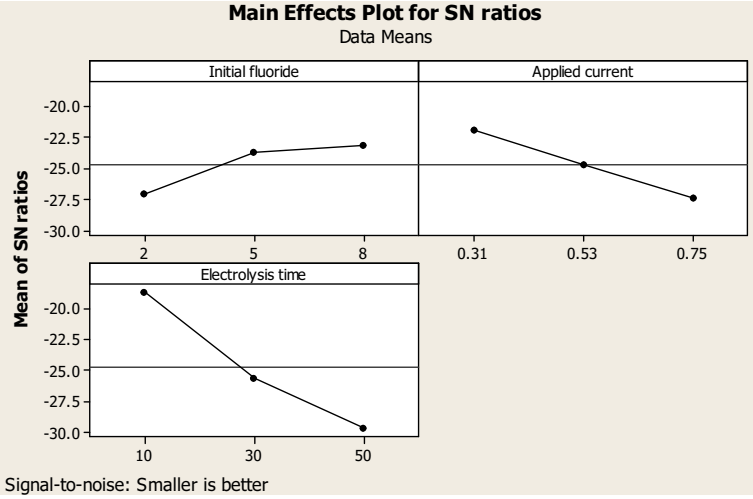

(b)

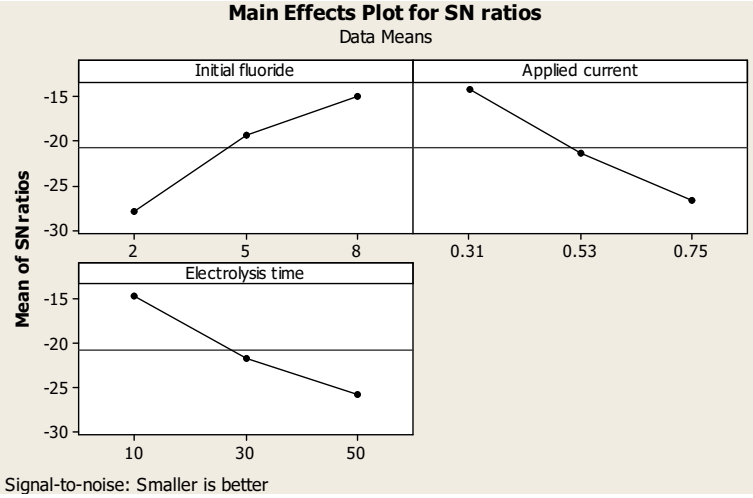

(c)

Figure 5.3: Main effect plot (a) residual fluoride (b) residual aluminium (c) SEEC.

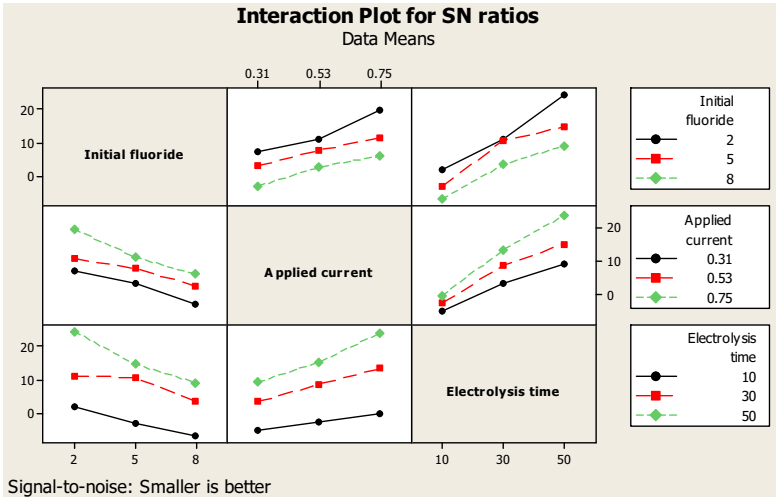

(a)

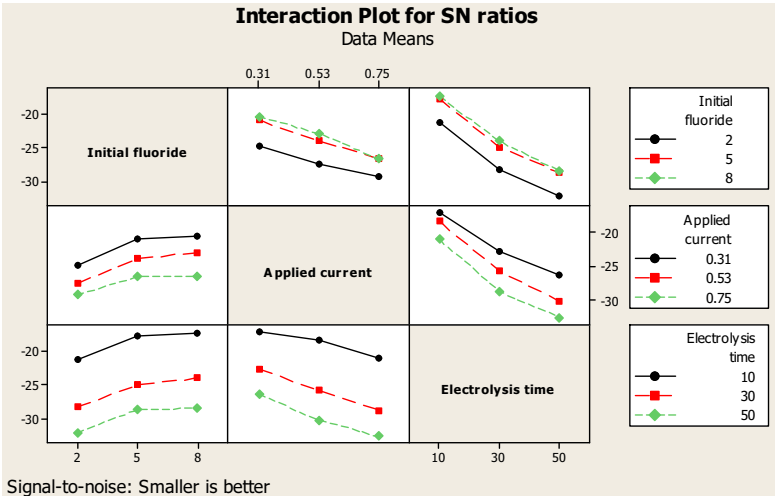

(b)

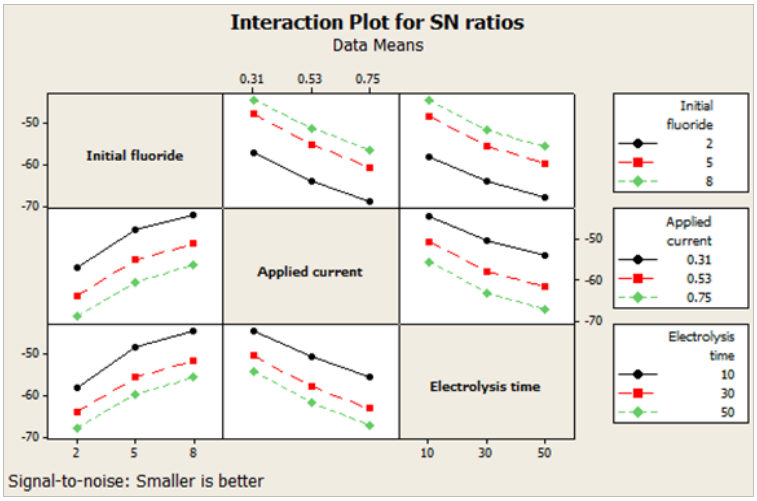

(c)

Figure 5.4: Interaction effect plot (a) residual fluoride (b) residual aluminium (c) SEEC.

5.2 Development of regression equations

The relationship between residual fluoride, residual aluminium and SEEC with combination of control factors is obtained using non-linear regression analysis with the help of SYSTAT 7.0. In order to express response in terms of mathematical expression the following form gave the best results. The relationship between residual fluoride, residual aluminium and SEEC with combination of control factors is obtained using non-linear regression analysis with the help of SYSTAT 7.0. In order to express response in terms of mathematical expression the following form gave the best results

$$E_r = K_0 + K_1{\times}A + K_2{\times}B + K_3{\times}C + K_4{\times}A{\times}B + K_5{\times}B{\times}C + K_6{\times}A{\times}C + K_7{\times}A^2 + K_8{\times}B^2 + K_9{\times}C^2 \quad (5.2)$$

Here, E_r is the response (output) term and K_i (i =0,1, ...,7) are the model constants. The settings for operational parameters and there corresponding response values (Table 5.2) were normalised by dividing each parameter with the largest value used for the parameter in the experimental study. These normalized values were used by the software. The constants are calculated using non-linear regression analysis with the help of SYSTAT 7.0 software and the relation obtained for each response is given in Equation 5.3-5.5.

$$Residual\ Fluoride(F_r) = 0.608 + (0.741{\times}F_i) - (0.557{\times}i) - (1.3{\times}t) - (0.559{\times}F_i{\times}i) + (0.424{\times}i{\times}t) - (0.622 \times F_i \times t) + (0.261 \times Fi^2) + (0.251 \times i^2) + (0.760 \times t^2) \quad (5.3)$$

$$Residual\ aluminium(Al_r) = 0.291 - (0.734{\times}F_i) - (0.09{\times}i) + (0.242{\times}t) - (0.01{\times}F_i{\times}i) + (0.757{\times}i{\times}t) - (0.322{\times}F_i{\times}t) + (0.549{\times}F_i^2) + (0.071{\times}i^2) + (0.024{\times}t^2) \quad (5.4)$$

$$SEEC = 0.190 - (0.626{\times}F_i) - (0.009{\times}i) + (0.169{\times}t) - (0.699{\times}F_i \times i) + (0.709{\times}i{\times}t) - (0.449{\times}F_i{\times}t) + (0.765{\times}F_i^2) + (0.315{\times}i^2) - (0.094{\times}t^2) \quad (5.5)$$

5.2.1 Verification of equations

To verify the correctness of the equations obtained by the SYSTAT 7.0, twenty set of random experiments, as mentioned in Table 5.6, were performed. The experimental results were plotted against predicted response and presented in Figure 5.5. The graphs and their respective R^2 value are displayed in the Figure 5.5. R^2 value for residual fluoride, residual aluminium and SEEC are 0.9614, 0.9732 and 0.9449 respectively.

Table 5.6: Operational parameter settings and their respective actual and predicted responses selected for verification of regression equations

S.No	***Operating parameters***			***Actual***			***Predicted***		
	F_i (mg/L)	i (A)	t (min)	F_r (mg/L)	Al_r (mg/L)	SEEC (J/mg)	F_r (mg/L)	Al_r (mg/L)	SEEC (J/mg)
1	2	0.31	10	1.12	9.40	454.43	1.15	10.14	605.22
2	2	0.31	25	0.43	15.71	632.75	0.39	16.76	1016.11
3	5	0.31	30	0.71	12.10	279.39	0.70	10.72	200.07
4	5	0.31	50	0.29	18.05	424.52	0.30	16.79	255.81
5	8	0.31	15	2.49	08.35	312.12	2.51	6.97	419.33
6	8	0.31	45	0.59	13.26	242.91	0.80	12.84	121.47
7	2	0.53	10	0.71	10.60	776.51	0.81	12.16	1056.98
8	2	0.53	20	0.52	19.68	1353.64	0.34	18.80	1546.79
9	5	0.53	25	0.59	16.02	567.85	0.52	14.41	542.95
10	5	0.53	30	0.25	17.50	632.65	0.33	17.09	683.14
11	5	0.53	35	0.39	20.71	744.36	0.19	19.74	814.20
12	2	0.75	10	0.61	14.90	1392.08	0.63	14.69	1754.88
13	2	0.75	30	0.18	18.90	3182.55	0.22	19.01	3097.81
14	5	0.75	10	1.27	09.25	518.76	1.00	8.73	395.84
15	5	0.75	30	0.14	25.80	1194.44	0.11	23.83	1411.32
16	8	0.75	10	1.37	10.00	291.85	1.61	10.25	82.85
17	8	0.75	20	0.90	09.01	534.53	0.85	9.88	445.15
18	3	0.45	10	1.00	10.86	441.60	1.11	8.55	460.11
19	6	0.60	20	0.75	13.54	432.00	0.81	12.38	339.90
20	7	0.31	10	2.3	05.92	170.00	2.60	4.54	174.26

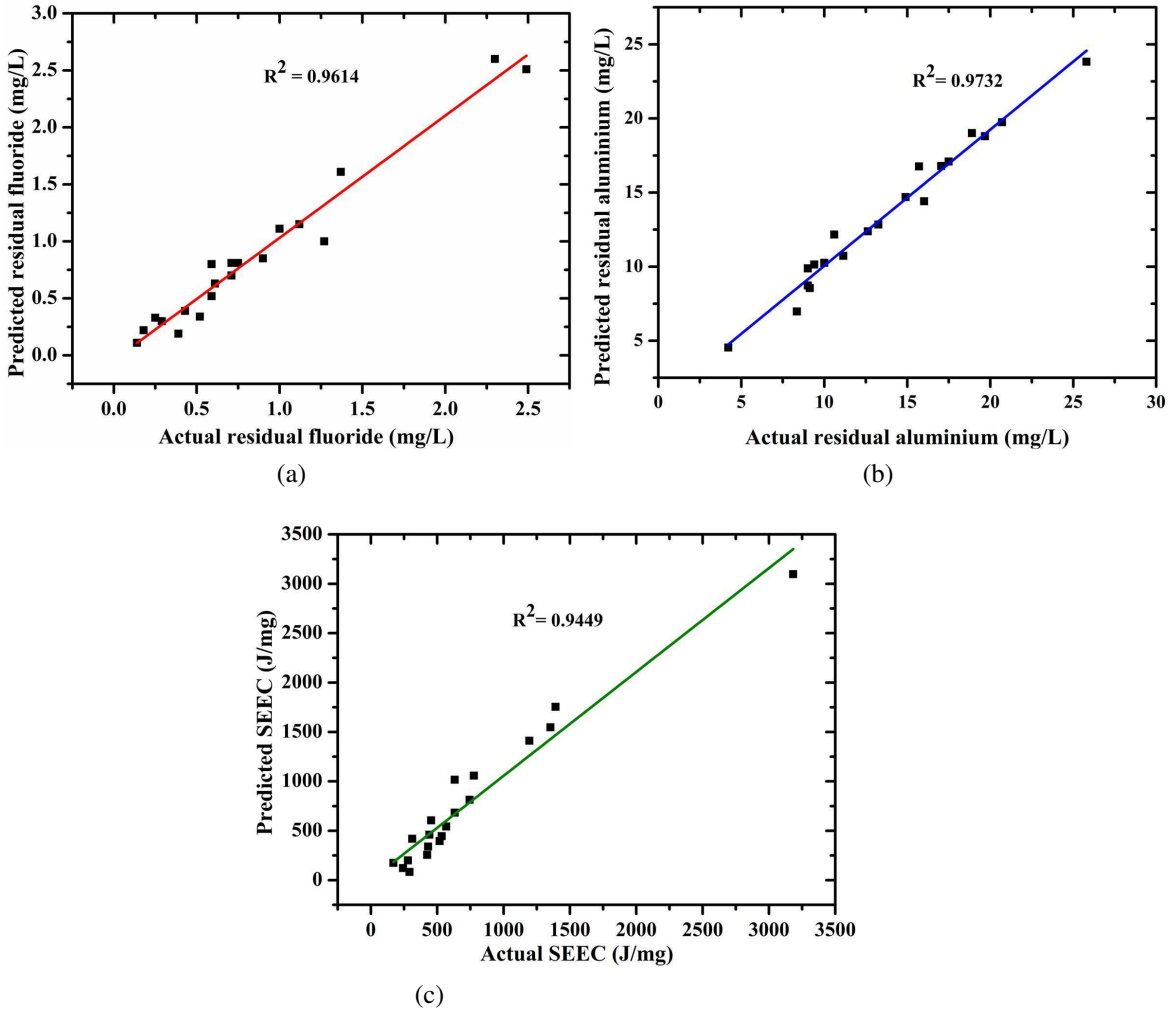

Figure 5.5: Actual v/s predicted plot (a) residual fluoride (b) residual aluminium (c) SEEC

5.3 Adsorption kinetics of EC

Fluoride is generally adsorbed at the surface of flocs produced by the coagulant which is generated electrochemically. Analysis of the electrocoagulation of fluoride contaminated water reveals that there are two separate processes taking place, i.e. electrochemical process through which the metal coagulants are generated and physio-chemical process through which the effluents are adsorbed on the surface of the coagulants [125]. The removal of pollutant is similar to conventional adsorption except the generation of coagulants. Generation of coagulants is in-situ and with the help of electric current. The electrode consumption can be estimated according to Faraday's Law (Refer Chapter 4) and the amount of coagulant generated can be estimated stoichiometrically [126]. At equilibrium a relationship exists between the concentration of the fluoride species in solution and the concentration of fluoride species

in the adsorbent (i.e. the amount of species adsorbed per unit mass of adsorbent). The amount of fluoride at equilibrium on aluminium species q_e (mg/g) was calculated from the Equation 5.6 [127] [128].

$$q_e = V(C_0 - C_e)/W \tag{5.6}$$

V= volume of solution (L)

C_0= initial fluoride concentration (mg/L)

C_e= equilibrium fluoride concentration (mg/L)

W= mass of anode dissolved (adsorbent) (gm)

Since the amount of coagulant can be estimated for a given time, the fluoride removal can be modeled by adsorption phenomenon. During EC the insoluble metal hydroxides removes pollutants by surface adsorption.

The kinetics of sorption is an important parameter for designing sorption system and is required for selecting optimum operating conditions before applying it at full scale process. The dynamics of the adsorption process can best be understood by the processing of kinetics adsorption data. Moreover, it helps in prediction of adsorption rate, which gives information for designing and modelling of the process [129]. Also adsorption kinetics is of great significance to evaluate the performance of a given adsorbent and gain insight into the underlying mechanisms.

5.3.1 Pseudo-first order kinetic model

The adsorption kinetic data of fluoride are analyzed using Lagergran rate equation. The first-order Lagergran model is [130]:

$$dq/dt = k_1(q_e - q) \tag{5.7}$$

where q is the amount of fluoride adsorbed on the adsorbent at time t (min), q_e is the amount of fluoride adsorbed at equilibrium and k_1 (min^{-1}) is the rate constant of first-order adsorption. The integrated form of the Equation 5.7 is given in Equation 5.8.

$$log(q_e - q) = logq_e - \frac{k_1 t}{2.303} \tag{5.8}$$

If the first order kinetics is applicable, a plot of log $(q_e - q)$ vs t will provide a linear relationship from which k_1 and predicted q_e can be determined from the slope and intercept of the plot respectively.

The results are shown in Table 5.7. The q_e and rate constant (k_1) were calculated from the slope of the plots of log $(q_e - q)$ versus time (t). A straight line obtained from the plots suggests the applicability of this kinetic model. It was found that points do not fit in a straight line. So the adsorption does not obey the first-order kinetics adsorption

[131].

5.3.2 Pseudo second order kinetic model

The second-order kinetic model is expressed as:

$$dq/dt = k_2(q_e - q) \tag{5.9}$$

Where k_2 is the rate constant of the second-order adsorption. The integrated form of Equation 5.9 is

$$\frac{1}{q_e - q} = \frac{1}{q_e} + k_2 t \tag{5.10}$$

$$\frac{t}{q} = \frac{1}{k_2 q_e^2} + \frac{t}{q_e} \tag{5.11}$$

The plot of t/q_t vs t will be a linear relationship if the second order kinetics is applicable. k_2 and predicted q_e can be determined from the slope and intercept of the plot respectively. Results are tabulated in Table 5.7

5.3.3 The intraparticle diffusion model

The adsorption process may follow a multi step transport of solute (adsorbate) molecules from the aqueous phase to the surface of solid particles followed by diffusion of the solute molecules into the interior of the pores, which is likely to be a slow process and is a rate determining step [129]. This type of adsorption behaviour can be explored by applying intraparticle diffusion model shown in the Equation 5.12 [132]:

$$q_t = k_{dif} t^{0.5} + C \tag{5.12}$$

Where C is the intercept and k_{dif} $(mg/g/min^{-0.5})$ is the intraparticle diffusion rate constant. The value of C provides information about the thickness of the boundary layer, since the resistance to the external mass transfer increases as the intercept increases.

The plot of q_t v/s $t^{0.5}$ may present a multilinearity correlation, which indicates that two or more steps occur during adsorption process. The rate constant K_{dif} is directly evaluated from the slope of the regression line and the intercept is C. Results are tabulated in Table 5.7.

5.4 Reaction Kinetics- Results

For the present study, the plots were made for three initial fluoride concentrations (2, 5, 8 mg/L) and three applied current values (0.31, 0.53, 0.75 A). The electrolysis time was

between $10-50\,min$. Value of C_e is the residual fluoride at varying time and is known experimentally. Value of q_e is calculated using Equation 5.6. The detailed results for all plots have been presented in the appendix B. All the plots have been shown in Figure 5.6-5.8. It can be clearly observed from the plots that second order kinetics fits the data well.

Parameters for reaction order kinetics have been summarised in Table 5.7. The various parameters were calculated by plotting the graphs as explained in the text in section 5.3.

The average R^2 value for pseudo first order kinetic model is 0.9276, for pseudo second order kinetic model it is 0.9815 and for intra-particle diffusion it is 0.8455. These results indicate that the adsorption system belongs to the pseudo second-order kinetic model. Similar results have been obtained by Khatibikamal *et al.* [133]. In this model, the rate-limiting step is the surface adsorption that involves chemisorption, where the removal from a solution is due to physicochemical interactions between the two phases [134]. Liu *et al.* [135] has also mentioned that pseudo-second order kinetic assumes that chemisorption controls the adsorption rate.

Table 5.7: Kinetic model used and their parameters at different initial fluoride concentrations and applied current.

Operating Parameters		***Pseudo first order kinetics***			***Pseudo second order kinetics***			***Intraparticle diffusion***	
Fi (mg/L)	i (A)	k_1 (min^{-1})	q_e (mg/g)	R^2	k_2 (min^{-1})	q_e (mg/g)	R^2	k_{dif} (min^{-1})	R^2
2	0.31	-0.036	1.589	0.9779	0.018	0.459	0.8554	5.479	0.8678
5	0.31	-0.031	1.742	0.8894	0.010	0.048	0.9975	6.823	0.7694
8	0.31	-0.029	2.076	0.9651	0.005	0.055	0.9973	17.641	0.8857
2	0.53	-0.023	1.207	0.9655	0.040	0.337	0.9938	2.421	0.9726
5	0.53	-0.024	1.393	0.8909	0.017	0.075	0.9985	4.240	0.8398
8	0.53	-0.043	1.772	0.9393	0.010	0.048	0.9986	7.456	0.7964
2	0.75	-0.026	1.124	0.9337	0.059	0.308	0.9948	1.203	0.9561
5	0.75	-0.035	1.501	0.8825	0.024	0.072	0.9984	2.486	0.7460
8	0.75	-0.039	1.697	0.9320	0.015	0.038	0.9997	3.559	0.7760

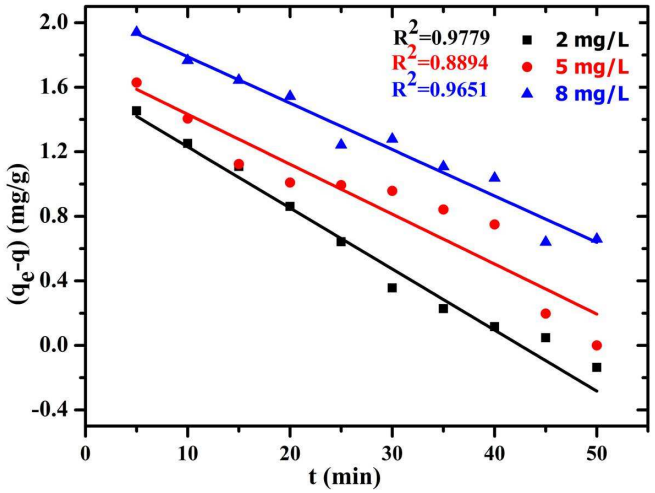

(a)

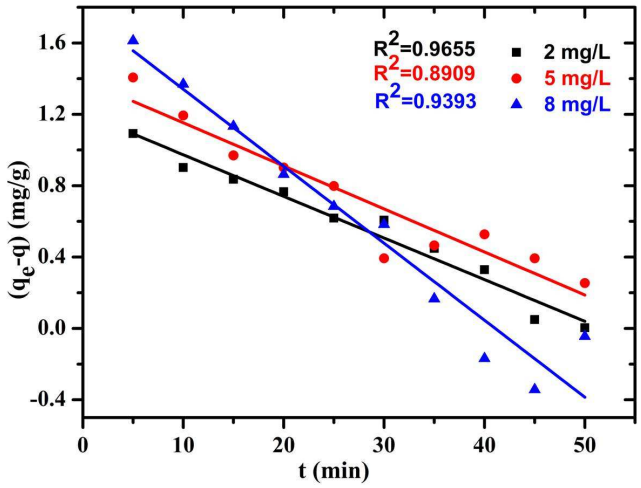

(b)

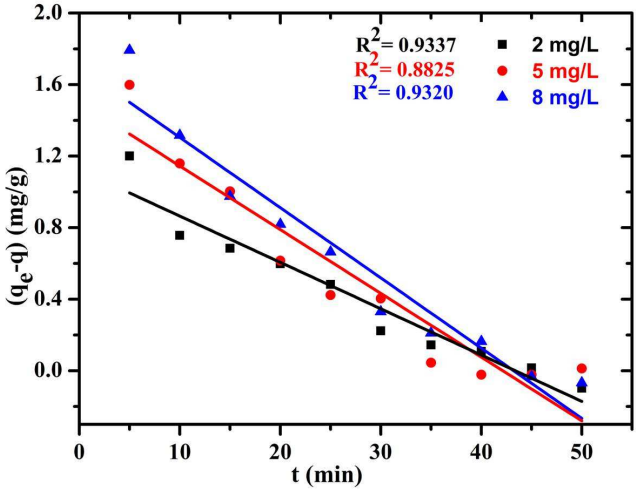

(c)

Figure 5.6: Pseudo first order kinetic model plot for varying applied current (a) 0.31 A (b) 0.53 A (c) 0.75 A.

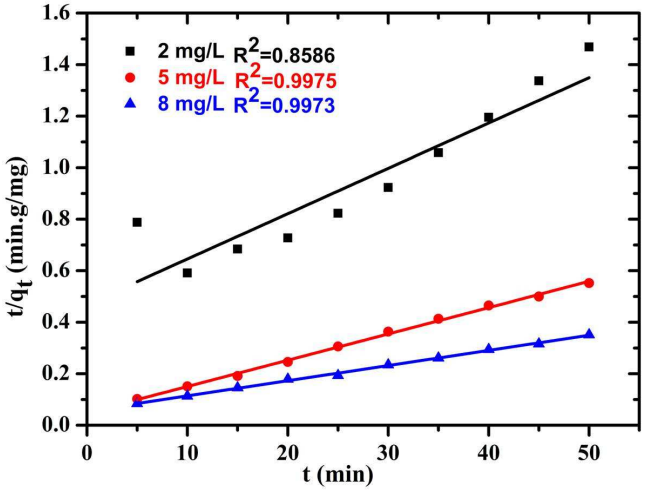

(a)

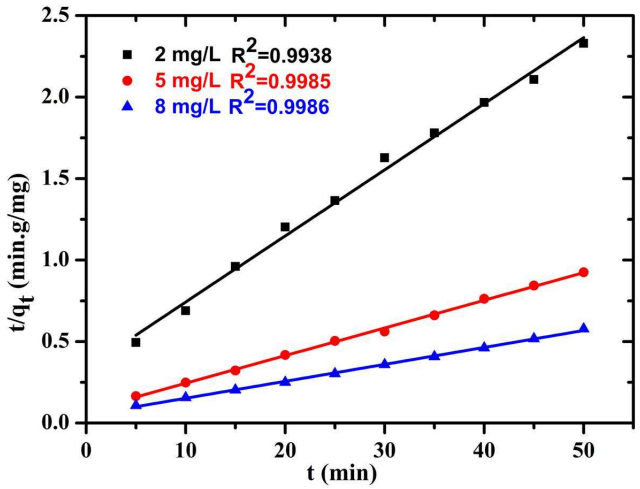

(b)

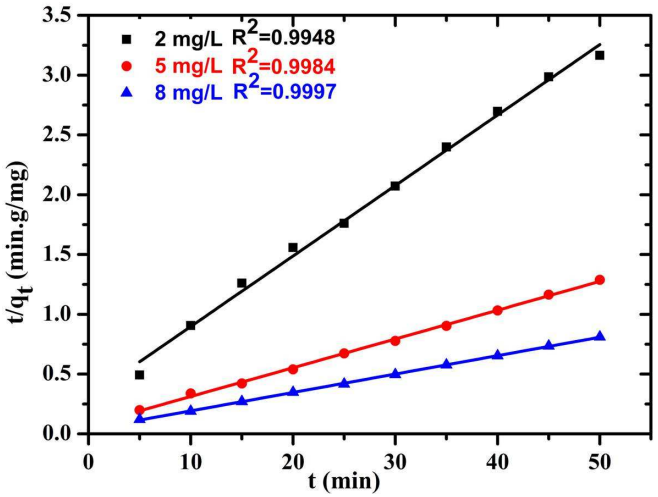

(c)

Figure 5.7: Pseudo second order kinetic model plot for varying applied current (a) 0.31 A (b) 0.53 A (c) 0.75 A

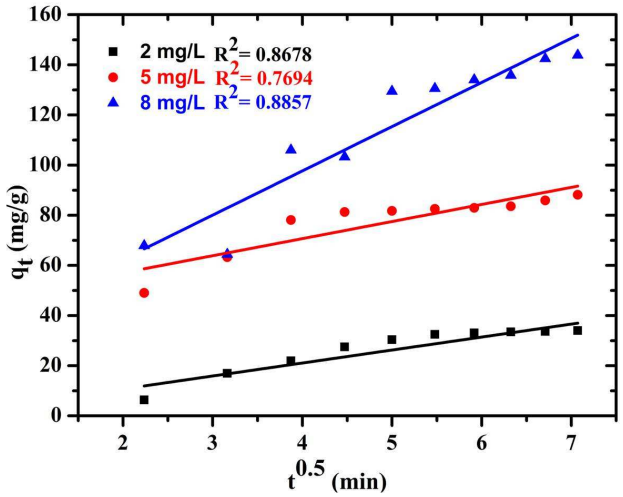

(a)

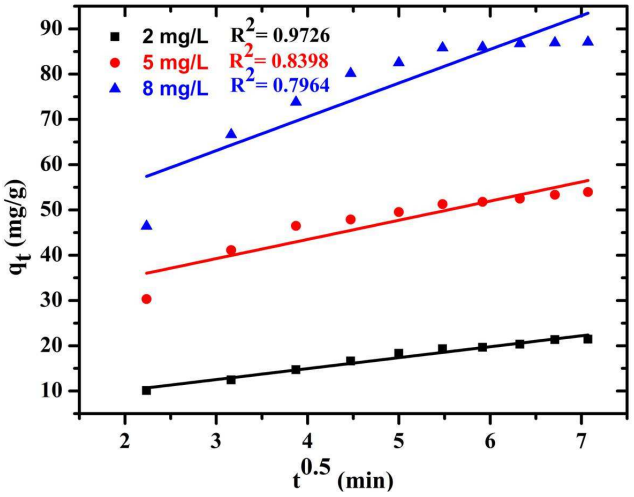

(b)

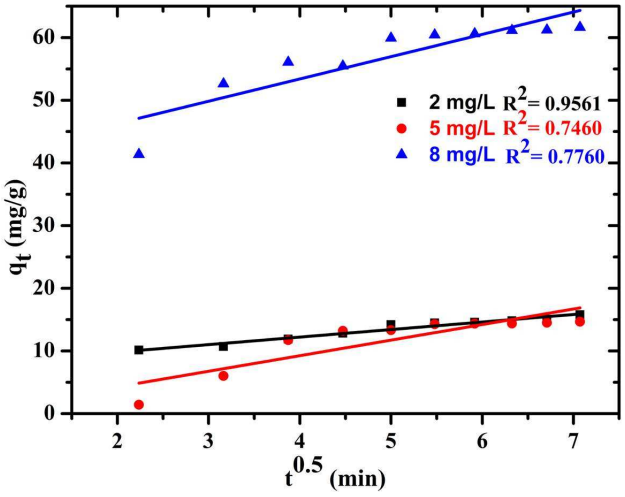

(c)

Figure 5.8: Intraparticle diffusion kinetic model plot for varying applied current (a) 0.31 A (b) 0.53 A (c) 0.75 A.

5.5 Adsorption isotherm studies

It is assumed that the pollutant can act as a ligand to bind hydrous aluminium in situ formed gelatinous precipitate, it is further attempted to extend the adsorption isotherm models for pollutant removal by Langmuir, Freundlich and Redlich Peterson models [125] [127] [128] [136]. The abilities of three widely used isotherms; the Langmuir, Freundlich, and Redlich Peterson were examined to model the adsorption equilibrium. In general, an adsorption isotherm is a curve describing the phenomenon governing the retention (or release) or mobility of a substance from the aqueous porous media or aquatic environments to a solid-phase at a constant temperature and pH [137]-[138].

For the present study the plots were made for three values of applied current ($0.31\,A$, $0.53\,A$ and $0.75\,A$). The concentration of adsorbate at equilibrium was calculated using varying initial fluoride concentration ($2-8\,mg/L$). Three isotherms namely, Langmuir, Freundlich and Redlich-Peterson have been considered for the study.

5.5.1 Langmuir isotherm

The Langmuir model [139] represents one of the first theoretical treatments of non-linear sorption and assumes monolayer deposition of adsorbate on homogenous adsorbent surface (coagulant). Langmuir represents the equilibrium distribution of metal ions between the solid and liquid phases [140]. In addition, the model assumes uniform energies of adsorption onto the surface and no transmigration of the adsorbate. The Langmuir isotherm assumes monolayer deposition of adsorbate on homogenous adsorbent surface (coagulant). It is well known that the Langmuir equation is intended for a homogeneous surface. The mathematical expression of Langmuir isotherm is given in Equation 5.13:

$$q_e = (q_{max} K_l C_e)/(1 + K_l C_e) \tag{5.13}$$

where q_e is the solid phase adsorbate concentration in equilibrium (mg/g), q_{max} the maximum adsorption capacity corresponding to complete monolayer coverage on the surface (mg/g), C_e the concentration of adsorbate at equilibrium (mg/L), and K_l the Langmuir constant (L/mg). Equation 5.13 can be linearized into four different forms shown in Table 5.8, which give different parameter estimates.

5.5.2 Freundlich isotherm

The freundlich isotherm [139] is commonly used to describe the adsorption characteristics for the heterogeneous surface [141]. It is empirical model relating the adsorption intensity of the sorbent towards adsorbent. The isotherm is adopted

to describe reversible adsorption and not restricted to monolayer formation. The mathematical expression of the Freundlich model is represented by:

$$q_e = K_f Ce(1/n) \tag{5.14}$$

K_f is Freundlich constant that indicate the adsorption capacity of the adsorbent (L/gm) and n is an empirical constant related to the magnitude of the adsorption driving force. The linear form of Freundlich isotherm is shown in Table 5.8.

5.5.3 Redlich-Peterson isotherm

The Redlich-Peterson isotherm [142] has three parameters and incorporates the features of Langmuir and Freundlich isotherms. It has a linear dependence on concentration in the numerator and an exponential function in the denominator. It can be represented as shown in Equation 5.15.

$$q_e = \frac{ACe}{1 + BCeg} \tag{5.15}$$

Where A and B are Redlich Peterson isotherm constants. The exponent 'g', as it lies between 0 and 1, has two limiting behaviours: Langmuir form for g = 1 and Henry's law form for g = 0. Since there are three unknown parameters A, B and g, so these have to be calculated by using the approach of maximizing R^2 between experimental q_e and predicted q_e by using Excel solver. So the results are shown in non-linear approach for adsorption isotherms.

Table 5.8: Different type of isotherm and their linearized form.

Name	***Linear form***	***Plot***	***Slope***	***Intercept***
Langmuir-1	$\frac{C_e}{q_e} = \frac{1}{K_l} + \frac{C_e}{q_{max}}$	C_e/q_e vs C_e	$1/q_{max}$	$1/(K_l q_{max})$
Langmuir-2	$\frac{1}{qe} = \frac{1}{K_l q_{max} C_e} + \frac{1}{qmax}$	$1/q_e$ vs $1/C_e$	$1/(K_l q_{max})$	$1/q_{max}$
Langmuir-3	$q_e = q_{max} + \frac{q_e}{K_l C_e}$	q_e vs q_e/C_e	$1/K_l$	q_{max}
Langmuir-4	$\frac{q_e}{C_e} = K_l q_{max} - K_l q_e$	q_e/C_e vs q_e	K_l	$K_l q_{max}$
Freundlich	$ln(q_e) = ln(K_f) + \frac{1}{n} lnC_e$	lnq_evs lnC_e	$1/n$	lnK_f

5.5.4 Linear regression method

Linear regression is frequently used to determine the best-fitting isotherm, and the method of least squares has been used for finding the parameters of the isotherms. Linear method assumes the experimental data to be linear and predicts the slope and intercept that makes a straight line. The linear method assumes that the scatter of points around the line follow a Gaussian distribution and the error distribution is the same at every point of X. But this is rarely true because the error distribution gets altered after

transforming the data to a linear form [143]. It considers error distribution along Y-axis irrespective of corresponding X-axis. The adsorption isotherms were developed for three current values $0.31\,A$, $0.53\,A$ and $0.75\,A$. C_e is the residual fluoride concentration at electrolysis time of $50\,min$ for initial fluoride concentration $(2-8\,mg/L)$ and q_e is calculated by Equation 5.6. Table 5.9 shows the isotherm parameters for all the mentioned isotherms.

Table 5.9: Isotherm parameters obtained using linear method.

Isotherm	***Parameters***	***Applied current (A)***		
		0.31	0.53	0.75
Langmuir Type 1	$q_{max}(mg/g)$	-625.00	-666.66	87.71
	K_l (L/mg)	-0.47	-0.45	14.25
	R^2	0.06	0.26	0.91
Langmuir Type2	$q_{max}(mg/g)$	-256.41	-416.67	55.86
	$K_l(L/mg)$	-0.78	-0.68	44.75
	R^2	0.71	0.97	0.83
Langmuir Type 3	$q_{max}(mg/g)$	7.39	-163.37	63.95
	$K_l(L/mg)$	2.89	1.46	-37.73
	R^2	0.20	0.30	0.57
Langmuir Type 4	$q_{max}(mg/g)$	1294.13	698.21	-77.85
	$K_l(L/mg)$	0.22	0.436	-20.05
	R^2	0.04	0.30	0.49
Freundlich	n	0.86	0.92	2.29
	K_f	334.59	386.02	127.14
	R^2	0.80	0.98	0.86

The above table shows that the result for R^2 value in most of the cases is not going beyond 0.9. So, the interpretation of which isotherm fits the data well could not be properly done. Therefore, a non-linear approach to make isotherms was used to fit the data.

5.5.5 Non Linear method

A significant limitation related to the linearized form of isotherm equation has recently been pointed out, which produces a vast amount of different outcomes, implicitly alter the error structure, violates the error variance and normality assumptions of standard least squares, leading to the bias of the adsorption data [144]-[145]. In this context, a non-linear form of the isotherm and kinetics models with error analyses and optimization techniques are required. In addition, evaluating the accuracy in parameters prediction is also needed. Moreover, a curve fitting is applied to describe experimental data in all fields of research. The better the fit, the more accurately the function describes the data. Over the past few decades, the exponential development of computer programming has provided scope to calculate and predict model parameters.

programming has provided scope to calculate and predict model parameters.

In this case of the non-linear method, a trial-and-error procedure, which is applicable to computer operation, was developed to determine the isotherm parameters using an optimization routine to maximize the coefficient of determination between the experimental data and isotherms in the solver add-in with Microsoft's spreadsheet, Microsoft Excel. The abilities of three widely used isotherms, the Freundlich, Langmuir, and Redlich-Peterson and isotherms to model the equilibrium sorption data were examined. The protocol which has been used is that experimental data was manually entered in MS-Excel, the formulated algorithm was carried out. The predicted curve was overlaid on the experimental data points and goodness of fit is observed. The experimental $q_{e.exp}$ was calculated by the Equation 5.6 and the predicted $q_{e.pred}$ is obtained from the non-linear expressions of the, Langmuir, Freundlich and Redlich Peterson isotherms as shown in Equation 5.13, 5.14 and 5.15 respectively. The detailed data is presented in the appendix B.

Goodness of fit is an essentially important parameter that estimates how well the curve (i.e. the prediction) pronounces the experimental data. For data not described by a linear function, it is crucial to apply a procedure that will fit a non-linear function to the data. A suitable method for this procedure is called iterative nonlinear least squares fitting. The following parameters are measured for judging the goodness of fit:

Coefficient of determination (R^2): It gives the proportion of the variance of one variable that is predictable from the other variable. The coefficient of determination is such that $0 < R^2 < 1$, and denotes the strength of the linear association between experimental data, $q_{e.exp}$ and prediction data, $q_{e.pred}$. The coefficient of determination represents the percent of the experimental data that is the closest to the line of best fit. R^2 is described by the expression in Equation 5.16 [146]:

$$R^2 = 1 - \frac{\sum_{n=1}^{n}(q_{e.exp.n} - q_{e.pred.n})^2}{\sum_{n=1}^{n}(q_{e.exp.n} - q_{e.pred.n})^2} \tag{5.16}$$

where, $q_{e.exp}$ is the equilibrium sorption capacity found from the batch experiment, $q_{e.pred}$ is the prediction from the isotherm model for corresponding to C_e and n is the number of observations.

Residual root mean square error (RMSE) and the chi-square test (χ^2): Non-linear error functions such as the residual root mean square error (RMSE) and the chi-square test (χ^2) are used to judge the equilibrium model with the optimal magnitude. Equation 5.17 and 5.18 shows the standard equation of RMSE and χ^2 respectively [146].

$$RMSE = \sqrt{\frac{1}{n-1}\sum_{n=1}^{n}(q_{e.exp.n} - q_{e.pred.n})^2} \tag{5.17}$$

$$\chi^2 = \sum_{n=1}^{n} \frac{(q_{e.exp.n} - q_{e.pred.n})^2}{q_{e.exp.n}} \tag{5.18}$$

The small values of RMSE and χ^2 indicate the better model fitting and the similarity of model with the experimental data respectively [147].

5.6 Adsorption isotherms-Results

Isotherm parameters for all the three isotherms have been tabulated in Table 5.10. Plots for all the isotherms are shown in Figure 5.9-5.11.

Table 5.10: Isotherm parameters obtained using non-linear method.

Isotherms	***Parameters***	***Applied current (A)***		
		0.31	0.53	0.75
Langmuir	q_{max}	2448.091	12584.01	113.684
	K_l	0.126	0.027	7.074
	RMSE	16.013	2.544	5.583
	χ^2	2.041	0.085	0.571
	R^2	0.8834	0.9918	0.9213
Freundlich	K_f	19.943	19.941	19.941
	n	0.068	0.058	0.055
	RMSE	16.150	2.480	10.372
	χ^2	2.076	0.081	1.973
	R^2	0.8814	0.9922	0.7286
Redlich Peterson	g	0.9	0.02	0.47
	RMSE	16.024	2.476	2.974
	χ^2	2.044	0.081	0.162
	R^2	0.8832	0.9922	0.9777

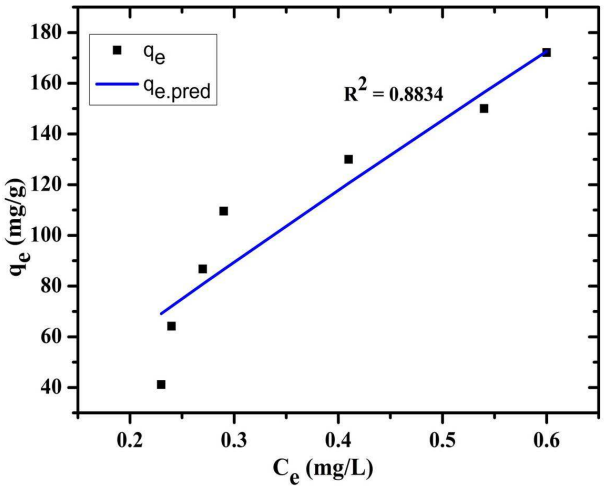

(a)

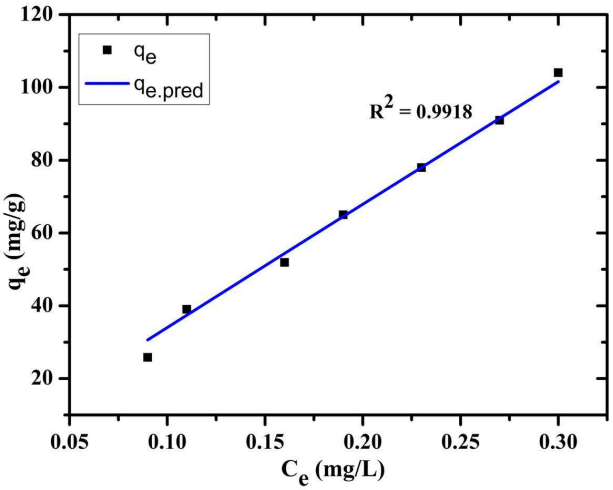

(b)

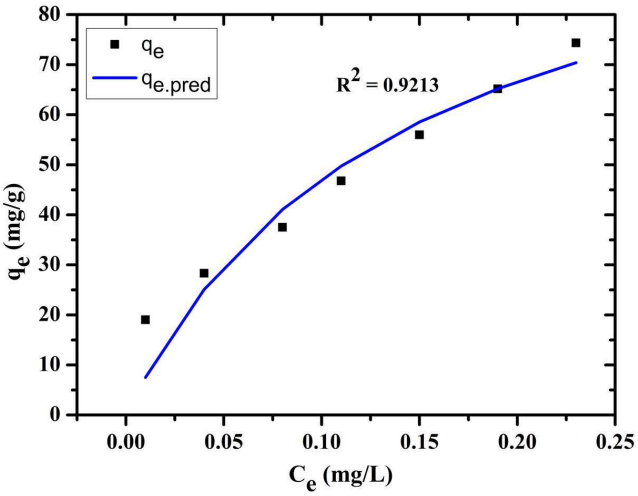

(c)

Figure 5.9: Langmuir isotherm plot (a) 0.31 A (b) 0.53 A (c) 0.75 A.

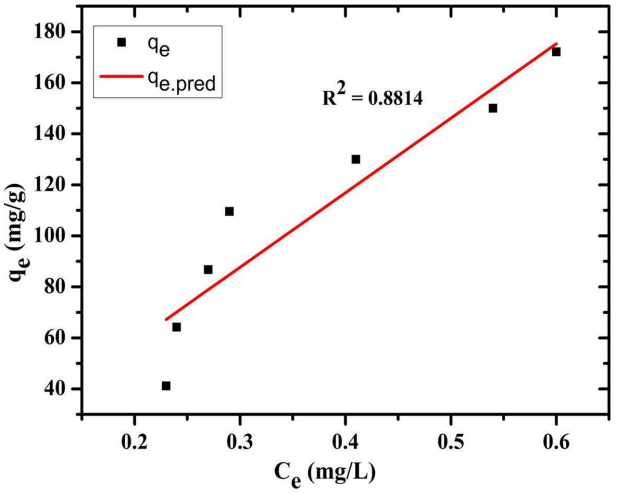

(a)

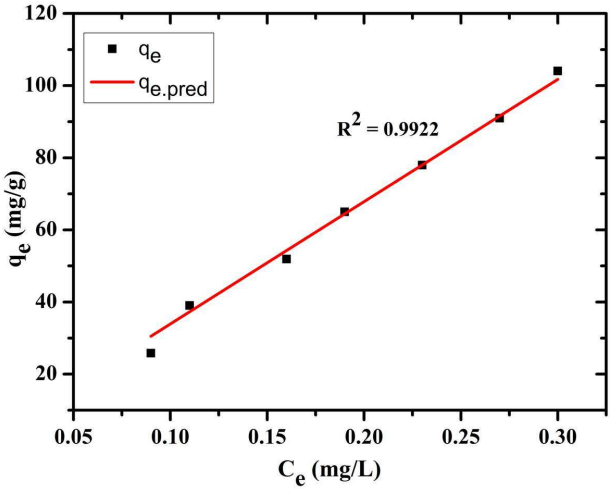

(b)

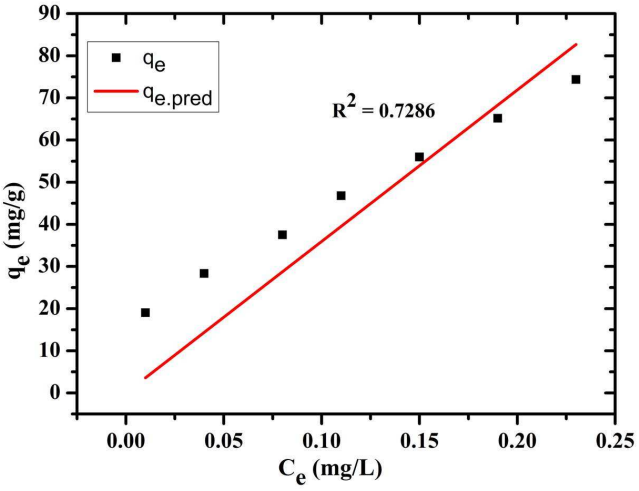

(c)

Figure 5.10: Freundlich isotherm plot (a) 0.31 A (b) 0.53 A (c) 0.75 A.

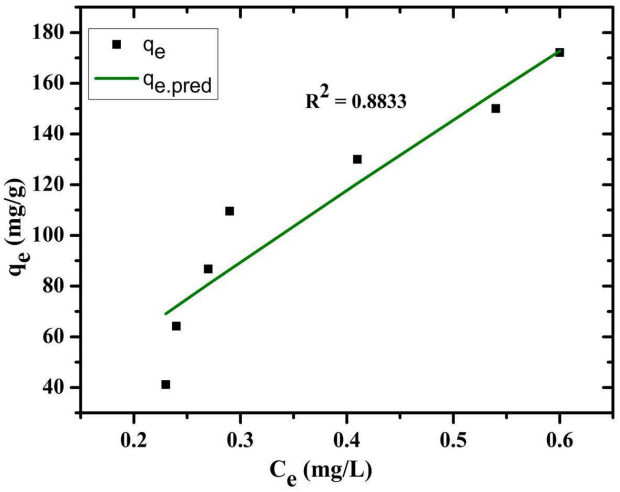

(a)

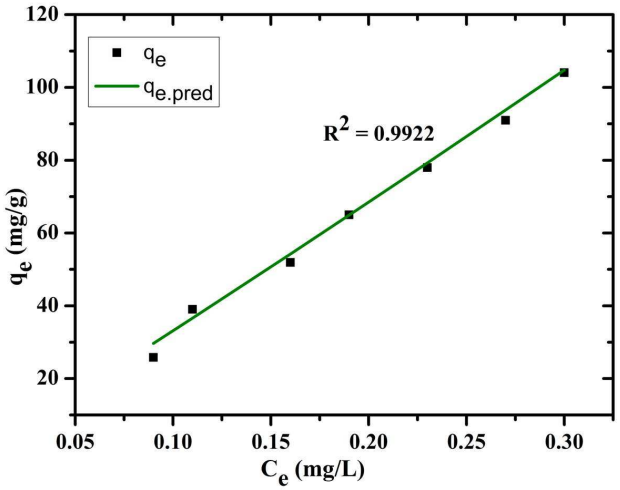

(b)

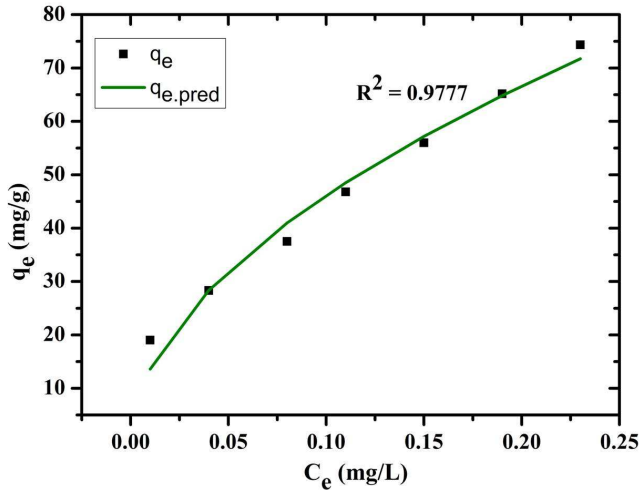

(c)

Figure 5.11: Redlich-Peterson isotherm plot (a) 0.31 A (b) 0.53 A (c) 0.75 A.

It can be clearly observed that at current of 0.31 A, Langmuir isotherm gave maximum R^2 value and for all other values of applied current the Redlich Peterson

isotherm gave the maximum R^2 value. Redlich Peterson isotherm has features of both Langmuir and Freundlich [142]. The model has a linear dependence on concentration in the numerator and an exponential function in the denominator [148] to represent adsorption equilibria over a wide concentration range, that can be applied either in homogeneous or heterogeneous systems due to its versatility [149]. In the limit, it approaches Freundlich isotherm model at high concentration (as the exponent g tends to zero) and is in accordance with the low concentration limit of the ideal Langmuir condition (as the g values are all close to one) [150]. Also, when the constants A and B are greater than unity Freundlich isotherm approaches [147]. It can be observed from Table 5.10, that g value at 0.53 and $0.75\,A$ of applied current is 0.02 and 0.47 respectively. This indicates that Freundlich isotherm is approaching. Thus it can be concluded that when the current is low ($0.31\,A$) then monolayer is formed and adsorption occurs at finite number of defined localized sites [151]. When current value is increased then Freundlich isotherm governs and multilayer adsorption takes place.

Chapter Summary

In this chapter Taguchi method was employed for designing the experiments. This method helps us to know how different parameters affect the process performance. This allows for the collection of the necessary data to determine which parameters affect the response values the most, with a minimum amount of experimentation, thus saving time and resources. The three parameters selected for development of Taguchi design were: initial fluoride concentration, applied current and electrolysis time. Three responses were selected namely: residual fluoride, residual aluminium and SEEC. The model developed using Taguchi design was validated by ANOVA. High R^2 suggested that the model is appropriate for use. But only R^2 value is not considered sufficient for validation. Straight line in the normal probability plots and constant variance in the residual v/s fit plot was observed which suggest that the model is well behaved. The relationship between residual fluoride, residual aluminium and SEEC with combination of control factors is obtained using non-linear regression analysis with the help of SYSTAT 7.0. Actual v/s predicted response graphs were plotted to verify the obtained equations. High R^2 values in the tune of 0.95 and above indicates that the equations can be used for prediction of data.

After the development of model, kinetics and adsorption isotherms were studied. This study was performed to understand the underlying mechanisms of the fluoride removal by EC. The kinetics study reveal that the second order kinetics fits the data well which suggests that removal of fluoride is due to physico-chemical reactions between the fluoride and aluminium hydroxide flocs. Also chemisorptions is the rate limiting step and hence this step governs the adsorption rate. The isotherm study reveals that at applied current of $0.31\,A$, Langmuir isotherm fits the data well and at higher applied current values, Redlich-Peterson isotherm fits the data well. Depending on the applied current, the surface of the adsorbate can be homogenous or hetrogenous. The result also suggests that the chemisorptions of fluoride onto the aluminium hydroxide flocs can be monolayer or multilayer.

The study also indicates that the treating the water for removing fluoride, introduces aluminium in the water. The concentration of aluminium in the treated water is beyond permissible level and hence steps have to be taken to control it. The next chapter marks the beginning of aluminium control in the treated water.

CHAPTER 6

Chapter 6

Model development for aluminium removal

From previous findings it is evident that defluoridation by the EC process using aluminium electrodes introduces aluminium in the water, besides removing fluoride from it. Aluminium is found to be a potential neuro-toxicant and medical research and epidemiological surveys suggest that dissolved aluminium entering the bloodstream may cause Alzheimer's disease, Lou Gehrig's disease and other forms of senile dementia. Synergistic associations of aluminium and fluoride have been shown by several researchers. Aluminium -fluoride complexes also increase the risk of developing Alzheimer's disease. Therefore, there is a need to control the aluminium concentration in the treated water.

The present chapter discusses the measures to control the aluminium content in the treated water introduced during defluoridation. Also statistical models for aluminium removal, using bentonite and activated silica sol have been developed and presented in the later part of the chapter. In the last section adsorption isotherms for the process are presented.

6.1 Measures to control aluminium

The experiments conducted for defluoridation through EC using aluminium electrodes have indicated that high aluminium is introduced in water after EC treatment. Therefore, it is imperative to control the aluminium in the treated water, to offset ill-effects of aluminium on human health. Based on previous findings it is evident that energy input governs the dissolution of aluminium in water. Energy input is a function of voltage, applied current and electrolysis time. The voltage was constant during experimental run, thus, it can be safely assumed that, aluminium dissolution depends on "i" and "t". To control aluminium, "i and t" were minimized for target fluoride removal. With the

use of optimized energy input, the residual aluminum in water could be lowered down, but it was still more than permissible value of aluminium in drinking water.

It was observed that the treated water after EC (with optimized energy input) has high turbidity and high aluminium content. The turbidity is due to the flocs (alumino-fluoro complexes) formed in the EC process during fluoride removal. Thus, it was necessary to remove these flocs to control turbidity and in turn aluminium.

As a first step to control aluminium, flocculation and settling was attempted. The results showed an appreciable decrease in turbidity and aluminium content, but were still not close to the IS:10500:2012 [25] permissible standards of aluminium in drinking water. It was now understandable that the efficient settling of flocs could lead to lesser residual aluminium. Therefore, as a second step for efficient settling of flocs, coagulant aids were used. Use of coagulant aids brought down the aluminium within permissible standards.

So, two strategies were attempted to control the aluminium in the treated water.

a. Control of aluminium by optimisation of energy input followed by flocculation, settling and filtration.

b. Control of aluminium by optimisation of energy input, followed by use of coagulant aid for better settling.

6.2 Control of aluminium by optimisation of energy input

In the previous Chapter the regression equations were validated and were suggested to be fit for use in further investigations. These equations were used to optimize the energy input, for desired fluoride removal. It has also been discussed earlier that aluminium introduced depends on the energy input. Hence, to minimize the aluminium content, energy input has to be minimized, which in turn means that product of applied current and electrolysis time needs to be minimized. To achieve this, a program has been developed in FORTRAN using the technique of grid search method. The objective of the program was to obtain minimum "i and t" for achieving target residual fluoride as $0.7\,mg/L$.

The minimum and maximum range for operational parameters (applied current and electrolysis time) was declared in the program. Equation 5.3 was used in the program and the response (residual fluoride, F_r) was fixed to $0.7\,mg/L$. The program was executed to determine the minimum "i" and "t" for a given initial fluoride concentration. The program in FORTRAN calculates the minimum point of a multi-variable function using the grid search method. This method performs a multi-dimensional grid search. Each dimension has a range of values. Each range is divided into a set of equal-value

intervals. The multi-dimensional grid has a centroid which locates the optimum point. The search involves multiple passes. In each pass, the method locates a node (point of intersection) with the least function value. This node becomes the new centroid and builds a smaller grid around it. Successive passes end up shrinking the multidimensional grid around the optimum [152].

In the present study minimum values of applied current and electrolysis time required were determined for each initial fluoride concentration to bring down the final fluoride concentration to $0.7\,mg/L$ (within IS:10500:2012 permissible limit [25]). The target value of fluoride in treated water was kept as $0.7\,mg/L$ to take care of any possible error in prediction/measurement. Table 6.1 gives the details of optimized sets which are obtained with the help of a program. The value of minimum applied current and electrolysis time for each initial fluoride concentration was calculated by the program and has been presented in Table 6.1 (Column 3 and 4). The respective values for residual aluminium and SEEC were calculated by Equation 5.4 and 5.5 and have been presented in Table 6.1 (Column 5 and 7 respectively).

Table 6.1: Details of optimized sets (Minimum value of applied current and time for target value of residual fluoride as $0.7\,mg/L$).

Set No.	***Operating parameters***			***Residual aluminium*** (mg/L)		***SEEC*** (J/mg)	
	F_i (mg/L)	i (A)	t (min)	Predicted	Experimental	Predicted	Experimental
1	2	0.33	17.05	13.659	14.018	862.508	584.29
2	3	0.32	20.93	12.097	12.723	566.93	384.38
3	4	0.39	22.41	11.596	11.926	429.46	405.21
4	5	0.36	27.85	11.304	11.732	258.83	335.75
5	6	0.32	34.90	11.249	11.586	133.34	278.14
6	7	0.31	41.08	12.204	12.504	95.49	260.71
7	8	0.37	43.84	14.990	15.320	212.8	326.63

It is apparent from Table 6.1 that the residual aluminium in water after energy optimisation for EC, is still higher than IS:10500:2012 [25] permissible limit ($0.2\,mg/L$) and needs further removal. Therefore, further steps were taken to control the aluminium.

6.3 Particle size and turbidity analysis

Particle size is an important parameter for flocculation studies [153]. Particle sizes in water sample after EC were measured to make a decision for further treatment. Turbidity of the samples was also recorded. Table 6.2 presents the results of particle size and turbidity, of the set no. 1, 4 and 7 (Refer Table 6.1).). D(0.5), D(0.1) and D(0.9) are standard percentile readings from the analysis. D(0.5) is the size in microns

at which 50% of the sample is smaller and 50% is larger. D(0.1) is the size of particle below which 10% of the sample lies. D(0.9) is the size of particle below which 90% of the sample lies.

The high turbidity in the range of $21-54$ NTU (Table 6.2) and high aluminium after EC with optimised energy input (Table 6.1) indicates requirement of further treatment. The turbidity is due to the aluminium complexes formed during the EC treatment for fluoride removal. The particle size of these flocs (Table 6.2) is less than $100\,\mu m$; this indicates that flocculation and settling will be a good choice to remove flocs [153].

Table 6.2: Particle size and turbidity for EC runs

Set No.	***Particle Size*** (μm)			***Turbidity (NTU)***
	D0.1	***D0.5***	***D0.9***	
1	4.282	13.306	24.488	21
4	4.244	14.386	45.721	32
7	6.186	21.496	62.410	54

6.4 Aluminium control by flocculation, settling and filtration

The next step to control aluminium is by flocculation and settling. A preliminary investigation was carried out to find a suitable flocculation time. This study was performed on set no. 1, 4 and 7 (Table 6.1), by varying the flocculation time ($10-30\,min$) and keeping the settling time constant ($30\,min$). The flocculation intensity was kept as $10\,rpm$ for all experiments. Residual aluminium was measured after $30\,min$ of settling time and filtration.

It can be observed from Figure 6.1 that when flocculation time was increased from 10 to $20\,min$ residual aluminium decreases. But further increase in flocculation time, increases the residual aluminium. Therefore, $20\,min$ of flocculation time was found suitable and was kept constant for all experiments.

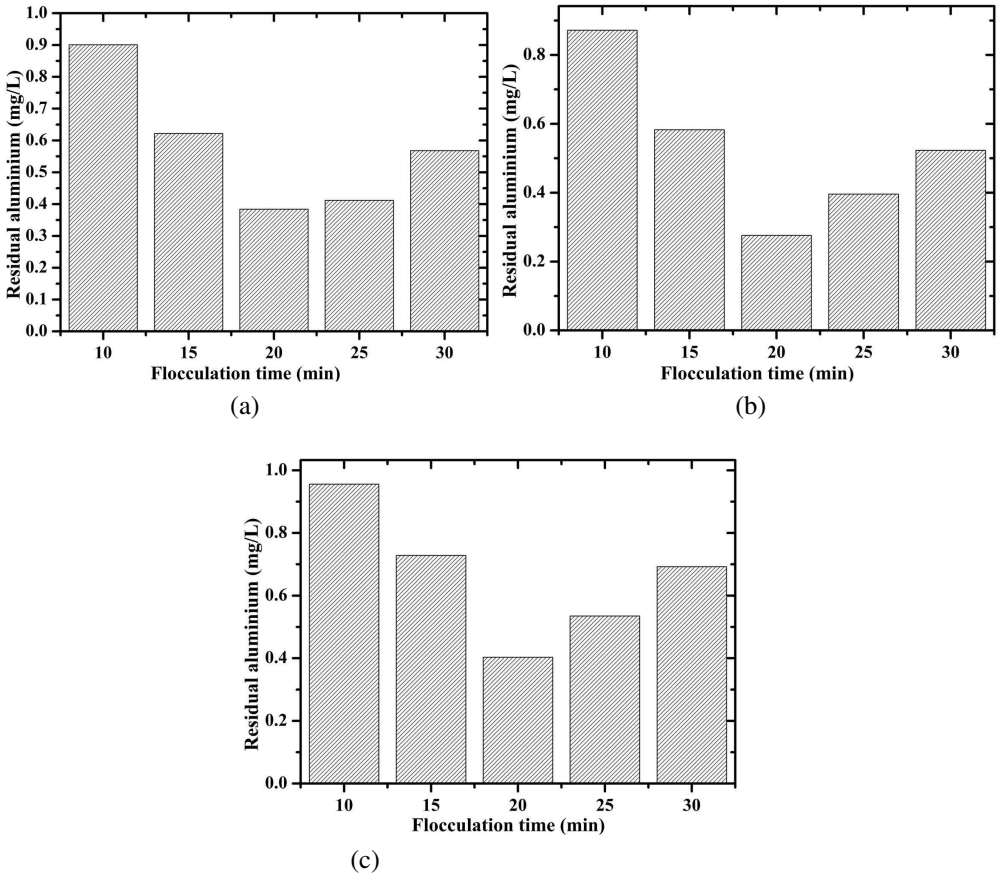

Figure 6.1: Effect of flocculation time on residual aluminium (a) Set 1 (b) Set 4 (c) Set 7.

To control the aluminium concentration in treated water flocculation, settling and filtration was attempted for all the optimized sets. After EC process is completed the sample was stirred for 20 min at 10 rpm and settled for 30 min. The supernatant was filtered with 2.2 μm filter (Whatman Grade 42) and the aluminium concentration was measured. The results are shown in Table 6.3.

Table 6.3: Residual aluminium concentration after flocculation, settling and filtration.

S.No	F_i ***(mg/L)***	Al_{EC} ***(mg/L)***	***Aluminium after flocculation and settling (mg/L)***	***Aluminium after flocculation, settling and filtration (mg/L)***
1	2	14.018	1.854	0.384
2	3	12.723	1.693	0.357
3	4	11.926	1.525	0.295
4	5	11.732	1.510	0.276
5	6	11.586	1.480	0.252
6	7	12.504	1.685	0.384
7	8	15.320	1.972	0.403

The pH measured after EC is in the range of 6.52–7.13; at this pH range, the aluminium has minimum solubility [44], which indicates that majority of aluminium present in water is contributed by aluminium hydroxide flocs formed during electrolysis. The turbidity of the samples was in the range of 4.8–6.9 NTU, which also confirms the hypothesis pertaining to presence of aluminium in bind forms. Therefore, it was necessary to remove these flocs efficiently to reduce the aluminium concentration in water. In the present study the aluminium concentration after EC was in the range of $6.2 - 48.5\, mg/L$ which was brought down to range $11.586 - 15.320\, mg/L$ through optimized energy usage. It is apparent from Table 6.3 that aluminium concentration in water after flocculation, settling and filtration is reduced, but is still more than the permissible limits. Thus, to improve settling efficiency, coagulant aid was used followed by flocculation, settling and filtration.

6.5 Addition of coagulant aid

The results in Table 6.3 explain that to control the residual aluminium, flocculation and settling was important. The results of aluminium obtained by plain flocculation and settling are close to the permissible limit. This suggests that aluminium in the water after EC is because of flocs. Settling alone (without coagulant aid) is not sufficient for efficient removal of these flocs and thus indicates the requirement of addition of coagulant aid to promote coagulation for better settling.

Today, the prime concern of the environmental engineers is how to lower the coagulants cost and to improve the characteristics of the produced sludge for safe disposal/reuse. In the present work, the first choice was bentonite clay, which is a natural coagulant aid. The usage of natural coagulant aid like bentonite is increasing due to its abundance, low price, and good adsorption capabilities [154]. Bentonite is

cheaper than chemicals and it fulfils the economic benefits of the operators as well as environmental concerns.

The second coagulant aid chosen was activated silica sol. Activated silica sol is a short chain polymer which is capable of binding aluminium hydrate particles used in coagulation processes. Activated silica sol is formed by polymerization of silicic acid which has no harmful effects and silica has a strong and unique affinity for aluminium [155]. Evidence is accumulating, largely through the pioneering work of the late J.D.Birchall and coworkers, that silicic acid ($Si(OH)_4$(aq)) interacts with aqueous $Al(III)$ so as to reduce the bioavailability (and hence the toxicity) of the latter [156]. In humans, silicic acid seems to reduce gastro-intestinal absorption of $Al(III)$ and to enhance its excretion through the kidneys [156]. Also few researches have reported that correlation of aluminium and Alzheimer's disease has lead to the use of silicic acid in beverages [157], due to its abilities to both reduce aluminium uptake in the digestive system as well as cause renal excretion of aluminium.

In the present study, two coagulant aids (bentonite and activated silica sol) were used for removing aluminium, owing to their above mentioned benefits.

6.6 Bentonite dosing

Bentonite, which is predominantly montmorillonite clay, is characterized by one Al octahedral sheet placed between two Si tetrahedral sheets. The isomorphous substitution of Al^{3+} for Si^{4+} in the tetrahedral layer and Mg^{2+} for Al^{3+} in the octahedral layer results in a net negative surface charge on the bentonite [158]. This charge imbalance is offset by exchangeable cations (Na^+ and Ca^{2+}, etc.) at the bentonite surface. Since bentonite is negatively charged, all the positively charged aluminium species are adsorbed by bentonite. The layered structure of the clay expands after wetting. Na^+ and Ca^{2+} are strongly hydrated in the presence of water, resulting in a hydrophilic environment at the bentonite surface [159]. Bentonite disperses into colloidal particles and provides large surface area per unit weight of clay [160]. When bentonite disaggregates in water, swelling takes place and the average clay particle size decreases. As a function of decreasing particle size, the number of particles per unit weight of clay increases and hence the available surface area increases [160]. Moreover, swelling of clay particles also helps in availability of more surface area. This large surface area provides greater contact opportunity and leads to destabilization by charge neutralization. Their sorption capabilities come from their high surface areas and exchange capacities [161]. It is a highly effective natural clay mineral, especially in granular form, used for the purification. The second advantage of using bentonite is improvement of floc properties. It adds weight to the flocs and cause them to settle more rapidly than flocs containing mostly $Al(OH)_3$.

The usage of natural clay minerals such as bentonite for water and wastewater treatment are increasing because of their abundance, low price, and adsorption capabilities, as well as ion exchange that is highly capable of adsorbing all kinds of pollutants for some organic and inorganic compounds, including heavy metals in waters [154]. This outstanding capability is due to the presence of the mineral montmorillonite [162]. Moreover, bentonite is cheaper than chemicals and it fulfils the economic benefits of the operators as well as environmental concerns [163]. However, coagulants that are commercialised in the market are mostly chemical-based, which are non-environmental friendly and may create adverse impacts on the surrounding environment [158].

The experimental investigations were carried out to determine appropriate flocculation time. These investigations were performed for set no. 1, 4 and 7. The dose of bentonite ($1\,g/L$) and settling time ($30\,min$) was kept constant, while the flocculation time was varied from $10-30\,min$. Results for residual aluminium at varying flocculation time are shown in Figure 6.2.

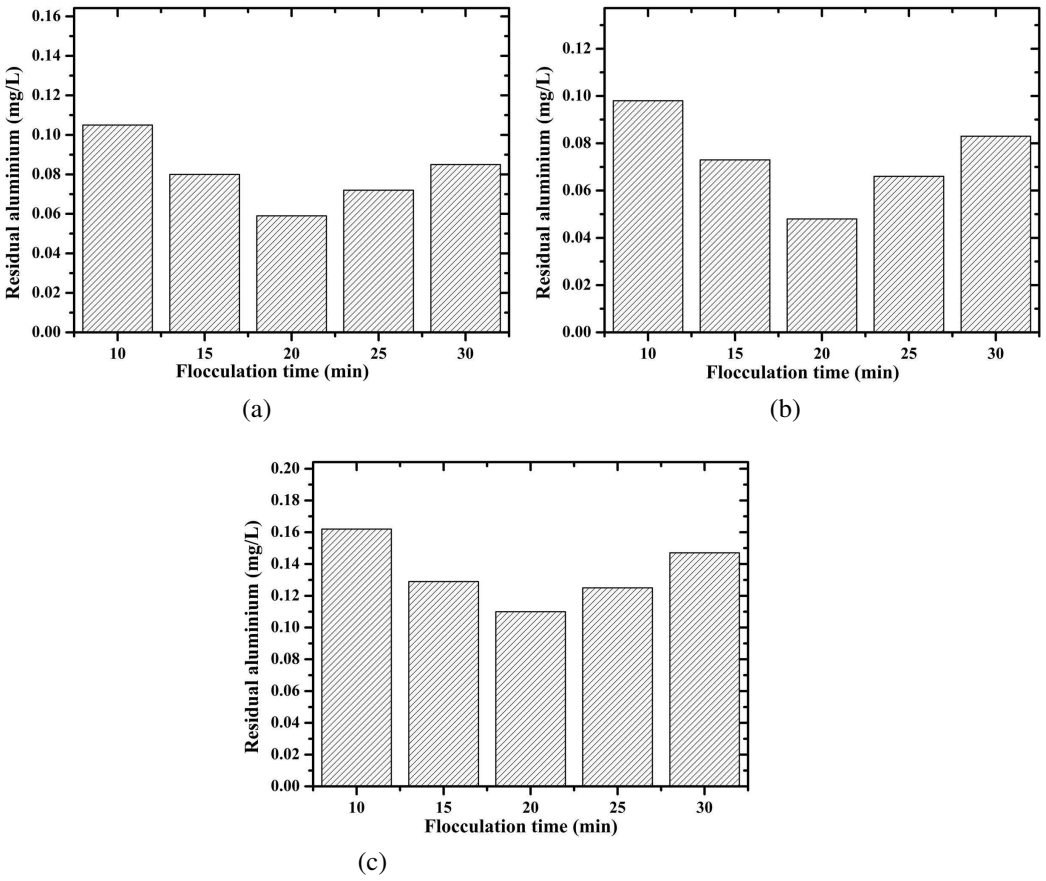

Figure 6.2: Effect of flocculation time on residual aluminium after addition of bentonite (a) Set 1 (b) Set 4 (c) Set 7.

It is evident from Figure 6.2 that $20\,min$ flocculation time gave better removal efficiency. Therefore, it was kept constant for all experiments.

Preliminary investigations were carried out on set no.1, 4 and 7 (Table 6.4-6.6). Bentonite was added after the EC process, and mixed thoroughly for 1 min at 40 rpm. Four doses of bentonite clay, $1-4\,g/L$ were used for the analysis. This was followed by flocculation (20 min) and settling (30 min). For aluminium analysis the supernatant was analyzed directly as well as after filtration (2.2 μm filter). The detailed results for analysis of pH, alkalinity, turbidity and residual aluminium has been presented in (Table 6.4-6.6) for the above mentioned sets.

Table 6.4: Detailed investigation on Set 1(F_i=2 mg/L) for assessment of turbidity, pH, alkalinity and residual aluminium.

Bentonite dose	***Parameters***	***After EC***	***After bentonite dosing and settling***	***After settling and filtration***
$1\,g/L$	Aluminium (mg/L)	14.018	0.462	0.082
	Turbidity (NTU)	32	4.3	1.5
	pH	6.32	6.45	7.13
	Alkalinity (mg/L as $CaCO_3$)	106	80	-
$2\,g/L$	Aluminium (mg/L)	14.018	0.381	0.072
	Turbidity (NTU)	32	3.9	1.5
	pH	6.35	6.55	7.12
	Alkalinity (mg/L as $CaCO_3$)	108	75	-
$3\,g/L$	Aluminium (mg/L)	14.018	0.490	0.087
	Turbidity (NTU)	32	6.15	2.4
	pH	6.35	6.55	7.12
	Alkalinity (mg/L as $CaCO_3$)	106	80	-
$4\,g/L$	Aluminium (mg/L)	14.018	0.534	0.101
	Turbidity (NTU)	32	7.9	2.5
	pH	6.32	6.62	7.30
	Alkalinity (mg/L as $CaCO_3$)	106	85	-

Table 6.5: Detailed investigation on Set 4 (F_i=5 mg/L), for assessment of turbidity, pH, alkalinity and residual aluminium.

Bentonite dose	***Parameters***	***After EC***	***After bentonite dosing and settling***	***After settling and filtration***
1 g/L	Aluminium (mg/L)	11.732	0.301	0.048
	Turbidity (NTU)	21	3.7	1.4
	pH	6.58	6.72	7.12
	Alkalinity (mg/L as $CaCO_3$)	102	67	-
2 g/L	Aluminium (mg/L)	11.732	0.282	0.032
	Turbidity (NTU)	21	3.3	1.0
	pH	6.60	6.75	7.10
	Alkalinity (mg/L as $CaCO_3$)	104	80	-
3 g/L	Aluminium (mg/L)	11.732	0.421	0.039
	Turbidity (NTU)	21	5.2	1.7
	pH	6.65	6.70	7.10
	Alkalinity (mg/L as $CaCO_3$)	104	82	-
4 g/L	Aluminium (mg/L)	11.732	0.490	0.054
	Turbidity (NTU)	21	6.9	2.0
	pH	6.65	6.78	7.12
	Alkalinity (mg/L as $CaCO_3$)	106	100	-

Table 6.6: Detailed investigation on Set 7 (F_i=8 mg/L), for assessment of turbidity, pH, alkalinity and residual aluminium.

Bentonite dose	***Parameters***	***After EC***	***After bentonite dosing and settling***	***After settling and filtration***
1 g/L	Aluminium (mg/L)	15.320	0.592	0.110
	Turbidity (NTU)	54	4.0	1.5
	pH	6.93	7.10	7.20
	Alkalinity (mg/L as $CaCO_3$)	106	100	-
2 g/L	Aluminium (mg/L)	15.320	0.456	0.080
	Turbidity (NTU)	54	3.5	1.3
	pH	6.90	7.12	7.25
	Alkalinity (mg/L as $CaCO_3$)	106	80	-
3 g/L	Aluminium (mg/L)	15.320	0.619	0.130
	Turbidity (NTU)	54	7.4	2.6
	pH	6.90	7.10	7.22
	Alkalinity (mg/L as $CaCO_3$)	104	70	-
4 g/L	Aluminium (mg/L)	15.320	0.704	0.149
	Turbidity (NTU)	56	8.4	2.6
	pH	6.95	7.12	7.24
	Alkalinity (mg/L as $CaCO_3$)	108	85	-

The results shown above indicate that the water treated after EC has high turbidity ($21-54\,NTU$) and low alkalinity ($104-108\,mg/L$ as $CaCO_3$). The pH after EC treatment is in the range of $6.32-6.95$. This suggests that aluminium hydroxides in this pH range are mostly positively charged hydroxymetal polymers. On addition of bentonite, which is negatively charged, these positively charged particles are destabilized by negatively charged bentonite. Also, bentonite increases the particle concentration in the system which may also favour sweep coagulation to occur. These investigations also show that filtration was required after settling to bring down the aluminium concentration to permissible levels.

This study leads to the development of a statistical model for aluminium removal by bentonite dosing. The further sections explain the statistical model developed for this technique.

6.7 Implementation of Taguchi design (Bentonite dosing)

To achieve a better design covering the entire parametric space; the experimental study was designed using 4 level Taguchi design method (L16 2^4). The operating parameters were aluminium after EC (Al_{EC}) and bentonite dose (D_b) for estimation of response (aluminium after bentonite dosing). Levels for the operating parameter "Al_{EC}" were selected by the results obtained in Table 6.1 (Column 2). The minimum and maximum value of aluminium was selected as Level 1 and Level 4. The values of Level 2 and Level 3 were selected between these two extreme values. The levels of operating parameters are presented in Table 6.7. MINITAB 14 software was used for analysis of results.

Table 6.7: Levels used for operational parameters.

Parameters	***Notation***	***Units***	***Level*** 1	***Level*** 2	***Level*** 3	***Level*** 4
Aluminium after EC	Al_{EC}	mg/L	11.586	12.723	14.018	15.320
Bentonite dose	D_b	g/L	1	2	3	4

Sixteen experiments were performed to determine residual aluminium (response parameter). The input settings and respective responses are presented in Table 6.8.

Table 6.8: Orthogonal array for L16 (2^4) Taguchi Design.

S.No	***Operating parameters***		***Response***
	Al_{EC} (mg/L)	D_b(g/L)	Al_{bd}(mg/L)
1	11.586	1	0.048
2	11.586	2	0.030
3	11.586	3	0.037
4	11.586	4	0.053
5	12.723	1	0.054
6	12.723	2	0.044
7	12.723	3	0.050
8	12.723	4	0.060
9	14.018	1	0.082
10	14.018	2	0.072
11	14.018	3	0.087
12	14.018	4	0.101
13	15.320	1	0.110
14	15.320	2	0.080
15	15.320	3	0.130
16	15.320	4	0.149

The experiments were performed in duplicate sets and the average results have been reported in the Table 6.8. It can be clearly observed that aluminium concentration was within permissible limit for all the applied doses of bentonite. Maximum removal was observed at the dose of $2\,g/L$. The response values were transformed into S/N ratios. In this study also, the aim was to minimize the aluminium after bentonite dosing, so S/N ratio was calculated by "smaller-the-best" formulation as given in Equation 5.1. This suggests that the largest S/N ratio value denotes the minimum response value.

6.7.1 Validation of the model

As explained earlier in Chapter 5, the model is validated by ANOVA and residual plots. High R^2 value of 0.9355 suggests towards the validity of the model (Table 6.9). Further confirmation was provided by residual plots. Minimum deviation of points from the straight line as shown in Figure 6.3 and constant variance of points as shown in Figure 6.4 also indicates towards the validity of the model developed.

Table 6.9: ANOVA table for residual aluminium after bentonite dosing.

Source	***DF***	***Seq SS***	***Adj SS***	***Adj MS***	***F***	***P***
Al_{EC}	3	186.067	186.067	62.022	37.06	0.000
D_b	3	32.369	32.369	10.790	6.45	0.013
Error	9	15.064	15.064	1.674		
Total	15	233.500				
S = 1.293 R^2 = 0.9355						

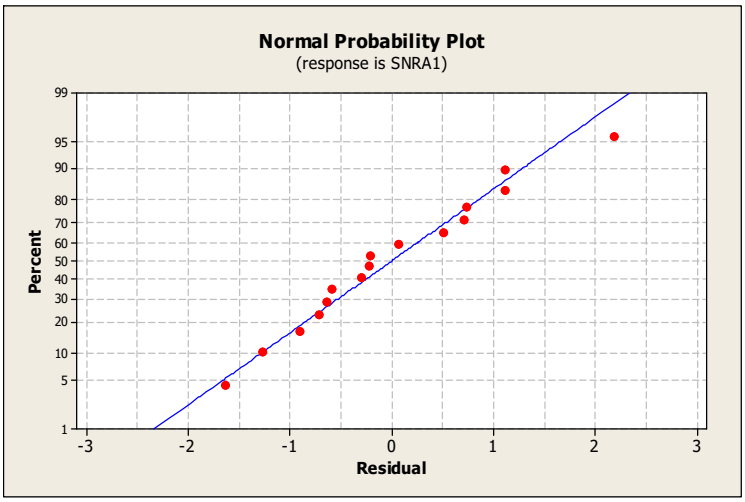

Figure 6.3: Normal probability plot for residual aluminium after bentonite dosing.

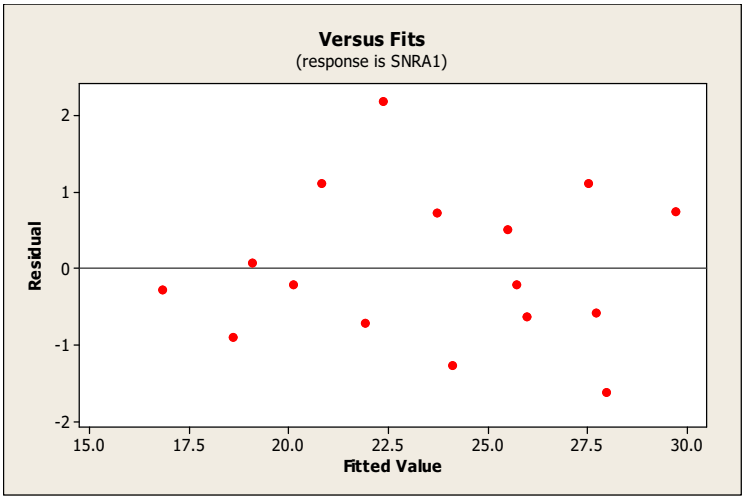

Figure 6.4: Residual v/s fit plot for residual aluminium after bentonite dosing.

6.7.2 Main effect and interaction effect plots

The main effect and interaction plots were prepared by using MINITAB 16.0 software. The plots are shown in Figure 6.5 and 6.6.

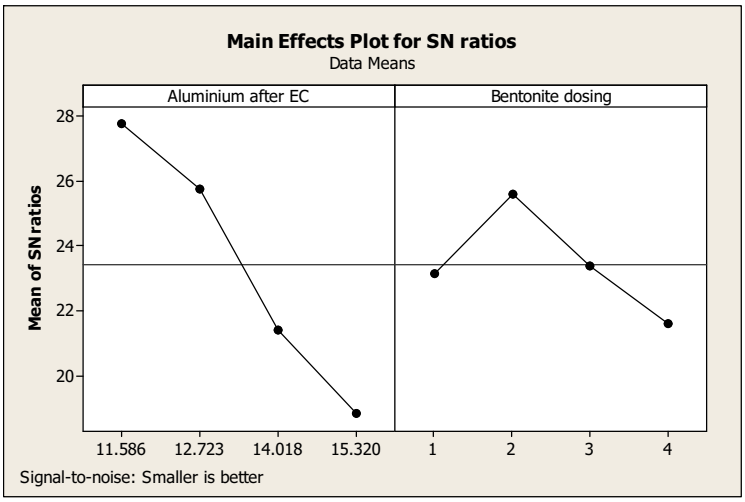

Figure 6.5: Main effect plot for residual aluminium after bentonite dosing.

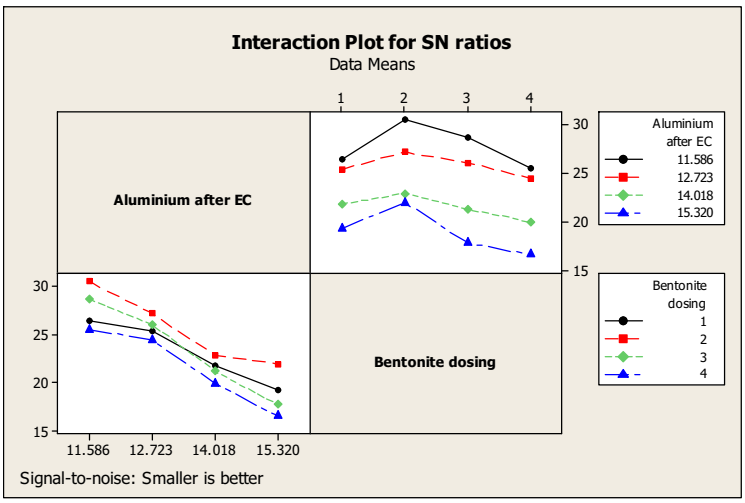

Figure 6.6: Interaction plot for residual aluminium after bentonite dosing.

It is apparent from the plots that aluminium after settling with coagulant aid is proportional to the aluminium in water after EC. This underlines requirement of optimization of energy input to control aluminium dissolution during electrolysis. A preliminary control of aluminium is helpful to make the dosing process efficient. These plots further explain that, dose of $2\,g/L$ was the optimum dose for controlling the aluminium content. On further increasing the dose, the aluminium content also starts increasing.

6.7.3 Development of regression equation and its verification

The expression to calculate residual aluminium after bentonite dosing was developed using normalised values of data, presented in Table 6.8. The data is normalised by dividing each value with the maximum existing value in the column. SYSTAT 7.0 was used for this purpose and the expression is presented in Equation 6.1.

$$Al_{bd} = 4.435 - (9.893 \times Al_{EC}) - (2.235 \times D_b) + (1.828 \times Al_{EC} \times D_b) + (6.174 \times Al_{EC}^2) + (0.698 \times D_b^2) \quad (6.1)$$

To verify the correctness of the equations obtained, actual v/s predicted response graphs were plotted. Fourteen set of experiments as mentioned in Table 6.10 were performed to verify the equations. The graphs and their respective R^2 value are displayed in the Figure 6.7.

Table 6.10: Operational parameter settings and their respective actual and predicted responses selected for verification of regression equations.

S.No	***Operational parameters***		Al_{bd}***(mg/L)***	
	Al_{EC} ***(mg/L)***	D_b***(g/L)***	***Predicted***	***Experimental***
1	11.586	2	0.035	0.030
2	11.732	2	0.035	0.032
3	11.926	2	0.036	0.036
4	12.504	2	0.041	0.040
5	12.723	2	0.044	0.044
6	14.018	2	0.066	0.072
7	15.320	2	0.102	0.080
8	15.320	4	0.150	0.150
9	14.018	4	0.102	0.102
10	14.018	3	0.077	0.078
11	11.586	3	0.035	0.036
12	12.504	1	0.049	0.053
13	11.926	1	0.047	0.050
14	12.504	1	0.049	0.053

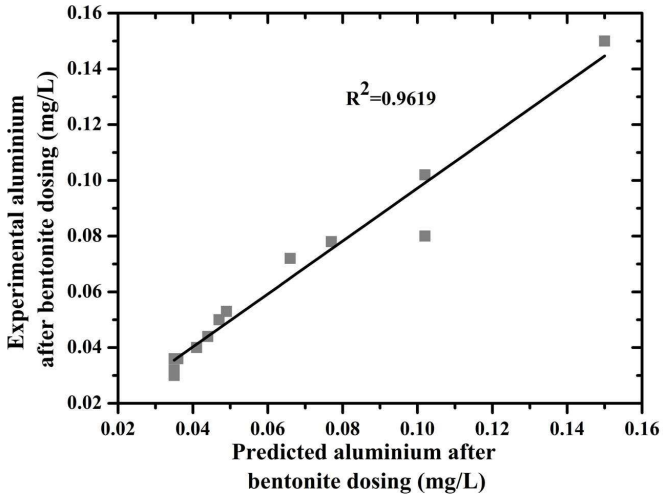

Figure 6.7: Actual v/s predicted values for aluminium after bentonite dosing.

Figure 6.7 explains that the model is fit for use and can be used for prediction of results, owing to the high R^2 value (0.9619) obtained.

6.8 Activated silica sol dosing

Colloidal silica or Activated silica sol have been used for many years to coagulate suspended particles in water. The silica sols envelop the particles and settle out of solution, thereby clarifying the water. They are prepared by using sodium silicate solution and activating it by adding acid which permits the growth of silicate micelles. The first activated silica sol successfully used as a coagulant aid in the treatment of raw water was developed by J.R. Baylis of the Department of Public Works, Chicago and reported his investigations in 1937. For better use of activated silica sol as coagulant aid, understanding the nature of silicate solution is essential. The solution of sodium silicate which is highly alkaline in nature is neutralized by addition of acid. During this process the silicate ion decomposes to silicic acid. Polymerized silica formation takes place in two stages; in the first initially formed silicic acid condenses into colloidal particles. Further dilution of the solution causes slow increase in particle size. Under certain conditions, aggregation of particles increases and a certain degree of rigidity is bestowed in the medium.

The precipitation process begins with the formation of polysilicate polymers that contain –Si—O—Si—linkages. These polysilicates react further by cross linking and aggregation to form negatively charged silica sols.

Si(OH)4→Polymerizes→Colloidal particles (sol)→Aggregation

Activated silica sol was prepared by the following method. A 3% of sodium silicate solution was prepared and mixed with equal volume of 0.33N sulphuric acid. This results into a 1.5% silica solution. By this process the initial alkalinity of the solution was neutralized and the pH of the current solution is 8.5.

The experimental investigations were carried out to determine appropriate flocculation time. These investigations were performed for set nos. 1,4 and 7. The dose of activated silica sol ($10\,mg/L$) and settling time ($30\,min$) was kept constant, while the flocculation time was varied from $10-30\,min$. Results of residual aluminium at varying flocculation time are shown in Figure 6.8.

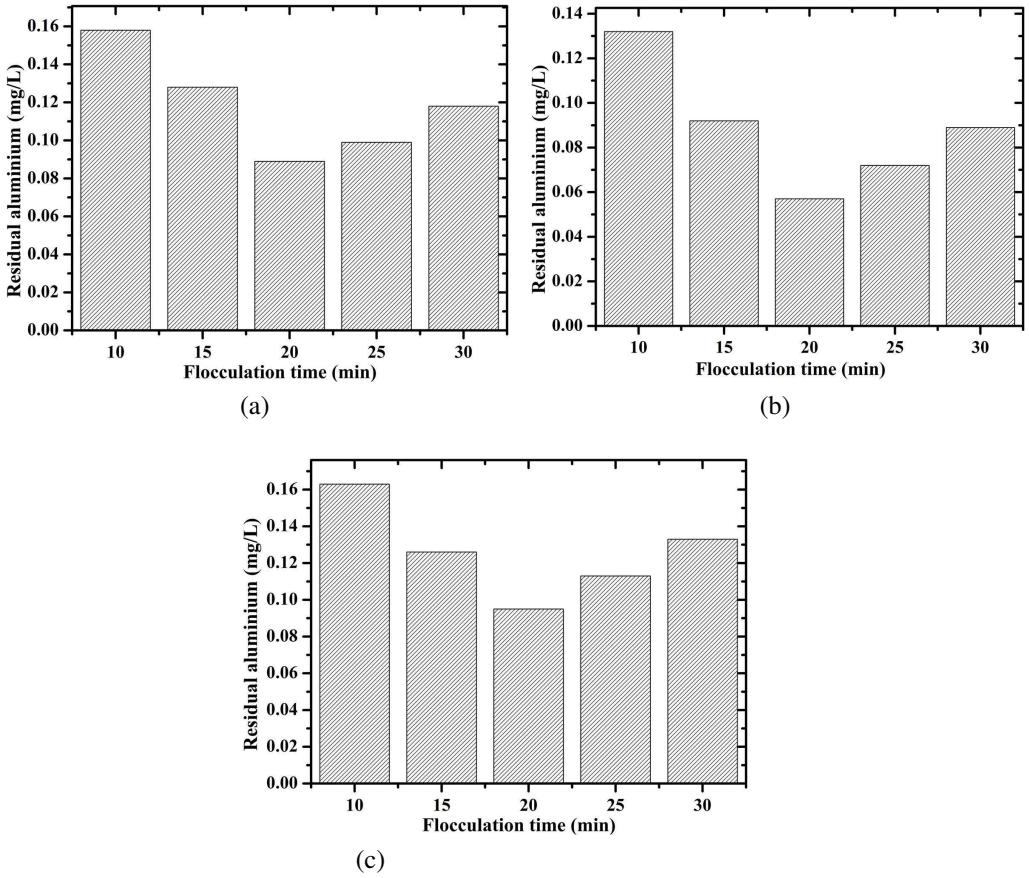

Figure 6.8: Effect of flocculation time on residual aluminium (a) Set 1 (b) Set 4 (c) Set 7.

It is evident from Figure 6.8 that 20 *min* flocculation time gave better removal efficiency. Therefore, it was kept constant for all experiments.

Preliminary investigations were carried out on set no 1, 4 and 7 (Table 6.11-6.13). Activated silica sol was added after EC process, and mixed thoroughly for 1 *min* at 40 *rpm*. The doses of activated silica sol are 10, 30, 50 and 70 mg/L. This was followed by flocculation (20 *min*) and settling (30 *min*). For aluminium analysis the supernatant was analyzed before and after filtration (2.2 μm filter). The detailed results are presented in Table 6.11-6.13.

Table 6.11: Detailed investigation on Set 1(F_i=2 mg/L) for assessment of turbidity, pH, alkalinity and residual aluminium.

Activated silica sol dose	***Parameters***	***After EC***	***After activated silica sol dosing and settling***	***After settling and filtration***
10 mg/L	Aluminium (mg/L)	14.018	0.097	0.089
	Turbidity (NTU)	32	4.3	1.4
	pH	6.32	6.45	7.13
	Alkalinity (mg/L as $CaCO_3$)	106	75	-
30 mg/L	Aluminium (mg/L)	14.018	0.050	0.029
	Turbidity (NTU)	32	3.9	1.0
	pH	6.35	6.55	7.12
	Alkalinity (mg/L as $CaCO_3$)	108	80	-
50 mg/L	Aluminium (mg/L)	14.018	0.065	0.037
	Turbidity (NTU)	32	6.1	1.7
	pH	6.35	6.55	7.12
	Alkalinity (mg/L as $CaCO_3$)	106	80	-
70 mg/L	Aluminium (mg/L)	14.018	0.101	0.085
	Turbidity (NTU)	32	7.9	2.0
	pH	6.32	6.62	7.30
	Alkalinity (mg/L as $CaCO_3$)	106	80	-

Table 6.12: Detailed investigation on Set 4(F_i=5 mg/L) for assessment of turbidity, pH, alkalinity and residual aluminium.

Activated silica sol dose	***Parameters***	***After EC***	***After activated silica sol dosing and settling***	***After settling and filtration***
10 mg/L	Aluminium (mg/L)	11.732	0.069	0.057
	Turbidity (NTU)	21	1.3	0.3
	pH	6.55	6.60	7.10
	Alkalinity (mg/L as $CaCO_3$)	106	70	-
30 mg/L	Aluminium (mg/L)	11.732	0.012	0.005
	Turbidity (NTU)	21	0.5	0.63
	pH	6.53	6.60	7.12
	Alkalinity (mg/L as $CaCO_3$)	108	75	-
50 mg/L	Aluminium (mg/L)	11.732	0.035	0.016
	Turbidity (NTU)	21	1.8	0.6
	pH	6.52	6.65	7.30
	Alkalinity (mg/L as $CaCO_3$)	106	85	-
70 mg/L	Aluminium (mg/L)	11.732	0.080	0.062
	Turbidity (NTU)	21	2.5	0.8
	pH	6.50	6.73	7.35
	Alkalinity (mg/L as $CaCO_3$)	106	80	-

Table 6.13: Detailed investigation on Set 7(F_i=8 mg/L) for assessment of turbidity, pH, alkalinity and residual aluminium

Activated silica sol dose	***Parameters***	***After EC***	***After activated silica sol dosing and settling***	***After settling and filtration***
10 mg/L	Aluminium (mg/L)	15.320	0.110	0.095
	Turbidity (NTU)	54	2.2	1.0
	pH	6.85	7.01	7.20
	Alkalinity (mg/L as $CaCO_3$)	106	82	-
30 mg/L	Aluminium (mg/L)	15.320	0.055	0.034
	Turbidity (NTU)	54	1.5	0.8
	pH	6.83	7.05	7.25
	Alkalinity (mg/L as $CaCO_3$)	108	75	-
50 mg/L	Aluminium (mg/L)	15.320	0.071	0.045
	Turbidity (NTU)	54	3.2	0.8
	pH	6.82	7.10	7.30
	Alkalinity (mg/L as $CaCO_3$)	106	80	-
70 mg/L	Aluminium (mg/L)	15.320	0.108	0.093
	Turbidity (NTU)	54	4.0	1.2
	pH	6.80	7.12	7.38
	Alkalinity (mg/L as $CaCO_3$)	106	70	-

The results shown in Table 6.11-6.13 indicate that the water treated after EC has high turbidity ($21-54\,NTU$) and low alkalinity ($106-108\,mg/L$ as $CaCO_3$). The pH after EC treatment is in the range of $6.32-6.85$. High turbidity and low alkalinity suggests the mechanism of charge neutralization for coagulation. To understand the mechanism of removal it is required to study the surface groups present on the activated silica sol. Flocculation of activated silica sol with polymeric aluminium should begin with the formation of negatively charged aluminosilicate sites. Aluminosilicate sites originate when aluminium polycation is contacted with silanol groups of specific surface sites of silica. Aluminum changing its coordination from 6-fold to 4-fold upon contact with the silica tetrahedral structure and giving rise to a negative charge [164]. These sites, similar to those found in clay minerals and zeolitic materials, represent potential anchors to aluminum polycations [165]. The second stage of destabilization involves the charge compensation of the newly created aluminosilicate sites. Al polymers are expected to remain in the vicinity of the silica surface after reaction and represent therefore the principal cations available for charge balance. Hence, aggregation of silica particles proceeds with either charge neutralization or bridging [166]. In the process of forming colloidal silica, silanol groups are formed on the silica surface in the course of its synthesis during the condensation-polymerization of $Si(OH)_4$ (silicic acid). It is generally agreed that the aluminosilicate sites are formed by condensation of the

silanol groups present on the silica surface with the hydroxyl groups of the hydrolyzed aluminum ions [165] [167]. Thus efficient removal of aluminium takes place from the solution.

These results are used for development of statistical model and presented in next section.

6.9 Implementation of Taguchi Design (Activated silica sol dosing)

Similar procedure as used for bentonite dosing, was implemented for activated silica sol dosing. The levels used in the Taguchi design are presented in Table 6.14.

Table 6.14: Levels used for operational parameters.

Parameters	***Notation***	***Units***	***Level*** 1	***Level*** 2	***Level*** 3	***Level*** 4
Aluminium after EC	Al_{EC}	mg/L	11.586	12.723	14.018	15.320
Bentonite dose	D_{as}	mg/L	10	30	50	70

Sixteen experiments were performed to determine residual aluminium (response parameter). The input settings and respective responses are presented in Table 6.15.

Table 6.15: Orthogonal array for L16 (2^4) Taguchi Design.

S.No	***Operating parameters***		***Response***
	Al_{EC} (mg/L)	D_{as}(mg/L)	Al_{as}(mg/L)
1	11.586	10	0.056
2	11.586	30	0.003
3	11.586	50	0.015
4	11.586	70	0.062
5	12.723	10	0.077
6	12.723	30	0.018
7	12.723	50	0.030
8	12.723	70	0.080
9	14.018	10	0.089
10	14.018	30	0.029
11	14.018	50	0.037
12	14.018	70	0.085
13	15.320	10	0.095
14	15.320	30	0.034
15	15.320	50	0.045
16	15.320	70	0.093

The experiments were performed in duplicate sets and the average results have been reported in the Table 6.15. It can be clearly observed that aluminium concentration

was within permissible limit for all the applied doses of bentonite. Maximum removal was observed at the dose of $30\,mg/L$. The response values were transformed into S/N ratio. In this study also, the aim was to minimize the aluminium after activated silica sol dosing, so S/N ratio was calculated by "smaller-the-best" formulation as given in Equation 5.1. This suggests that the largest S/N ratio value denotes the minimum response value.

6.9.1 Validation of the model

The model is validated by ANOVA and residual plots. High R^2 value of 0.9488 suggests towards the validity of the model as shown in Table 6.16. Further confirmation was provided by residual plots.

Table 6.16: ANOVA table for residual aluminium after bentonite dosing.

Source	*DF*	*Seq SS*	*Adj SS*	*Adj MS*	*F*	*P*
Al_{EC}	3	219.63	219.63	73.21	11.30	0.002
D_{as}	3	853.47	853.47	284.49	44.24	0.000
Error	9	57.88	57.88	6.44		
Total	15	1130.98				
S = 2.535 R^2 = 0.9488						

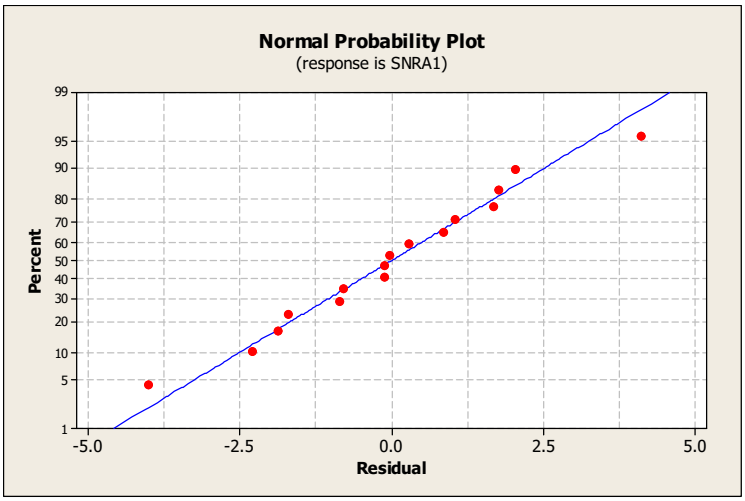

Figure 6.9: Normal probability plot for residual aluminium after activated silica sol dosing.

Minimum deviation of points from the straight line as shown in Figure 6.9 and constant variance of points as shown in Figure 6.10 also indicates towards the validity of the model developed.

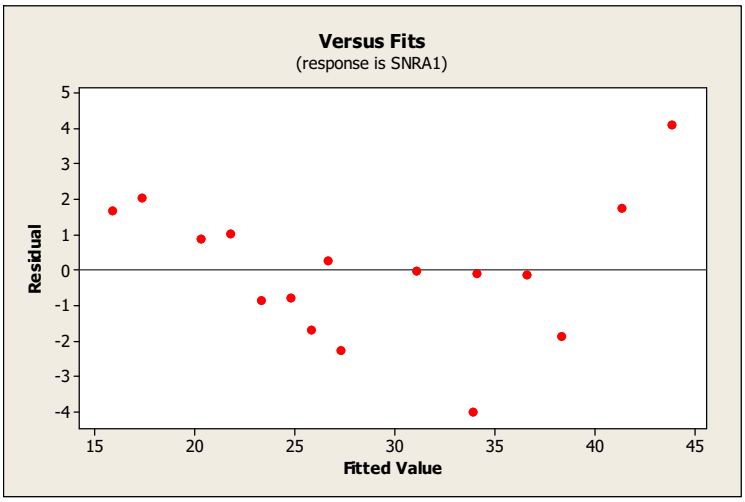

Figure 6.10: Residual v/s fit plot for residual aluminium after activated silica sol dosing.

6.9.2 Main effect and interaction effect plots

The main effects and interaction plot prepared by using Taguchi design and the plots are shown in Figure 6.11 and 6.12. Figure 6.11 explains that as the activated silica dose increases from 10 mg/L to 30 mg/L, the residual aluminium decreases but on increasing the dose further increase in activated silica dose from 30 mg/L to 50 mg/L, the residual aluminium increases. So it can be clearly observed that 30 mg/L is the optimum dose for the performed experiments.

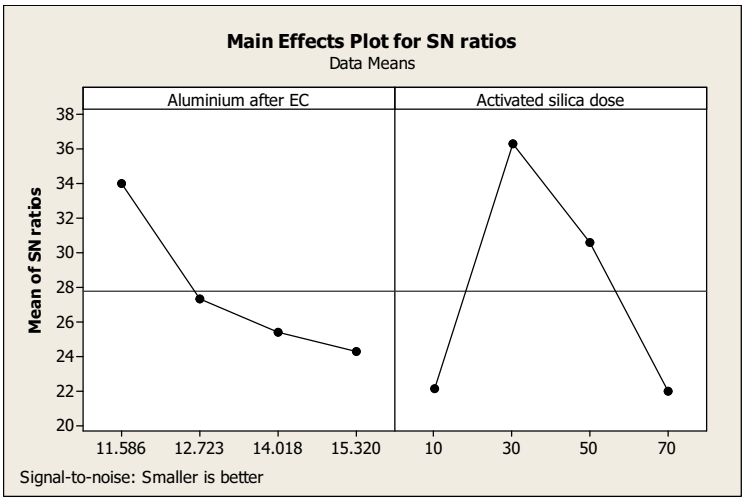

Figure 6.11: Main effect plot for residual aluminium after activated silica sol dosing

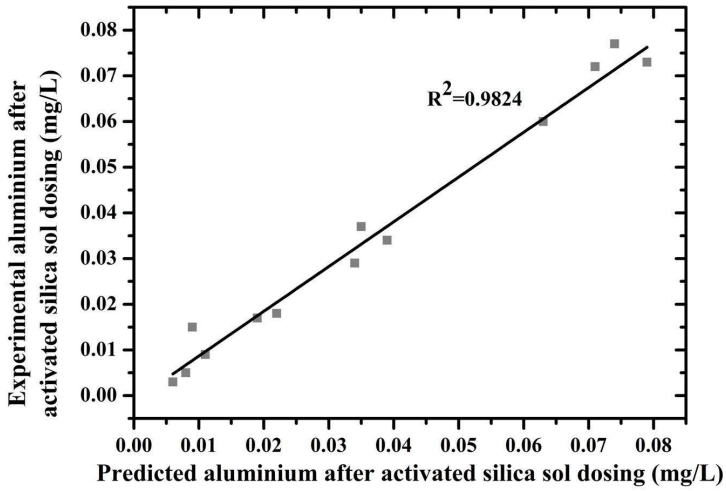

Figure 6.13: Actual v/s predicted values for aluminium after activated silica sol dosing.

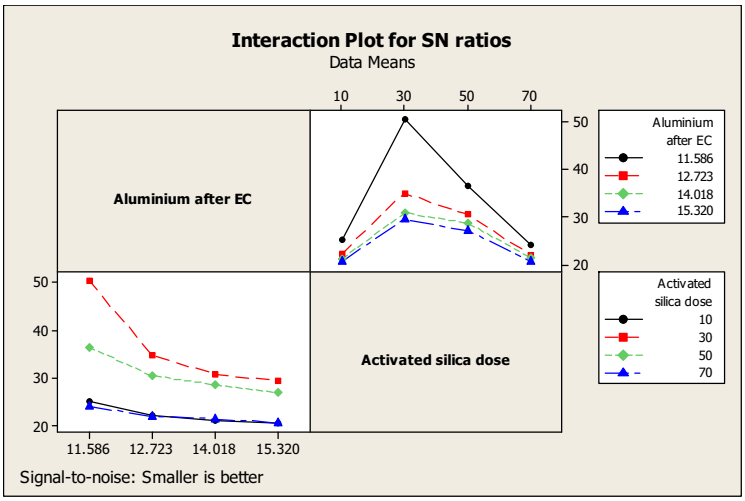

Figure 6.12: Interaction plot for residual aluminium after activated silica sol dosing

6.9.3 Development of regression equation and its verification

The regression equation is obtained by SYSTAT 7.0 software. The expression to obtain residual aluminium after bentonite dosing is shown in Equation 6.2

$$Al_{as} = -3.815 + (10.153 \times Al_{EC}) - (3.588 \times D_{as}) - (0.458 \times Al_{EC} \times D_{as}) - (4.833 \times Al_{EC}^2) + (3.507 \times D_{as}^2) \quad (6.2)$$

To verify the correctness of the equations obtained, actual v/s predicted response graphs were plotted. Fourteen set of experiments as mentioned in Table 6.17 were performed to verify the equations. The graphs and their respective R^2 value are displayed in the Figure 6.13.

Table 6.17: Operational parameter settings and their respective actual and predicted responses selected for verification of regression equations.

S.No	***Operating parameters***		Al_{as}***(mg/L)***	
	Al_{EC} ***(mg/L)***	D_{as}***(g/L)***	***Predicted***	***Experimental***
1	11.586	30	0.006	0.003
2	11.586	50	0.009	0.015
3	12.723	10	0.074	0.077
4	12.723	70	0.079	0.073
5	12.723	30	0.022	0.018
6	14.018	30	0.034	0.029
7	14.018	50	0.035	0.037
8	15.320	30	0.039	0.034
9	11.732	30	0.008	0.005
10	11.926	30	0.011	0.009
11	12.504	30	0.019	0.017
12	12.723	10	0.079	0.073
13	12.504	10	0.071	0.072
14	11.926	10	0.063	0.060

High R^2 value of 0.9824 as shown in Figure 6.13 suggests that the equations are validated and are fit for prediction of results.

It is evident from experimental investigations that bentonite clay and activated silica sol can be effectively used to control aluminium concentration in the water treated by EC. With optimised dose of bentonite, residual aluminium was brought down to a range of $0.03 - 0.08\,mg/L$. Similarly with optimised dose of activated silica sol, residual aluminium was brought down to a much lower range of $0.003 - 0.034\,mg/L$. Thus, it can be concluded that both coagulant aids can effectively bring down the aluminium to IS:10500:2012 [25] permissible limits ($0.2\,mg/L$) in the final water.

Activated silica sol was found to be better than bentonite clay as it reduces aluminium concentration in water to a much lower range than bentonite clay. This result can be attributed to the fact that bentonite clay is negatively charged due to isomorphous substitution of Al^{3+} for Si^{4+} in the tetrahedral layer and Mg^{2+} for Al^{3+} in the octahedral layer. This arrangement is already present in the bentonite which is added. But, in colloidal silica sol the negatively charged aluminosilicates are formed after its addition to the water treated by EC. So, the removal of aluminium occurs in two steps; first aluminium is utilised in the formation of negatively charged aluminosilicates and second the positively charges aluminium polymers are removed by these aluminosilicates as a result of charge neutralization. FTIR scan results further substantiate this fact, which is presented in the next chapter.

6.10 Adsorption isotherms

Adsorption isotherms are studied for removal of aluminium using coagulant aid. Study of adsorption isotherms is the most common way of describing adsorption phenomena.

The experimental data were fitted with Langmuir, Freundlich and Redlich Peterson isotherms. Isotherms were calculated using optimised set of results. Set of six varying initial fluoride concentrations and their respective aluminium concentration after EC (C_0) was used for calculations. The amount of aluminium adsorbed by bentonite was determined using a mass balance equation expressed in Equation 5.6. All the doses for bentonite and activated silica sol were used for developing the isotherms. The experimental q_e was calculated by the Equation 5.6. and the predicted q_e is obtained from the non-linear expressions of the, Langmuir, Freundlich and Redlich Peterson isotherms as shown in Equation 5.13-5.15. In the case of the non-linear method, a trial-and-error procedure was developed to determine the isotherm parameters using an optimization routine to maximize the coefficient of determination between the experimental data and isotherms [168]. This was performed in the solver add-in with Microsoft's spreadsheet, Microsoft Excel. The protocol which has been used is, that experimental data is manually entered in MS-Excel, the formulated algorithm was carried out and the predicted curve was overlaid on the experimental data points and goodness of fit was observed [169]. Goodness of fit was used to estimate the best fit isotherm as explained in Chapter 5.

Data for isotherms for bentonite dosing and activated silica sol dosing has been presented in the appendix C. Table 6.18 and 6.19 presents the isotherm parameters for studied doses of bentonite and activated silica sol respectively.

Table 6.18: Isotherm parameters obtained using non-linear method for bentonite dosing.

Isotherms	***Parameters***	***Bentonite dose (g/L)***			
		1	2	3	4
Langmuir	q_{max}	20.039	17.923	17.245	18.091
	K_l	30.887	57.336	53.349	35.153
	RMSE	0.485	0.322	0.185	0.246
	χ^2	0.016	0.007	0.002	0.004
	R^2	0.8714	0.9430	0.9813	0.9668
Freundlich	K_f	30.250	28.707	23.734	24.525
	n	3.297	3.822	4.619	4.043
	RMSE	0.550	6.269	0.167	0.277
	χ^2	0.020	0.004	0.002	0.005
	R^2	0.8346	0.9602	0.9847	0.9578
Redlich Peterson	g	0.700	0.744	0.788	0.750
	RMSE	0.549	0.271	0.166	0.277
	χ^2	0.020	0.004	0.002	0.005
	R^2	0.8351	0.9600	0.9850	0.9581

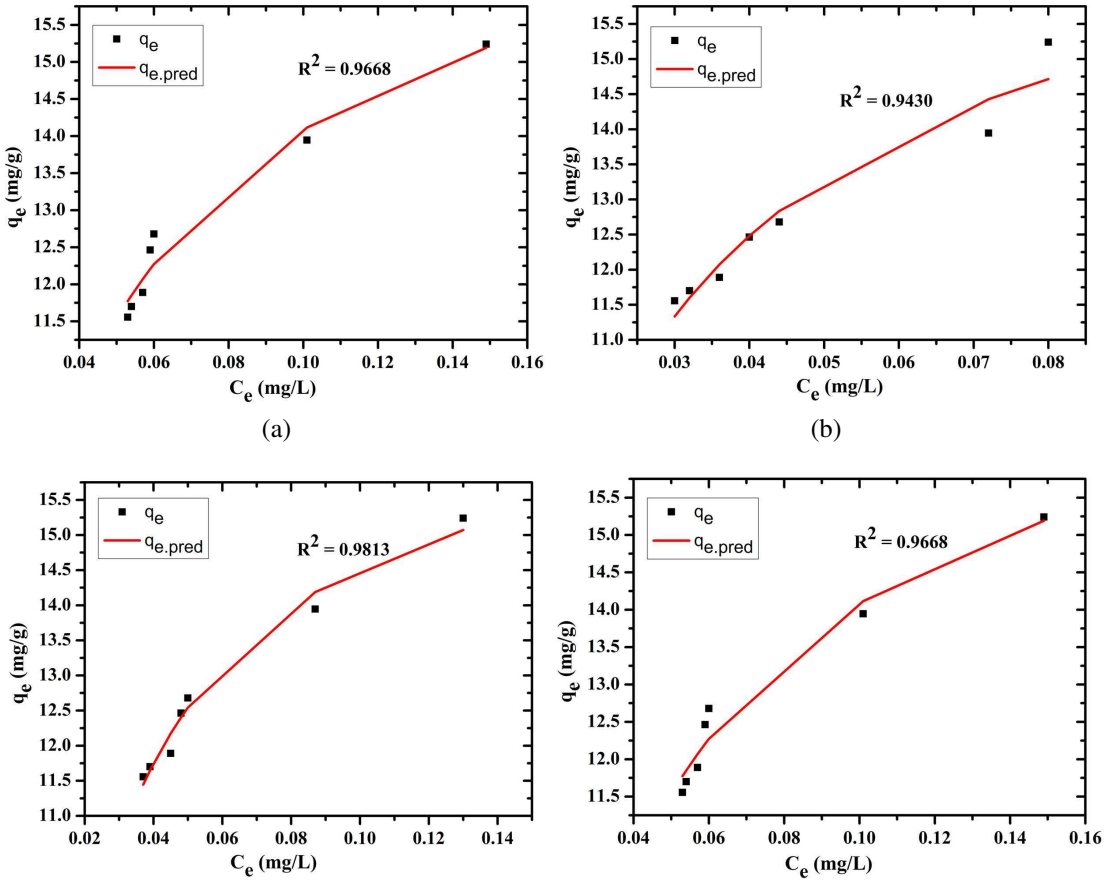

Figure 6.14: Langmuir isotherm at varying doses of bentonite (a) $1\,g/L$ (b) $2\,g/L$ (c) $3\,g/L$ (d) $4\,g/L$.

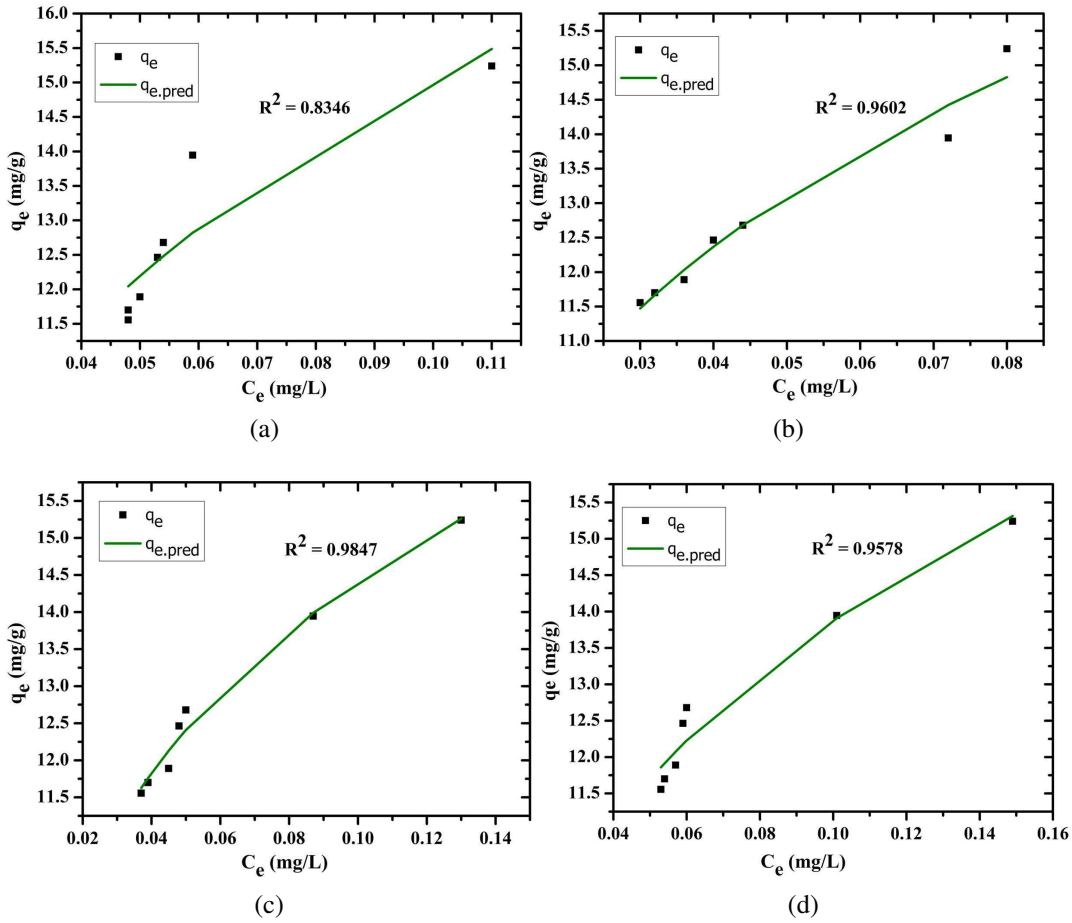

Figure 6.15: Freundlich isotherm at varying doses of bentonite (a) $1\,g/L$ (b) $2\,g/L$ (c) $3\,g/L$ (d) $4\,g/L$.

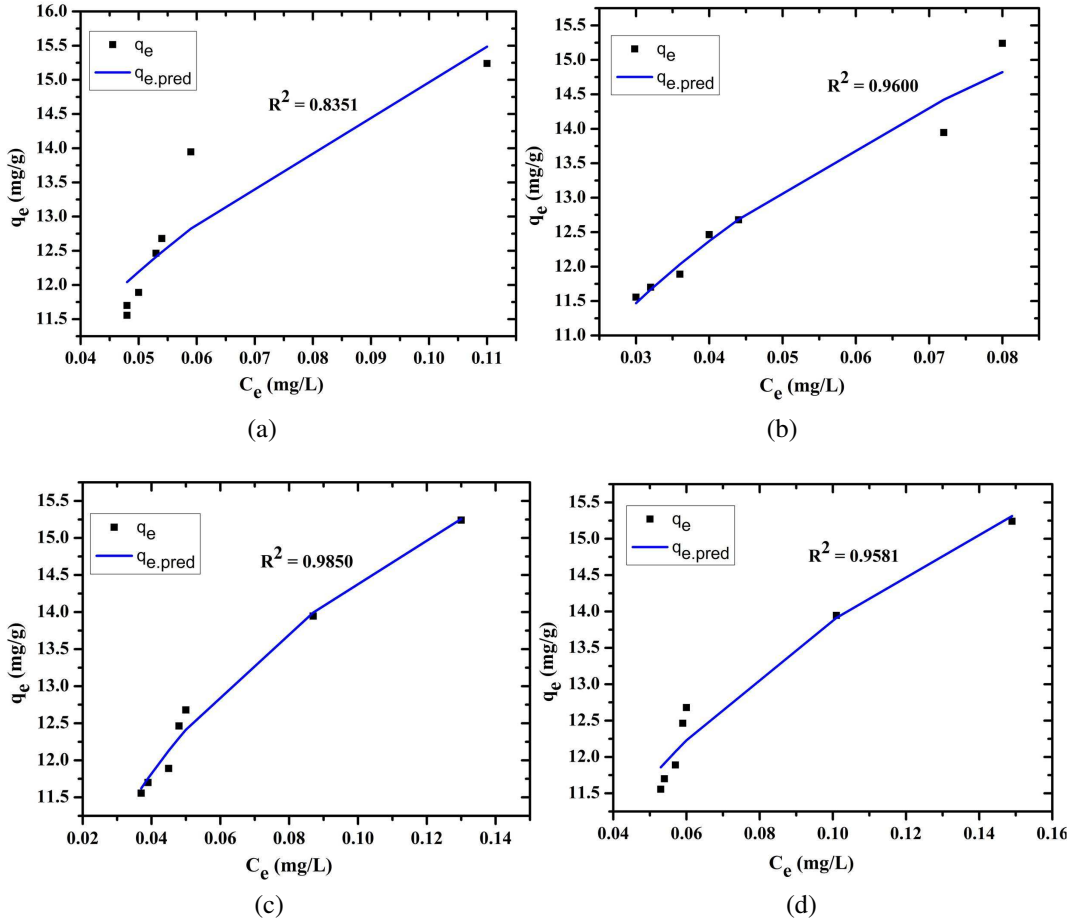

Figure 6.16: Redlich-Peterson isotherm at varying doses of bentonite (a) 1 g/L (b) 2 g/L (c) 3 g/L (d) 4 g/L.

It can be observed clearly from the above results that at bentonite dose of 1 g/L, Langmuir isotherm fits the data well. At this dose only monolayer adsorption is taking place. But as the dose is increased Freundlich isotherm and Redlich-Peterson isotherm fits the data well. Also, the Freundlich isotherm has the best fit if compared with Langmuir. This suggests that features of Freundlich isotherm are applicable to the present adsorption. So, it can be concluded that it is non-ideal and reversible adsorption, not restricted to the formation of monolayer. The amount adsorbed is the summation of adsorption on all sites (each having bond energy), with the stronger binding sites occupied first, until adsorption energy is exponentially decreased upon the completion of adsorption process [29]. The slope ranges of Freundlich isotherm, between 0 and 1, is a measure of adsorption intensity or surface heterogeneity, becoming more heterogeneous as its value gets closer to zero. Whereas, a value below unity implies chemisorptions process, where 1/n above one is an indicative of co-operative adsorption [30]. The slope in the present study is in the range of $0.22 - 0.26$, which is indicative of chemisorptions taking place. Again when the dose is 4 g/L, Langmuir isotherm fits the data well. The probable reason of this could be attributed to the fact that when the dose

is increased beyond a certain value, negative charge due to bentonite accumulates in the system and causes repulsion to an extent which prevents the formation of multilayer.

Table 6.19: Isotherm parameters obtained using non-linear method for activated silica sol dosing.

Isotherms	***Parameters***	***Activated silica sol dose (mg/L)***			
		10	30	50	70
Langmuir	q_{max}	24.507	13.984	16.973	37.048
	K_l	15.392	1164.510	128.691	7.100
	RMSE	0.445	0.926	0.517	0.421
	χ^2	0.013	0.057	0.018	0.012
	R^2	0.8915	0.5309	0.8537	0.9030
Freundlich	K_f	44.478	20.355	31.081	66.684
	n	2.115	9.384	4.148	1.544
	RMSE	0.402	0.647	0.385	0.397
	χ^2	0.011	0.028	0.009	0.010
	R^2	0.9116	0.7711	0.9191	0.9137
Redlich Peterson	g	0.530	0.931	0.771	0.354
	RMSE	0.402	0.761	0.391	0.397
	χ^2	0.011	0.039	0.010	0.010
	R^2	0.9115	0.6832	0.9163	0.9137

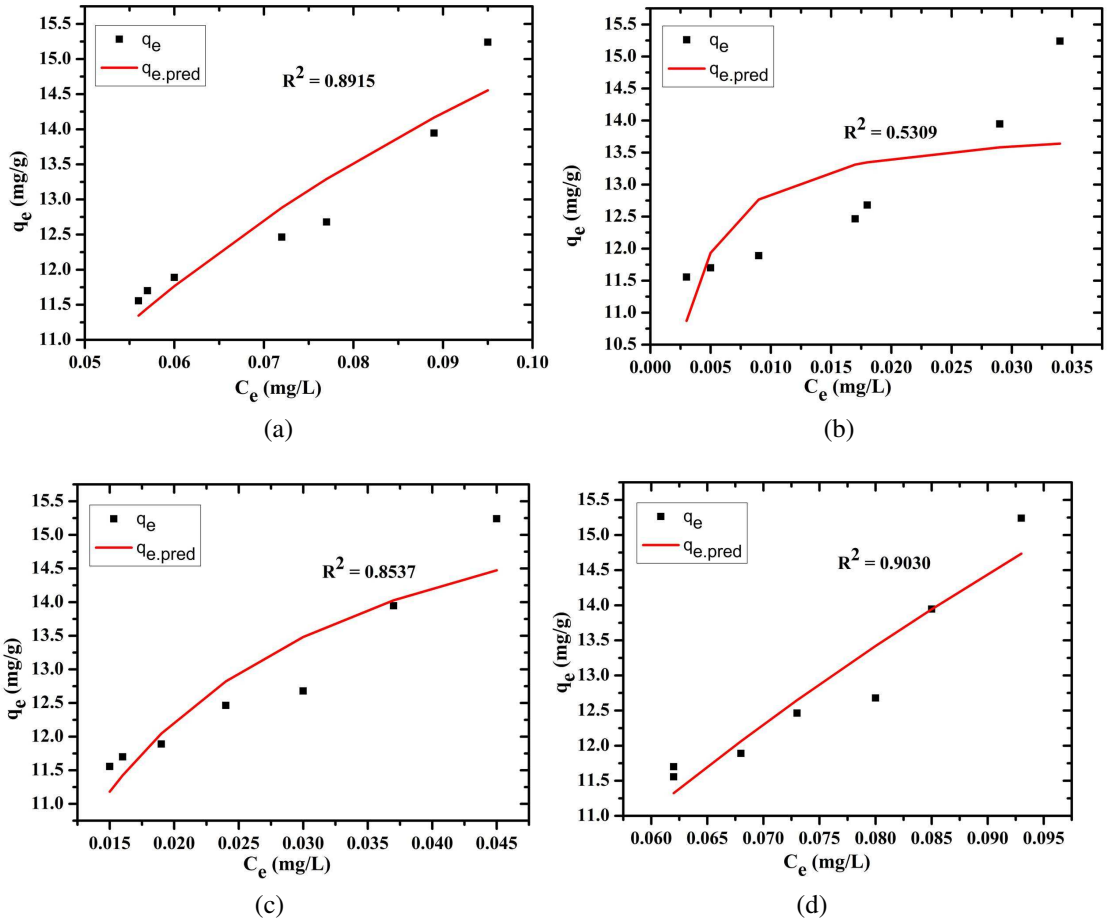

Figure 6.17: Langmuir isotherm at varying doses of activated silica sol (a) 10 mg/L (b) 30 mg/L (c) 50 mg/L (d) 70 mg/L.

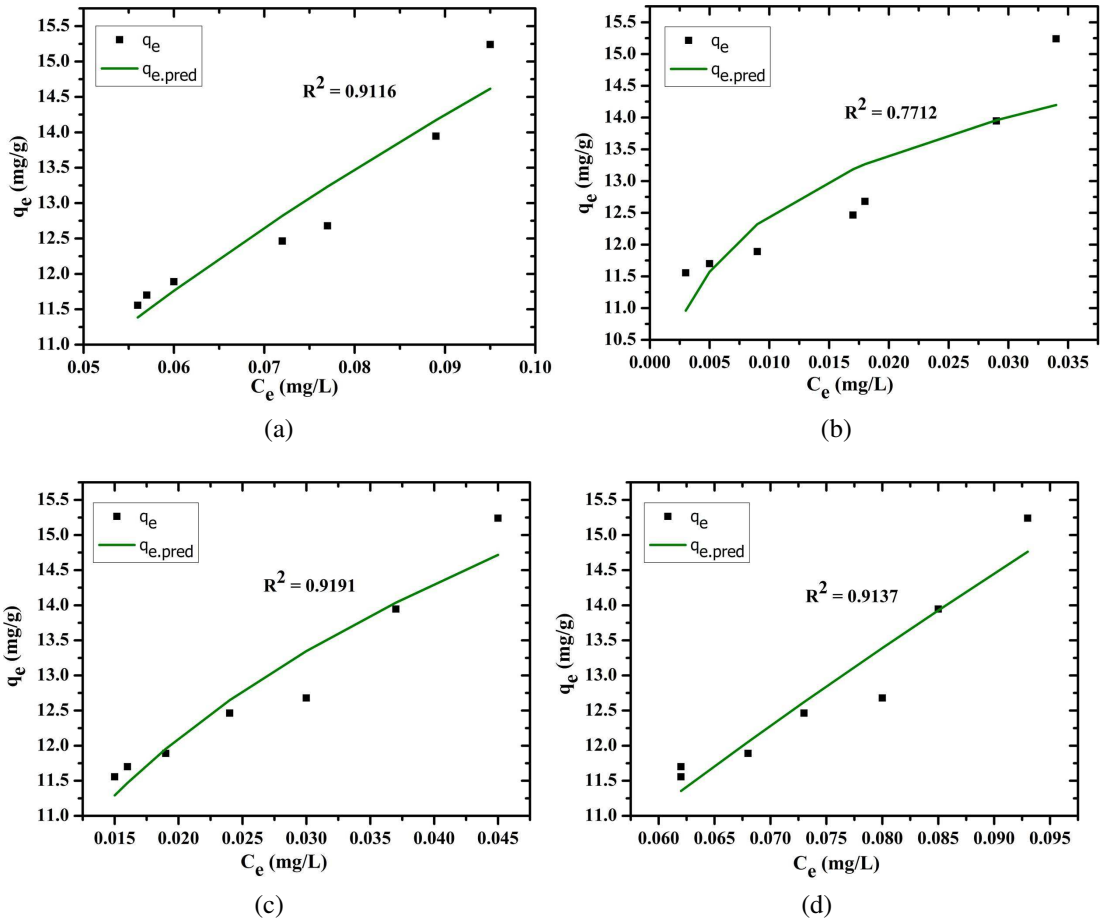

Figure 6.18: Freundlich isotherm at varying doses of activated silica sol (a) 10 mg/L (b) 30 mg/L (c) 50 mg/L (d) 70 mg/L.

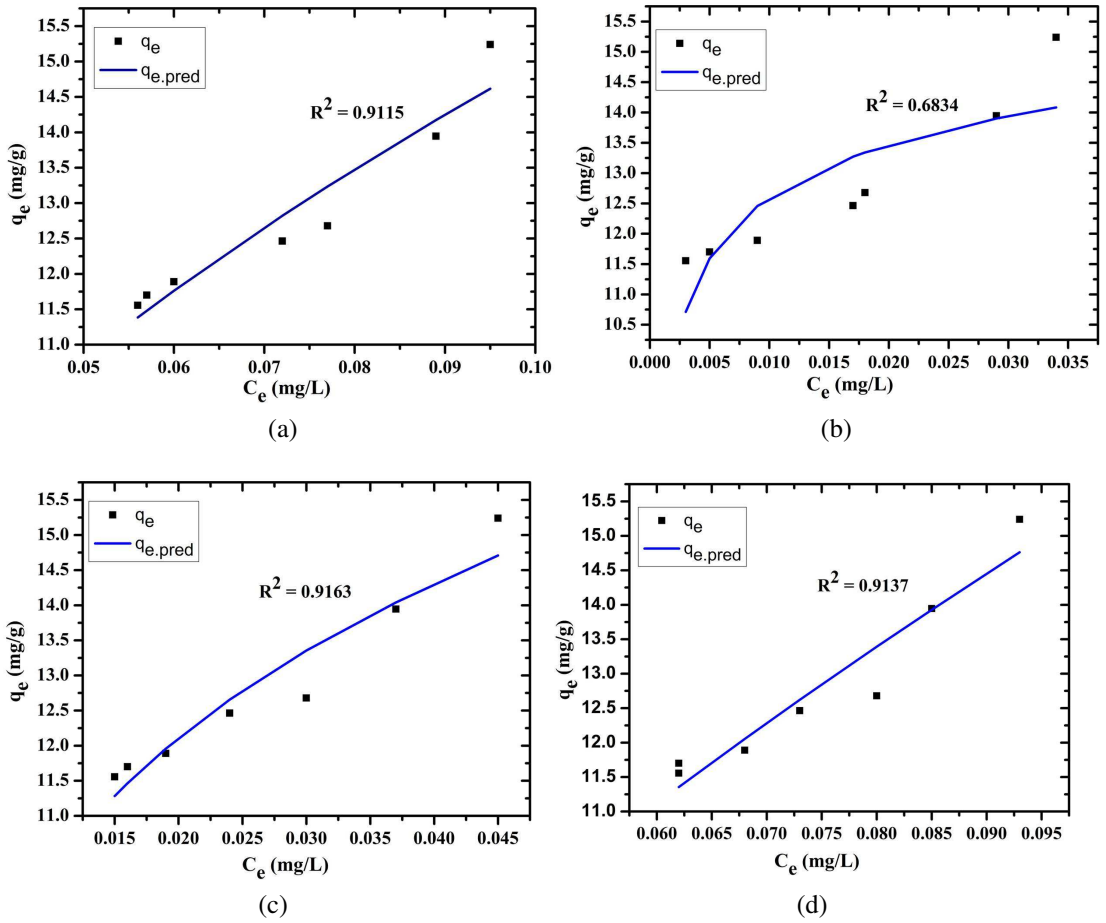

Figure 6.19: Redlich-Peterson isotherm at varying doses of activated silica sol (a) $10\,mg/L$ (b) $30\,mg/L$ (c) $50\,mg/L$ (d) $70\,mg/L$.

In the case of activated silica sol dosing, for all the doses Freundlich isotherm fits the data well. Hence it can be clearly said that in this case multilayer adsorption is taking place. The slope in case of activated silica sol was found to be in the range of $0.11 - 0.47$, which indicates that chemisorption is taking place.

Chapter Summary

This Chapter focusses on the stategies to control the aluminium. Two stategies: optimization of energy input followed by flocculation and settling & optimization of energy input followed by addition of coagulant aid were used to control the aluminium from water treated by EC.

For optimization of energy input, a program was developed in FORTRAN to minimize energy used for target fluoride removal. It helps in controlling aluminium dissolution and only amount necessary for desired fluoride removal is introduced in the solution. Use of optimized energy alone is not sufficient to bring the aluminium below permissible limits of aluminum in drinking water.

In next step, flocculation and settling followed by filtration was attempted. It appreciably reduces the aluminium concentration but not below the permissible limit. Performing this step, gave a clear insight that the aluminium concentration was mostly due to the flocs present in the water and efficient settling of these flocs is required for aluminium control. Therefore, coagulants aids (bentonite clay and activated silica sol) were used to improve settling efficiency Both coagulant aids brought down the aluminium content below permissible limits.

With optimised dose of bentonite, residual aluminium was brought down to a range of $0.03 - 0.08\, mg/L$. With optimised dose of activated silica sol, residual aluminium was brought down to a much lower range of $0.003 - 0.034\, mg/L$.

Also, this chapter evaluated the adsorption isotherms for both bentonite clay dosing and activated silica sol dosing. The results suggested that features of Freunlich isotherm are best suited for this study.

CHAPTER 7

Chapter 7

Sludge characterization and cost analysis

This Chapter includes the characteristics of the sludge formed in the treatment process. Sludge can be defined as precipitated solid matter which is an outcome of water treatment process. The sludge characterization in the present study includes the information about settled sludge volume and analysis of sludge using techniques like: settled sludge volume (SSV), scanning electron microscopy- energy dispersive x-ray spectroscopy (SEM-EDX), fourier transform infra-red spectroscopy (FTIR) and x-ray diffraction (XRD).

In the present study three types of sludge were studied as mentioned below:

1. Sludge produced after EC process, flocculation and settling (Sludge A).
2. Sludge produced after bentonite dosing, flocculation and settling (Sludge B).
3. Sludge produced after activated silica sol dosing, flocculation and settling (Sludge C).

The characterization of the above mentioned sludge using various techniques has been discussed below.

7.1 Settled Sludge Volume

Sludge quantity is important to plan for management of sludge. The method to handle sludge, cost, treatment and disposal are influenced by the amount and characteristics of sludge. The sludge quantity and its characteristics are affected by raw water quality and the chemicals which are used for treatment. Raw water quality cannot be altered. However the process of water treatment can be changed/modified to minimize the sludge production. The reduction of waste volume results in saving the operational cost of a

treatment plant. Sludge produced in the treatment process is high in gelatinous metal hydroxides. These types of sludges are difficult to handle because of their low settling rates and thixotropic characteristics [170]. The sludge consists of solids removed from coagulated water; mainly hydroxide precipitates from the coagulant, materials present in the raw water and chemicals or coagulant aids used for water treatment.

The settled sludge volume (SSV) gives an idea about the compaction of sludge [171]. SSV is the volume occupied by sludge after a specified time. The settling time is shown as a subscript. In the present study SSV was measured after 30 min so it is known as SSV_{30}. It is reported as ml of sludge per litres of sample (mL/L). The water after the treatment process was poured in an imhoff cone as shown in Figure 7.1, after which it was allowed to settle for 30 min. Imhoff cone is an graduated cone (Figure 7.1a) which allows us to measure the volume of settled sludge.

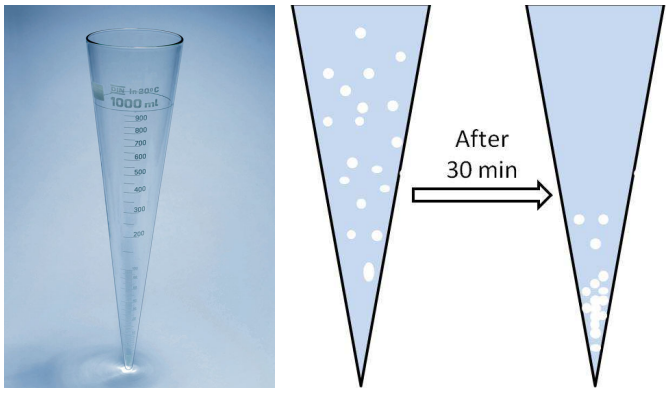

(a) (b)

Figure 7.1: (a) Imhoff cone (b) Schematic diagram of settling process in imhoff cone

The amount of sludge produced during coagulation-flocculation process using chemical coagulants remains a serious problem to the operator in handling the sludge [172]. Mishandling of chemical sludge will lead to deterioration of the environment [173]. Therefore, various types of coagulants with little sludge at final discharge of the treatment process should be preferred. It can be observed from the Figure 7.2 that the order of compaction was more in sludge obtained after activated silica sol dosing than sludge obtained after bentonite dosing. The results for SSV_{30} for all the three types of sludge are shown in the Figure 7.2. It can be observed that SSV_{30} is least in the case of activated silica sol dosing, followed by bentonite dosing and EC alone. It shows that addition of coagulant aid causes compaction of sludge volume and hence makes the handling process easier. Coagulant aids are added to aid in coagulation and to increase sludge density. The use of bentonite and activated silica sol improves floc settleability and lowers sludge volume [174]. This sludge can be easily used in brick making industries, to solve the issue of disposal of sludge. A review done by Kadir and Rahim [175], states that utilization of various kinds of sludge in making of fire clay

bricks usually have a positive impact on the bricks. Therefore it may be suggested as a method for sludge disposal.

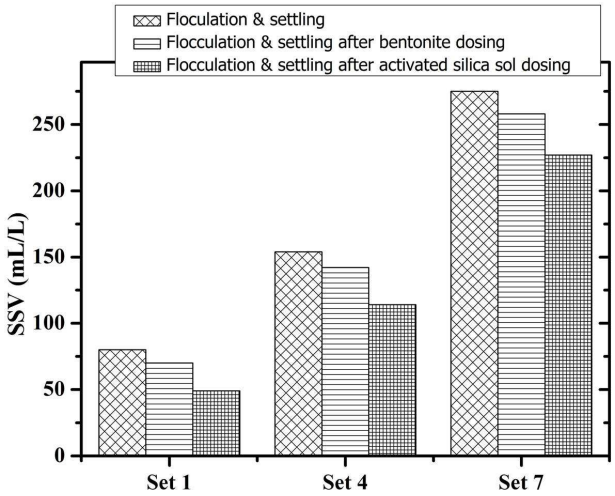

Figure 7.2: SSV_{30} at varying initial fluoride concentrations

7.2 SEM-EDX analysis

The SEM-EDX analysis of sludge was conducted to know about the morphology and elemental composition of sludge. In the present study three different sludges (A, B and C) produced by varying strategies; sludge after flocculation and settling (without coagulant aid), sludge after bentonite dosing and sludge after activated silica sol dosing were analyzed. The morphology of the sludge formed using above mentioned processes is shown in Figure 7.3. The images indicate the presence of micron level ultrafine structure at the surface [99].

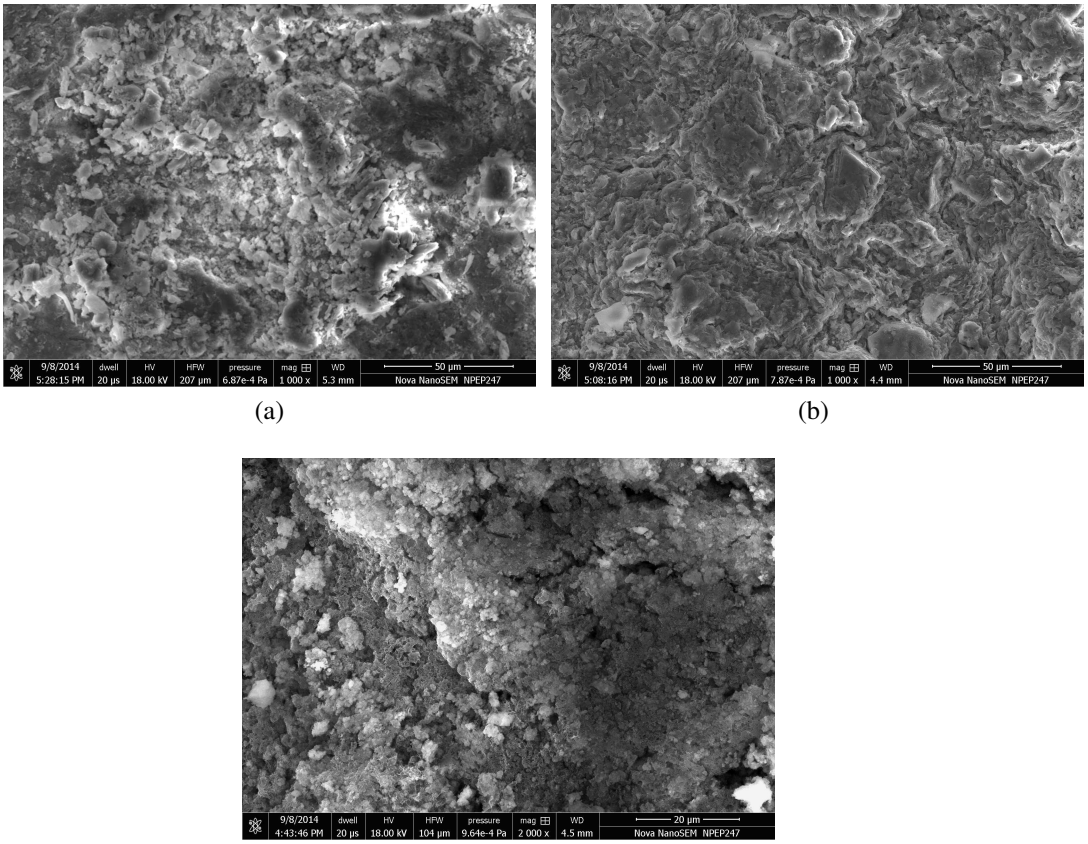

(a) (b)

(c)

Figure 7.3: SEM images of (a) sludge A (b) sludge B (c) sludge C

The EDX analysis of sludge A is shown in Figure 7.4a. The main components of sludge are fluoride and aluminium. The peak of oxygen is mainly due to the presence of oxides of aluminium. Other peaks of sodium, magnesium and calcium are due to the presence of these elements in tap water that were adsorbed on the surface of the colloids; were destabilized and precipitated. The peak of chlorine is due to the addition of HCl for maintaining pH and dissociation of sodium chloride which was added for enhancement of conductivity.

The EDX analysis of sludge B and C are shown in Figure 7.4b and 7.4c respectively. All elements as mentioned for sludge after EC process are present in this also. Silica is the new element introduced which is present in the sludge due to addition of bentonite and activated silica sol in the process.

The atomic% and weight% of the elements present in the sludge A, B and C are tabulated in Table 7.1-7.3.

Elements	***Weight%***	***Atomic%***
O	51.23	65.83
Al	13.30	10.13
Cl	9.29	5.32
Mg	4.36	3.69
Na	2.86	2.56
Ca	8.35	5.28
F	2.08	2.25
Cl	8.53	4.94

Table 7.1: Elemental composition of sludge A

Elements	***Weight%***	***Atomic%***
O	49.81	65.90
Al	14.47	11.23
Si	20.31	10.02
Cl	1.47	0.78
Mg	7.25	7.08
Na	2.07	1.98
Ca	1.44	0.75
F	1.09	0.70
K	1.09	0.56

Table 7.2: Elemental composition of sludge B

Elements	***Weight%***	***Atomic%***
O	52.52	65.42
Al	16.71	12.34
Si	14.11	11.34
Cl	6.09	3.42
Mg	4.63	3.36
Na	2.76	2.39
Ca	2.01	1.00
F	1.17	0.72

Table 7.3: Elemental composition of sludge C

It can be clearly seen that atomic% of aluminium shows an increase from 10.13% (sludge A) to 11.23% (sludge B) and further increased to12.34% (sludge C). This increase in aluminium percentage in sludge may also be considered as an indicative of aluminium removal using bentonite and activated silica sol.

EDX analysis is not able to differentiate much between the sludge generated by addition of bentonite or activated silica sol. This clarity was achieved when XRD analysis of the sludge was done.

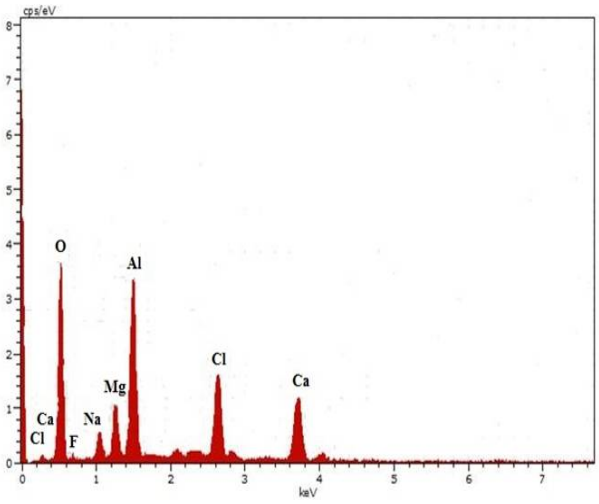

(a)

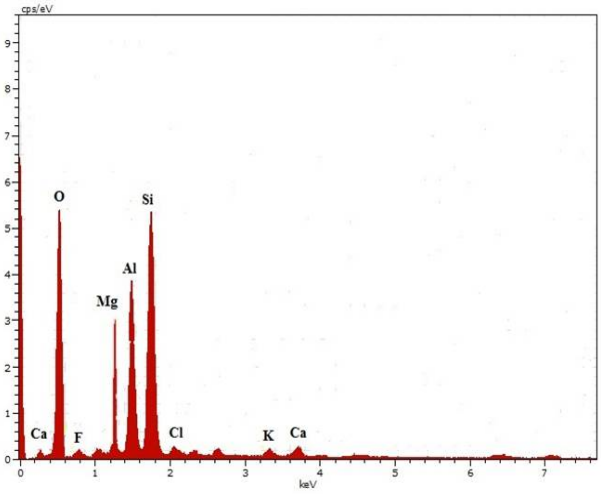

(b)

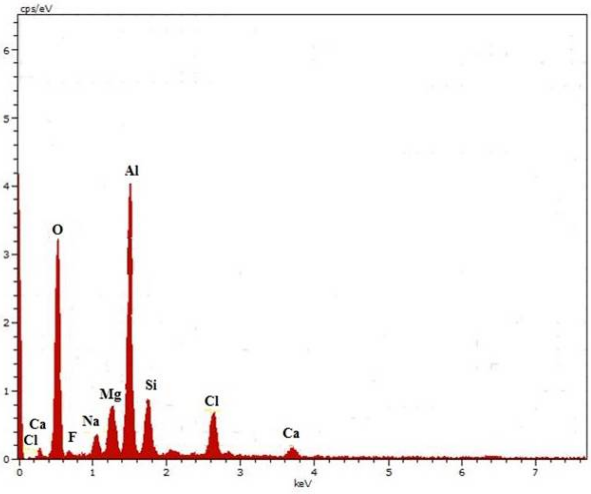

(c)

Figure 7.4: EDX analysis (a) sludge A (b) sludge B (c) sludge C

7.3 FTIR analysis

FTIR analysis is useful to investigate the functional groups present in the sludge and indicates towards the removal mechanism used in the treatment process. FTIR analysis was conducted for three different sludge produced, raw bentonite and activated silica sol.

7.3.1 FTIR scan of Sludge A

The FTIR scan result of sludge A is shown in Figure 7.5. The FTIR scan peaks at 3366 $cm^{-1}$and 1631 cm^{-1} correspond to H-O-H bond stretching and H-O-H bending respectively [176]. Al-F-Al bond stretching peak was found at 604 cm^{-1}. Al-F-Al bond stretching was matched with analysis made by Gross *et al.* [177]. This indicates that fluoride was linked with aluminium hydroxide complexes and precipitated in the reactor.

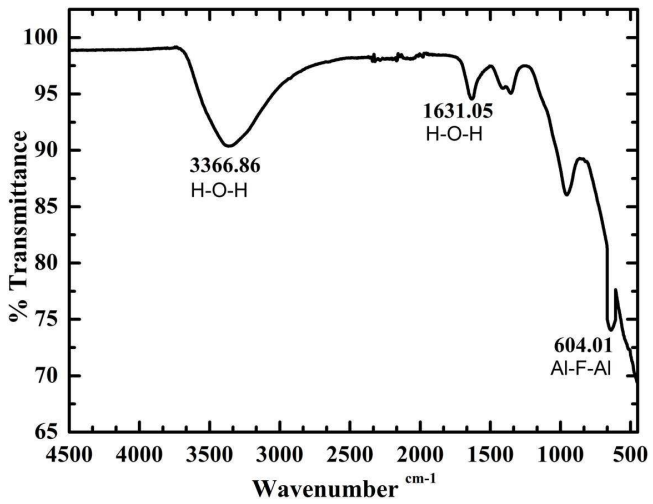

Figure 7.5: FTIR scans of sludge A

7.3.2 FTIR scan of bentonite and sludge B

FTIR scans of bentonite and sludge B are shown in Figure 7.6a and 7.6b respectively. The scans of bentonite show peak at 1634 cm^{-1} corresponding to H-O-H bending, peak at 3620 cm^{-1} corresponds to OH stretching or crystalline hydroxyl, at 520 cm^{-1} corresponds to Si-O-Al and peak at 998 cm^{-1} confirms Si-O stretching.

The sludge scans of sludge B show peaks at 1630 cm^{-1} corresponding to H-O-H bending; peak at 3620 cm^{-1} corresponds to OH stretching or crystalline hydroxyl, at 519 cm^{-1} corresponds to Si-O-Al and peaks at 1000 cm^{-1} confirms Si-O stretching. These results corroborates the results of Bhaskar and Parthasarathy [176].

It may be noted that the peaks found in the FTIR of raw bentonite and sludge B are almost similar, but there is a decrease in transmittance of Si-O-Al peak in case of sludge

B when compared to raw bentonite. This may be suggested as an evidence of adsorption taking place in sludge B.

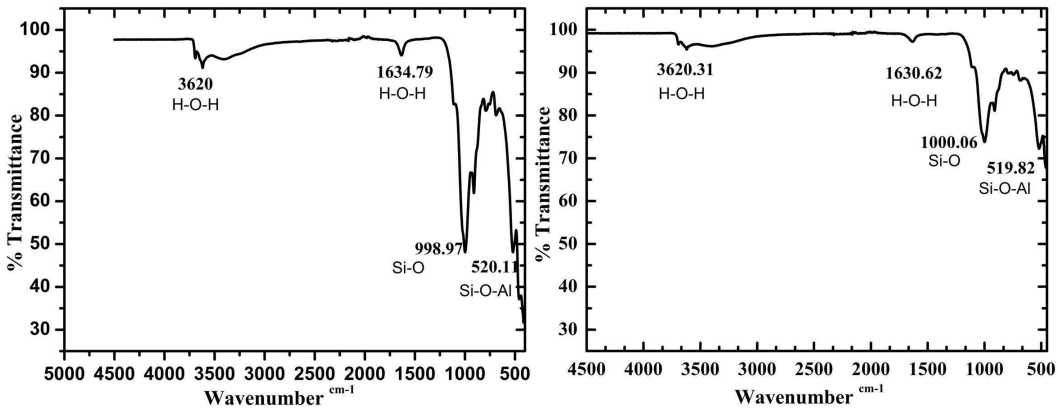

(a) (b)

Figure 7.6: FTIR scans of (a) bentonite (b) sludge B

7.3.3 FTIR of activated silica sol and sludge C

FTIR scans were conducted for activated silica sol and sludge C to understand the removal mechanisms. FTIR scans of activated silica sol (Figure 7.7a) peaks at 3307.39 cm^{-1} and 1634.25 cm^{-1} correspond to H-O-H bond stretching and H-O-H bending respectively. FTIR scans of sludge C (Figure 7.7b) peaks at 3390.21 cm^{-1} and 1633.90 cm^{-1}correspond to H-O-H bond stretching and H-O-H bending respectively. The results corroborates the findings of Hayati-Ashtiani [178]. Si-O stretching bond peak was found at 1008.64 $cm^{-1}$for activated silica sol and at 967.16 $cm^{-1}$for sludge C. These findings are in line with Stubican and Roy [179].

The presence of Si-O-Al peak at 538 cm^{-1}[179] is found in the scans of sludge only. This finding supports the results that activated silica sol is better than bentonite for removing aluminium from treated water. Si-O-Al peak is already present in the case of raw bentonite. But, in colloidal silica sol the negatively charged aluminosilicates are formed after its addition to the water treated by EC. So, the removal of aluminium occurs in two steps; first aluminium is utilised in the formation of negatively charged aluminosilicates and second the positively charges aluminium polymers are removed by these aluminosilicates as a result of charge neutralization.

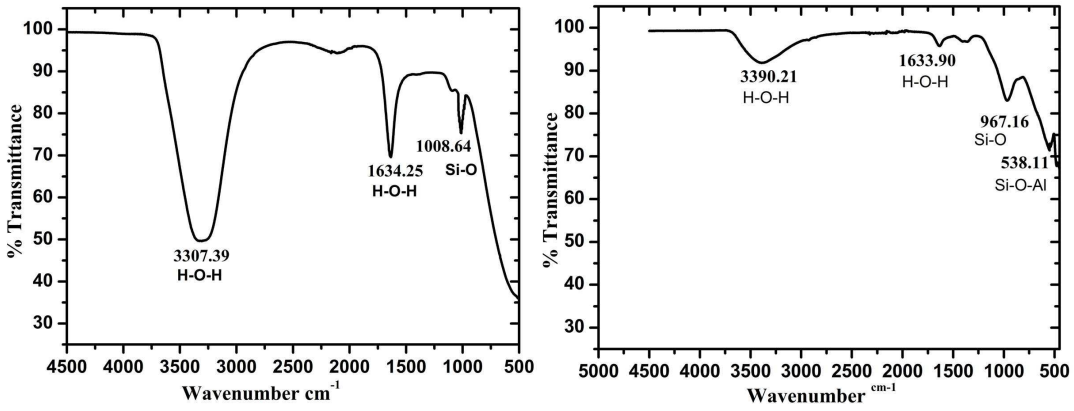

(a) (b)

Figure 7.7: FTIR scans for (a) activated silica sol (b) sludge C

7.4 XRD analysis

The sludge A, B and C have been characterised using the XRD spectrum. The spectrum of the analyzed by-products showed broad and diffuse peaks. Therefore, the identification of peaks with such broad humps is a well known confirmed characteristic of phases which are amorphous or poorly crystalline in nature [90].

7.4.1 XRD analysis of sludge A

The strongest peaks identified in XRD spectrum of sludge A (Figure 7.8a and 7.8b) were of sodium aluminium fluoride, aluminium fluoride hydrate and aluminium oxide hydrate. The formation of these compounds suggests the removal mechanism of fluoride in EC process. It shows that the fluoride may occur in solids particles such as aluminium fluoride hydroxide complexes.

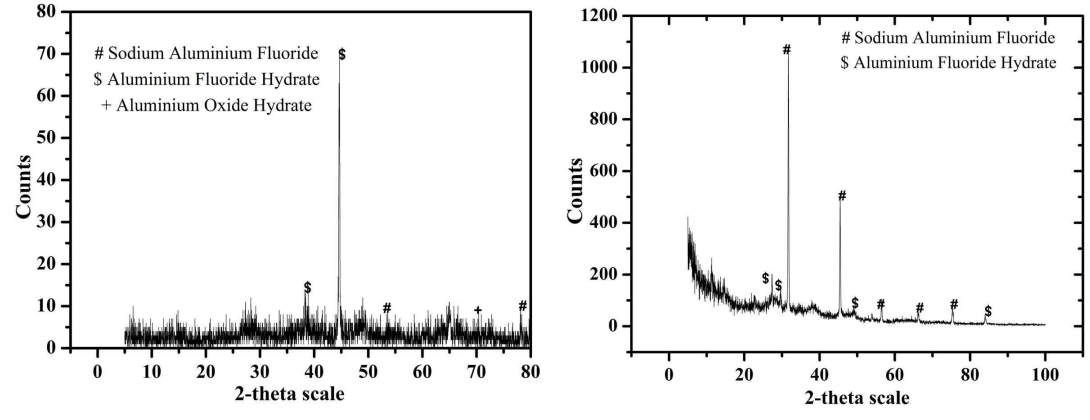

(a) (b)

Figure 7.8: XRD pattern of sludge A (a) F_i=5 mg/L i=0.31 A t=30 min (b) F_i=8 mg/L i=0.37 A t=43.84 min

7.4.2 XRD analysis of raw bentonite and sludge B

XRD was performed for raw bentonite (Figure 7.9) and sludge B (Figure 7.10). XRD patterns of raw bentonite indicate that it is mostly made up of montmorillonite, quartz and kaolinite. Chemically, montmorillonite is described as a hydrous aluminium silicate containing small amounts of alkali and alkaline-earth metals. XRD confirms that the metal present in bentonite used for this study is sodium and magnesium. Sodium bentonite swells or expands to a greater degree than its calcium equivalent and hence develops larger surface area [180].

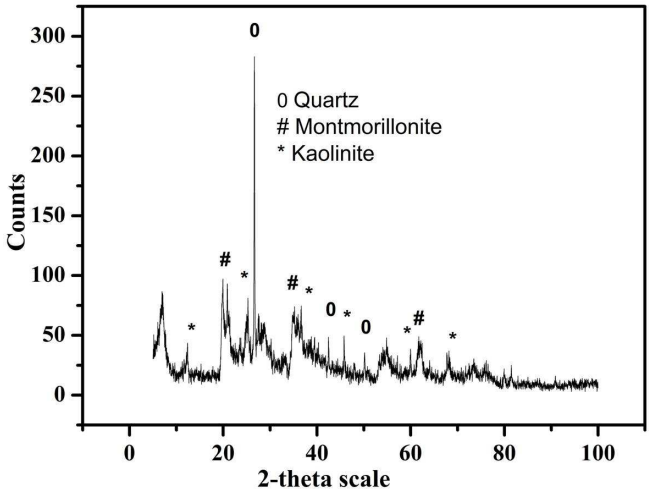

Figure 7.9: XRD spectrum of raw bentonite

In the XRD spectrum of sludge B (Figure 7.10), the peaks of Sodium Magnesium Aluminum Fluoride Silicate, Sodium Aluminum Fluoride, and Aluminum Fluoride Silicate were identified. Other peaks of Sodium Aluminum Fluoride, and Aluminum Silicate Hydroxide Fluoride were also present. The presences of these compounds indicate towards the chemisorption of alumino complexes in the form of flocs on to the bentonite clay particles and hence verify the role of bentonite clay in better settling of flocs.

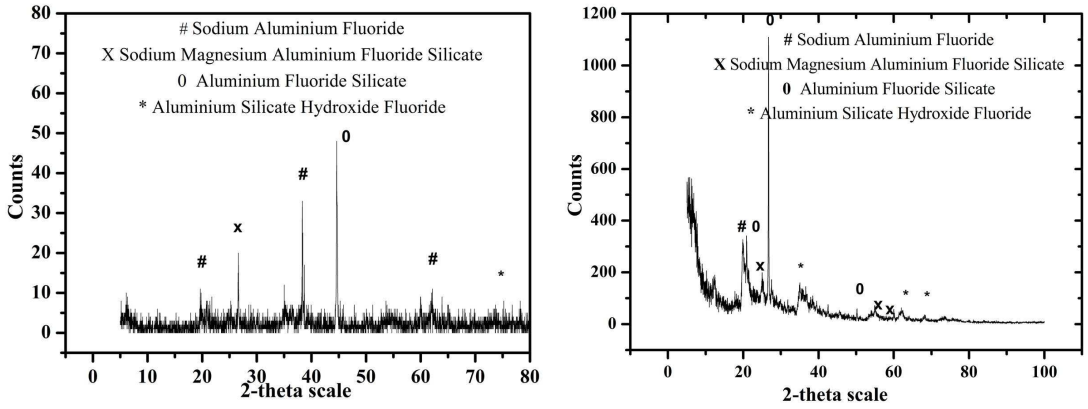

Figure 7.10: XRD pattern of sludge B (a) F_i=5 mg/L i=0.31 A t=30 min (b) F_i=8 mg/L i=0.37 A t=43.84 min

7.4.3 XRD patterns of sludge C

XRD pattern of sludge C were studied and are presented in Figure 7.11. The strongest peak was identified as sodium aluminium silicate hydrate. Other peaks were identified as sodium aluminium fluoride, aluminium silicate hydroxide fluoride and aluminium fluoride silicate. The presence of these compounds indicates towards the chemisorption of alumino complexes to activated silica sol and verifies the role of activated silica sol as coagulant aid for removal of aluminium from water treated by EC. Coagulant aid used was activated silica sol, therefore magnesium compounds are absent in the XRD patterns.

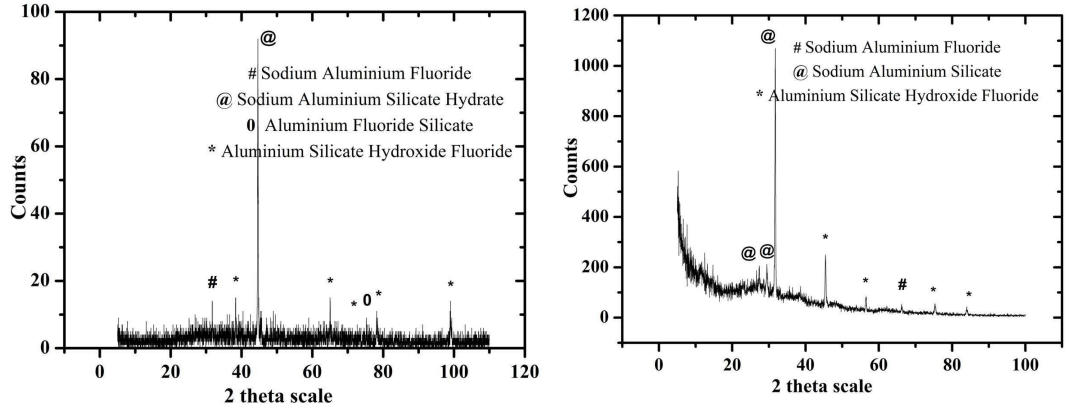

Figure 7.11: XRD pattern of sludge C (a) F_i=5 mg/L i=0.31 A t=30 min (b) F_i=8 mg/L i=0.37 A t=43.84 min

7.5 Cost analysis

Like all other electrolytic processes, energy consumption and sacrificial electrodes are important parameters from economic considerations [181]. These two parameters were considered for calculation of operating cost as $USD/m^3$of water treated. Other cost parameters such as labour, maintenance, sludge dewatering, disposal and other costs are assumed fixed and are not included in the calculations [181]. Therefore, main operating cost of the EC process is due to three components as explained in the Equation 7.1

$$Operating\ cost = xC_{energy} + yC_{electrode} + zC_{aid} \tag{7.1}$$

where C_{energy} ,$C_{electrode}$ and C_{aid} are quantities consumed per liter of water treated. Unit prices, x, y and z, obtained from Indian Market, 2014, are as follows (a) electrical energy price $0.09\,USD/kWh$, (b) electrode material price $1.7\,USD/kg$ for aluminium. C_{aid} is the cost of coagulant aid used; bentonite is $0.005\,USD/kg$ and activated silica sol is $0.12\,USD/L$.

The value of energy consumption was calculated using Equation 7.2

$$E = V \times i \times t \tag{7.2}$$

Where,

E is the electrical energy in kWh,

V the cell voltage in volt (V),

I the current in ampere (A) and

t is the time of EC process (sec).

The aluminium consumed in the process is the loss of electrode material during the EC process. This loss can be calculated by subtracting the weight of the electrodes taken at the end of the experiments from the weight taken before the experiments of the same electrode [101]. It has been discussed in Chapter 4, that theoretical aluminium dissolution can be calculated using the Equation 4.6, as explained by Faraday's law. From the results obtained in chapter 4, it is evident that the current efficiency of the EC process is more than 100% due to pitting corrosion. Therefore, aluminium dissolution calculated by weighing the electrode is slightly higher than the dissolution calculated by using Equation 4.6. Figure 7.12 clearly explains that the variation in aluminium consumed between theoretical and experimental values is very small. Therefore, in the present study Equation 4.6 was used for calculating the aluminium dissolution.

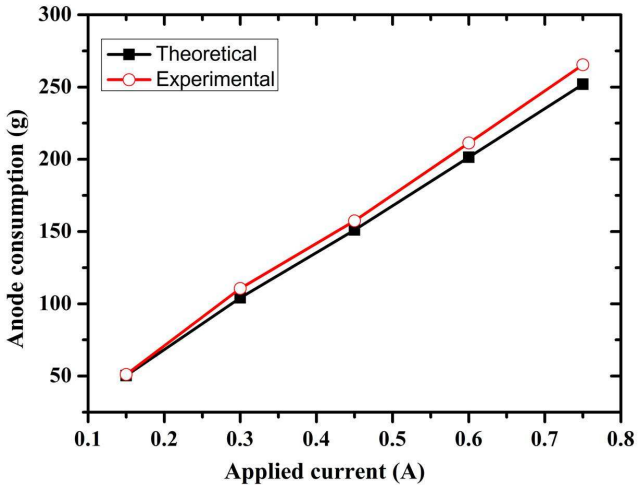

Figure 7.12: Relation between theoretical and experimental anode consumption.

After EC treatment for fluoride removal, flocculation and settling was attempted for aluminium removal. The cost of filtration is again fixed cost, so not included in the discussion. But the cost of power consumption due to flocculation (rapid mix and slow mix) has been calculated. Power of flocculation is calculated using the formula in Equation 7.3

$$P = G^2 \times V \times \mu \tag{7.3}$$

Where,

G is the velocity gradient, $/s$

P is power input in W

V is volume of suspension in m^3

μ is viscosity of water in $N.s/m^2$

Rapid mix was given for 1 min at 40 rpm. (G$\sim 120/s$)

Slow mix was give for 20 min at 10 rpm (G$\sim 10/s$)

All the above costs were added to estimate operational cost of the treatment process. In the present study initial fluoride concentration $2-8\,mg/L$ was treated using the EC process and both aluminium and fluoride were brought within the permissible limits. The EC process was optimized for target fluoride removal of $0.7\,mg/L$ with minimum energy input. Cost associated with the optimized treatment process is $0.06-0.13\,USD/m^3$ of water treated when bentonite is used as a coagulant aid. The cost is $0.29-0.36\,USD/m^3$ of water treated when activated silica sol is used as a coagulant aid.

In the present study it has been found that the use of optimized energy controls the dissolution of aluminium in water, which subsequently helps in controlling residual aluminium in water after defluoridation. Optimized energy usage not only controls the residual aluminium in water but also maintains the economics of the treatment process.

It is also evident that operating cost depends on the applied current and electrolysis time of the treatment process [101]. Increase in applied current and electrolysis time, increases the energy consumption and aluminium consumption which in turn increases the operational cost. Thus, it can be concluded that careful selection of both operating parameters applied current and electrolysis time is required to maintain the efficiency and economics of the process. Table 7.4 presents the cost of treatment estimated for optimized sets.

Table 7.4: Cost of treatment for optimized sets.

F_i (mg/L)	i (A)	t (min)	Total cost of treatment (USD/m^3)	
			Using Bentonite	Using Activated silica sol
2	0.33	17.05	0.06	0.29
3	0.32	20.93	0.07	0.30
4	0.39	22.41	0.09	0.32
5	0.36	27.85	0.06	0.29
6	0.32	34.9	0.08	0.31
7	0.31	41.08	0.09	0.32
8	0.37	43.84	0.13	0.36

Rao *et al.* [182] reported the recurring cost of Nalgonda process and AA process, to treat water of $5\,mg/L$ initial fluoride concentration as $0.33\,USD/m^3$ and $4.44\,USD/m^3$ respectively. The cost of treatment to treat water of $5\,mg/L$ initial fluoride concentration using EC and bentonite as coagulant aid is estimated as $0.06\,USD/m^3$. The cost of treatment to treat water of $5\,mg/L$ initial fluoride concentration using EC and activated silica sol as coagulant aid is estimated as $0.29\,USD/m^3$.

Agarwal *et al.* [59] reported that the residual aluminium ranges from $2.01 - 6.86\,mg/L$ in Nalgonda process which exceeds the permissible limit of $0.2\,mg/L$ as prescribed in IS 10500:2012 [25]. Agarwal *et al.* [59] also reported moderately high residual aluminium in output water ranging from $0.1 - 0.3\,mg/L$ in AA process. The residual aluminium after the present treatment is in the range of $0.03 - 0.08\,mg/L$ (using bentonite as coagulant aid) and $0.003 - 0.034\,mg/L$ (using activated silica sol as coagulant aid); which is well within the IS:10500:2012 [25] permissible range. A comparative cost estimation to treat water of $5\,mg/L$ initial fluoride concentration using Nalgonda, AA and present treatment process has been presented in Table 7.5

Table 7.5: Cost comparison of present treatment process with Nalgonda and AA process to treat water with F_i= 5 mg/L.

Treatment process	***Estimated cost*** (USD/m^3)	***Residual aluminium*** (mg/L)
Nalgonda	0.33 [182]	$2.01-6.86$ [59]
AA	4.44 [182]	$0.1-0.3$[59]
EC process using bentonite as coagulant aid	0.06	$0.03-0.08$
EC process using activated silica sol as coagulant aid	0.29	$0.003-0.034$

Table 7.5 indicates that the present treatment process offers better economy and better quality of final water.

Chapter Summary

This chapter included details of sludge characterization and cost analysis. Sludge was characterized using SEM-EDX, FTIR and XRD. The investigations explain the importance of silica in removal of aluminium from the water.

The EDX analysis identified the elements present in the sludge. FTIR analysis identified the functional groups present in the sludge and finally XRD analysis identified the compounds present in the sludge. These all analysis gave an insight into the removal mechanism of fluoride and aluminium.

The estimated operational cost of the treatment process used in the present study was calculated to be $0.06 - 0.13\,USD/m^3$ when bentonite was used and $0.29 - 0.36\,USD/m^3$ when activated silica sol was used.

CHAPTER 8

Chapter 8

CONCLUSION

This chapter summarizes the the present work and its major findings.

High concentration of fluoride in ground water, used for human consumption has severe implications on human healh. It is a big challenge for public health engineers across the globe in general, and for developing countries in particular. Fluoride is the most electronegative element and has a strong affinity for aluminium. Owing to this fact, use of aluminium compounds is more prevalent for defluoridation. In the present work experimental investigations were carried out to reduce fluoride concentration in drinking water below permissible levels prescribed by IS: 10500:2012 using EC with aluminium electrodes. The aluminium dissolution assists in fluoride removal, but it also introduces aluminium compounds in the water. From the present investigations it was found that the aluminium introduced in the water during defluoridation process is more than the permissible limit.

The high aluminium in defluoridated water suggests the necessity of further treatment for bringing down the aluminium concentration in treated water. The treated water after the EC process is found to have high turbidity and low alkalinity. The turbidity is due to high concentration of flocs present in the water and low alkalinity is due to the neutralization of alkalinity by hydrogen ions formed during the EC process. This high turbidity-low alkalinity water can be easily coagulated by adsorption and charge neutralization. Assuming that high concentration of aluminium is mainly due to flocs present in water, the control of residual aluminium through efficient floc removal has been attempted. Flocculation with and without coagulant aid was attempted for better settling of flocs formed during EC. Two coagulant aids , namely bentonite and activated silica sol were used for the present experimental investigations.

Results of flocculation without coagulant aid showed an appreciable decrease in turbidity and aluminium concentration, but were still not close to permissible standards of aluminium in drinking water. It was now understandable that the efficient settling of flocs could lead to lesser residual aluminium. Two coagulant aids (bentonite clay and activated silica sol) were used to improve settling. Both coagulant aids brought down

the aluminium concentration below permissible limits.

Statistical models were developed for both fluoride and aluminium removal. Mathematical equations were developed for prediction of responses which can be used for design of such treatment systems.

8.1 Parametric investigations for fluoride removal

This Chapter elucidates the effect of operational parameters like pH, inter-electrode distance, initial fluoride concentration, applied current and electrolysis time which governs the EC process for fluoride removal. Other parameters like specific electrical energy consumption (SEEC), charge loading, anode consumption, fluoride uptake capacity (FUC) were also studied.

- The initial pH of 6 gave maximum fluoride removal efficiency and the final pH attained after treatment was close to 7 (suitable for drinking purposes). No readjustment of pH was required during or after the treatment. Therefore, the pH value of the influent was kept constant (pH = 6) for all the experiments.

- In the present study inter-electrode distance of $10\,mm$ gave the best defluoridation efficiency. Increasing the inter-electrode distance above this leads to decrease in defluoridation efficiency due to increase in resistance. Decreasing the distance below $10\,mm$ also decreases the efficiency due to short circuiting.

- The parametric investigations and there corroboration with literature gave an insight that initial fluoride concentration, applied current and electrolysis time are the three major parameters which governs the EC process.

- It was found that on increasing the initial fluoride concentration at constant applied current and electrolysis time, the residual fluoride decreases. This is due to formation of insufficient aluminium hydroxide complexes to remove available fluoride in water. It was also observed that higher initial fluoride concentration requires a higher value of applied current or longer electrolysis time for bringing down the residual fluoride below permissible limit of $1\,mg/L$.

- It was observed from the present study that up to $60-70\%$ of the initial fluoride concentration decreases within $10\,min$ from the start of the process. In the beginning of the process the fluoride removal is rapid and later it decreases gradually over almost the entire process examined. It is so as the fluoride ions are more abundant in the beginning of the EC process.

- Applied current and electrolysis time are important parameters of concern in EC process. They both together determine the coagulant produced and the bubble

generation rate. The applied current and electrolysis time go hand in hand. If the applied current is less, more electrolysis time is required for removal of fluoride and vice versa.

- It was observed that FUC decreases with increase in electrolysis time and then tends to stabilise. It is because of this fact, that treatment time should be carefully decided to minimize the wastage of energy and dissolution of aluminium in water.
- SEEC increases with increase in applied current and electrolysis time. With the increase in SEEC the fluoride removal also increases but after a certain value of energy consumed the fluoride removal is insignificant and most of the energy consumed is wasted in heating of electrodes.
- For desired removal a balance between electrolysis time and applied current has to be made so as to maintain the efficiency as well as economics of the process.
- In light of the above findings, applied current was kept between $0.30 - 0.75\,A$ for all experimental investigations. It was found, that for a minimum value of initial fluoride concentration ($2\,mg/L$) and minimum value of applied current ($0.30\,A$), $15\,min$ of electrolysis time was sufficient to bring down the fluoride within acceptable limits (IS:10500:2012, less than $1\,mg/L$). Similarly for maximum value of initial fluoride concentration ($8\,mg/L$) at a minimum value of applied current ($0.30\,A$), $40\,min$ was sufficient to lower the residual fluoride to prescribed limit. Therefore, the range of electrolysis time, for experimental investigations was kept as $10 - 50\,min$ (allowing a sufficient margin for desired fluoride removal).

8.2 Development of statistical model for fluoride removal

This Chapter implements the design of experiments for the development of statistical model. Taguchi design has been used to develop the statistical model. The model for fluoride removal was developed to understand the interaction between operating parameters and responses. The equations developed through statistical model development were used to optimize the operational parameters for better economy of treatment and efficiency of the process.

- The three parameters used for development of Taguchi design were: initial fluoride concentration, applied current and electrolysis time. The three responses were: residual fluoride, residual aluminium and SEEC.

- The model developed using Taguchi design, was validated by ANOVA. High R^2 value of 0.9468, 0.9959 and 0.9985 was obtained for residual fluoride, residual aluminium and SEEC respectively.

- In case of residual fluoride as a response; all the three parameters, initial fluoride, applied current and electrolysis time have p-values of 0.003, 0.005 and 0.000 respectively which accounts for the significance of these factors, electrolysis time being the highly significant of them.

- In case of residual aluminium as a response, initial fluoride, applied current, electrolysis time and interaction effect (ixt) were significant parameters while (F_ixt) are marginally significant. This suggests that the combined effect of the factors "i" and "t" plays an important role in the dissolution of aluminium anode.

- In case of SEEC as a response, initial fluoride, applied current and electrolysis time are significant factors.

- Residuals were tested using normal probability plots and residual v/s fit plots. Straight line in the normal probability plots and constant variance in the residual v/s fit plot was observed, which suggests that the model is well behaved.

- Main effect plots were studied for all three responses.

1. It was observed that with increase in initial fluoride the residual fluoride increases. It was also observed that with increase in applied current and time the residual fluoride decreases.

2. With an increase in initial fluoride, residual aluminium decreases. It can be observed that as the initial fluoride increases from 2 to 8 mg/L, more fluoride is available to bind with aluminium and hence lesser aluminium is in the solution. But with increase in electrolysis time and applied current, the residual aluminium increases.

3. With increase in initial fluoride, SEEC decreases; as there is availability of more fluoride so per unit removal is increased. With more current and time, SEEC increases as it is directly proportional to applied current and time.

- The relationship between residual fluoride, residual aluminium and SEEC with a combination of control factors was obtained using non-linear regression analysis with the help of SYSTAT 7.0.

- Actual v/s predicted response graphs were plotted to verify the obtained equations. High R^2 values in the tune of 0.95 and above indicates that the equations can be used for prediction of data.

- The study of kinetics of process study indicates the second order kinetics fits the data well, which suggests that removal of fluoride is due to physico-chemical reactions between the fluoride and aluminium hydroxide flocs. Also chemisorption is the rate limiting step and hence this step governs the adsorption rate.

- The isotherm study reveals that for applied current of $0.31\,A$, Langmuir isotherm fits the data well and for higher applied current values, Redlich-Peterson isotherm fits the data well. Depending on the applied current, the surface of the adsorbate can be homogenous or hetrogenous.

8.3 Development of model for aluminium removal

From previous findings it is evident that defluoridation by EC process using aluminium electrodes introduces aluminium in the water, besides removing fluoride from it. Aluminium is reported in literature as a potential neuro-toxicant. Therefore, there is a need to control the aluminium concentration in the treated water to offset ill-effects of aluminium on human health. The present chapter discusses the measures to control the aluminium concentration in the treated water introduced during defluoridation.

- It is evident that energy input governs the dissolution of aluminium in water. As a first step to control aluminium, energy input was minimized (optimizing "i and t") using a program in FORTRAN for desired target value of fluoride in water after treatment. ($0.7\,mg/L$). The controlled aluminium dissolution at this stage helps in subsequent steps of treatment for aluminium control.

- As a second step to control aluminium, flocculation and settling was attempted. The results showed an appreciable decrease in turbidity and aluminium concentration, but were still not close to permissible standards of aluminium in drinking water. It was now understandable that the efficient settling of flocs could lead to lesser residual aluminium. Therefore, coagulant aids were used for efficient settling of flocs. Use of coagulant aids brought down the aluminium within permissible standards.

- Coagulant aids (bentonite and activated silica sol) were used to improve settling efficiency. Both coagulant aids brought down the aluminium concentration in funal water below permissible limits of IS:10500:2012 ($0.2\,mg/L$).

- Taguchi design was used to develop model for bentonite clay and activated silica sol. ANOVA study was performed to assess the adequacy of the model. R^2 value of 0.9355 and 0.9488 was obtained for bentonite dosing and activated silica sol dosing repectively.

- With optimised dose of bentonite ($2\,g/L$), residual aluminium was brought down to a range of $0.03 - 0.08\,mg/L$. With optimised dose of activated silica sol ($30\,mg/L$), residual aluminium was brought down to a much lower range of $0.003 - 0.034\,mg/L$.
- Regression equations were developed using SYSTAT software for both aluminium after bentonite and activated silica sol dosing.
- The R2 value obtained for validation of equation were 0.9619 and 0.9824 for aluminium after bentonite and activated silica sol dosing respectively. This renders the model fit for prediction of data .
- Also, this chapter evaluated the adsorption isotherms for both bentonite dosing and activated silica sol dosing. The results suggested that features of Freundlich isotherm are best suited for this study.

8.4 Sludge characterization and cost analysis

This Chapter includes the characterization of the sludge formed during the treatment process. In the present study three sludges were studied; sludge produced after EC, flocculation and settling (sludge A), sludge produced after EC, bentonite dosing , flocculation and settling (sludge B) and sludge produced after EC, activated silica sol dosing , flocculation and settling (sludge C).

- Sludge quantity is important to plan for management of sludge. The reduction of waste volume leads to saving of the operational cost. Coagulant aids are added to aid in coagulation and to increase sludge density. The use of bentonite and activated silica sol improves floc settleability and lowers sludge volume.
- SSV_{30} is least in the case of activated silica sol dosing, followed by bentonite dosing and EC alone. This suggests that addition of activated silica sol increases the compaction of the sludge more than bentonite.
- The SEM-EDX analysis of sludge was conducted to know about the morphology and elemental composition of sludge.
- Atomic% of aluminium shows an increase from 10.13% (sludge A) to 11.23% (sludge B) and further increased to 12.34% (sludge C). This increase in aluminium percentage in sludge indicates role of bentonite and activated silica sol in aluminium removal .

- In FTIR scans of sludge A, Al-F-Al bond stretching peak was found at 604 cm^{-1}. This indicates that fluoride was linked with aluminium hydroxide complexes and precipitated in the reactor.
- FTIR scans show that there is a decrease in transmittance of Si-O-Al peak in case of sludge B when compared to raw bentonite. This may be suggested as an evidence of adsorption taking place in sludge B
- In FTIR scans of sludge C, Si-O-Al peak was present at 538 cm^{-1}. This peak was absent in FTIR scan of activated silica sol. This finding supports the results that activated silica sol is better than bentonite for removing aluminium from treated water. The removal of aluminium occurs in two steps; first aluminium is utilised in the formation of negatively charged aluminosilicates and second the positively charges aluminium polymers are removed by these aluminosilicates as a result of charge neutralization.
- XRD analysis of sludge A shows the presence of compounds like sodium aluminium fluoride, aluminium fluoride hydrate and aluminium oxide hydrate. It indicates the mechanism of fluoride remaining through alumino-fluoro complexes.
- XRD analysis of sludge B shows the presence of compounds like sodium magnesium aluminium fluoride silicate, sodium aluminium fluoride, aluminium fluoride silicate and aluminium silicate hydroxide fluoride. The presences of these compounds indicate towards the chemisorption of alumino complexes in the form of flocs on to the bentonite clay particles.
- XRD analysis of sludge C shows the presence of compounds like sodium aluminium silicate hydrate, sodium aluminium fluoride, aluminium silicate hydroxide fluoride and aluminium fluoride silicate. The presence of these compounds indicates towards the chemisorption of alumino complexes to activated silica sol.
- The operating cost of the process used in the present study is $0.06 - 0.13\,USD/m^3$ of water treated when bentonite is used as a coagulant aid and$0.29 - 0.36\,USD/m^3$of water treated when activated silica sol is used as coagulant aid.

The present study was able to successfully remove fluoride and aluminium from water and render it fit for drinking purpose. Table 8.1 summarizes the details of treatment.

Table 8.1: Operational parameter settings and their respective responses

Operating Parameters			***After EC***		***After bentonite dosing*** $(2\,g/L)$***, settling, filtration***		***After activated silica sol dosing*** $(30\,mg/L)$***, settling, filtration***	
F_i (mg/L)	i (A)	t (min)	F_r (mg/L)	Al_r (mg/L)	Al_{bd} (mg/L)	pH_{bd}	Al_{as} (mg/L)	pH_{as}
2	0.33	17.05	0.72	14.018	0.072	7.12	0.029	7.10
3	0.32	20.93	0.75	12.723	0.044	7.14	0.018	7.10
4	0.39	22.41	0.72	11.926	0.036	7.12	0.009	7.12
5	0.36	27.85	0.70	11.732	0.032	7.10	0.005	7.12
6	0.32	34.90	0.73	11.586	0.030	7.15	0.003	7.14
7	0.31	41.08	0.73	12.504	0.040	7.18	0.017	7.16
8	0.37	43.84	0.74	15.320	0.080	7.25	0.034	7.25

The results presented in 8.1 show that the process used in the present study brings down both fluoride as well as aluminium within the IS:10500:2012 permissible limits.

Recommendations for further research

The EC process is sensitive process for fluoride removal and a lot of literature is available about the process. But there is still scope for further research in this area and following recommendations may help to improve the treatment.

- Deeper understanding of the process is required to develop a better reactor design.
- Bubble size in the treatment helps in removal by flotation. Evaluation of role of electrolytic bubbles in the removal process requires deeper knowledge of bubble characteristics.
- Different electrode materials can be used. Inert material for cathode and aluminium alloys for anode may be attempted. This might help in better control of dissolution of aluminium during electrolysis.
- The rate of mixing in the EC reactor might affect the performance of the process which was not studied in the present work. Further investigations for flocculation and their interactions need to be studied for better understanding.
- Different ways of connecting electrodes might be studied in future research. Use of alternating current instead of direct current may also be studied. Alternating current prevents the formation of impermeable oxide layer on the cathode.
- Solar energy could be considered as a source of power for running the EC process, and make process useful for remote locations with limited or no power supply.
- In the present research only two coagulant aids were used for removal of aluminium. More coagulant aids may be evaluated to get better understanding for aluminium removal.
- Cost analysis made in the present study is an approximate cost given on the basis of batch experiments performed on laboratory scale. Detailed cost investigations for the treatment process, covering all aspects can be done.

Bibliography

[1] UNESCO, "Political inertia exacerbates water crisis, world water development report, first UN system wide evaluation of global water resources," 2003.

[2] R. Liteplo, P. Howe, and H. H. Malcolm, Environmental health Criteria 227: Fluorides, 2002.

[3] C. A. Tylenda, "Toxicological profile for fluorides, hydrogen fluoride and fluorine," Atlanta, September, 2003.

[4] K. Brindha and L. Elango, "Fluoride in groundwater: causes, implications and mitigation measures," Fluoride Properties, Applications and Environmental Management, pp. 111–136, 2011.

[5] S. Teotia and M. Teotia, "Endemic fluorosis in India: a challenging national health problem." The Journal of the Association of Physicians of India, vol. 32, no. 4, pp. 347–352, 1984.

[6] A. Susheela, "Fluorosis management programme in India," Current Science, vol. 77, no. 10, pp. 1250–1256, 1999.

[7] N. Mondal, R. Prasad, V. Saxena, Y. Singh, and V. Singh, "Appraisal of highly fluoride zones in groundwater of Kurmapalli watershed, Nalgonda district, Andhra Pradesh (India)," Environmental Earth Sciences, vol. 59, no. 1, pp. 63–73, 2009.

[8] N. R. Rao, N. Rao, K. S. P. Rao, and R. Schuiling, "Fluorine distribution in waters of Nalgonda district, Andhra Pradesh, India," Environmental Geology, vol. 21, no.1-2, pp. 84–89, 1993.

[9] N. S. Rao, "Fluoride in groundwater, Varaha river basin, Visakhapatnam district, Andhra Pradesh, India," Environmental monitoring and assessment, vol. 152, no. 1-4, pp. 47–60, 2009.

[10] B. Prasad and K. Kr. Mondal, "Leaching characteristics of fluoride from coal ash," Asian Journal of Water, Environment and Pollution, vol. 4, no. 2, pp. 17–21, 2007.

[11] B. Das, J. Talukdar, S. Sarma, B. Gohain, R. K. Dutta, H. B. Das, and S. C. Das, "Fluoride and other inorganic constituents in groundwater of Guwahati, Assam, India," Current Science Banglore, vol. 85, no. 5, pp. 657–660, 2003.

[12] P. Datta, D. Deb, and S. Tyagi, "Stable isotope (^{18}O) investigations on the processes controlling fluoride contamination of groundwater," Journal of contaminant hydrology, vol. 24, no. 1, pp. 85–96, 1996.

[13] P. Salve, A. Maurya, P. Kumbhare, D. Ramteke, and S. Wate, "Assessment of groundwater quality with respect to fluoride," Bulletin of environmental contamination and toxicology, vol. 81, no. 3, pp. 289–293, 2008.

[14] V. K. Garg, S. Suthar, S. Singh, A. Sheoran, S. Jain et al., "Drinking water quality in villages of Southwestern Haryana, India: assessing human health risks associated with hydrochemistry," Environmental geology, vol. 58, no. 6, pp. 1329–1340, 2009.

[15] B. Wodeyar and G. Srinivasan, "Occurrence of fluoride in the ground-waters and its impact in Pedda-Vankahalla basin, Bellary district, Karnataka-A preliminary study," Curr Sci, vol. 70, pp. 71–74, 1996.

[16] E. Shaji, J. V. Bindu, D.S. Thambi,. High fluoride in groundwater of Palghat district, Kerala," Current Science, vol. 92, no. 2, pp. 240–245, 2007.

[17] P. Madhnure, D. Sirsikar, A. Tiwari, B. Ranjan, and D. Malpe, "Occurrence of fluoride in the groundwaters of Pandharkawada area, Yavatmal district, Maharashtra, India," Current Science Banglore, vol. 92, no. 5, p. 675, 2007.

[18] S. Suthar, V. K. Garg, S. Jangir, S. Kaur, N. Goswami, and S. Singh, "Fluoride contamination in drinking water in rural habitations of northern Rajasthan, India," Environmental monitoring and assessment, vol. 145, no. 1-3, pp. 1–6, 2008.

[19] K. Karthikeyan, K. Nanthakumar, P. Velmurugan, S. Tamilarasi, and P. Lakshmanaperumalsamy, "Prevalence of certain inorganic constituents in groundwater samples of erode district, Tamil Nadu, India, with special emphasis on fluoride, fluorosis and its remedial measures," Environmental monitoring and assessment, vol. 160, no. 1-4, pp. 141–155, 2010.

[20] N. Sankararamakrishnan, A. K. Sharma, and L. Iyengar, "Contamination of nitrate and fluoride in ground water along the Ganges alluvial plain of Kanpur district, Uttar Pradesh, India," Environmental monitoring and assessment, vol.146, no. 1-3, pp. 375–382, 2008.

[21] M. C. Kundu and B. Mandal, "Assessment of potential hazards of fluoride contamination in drinking groundwater of an intensively cultivated district in West Bengal, India," Environmental monitoring and assessment, vol. 152, no. 1-4, pp. 97–103, 2009.

[22] J. Hussain, K. Sharma, and I. Hussain, "Fluoride in drinking water in Rajasthan and its ill effects on human health," J Tissue Res, vol. 4, pp. 263–273, 2004.

[23] P. Fottrell, Forum on Fluoridation 2002: Report Presented to Micheál Martin TD, Minister for Health and Children. Stationery Office, 2002.

[24] M. D. Grynpas, "Fluoride effects on bone crystals," Journal of Bone and Mineral Research, vol. 5, no. S1, pp. S169–S175, 1990.

[25] Bureau of Indian standards, "Indian standard- drinking water specification, second revision," 2012.

[26] S. Modi and R. Soni, "Merits and demerits of different technologies of defluoridation for drinking water," J Environ Sci Toxicol Food Technol, vol. 3, pp. 24–7, 2013.

[27] WHO, "Guidelines for drinking-water quality volume 1. Recommendations. 3rd Edition," 2004.

[28] H. Lounici, L. Adour, D. Belhocine, A. Elmidaoui, B. Bariou, and N. Mameri, "Novel technique to regenerate activated alumina bed saturated by fluoride ions," Chemical Engineering Journal, vol. 81, no. 1, pp. 153–160, 2001.

[29] N. Parthasarathy and J. Buffle, "Study of polymeric aluminium (iii) hydroxide solutions for application in waste water treatment. properties of the polymer and optimal conditions of preparation," Water Research, vol. 19, no. 1, pp. 25–36, 1985.

[30] M. Sujana, R. Thakur, and S. Rao, "Removal of fluoride from aqueous solution by using alum sludge," Journal of colloid and interface science, vol. 206, no. 1, pp. 94–101, 1998.

[31] A. Toyoda and T. Taira, "A new method for treating fluorine wastewater to reduce sludge and running costs," Semiconductor Manufacturing, IEEE Transactions on, vol. 13, no. 3, pp. 305–309, 2000.

[32] Z. Amor, B. Bariou, N. Mameri, M. Taky, S. Nicolas, and A. Elmidaoui, "Fluoride removal from brackish water by dialysis," Desalination, vol. 133, no. 3, pp. 215–223, 2001.

[33] N. Mameri, A. Yeddou, H. Lounici, D. Belhocine, H. Grib, and B. Bariou, "Defluoridation of septentrional Sahara water of North Africa by electrocoagulation process using bipolar aluminium electrodes," Water Research, vol. 32, no. 5, pp. 1604–1612, 1998.

[34] M. M. Emamjomeh and M. Sivakumar, "Fluoride removal by a continuous flow electrocoagulation reactor," Journal of Environmental Management, vol. 90, no. 2, pp. 1204–1212, 2009.

[35] A. Susheela, "Defluoridation of drinking water: merits of alternative technologies," Bull Nutr Found India, vol. 13, pp. 6–7, 1992.

[36] M. M. Emamjomeh, M. Sivakumar, and A. S. Varyani, "Analysis and the understanding of fluoride removal mechanisms by an electrocoagulation/flotation (ecf) process," Desalination, vol. 275, no. 1, pp. 102–106, 2011.

[37] D. Mills et al., "A new process for electrocoagulation (pdf)," Journal-American Water Works Association, vol. 92, no. 6, pp. 34–43, 2000.

[38] P. R. Kumar, S. Chaudhari, K. C. Khilar, and S. Mahajan, "Removal of arsenic from water by electrocoagulation," Chemosphere, vol. 55, no. 9, pp. 1245–1252, 2004.

[39] C.-Y. Hu, S.-L. Lo, and W.-H. Kuan, "Simulation the kinetics of fluoride removal by electrocoagulation (ec) process using aluminum electrodes," Journal of hazardous materials, vol. 145, no. 1, pp. 180–185, 2007.

[40] J. Zhu, H. Zhao, and J. Ni, "Fluoride distribution in electrocoagulation defluoridation process," Separation and Purification Technology, vol. 56, no. 2, pp. 184–191, 2007.

[41] P. K. Holt, G. W. Barton, M. Wark, and C. A. Mitchell, "A quantitative comparison between chemical dosing and electrocoagulation," Colloids and Surfaces A: Physicochemical and Engineering Aspects, vol. 211, no. 2, pp. 233–248, 2002.

[42] USEPA, "Secondary drinking water regulations: Guidance for nuisance chemicals."

[43] "Summary of guidelines for Canadian drinking water quality," 2003. [Online]. Available: www.hc-sc.gc.ca/waterquality

[44] P. Srinivasan, T. Viraraghavan, and K. Subramanian, "Aluminium in drinking water: An overview," Water SA, vol. 25, no. 1, pp. 47–55, 1999.

[45] W. D. Schecher and C. T. Driscoll, "Alchemi: A chemical equilibrium model to assess the acid-base chemistry and speciation of aluminum in dilute solutions," Chemical Equilibrium and Reaction Models, pp. 325–356, 1995.

[46] A. Rahman, "Residual aluminum in treated water," M.Sc Thesis, State university of Newyork at Buffalo, NY, 1992.

[47] A. I. C. R. Committee et al., "Committee report–research needs for inorganic contaminants (pdf)," Journal-American Water Works Association, vol. 85, no. 5, pp. 106–113, 1993.

[48] S. Masten, "Research triangle park, north carolina 27709," 2002.

[49] A. Strunecka and J. Patocka, "Pharmacological and toxicological effects of aluminofluoride complexes," Fluoride, vol. 32, no. 4, pp. 230–242, 1999.

[50] H. Jacqmin, D. Commenges, L. Letenneur, P. Barberger-Gateau, and J.-F. Dartigues, "Components of drinking water and risk of cognitive impairment in the elderly," American journal of epidemiology, vol. 139, no. 1, pp. 48–57, 1994.

[51] S. S. Gupta A.B., Gupta Sunil K., "Aluminium-fluoride interactions in drinking water and their synergistic effects on human health : A case study," Paper communicated to Fluoride, NZ, 2000.

[52] B. Jajoo, "The synergistic role of aluminium and fluoride in fluorosis- a case study of Chaksu block, Jaipur," M.E. (Environmental Engineering) dissertation, MREC, University of Rajasthan, Jaipur, 2002.

[53] D. Sayal, "The synergistic role of aluminium and fluoride in fluorosis," M.E. (Environmental Engineering) dissertation, MREC, University of Rajasthan, Jaipur, 2001.

[54] W. Nawlakhe, D. Kulkarni, B. Pathak, and K. Bulusu, "Defluoridation of water by Nalgonda technique," Indian Journal of Environmental Health, vol. 17, no. 1, pp. 26–67, 1978.

[55] B. K. Shrivastava, A. Vani., "Comparative study of defluoridation technologies in India," Asian J. Exp. Sci, vol. 23, no. 1, pp. 269–274, 2009.

[56] S. Gupta, "A process for defluoridation of water by a filter bed using indigenous material," Indian J. Environ. Sci, vol. 1, no. 2, pp. 149–156, 1997.

[57] R. C. Maheshwari, "Fluoride in drinking water and its removal," Journal of

Hazardous Materials, vol. 137, no. 1, pp. 456–463, 2006.

[58] O. J. Hao and C. Huang, "Adsorption characteristics of fluoride onto hydrous alumina," Journal of environmental engineering, vol. 112, no. 6, pp. 1054–1069, 1986.

[59] K. C. Agarwal, S. K. Gupta, and A. B. Gupta, "Development of new low cost defluoridation technology (krass)," Water science and technology, vol. 40, no. 2, pp. 167–173, 1999.

[60] S. Ayoob, A. Gupta, and V. T. Bhat, "A conceptual overview on sustainable technologies for the defluoridation of drinking water," Critical reviews in environmental science and technology, vol. 38, no. 6, pp. 401–470, 2008.

[61] M. Agarwal, K. Rai, R. Shrivastav, and S. Dass, "A study on fluoride sorption by montmorillonite and kaolinite," Water, air, and soil pollution, vol. 141, no. 1-4, pp. 247–261, 2002.

[62] G. Karthikeyan, A. Pius, G. Alagumuthu., "Fluoride adsorption studies of montmorillonite clay," Indian Journal of Chemical Technology, vol. 12, no. 3, pp.263–272, 2005.

[63] Y. Çengelog lu, E. Kır, and M. Ersöz, "Removal of fluoride from aqueous solution by using red mud," Separation and Purification Technology, vol. 28, no. 1, pp. 81–86, 2002.

[64] R. Piddennavar and P. Krishnappa, "Review on defluoridation techniques of water," Int J Eng Sci, vol. 2, pp. 86–94, 2013.

[65] S. Adhikary, U. Tipnis, W. Harkare, and K. Govindan, "Defluoridation during desalination of brackish water by electrodialysis," Desalination, vol. 71, no. 3, pp. 301–312, 1989.

[66] H. Deng and X. Yu, "Fluoride removal from drinking water by zirconium-impregnated fibrous protein," Desalination and Water Treatment, no. ahead-of-print, pp. 1–10, 2014.

[67] K. Matis, A. Zouboulis, S. Mandjiny, and D. Zamboulis, "Removal of cadmium from dilute solutions by hydroxyapatite. (III) flocculation studies," Separation science and technology, vol. 32, no. 13, pp. 2127–2148, 1997.

[68] J. Eastoe and T. Cosgrove, "Colloid science, principles methods and applications," 2005.

[69] W. Stumm and C. R. O'Melia, "Stoichiometry of coagulation," Journal of American Water Works Association, pp. 514–539, 1968.

[70] Y. Ş. Yildiz, A. S. Koparal, Ş. Irdemez, and B. Keskinler, "Electrocoagulation of synthetically prepared water containing high concentration of NOM using iron cast electrodes," Journal of hazardous materials, vol. 139, no. 2, pp. 373–380, 2007.

[71] R. D. Letterman, Water quality and treatment: a handbook of community water supplies. McGraw-Hill Professional, 1999.

[72] B. A. Dempsey and C. R. O'Melia, "Removal of naturally occurring compounds by coagulation and sedimentation," Critical Reviews in Environmental Science and Technology, vol. 14, no. 4, pp. 311–331, 1984.

[73] A. Amirtharajah and K. M. Mills, "Rapid-mix design for mechanisms of alum coagulation," Journal of American Water Works Association, pp. 210–216, 1982.

[74] N. Meunier, P. Drogui, C. Montané, R. Hausler, G. Mercier, and J.-F. Blais, "Comparison between electrocoagulation and chemical precipitation for metals removal from acidic soil leachate," Journal of hazardous materials, vol. 137, no. 1, pp. 581–590, 2006.

[75] S. K. Dentel and J. M. Gossett, "Mechanisms of coagulation with aluminum salts," Journal of American Water Works Association, pp. 187–198, 1988.

[76] W. Stumm and J. J. Morgan, Aquatic chemistry: An introduction emphasizing chemical equilibria in natural waters. John Wiley & Sons, 1981.

[77] R. W. Smith, "Kinetic aspects of aqueous aluminum chemistry: environmental implications," Coordination chemistry reviews, vol. 149, pp. 81–93, 1996.

[78] Y. Avsar, U. Kurt, and T. Gonullu, "Comparison of classical chemical and electrochemical processes for treating rose processing wastewater," Journal of hazardous materials, vol. 148, no. 1, pp. 340–345, 2007.

[79] P. Srinivasan and T. Viraraghavan, "Characterisation and concentration profile of aluminium during drinking-water treatment," Water SA, vol. 28, no. 1, pp. 99–106, 2002.

[80] N. Radic and M. Bralic, "Aluminium fluoride complexation and its ecological importance in the aquatic environment," Science of the total environment, vol. 172, no. 2, pp. 237–243, 1995.

[81] N. Mameri, H. Lounici, D. Belhocine, H. Grib, D. Piron, and Y. Yahiat, "Defluoridation of Sahara water by small plant electrocoagulation using bipolar aluminium electrodes," Separation and Purification Technology, vol. 24, no. 1, pp. 113–119, 2001.

[82] C. R. O'Melia, "Review of the coagulation process," Public works, vol. 100, p. 11, 1969.

[83] L. D. Benefield, J. F. Judkins, and B. L. Weand, Process chemistry for water and wastewater treatment. Prentice Hall Inc, 1982.

[84] H. A. Moreno C, D. L. Cocke, J. A. Gomes, P. Morkovsky, J. Parga, E. Peterson, and C. Garcia, "Electrochemical reactions for electrocoagulation using iron electrodes," Industrial & Engineering Chemistry Research, vol. 48, no. 4, pp. 2275–2282, 2009.

[85] E. A. Vik, D. A. Carlson, A. S. Eikum, and E. T. Gjessing, "Electrocoagulation of potable water," Water Research, vol. 18, no. 11, pp. 1355–1360, 1984.

[86] K. Rajeshwar, J. Ibanez, and G. Swain, "Electrochemistry and the environment," Journal of Applied Electrochemistry, vol. 24, no. 11, pp. 1077–1091, 1994.

[87] G. Sposito et al., The environmental chemistry of aluminum., 1989.

[88] F. Shen, X. Chen, P. Gao, and G. Chen, "Electrochemical removal of fluoride ions from industrial wastewater," Chemical Engineering Science, vol. 58, no. 3, pp. 987–993, 2003.

[89] G. Chen, "Electrochemical technologies in wastewater treatment," Separation and purification Technology, vol. 38, no. 1, pp. 11–41, 2004.

[90] J. A. Gomes, P. Daida, M. Kesmez, M. Weir, H. Moreno, J. R. Parga, G. Irwin, H. McWhinney, T. Grady, E. Peterson, "Arsenic removal by electrocoagulation using combined Al–Fe electrode system and characterization of products," Journal of Hazardous Materials, vol. 139, no. 2, pp. 220–231, 2007.

[91] R. Katal and H. Pahlavanzadeh, "Influence of different combinations of aluminum and iron electrode on electrocoagulation efficiency: Application to the treatment of paper mill wastewater," Desalination, vol. 265, no. 1, pp. 199–205, 2011.

[92] L. Ming, S. R. Yi, Z. J. Hua, B. Yuan, W. Lei, L. Ping, and K. C. Fuwa, "Elimination of excess fluoride in potable water with coacervation by electrolysis using an aluminum anode." Fluoride, vol. 20, no. 2, pp. 54–63, 1987.

[93] C. Hu, S. Lo, and W. Kuan, "Effects of co-existing anions on fluoride removal in electrocoagulation (ec) process using aluminum electrodes," Water research, vol. 37, no. 18, pp. 4513–4523, 2003.

[94] Q. Zuo, X. Chen, W. Li, and G. Chen, "Combined electrocoagulation and electroflotation for removal of fluoride from drinking water," Journal of hazardous materials, vol. 159, no. 2, pp. 452–457, 2008.

[95] M. Y. A. Mollah, R. Schennach, J. R. Parga, and D. L. Cocke, "Electrocoagulation (ec) science and applications," Journal of hazardous materials, vol. 84, no. 1, pp. 29–41, 2001.

[96] M. M. Emamjomeh and M. Sivakumar, "An empirical model for defluoridation by batch monopolar electrocoagulation/flotation (ecf) process," Journal of hazardous materials, vol. 131, no. 1, pp. 118–125, 2006.

[97] C.-Y. Hu, S.-L. Lo, W.-H. Kuan, and Y.-D. Lee, "Treatment of high fluoride-content wastewater by continuous electrocoagulation–flotation system with bipolar aluminum electrodes," Separation and Purification Technology, vol. 60, no. 1, pp. 1–5, 2008.

[98] D. Ghosh, C. Medhi, and M. Purkait, "Treatment of fluoride containing drinking water by electrocoagulation using monopolar and bipolar electrode connections," Chemosphere, vol. 73, no. 9, pp. 1393–1400, 2008.

[99] N. Drouiche, N. Ghaffour, S. Aoudj, M. Hecini, and T. Ouslimane, "Fluoride removal from photovoltaic wastewater by aluminium electrocoagulation and characteristics of products," Chemical Engineering Transactions, vol. 17, pp.1651–1656, 2009.

[100] N. Drouiche, S. Aoudj, H. Lounici, H. Mahmoudi, N. Ghaffour, and M. Goosen, "Development of an empirical model for fluoride removal from photovoltaic wastewater by electrocoagulation process," Desalination and Water Treatment, vol. 29, no. 1-3, pp. 96–102, 2011.

[101] M. Behbahani, M. A. Moghaddam, and M. Arami, "Techno-economical evaluation of fluoride removal by electrocoagulation process: Optimization

through response surface methodology," Desalination, vol. 271, no. 1, pp. 209–218, 2011.

[102] N. Drouiche, S. Aoudj, H. Lounici, M. Drouiche, T. Ouslimane, and N. Ghaffour, "Fluoride removal from pretreated photovoltaic wastewater by electrocoagulation: an investigation of the effect of operational parameters," Procedia Engineering, vol. 33, pp. 385–391, 2012.

[103] A. Takdastan, S. E. Tabar, A. Neisi, and A. Eslami, "Fluoride removal from drinking water by electrocoagulation using iron and aluminum electrodes" Jundishapur J.Health Sci., vol. 6, 2014.

[104] M. M. Naim, A. A. Moneer, and G. F. El-Said, "Predictive equations for the defluoridation by electrocoagulation technique using bipolar aluminum electrodes in the absence and presence of additives: a multivariate study," Desalination and Water Treatment, no. ahead-of-print, pp. 1–13, 2015.

[105] M. M. Emamjomeh, "Electrocoagulation technology as a process for defluoridation in water treatment," 2006.

[106] S. C. Lenore, E. G. Arnold, and D. E. Andrew, "Standard methods for the examination of water and wastewater," American Public Health Association. American Water Works Association and World Environment Federation. 20th Edition, Washington DC, 1998.

[107] G. Chen, X. Chen, and P. L. Yue, "Electrocoagulation and electroflotation of restaurant wastewater," Journal of environmental engineering, vol. 126, no. 9, pp. 858–863, 2000.

[108] C. Zhang, S. Tan, X. Niu, and P. Su, "Treatment of geothermal water with high fluoride content by electrocoagulation," Desalination and Water Treatment, no. ahead-of-print, pp. 1–5, 2014.

[109] G. Karthikeyan, B. Apparao, and S. Meenakshi, "Mechanistic studies of the defluoridation property of activated alumina," in Proceedings of the Second International Workshop on Fluorosis and Defluoridation of Water, pp. 19–25, 1997.

[110] L. Iyengar, "Defluoridation of water using activated alumina technology studies carried out at IIT Kanpur. A report prepared in March 2005 for UNICEF, New Delhi. pp. 1-9."

[111] R. Sinha, A. Singh, and S. Mathur, "Multiobjective optimization for minimum residual fluoride and specific energy in electrocoagulation process," Desalination and Water Treatment, no. ahead-of-print, pp. 1–11, 2014.

[112] R. Foley, "Localized corrosion of aluminum alloys-a review," Corrosion, vol. 42, no. 5, pp. 277–288, 1986.

[113] A. C. Davison, Statistical models. Cambridge University Press, 2003, vol. 11.

[114] S. P. Kondapalli, S. R. Chalamalasetti, and N. R. Damera, "Application of Taguchi based design of experiments to fusion arc weld processes: A review," International Journal of Technology and Management (IJTM), vol. 2, no. 1, 2013.

[115] S. Athreya and Y. Venkatesh, "Application of taguchi method for optimization of process parameters in improving the surface roughness of lathe facing operation," International Refereed Journal of Engineering and Science (IRJES) ISSN (Online), pp. 2319–1821, 2012.

[116] K. Vishwanatha, A. A. Rao, and S. A. Singh, "Acid protease production by solid-state fermentation using aspergillus oryzae mtcc 5341: optimization of process parameters," Journal of industrial microbiology & biotechnology, vol. 37, no. 2, pp. 129–138, 2010.

[117] P. J. Ross, "Taguchi techniques for quality engineering, 1996," Mcgraw-Hill International editions.

[118] T. J. S.An, "DOE based statistical approaches in modeling of laser processing– review & suggestion," 2010.

[119] S. Suresh, V. Srivastava, and I. Mishra, "Adsorptive removal of aniline by granular activated carbon from aqueous solutions with catechol and resorcinol," Environmental technology, vol. 33, no. 7, pp. 773–781, 2012.

[120] F. Kolahan, M. Manoochehri, and A. Hosseini, "Application of Taguchi method and anova analysis for simultaneous optimization of machining parameters and tool geometry in turning," in International Conference on Computer, Electrical and Systems Science and Engineering-ICCESSE 2011, 2011.

[121] K. Ravikumar, S. Krishnan, S. Ramalingam, and K. Balu, "Optimization of process variables by the application of response surface methodology for dye removal using a novel adsorbent," Dyes and Pigments, vol. 72, no. 1, pp. 66–74, 2007.

[122] A. Lohmann, English Coordinate Constructions. Cambridge University Press, 2014.

[123] A. R. Khataee, M. Zarei, and L. Moradkhannejhad, "Application of response surface methodology for optimization of Azo dye removal by oxalate catalyzed photoelectro-fenton process using carbon nanotube-ptfe cathode," Desalination, vol. 258, no. 1, pp. 112–119, 2010.

[124] J.J.Faraway,"Practical regression and anova using R, "2002.

[125] K. Chithra and N. Balasubramanian, "Modeling electrocoagulation through adsorption kinetics." Journal of Modelling & Simulation of Systems, vol. 1, no. 2, 2010.

[126] J. R. Parga, D. L. Cocke, V. Valverde, J. A. Gomes, M. Kesmez, H. Moreno, M. Weir, and D. Mencer, "Characterization of electrocoagulation for removal of chromium and arsenic," Chemical Engineering & Technology, vol. 28, no. 5, pp. 605–612, 2005.

[127] P. S. Kumar, K. Ramakrishnan, S. D. Kirupha, and S. Sivanesan, "Thermodynamic and kinetic studies of cadmium adsorption from aqueous solution onto rice husk," Brazilian Journal of Chemical Engineering, vol. 27, no. 2, pp. 347–355, 2010.

[128] M. Malakootian, M. Moosazadeh, N. Yousefi, and A. Fatehizadeh, "Fluoride removal from aqueous solution by pumice: case study on Kuhbonan water," African Journal of Environmental Science and Technology, vol. 5, no. 4, pp. 299–306, 2011.

[129] A. El Nemr, "Potential of pomegranate husk carbon for Cr (VI) removal from wastewater: Kinetic and isotherm studies," Journal of Hazardous Materials, vol. 161, no. 1, pp. 132–141, 2009.

[130] A. Celekli, M. Yavuzatmaca, and H. Bozkurt, "Kinetic and equilibrium studies on the adsorption of reactive red 120 from aqueous solution on spirogyra majuscula," Chemical Engineering Journal, vol. 152, no. 1, pp. 139–145, 2009.

[131] S. Vasudevan, J. Lakshmi, J. Jayaraj, and G. Sozhan, "Remediation of phosphate-contaminated water by electrocoagulation with aluminium, aluminium alloy and mild steel anodes," Journal of Hazardous Materials, vol. 164, no. 2, pp. 1480–1486, 2009.

[132] S. M. Maliyekkal, A. K. Sharma, and L. Philip, "Manganese-oxide-coated

alumina: a promising sorbent for defluoridation of water," Water Research, vol. 40, no. 19, pp. 3497–3506, 2006.

[133] V. Khatibikamal, A. Torabian, F. Janpoor, and G. Hoshyaripour, "Fluoride removal from industrial wastewater using electrocoagulation and its adsorption kinetics," Journal of hazardous materials, vol. 179, no. 1, pp. 276–280, 2010.

[134] H. Wang, A. Zhou, F. Peng, H. Yu, and J. Yang, "Mechanism study on adsorption of acidified multiwalled carbon nanotubes to Pb (II)," Journal of Colloid and Interface Science, vol. 316, no. 2, pp. 277–283, 2007.

[135] B. Liu, D. Wang, X. Gao, L. Zhang, Y. Xu, and Y. Li, "Removal of Arsenic from laminaria japonica aresch juice using As (III)-imprinted chitosan resin," European Food Research and Technology, vol. 232, no. 5, pp. 911–917, 2011.

[136] Z. Shahryari, A. S. Goharrizi, and M. Azadi, "Experimental study of methylene blue adsorption from aqueous solutions onto carbon nano tubes," Int J Water Res Environ Eng, vol. 2, no. 2, pp. 16–28, 2010.

[137] S. Allen, G. Mckay, and J. Porter, "Adsorption isotherm models for basic dye adsorption by peat in single and binary component systems," Journal of Colloid and Interface Science, vol. 280, no. 2, pp. 322–333, 2004.

[138] G. Limousin, J.-P. Gaudet, L. Charlet, S. Szenknect, V. Barthes, and M. Krimissa, "Sorption isotherms: a review on physical bases, modeling and measurement," Applied Geochemistry, vol. 22, no. 2, pp. 249–275, 2007.

[139] A. Ghanim, S. Ajjam., "Kinetic modelling of nitrate removal from aqueous solution during electrocoagulation," Civil and Environmental Research, vol. 3, no. 7, pp. 64–73, 2013.

[140] T. Vermeulan, K. Vermeulan, and L. Hall, "Fundamental," J. Ind. Eng. Chem, vol. 5, pp. 212–223, 1966.

[141] N. D. Hutson, S. C. Zajic, and R. T. Yang, "Influence of residual water on the adsorption of atmospheric gases in Li-x zeolite: Experiment and simulation," Industrial & Engineering Chemistry Research, vol. 39, no. 6, pp. 1775–1780, 2000.

[142] O. Redlich and D. L. Peterson, "A useful adsorption isotherm," Journal of Physical Chemistry, vol. 63, no. 6, pp. 1024–1024, 1959.

[143] B. Armagan and F. Toprak, "Optimum isotherm parameters for reactive azo dye onto pistachio nut shells: comparison of linear and non-linear methods," Polish

Journal of Environmental Studies, vol. 22, no. 4, 2013.

[144] R. Han, Y. Wang, W. Zou, Y. Wang, and J. Shi, "Comparison of linear and nonlinear analysis in estimating the Thomas model parameters for Methylene blue adsorption onto natural Zeolite in fixed-bed column," Journal of hazardous materials, vol. 145, no. 1, pp. 331–335, 2007.

[145] K. V. Kumar and S. Sivanesan, "Sorption isotherm for safranin onto rice husk: Comparison of linear and non-linear methods," Dyes and Pigments, vol. 72, no. 1, pp. 130–133, 2007.

[146] M. Hossain, H. Ngo, W. Guo, and T. Setiadi, "Adsorption and desorption of Copper (II) ions onto garden grass," Bioresource technology, vol. 121, pp. 386–395, 2012.

[147] Y.-S. Ho, "Selection of optimum sorption isotherm," Carbon, vol. 42, no. 10, pp. 2115–2116, 2004.

[148] J. Ng, W. Cheung, and G. McKay, "Equilibrium studies of the sorption of Cu (II) ions onto chitosan," Journal of Colloid and Interface Science, vol. 255, no. 1, pp. 64–74, 2002.

[149] F. Gimbert, N. Morin-Crini, F. Renault, P.-M. Badot, and G. Crini, "Adsorption isotherm models for dye removal by cationized starch-based material in a single component system: error analysis," Journal of Hazardous Materials, vol. 157, no. 1, pp. 34–46, 2008.

[150] L. Jossens, J. Prausnitz, W. Fritz, E. Schlünder, and A. Myers, "Thermodynamics of multi-solute adsorption from dilute aqueous solutions," Chemical Engineering Science, vol. 33, no. 8, pp. 1097–1106, 1978.

[151] K. Foo and B. Hameed, "Insights into the modeling of adsorption isotherm systems," Chemical Engineering Journal, vol. 156, no. 1, pp. 2–10, 2010.

[152] R. Sinha and S. Mathur, "Control of aluminium in treated water after defluoridation by electrocoagulation and modelling of adsorption isotherms," Desalination and Water Treatment, no. ahead-of-print, pp. 1–10, 2015.

[153] B. M. Moudgil, S. Behl, and T. Prakash, "Effect of particle size in flocculation," Journal of colloid and interface science, vol. 158, no. 2, pp. 511–512, 1993.

[154] R. Abdullah, I. Abustan, and A. N. M. Ibrahim., "Wastewater treatment using bentonite, the combinations of bentonite-zeolite, bentonite-alum, and bentonite-limestone as adsorbent and coagulant," International Journal of Environmental Sciences, vol. 4, no. 3, p. 379, 2013.

[155] J. Birchall, C. Exley, J. Chappell, and M. Phillips, "Acute toxicity of aluminium to fish eliminated in silicon-rich acid waters," 1989.

[156] T. W. Swaddle, "Silicate complexes of Aluminum (III) in aqueous systems," Coordination Chemistry Reviews, vol. 219, pp. 665–686, 2001.

[157] C. Exley, C. Schneider, and F. J. Doucet, "The reaction of aluminium with silicic acid in acidic solution: an important mechanism in controlling the biological availability of aluminium?" Coordination Chemistry Reviews, vol. 228, no. 2, pp. 127–135, 2002.

[158] A. S. Özcan and A. Özcan, "Adsorption of acid dyes from aqueous solutions onto acid-activated bentonite," Journal of Colloid and Interface Science, vol. 276, no. 1, pp. 39–46, 2004.

[159] Y.-H. Shen, "Preparations of organobentonite using nonionic surfactants," Chemosphere, vol. 44, no. 5, pp. 989–995, 2001.

[160] R. Sinha, S. Mathur, and U. Brighu, "Aluminium removal from water after defluoridation with electrocoagulation process," Environmental technology, DOI: 10.1080/09593330.2015.1043958, 2015.

[161] S. Babel and T. A. Kurniawan, "Low-cost adsorbents for heavy metals uptake from contaminated water: a review," Journal of hazardous materials, vol. 97, no. 1, pp. 219–243, 2003.

[162] A. Khenifi, B. Zohra, B. Kahina, H. Houari, and D. Zoubir, "Removal of 2, 4-DCP from wastewater by CTAB/bentonite using one-step and two-step methods: a comparative study," Chemical engineering journal, vol. 146, no. 3, pp. 345–354, 2009.

[163] M. Al-Qunaibit, W. Mekhemer, and A. Zaghloul, "The adsorption of Cu (II) ions on bentonite-a kinetic study," Journal of colloid and interface science, vol. 283, no. 2, pp. 316–321, 2005.

[164] L. Pauling, The Nature of the Chemical Bond. Cornell University press Ithaca, NY, 1960, vol. 3.

[165] P. Cloos, A. Li ., "Structural organization of amorphous silico-aluminas," in Clays & Clay Minerals. Citeseer, 1969.

[166] B. Lartiges, J. Bottero, L. Derrendinger, B. Humbert, P. Tekely, and H. Suty, "Flocculation of colloidal silica with hydrolyzed aluminum: And 27 Al solid state NMR investigation," Langmuir, vol. 13, no. 2, pp. 147–152, 1997.

[167] M. Tamele, "Chemistry of the surface and the activity of alumina-silica cracking catalyst," Discussions of the Faraday Society, vol. 8, pp. 270–279, 1950.

[168] K. V. Kumar, "Optimum sorption isotherm by linear and non-linear methods for malachite green onto lemon peel," Dyes and Pigments, vol. 74, no. 3, pp. 595–597, 2007.

[169] M. A. Hossain, H. H. Ngo, and W. Guo, "Introductory of microsoft excel solver function-spreadsheet method for isotherm and kinetics modelling of metals biosorption in water and wastewater," Journal of Water Sustainability, vol. 3, no. 4, pp. 223–237, 2013.

[170] S. D. Lin and C. D. Green, Wastes from water treatment plants: Literature review, results of an Illinois survey, and effects of alum sludge application to cropland. Illinois State Water Survey, Water Quality Section, 1987.

[171] T. González, J. R. Domínguez, J. Beltrán-Heredia, H. M. García, and F. Sanchez-Lavado, "Aluminium sulfate as coagulant for highly polluted cork processing wastewater: Evaluation of settleability parameters and design of a clarifier-thickener unit," Journal of hazardous materials, vol. 148, no. 1, pp. 6–14, 2007.

[172] J.-P. Wang, Y.-Z. Chen, X.-W. Ge, and H.-Q. Yu, "Optimization of coagulation–flocculation process for a paper-recycling wastewater treatment using response surface methodology," Colloids and Surfaces A: Physicochemical and Engineering Aspects, vol. 302, no. 1, pp. 204–210, 2007.

[173] A. Ndabigengesere, K. S. Narasiah, and B. G. Talbot, "Active agents and mechanism of coagulation of turbid waters using moringa oleifera," Water research, vol. 29, no. 2, pp. 703–710, 1995.

[174] T. Huang and T. M. T. Plant, "Enhanced treatment with the addition of activated silica polymer," 1998.

[175] A. B. A. Kadir and A. S. B. A. Rahim, "An overview of sludge utilization into fired clay brick." 2014.

[176] B. J. Saikia and G. Parthasarathy, "Fourier transform infrared spectroscopic characterization of kaolinite from Assam and Meghalaya, Northeastern India," Journal of Modern Physics, vol. 1, no. 04, p. 206, 2010.

[177] U. Gross, S. Rüdiger, E. Kemnitz, K.-W. Brzezinka, S. Mukhopadhyay, C. Bailey, A. Wander, and N. Harrison, "Vibrational analysis study of aluminum trifluoride phases," The Journal of Physical Chemistry A, vol. 111, no. 26, pp.

5813–5819, 2007.

[178] M. Hayati-Ashtiani, "Use of FTIR spectroscopy in the characterization of natural and treated nanostructured bentonites (montmorillonites)," Particulate Science and Technology, vol. 30, no. 6, pp. 553–564, 2012.

[179] V. Stubičan and R. Roy, "Infrared spectra of layer-structure silicates," Journal of the American Ceramic Society, vol. 44, no. 12, pp. 625–627, 1961.

[180] A. G. Clem, "Industrial applications of bentonite," Clays and Clay Minerals, vol. 10, pp. 272–283, 1961.

[181] N. Drouiche, N. Ghaffour, H. Lounici, N. Mameri, A. Maallemi, and H. Mahmoudi, "Electrochemical treatment of chemical mechanical polishing wastewater: removal of fluoride-sludge characteristics-operating cost," Desalination, vol. 223, no. 1, pp. 134–142, 2008.

[182] S. M. Rao, M. Pemmaraju, A. Kumar, S. Kundu, and M. Dhananjay, "Field studies on defluoridation using magnesium oxide," Proceedings of the ICE-Water Management, vol. 163, no. 3, pp. 147–155, 2010.

[183] H. T. Dean, "Distribution of mottled enamel in the United States," Public health reports, vol. 48, no. 25, pp. 703–734, 1933.

[184] P. K. Holt, G. W. Barton, and C. A. Mitchell, "The future for electrocoagulation as a localised water treatment technology," Chemosphere, vol. 59, no. 3, pp. 355–367, 2005.

[185] C. Hu, S. Lo, W. Kuan, and Y. Lee, "Removal of fluoride from semiconductor wastewater by electrocoagulation–flotation," Water Research, vol. 39, no. 5, pp.895–901, 2005.

[186] S. Tunali and T. Akar, "Zn (II) biosorption properties of botrytis cinerea biomass," Journal of Hazardous Materials, vol. 131, no. 1, pp. 137–145, 2006.

[187] S. Hong, C. Wen, J. He, F. Gan, and Y.-S. Ho, "Adsorption thermodynamics of methylene blue onto bentonite," Journal of Hazardous Materials, vol. 167, no. 1, pp. 630–633, 2009.

[188] E. Guibal, C. Milot, and J. M. Tobin, "Metal-anion sorption by Chitosan Beads: equilibrium and kinetic studies," Industrial & Engineering Chemistry Research, vol. 37, no. 4, pp. 1454–1463, 1998.

Appendix A

Table A.1: Effect of electrolysis time and applied current on fluoride removal. F_i=2 mg/L.

Electrolysis time (min)	*Applied current (A)*				
	0.15	*0.30*	*0.45*	*0.60*	*0.75*
0	2	2	2	2	2
5	1.72	1.67	1.53	1.1	0.72
10	1.2	1.12	0.924	0.74	0.61
15	0.95	0.86	0.645	0.56	0.5
20	0.69	0.57	0.418	0.4	0.383
25	0.53	0.42	0.3	0.25	0.211
30	0.48	0.31	0.23	0.2	0.176
35	0.40	0.28	0.22	0.18	0.162
40	0.35	0.26	0.19	0.15	0.131
45	0.33	0.25	0.17	0.12	0.101
50	0.30	0.23	0.11	0.07	0.01
55	0.28	0.21	0.09	0.04	0
60	0.25	0.20	0.05	0.01	0

Table A.2: Effect of electrolysis time and applied current on fluoride removal. F_i=8 mg/L.

Electrolysis time (min)	*Applied current (A)*				
	0.15	*0.30*	*0.45*	*0.60*	*0.75*
0	8	8	8	8	8
5	5.83	4.9	3.72	3.22	2.79
10	4.27	3.4	2.47	2.01	1.37
15	3.18	2.65	2.04	1.6	1.01
20	3.09	2.18	1.65	1.24	0.76
25	2.65	1.27	1.31	0.94	0.449
30	2.60	1.35	1.03	0.685	0.384
35	2.56	1.03	0.87	0.583	0.363
40	1.87	0.93	0.62	0.43	0.296
45	1.83	0.59	0.49	0.33	0.287
50	1.65	0.60	0.42	0.29	0.233
55	1.55	0.55	0.38	0.25	0.185
60	1.41	0.36	0.26	0.19	0.178

Appendix B

Table B.1: Data for pseudo first order kinetics (i=0.31 A)

t (min)	$q_e - q$ (mg/g)		
	F_i=2 mg/L	F_i=5 mg/L	F_i=8 mg/L
5	1.453	1.628	1.940
10	1.251	1.405	1.766
15	1.108	1.124	1.643
20	0.861	1.009	1.543
25	0.641	0.993	1.241
30	0.355	0.957	1.278
35	0.228	0.842	1.108
40	0.116	0.749	1.037
45	0.047	0.197	0.640
50	-0.136	6.171E-15	0.658

Table B.2: Data for pseudo first order kinetics (i=0.53 A))

t (min)	$q_e - q$ (mg/g)		
	F_i=2 mg/L	F_i=5 mg/L	F_i=8 mg/L
5	1.091	1.406	1.612
10	0.901	1.193	1.368
15	0.835	0.969	1.133
20	0.766	0.901	0.863
25	0.618	0.798	0.684
30	0.606	0.392	0.582
35	0.448	0.465	0.165
40	0.328	0.527	-0.168
45	0.049	0.392	-0.343
50	0.004	0.254	-0.044

Table B.3: Data for pseudo first order kinetics (i=0.75 A)

t (min)	$q_e - q$ (mg/g)		
	F_i=2 mg/L	F_i=5 mg/L	F_i=8 mg/L
5	1.200	1.598	1.792
10	0.756	1.159	1.316
15	0.684	1.003	0.975
20	0.598	0.615	0.819
25	0.482	0.422	0.663
30	0.223	0.404	0.330
35	0.144	0.044	0.211
40	0.108	-0.022	0.164
45	0.015	-0.022	-0.032
50	-0.097	0.012	-0.067

Table B.4: Data for pseudo second order kinetics (i=0.31 A)

t (min)	t/q_t (min.g/mg)		
	F_i=2 mg/L	F_i=5 mg/L	F_i=8 mg/L
5	0.787	0.101	0.083
10	0.590	0.151	0.113
15	0.684	0.191	0.145
20	0.727	0.245	0.178
25	0.822	0.305	0.193
30	0.923	0.363	0.234
35	1.058	0.413	0.261
40	1.195	0.465	0.294
45	1.337	0.500	0.315
50	1.468	0.552	0.351

Table B.5: Data for pseudo second order kinetics (i=0.53 A)

t (min)	t/q_t (min.g/mg)		
	F_i=2 mg/L	F_i=5 mg/L	F_i=8 mg/L
5	0.494	0.164	0.107
10	0.689	0.248	0.156
15	0.960	0.322	0.203
20	1.202	0.417	0.249
25	1.365	0.504	0.302
30	1.628	0.562	0.358
35	1.780	0.661	0.407
40	1.966	0.762	0.461
45	2.107	0.843	0.517
50	2.329	0.925	0.577

Table B.6: Data for pseudo second order kinetics (i=0.75 A)

t (min)	t/q_t (min.g/mg)		
	F_i=2 mg/L	F_i=5 mg/L	F_i=8 mg/L
5	0.492	0.198	0.120
10	0.906	0.337	0.190
15	1.260	0.421	0.270
20	1.558	0.540	0.348
25	1.760	0.673	0.417
30	2.072	0.777	0.496
35	2.399	0.903	0.577
40	2.696	1.032	0.654
45	2.985	1.164	0.735
50	3.165	1.288	0.811

Table B.7: Data for intraparticle diffusion (i=0.31 A)

$t^{0.5}$	q_t (mg/g)		
	F_i=2 mg/L	F_i=5 mg/L	F_i=8 mg/L
2.23607	6.346	49.038	67.884
3.16228	16.923	63.269	64.423
3.87298	21.923	78.096	105.961
4.47214	27.500	81.288	103.269
5	30.384	81.730	129.423
5.47723	32.500	82.576	130.576
5.91608	33.076	82.961	134.038
6.32456	33.461	83.596	135.807
6.7082	33.653	85.923	142.461
7.07107	34.038	88.192	143.865

Table B.8: Data for intraparticle diffusion (i=0.53 A)

$t^{0.5}$	q_t (mg/g)		
	F_i=2 mg/L	F_i=5 mg/L	F_i=8 mg/L
2.23607	10.112	30.337	46.404
3.16228	12.460	41.123	66.629
3.87298	14.707	46.494	73.820
4.47214	16.629	47.898	80.157
5	18.314	49.550	82.539
5.47723	19.325	51.292	85.831
5.91608	19.662	51.797	85.966
6.32456	20.337	52.494	86.730
6.7082	21.348	53.370	86.932
7.07107	21.460	53.966	87.089

Table B.9: Data for intraparticle diffusion (i=0.75 A)

$t^{0.5}$	q_t (mg/g)		
	F_i=2 mg/L	F_i=5 mg/L	F_i=8 mg/L
2.23607	10.158	1.428	41.349
3.16228	10.714	6.031	52.619
3.87298	11.904	11.746	56.079
4.47214	12.833	13.222	55.476
5	14.198	13.333	59.928
5.47723	14.476	14.269	60.444
5.91608	14.587	14.365	60.611
6.32456	14.833	14.388	61.142
6.7082	15.071	14.523	61.214
7.07107	15.793	14.682	61.642

Table B.10: Adsorption isotherm data for fluoride removal at applied current of 0.31 A

C_e (mg/L)	q_e (mg/g)	$q_{e.pred}$ (mg/g)		
		Langmuir	Freunlich	Redlich- Peterson
0.23	41.16	69.166	67.191	69.103
0.24	64.19	72.084	70.113	72.018
0.27	86.74	80.798	78.877	80.721
0.29	109.53	86.571	84.719	86.490
0.41	130	120.628	119.776	120.559
0.54	150	156.432	157.753	156.474
0.6	172.09	172.588	175.281	172.721

Table B.11: Adsorption isotherm data for fluoride removal at applied current of 0.53 A

C_e (mg/L)	q_e (mg/g)	$q_{e.pred}$ (mg/g)		
		Langmuir	Freunlich	Redlich- Peterson
0.09	25.81	30.651	30.526	29.688
0.11	39.05	37.442	37.309	36.620
0.16	51.89	54.388	54.268	54.206
0.19	65	64.533	64.443	64.898
0.23	77.97	78.035	78.010	79.287
0.27	90.94	91.507	91.578	93.806
0.3	104.05	101.593	101.753	104.771

Table B.12: Adsorption isotherm data for fluoride removal at applied current of 0.75 A

C_e (mg/L)	q_e (mg/g)	$q_{e.pred}$ (mg/g)		
		Langmuir	Freunlich	Redlich- Peterson
0.01	19.04	7.511	3.595	13.592
0.04	28.32	25.075	14.381	28.370
0.08	37.51	41.087	28.762	40.978
0.11	46.79	49.752	39.547	48.519
0.15	55.98	58.529	53.928	57.193
0.19	65.16	65.187	68.309	64.832
0.23	74.35	70.411	82.690	71.744

Appendix C

Table C.1: Adsorption isotherm data for aluminium removal using bentonite (Dose = $1\,g/L$)

C_e (mg/L)	q_e (mg/g)	$q_{e.pred}$ (mg/g)		
		Langmuir	Freunlich	Redlich- Peterson
11.586	11.538	11.607	11.530	11.543
11.732	11.684	11.745	11.676	11.687
11.926	11.876	11.929	11.869	11.879
12.504	12.451	12.475	12.444	12.449
12.723	12.669	12.681	12.662	12.665
14.018	13.959	13.892	13.951	13.941
15.320	15.210	15.096	15.247	15.223

Table C.2: Adsorption isotherm data for aluminium removal using bentonite (Dose = $2\,g/L$)

C_e (mg/L)	q_e (mg/g)	$q_{e.pred}$ (mg/g)		
		Langmuir	Freunlich	Redlich- Peterson
11.586	11.556	11.618	11.542	11.556
11.732	11.700	11.757	11.687	11.700
11.926	11.890	11.941	11.880	11.891
12.504	12.464	12.487	12.456	12.461
12.723	12.679	12.694	12.674	12.677
14.018	13.946	13.906	13.964	13.954
15.320	15.240	15.110	15.261	15.236

Table C.3: Adsorption isotherm data for aluminium removal using bentonite (Dose = $3\,g/L$)

C_e (mg/L)	q_e (mg/g)	$q_{e.pred}$ (mg/g)		
		Langmuir	Freunlich	Redlich- Peterson
11.586	11.549	11.607	11.528	11.553
11.732	11.693	11.745	11.673	11.696
11.926	11.881	11.929	11.866	11.886
12.504	12.456	12.475	12.441	12.451
12.723	12.673	12.681	12.659	12.664
14.018	13.931	13.892	13.947	13.928
15.320	15.190	15.096	15.243	15.195

Table C.4: Adsorption isotherm data for aluminium removal using bentonite (Dose = $4\,g/L$)

C_e (mg/L)	q_e (mg/g)	$q_{e.pred}$ (mg/g)		
		Langmuir	Freunlich	Redlich- Peterson
11.586	11.533	11.591	11.515	11.541
11.732	11.678	11.730	11.660	11.683
11.926	11.869	11.913	11.853	11.873
12.504	12.445	12.459	12.427	12.437
12.723	12.663	12.665	12.645	12.651
14.018	13.917	13.874	13.932	13.912
15.320	15.171	15.076	15.226	15.179

Table C.5: Adsorption isotherm data for aluminium removal using activated silica sol (Dose = $10\,mg/L$)

C_e (mg/L)	q_e (mg/g)	$q_{e.pred}$ (mg/g)		
		Langmuir	Freunlich	Redlich- Peterson
11.586	11.530	11.596	11.520	11.527
11.732	11.675	11.735	11.665	11.671
11.926	11.866	11.918	11.858	11.863
12.504	12.432	12.464	12.433	12.435
12.723	12.646	12.670	12.651	12.652
14.018	13.929	13.880	13.938	13.933
15.32	15.225	15.082	15.233	15.220

Table C.6: Adsorption isotherm data for aluminium removal using activated silica sol (Dose = 30 mg/L)

C_e (mg/L)	q_e (mg/g)	$q_{e.pred}$ (mg/g)		
		Langmuir	Freunlich	Redlich- Peterson
11.586	11.583	11.647	11.570	11.579
11.732	11.727	11.786	11.716	11.724
11.926	11.917	11.971	11.910	11.917
12.504	12.487	12.518	12.487	12.491
12.723	12.705	12.725	12.706	12.708
14.018	13.989	13.940	13.999	13.992
15.32	15.286	15.147	15.299	15.283

Table C.7: Adsorption isotherm data for aluminium removal using activated silica sol (Dose = 50 mg/L)

C_e (mg/L)	q_e (mg/g)	$q_{e.pred}$ (mg/g)		
		Langmuir	Freunlich	Redlich- Peterson
11.586	11.571	11.638	11.561	11.569
11.732	11.716	11.777	11.707	11.714
11.926	11.907	11.961	11.901	11.907
12.504	12.480	12.509	12.477	12.480
12.723	12.693	12.715	12.696	12.698
14.018	13.981	13.929	13.988	13.982
15.32	15.275	15.136	15.287	15.273

Table C.8: Adsorption isotherm data for aluminium removal using activated silica sol (Dose = 70 mg/L)

C_e (mg/L)	q_e (mg/g)	$q_{e.pred}$ (mg/g)		
		Langmuir	Freunlich	Redlich- Peterson
11.586	11.524	11.594	11.518	11.521
11.732	11.670	11.733	11.663	11.666
11.926	11.858	11.916	11.856	11.859
12.504	12.431	12.462	12.431	12.432
12.723	12.643	12.668	12.649	12.649
14.018	13.933	13.877	13.936	13.934
15.32	15.227	15.080	15.230	15.225

Desalination and Water Treatment
www.deswater.com
doi: 10.1080/19443994.2015.1084536

(2015) 1–10

Taylor & Francis
Taylor & Francis Group

Use of activated silica sol as a coagulant aid to remove aluminium from water defluoridated by electrocoagulation

Richa Sinha, Sanjay Mathur*

Department of Civil Engineering, Malaviya National Institute of Technology, Jaipur 302017, India, Tel. +91 7877290494; email: richamnit10@gmail.com (R. Sinha), Tel. +91 9549654213; email: smathur.ce@mnit.ac.in (S. Mathur)

Received 4 June 2015; Accepted 7 August 2015

ABSTRACT

Presence of fluorides in drinking water has become a public health problem. Aluminium compounds are popular for defluoridation of water owing to high affinity of fluoride toward aluminium. Use of these compounds may lead to high aluminium concentrations in drinking water. Aluminium is found to be a potential neurotoxicant. Synergistic associations of both aluminium and fluorides in the drinking water supply have been expounded by researchers. Aluminium–fluoride complexes also increase the risk of developing Alzheimer's disease. Therefore, it is imperative to control the residual aluminium in the water. In the present work, the electrocoagulation process with aluminium electrodes has been used for defluoridation of water. In subsequent steps, activated silica sol has been used as a coagulant aid to remove aluminium from defluoridated water. Taguchi design has been used to develop a statistical model for aluminium removal. The experimental investigations revealed that activated silica sol reduces residual aluminium to a range of 0.003–0.034 mg/L.

Keywords: Activated silica sol; Aluminium; Coagulant aid; Electrocoagulation; Fluoride

1. Introduction

Fluoride in drinking water is a matter of concern in present time. A study by UNICEF shows that fluorosis is widespread in at least 27 countries across the globe [1]. Problems associated with excessive or prolonged exposure to fluoride contaminated drinking water may cause dental or skeletal fluorosis. In dental fluorosis, excessive fluoride can cause yellowing of teeth, white spots, and pitting or mottling of enamel [2]. Common symptoms of chronic fluoride exposure are skeletal fluorosis, which can lead to permanent bone and joint deformation [3]. Therefore, fluoride removal has been an issue of concern for environmental engineers for the past few decades [2]. Aluminium-based compounds are useful adsorbent/coagulant for fluoride removal, owing to high affinity of fluoride toward aluminium [4]. Various treatment technologies have been developed for fluoride removal from drinking water using aluminium-based compounds. However, generation of large volume of sludge, hazardous waste categorization of metal hydroxides and high costs associated with chemical treatments have made them less acceptable [5].

Electrocoagulation (EC) process using aluminium electrodes is one such process for fluoride removal. Researchers [2,6–8] have demonstrated the effectiveness of EC with aluminium electrodes for defluoridation. EC has been suggested as an alternative to conventional coagulation [9,10]. Reduced sludge production, no

*Corresponding author.

Desalination and Water Treatment
www.deswater.com
doi: 10.1080/19443994.2015.1060538

(2015) 1–10

Taylor & Francis
Taylor & Francis Group

Control of aluminium in treated water after defluoridation by electrocoagulation and modelling of adsorption isotherms

Richa Sinha, Sanjay Mathur*

Department of Civil Engineering, Malaviya National Institute of Technology, Jaipur 302017, India, Tel. +91 7877290494; email: richamnit10@gmail.com (R. Sinha), Tel. +91 9549654213; email: smathur.ce@mnit.ac.in (S. Mathur)

Received 3 February 2015; Accepted 4 June 2015

ABSTRACT

The removal of fluoride from drinking water by use of aluminium compounds is more prevalent than other defluoridation techniques due to the strong affinity between aluminium and fluoride. Electrocoagulation (EC) with aluminium electrodes is one such technique which is successfully used for defluoridation of water. But various monomeric and polymeric hydroxyl species of aluminium and fluoride complexes are formed in the process. In the recent past, the adverse effects of aluminium have been recognized. The present study was carried out to control aluminium content in water after defluoridation by EC process. In the present study, the aluminium content after EC was in the range of 6.2–48.5 mg/L, which was brought down to range 11.25–14.99 mg/L through optimized energy usage and further brought down to 0.030–0.149 mg/L with use of bentonite as coagulant.

Keywords: Defluoridation; Aluminium control; Coagulation; Optimization and adsorption isotherm

1. Introduction

Presence of fluorides in groundwater is a major problem in many parts of the world including India. Detrimental effects of fluorides depend upon the concentration and exposure [1]. Aluminium-based compounds have been used for defluoridation of water because of high affinity between aluminium and fluorine. Electrocoagulation (EC) with aluminium electrodes has been demonstrated as an efficient process for defluoridation [2–5]. This process involves applying electric current to sacrificial electrodes inside an electrolytic cell where the current generates a coagulating agent and gas bubbles [6]. The advantages of electrocoagulation include high particulate removal efficiency, compact treatment facility and possibility of complete automation [7].

Aluminium was earlier regarded as a relatively innocuous element, but in the recent past, researchers have found that its various bond forms with fluoride and other inorganic/organic ions are toxic in nature. Aluminium is a potential neurotoxic agent in human beings and researchers like Strunecka and Patocka [8] and Gauthier et al. [9] have elucidated synergistic effects of aluminium and fluorides and its role in Alzheimer's disease.

A little information is available in literature about the residual aluminium content after use of EC for defluoridation of water and its removal. The present study was carried out to control aluminium content in water after defluoridation by the EC process. It has been observed that the aluminium content in

*Corresponding author.

Publisher: Taylor & Francis

Journal: *Environmental Technology*

DOI: 10.1080/09593330.2015.1043958

Aluminium removal from water after defluoridation with electrocoagulation process

Richa Sinha[1], Sanjay Mathur[1*] and Urmila Brighu[1]

[1]Department of Civil Engineering, Malaviya National Institute of Technology, Jaipur-302017, India, Tel. +917877290494, email: richamnit10@gmail.com (R. Sinha), Tel. +919549654213, email:smathur.ce@mnit.ac.in (S. Mathur), Tel. +919549654214, email: ubrighu@gmail.com (U. Brighu)

Abstract

Fluoride is the most electronegative element and has a strong affinity for aluminium. Owing to this fact most of the techniques used for fluoride removal utilised aluminium compounds for removing fluoride, which results in high concentrations of aluminium in the treated water. In the present paper a new approach is presented to meet WHO guideline for residual aluminium concentration as 0.2 mg/L. The Electrocoagulation (EC) process was used for fluoride removal in the present work. It was found that aluminium content in water increases with increase in energy input. Therefore experiments were optimised for minimum energy input to achieve target value (0.7mg/L) of fluoride in resultant water. These optimised sets were used for further investigations of aluminium control. The experimental investigations revealed that use of bentonite clay as coagulant in clariflocculation brings down the aluminium concentration of water below WHO guideline. Bentonite dose of 2g/L was found to be the best for efficient removal of aluminium.

Keywords: Bentonite, Electrocoagulation, Fluoride, Optimization, Aluminium removal

*[1] Corresponding author: Sanjay Mathur, email: smathur.ce@mnit.ac.in, contact no. Mobile No. +919549654213

Desalination and Water Treatment
www.deswater.com
doi: 10.1080/19443994.2014.990929

(2014) 1–11

Taylor & Francis
Taylor & Francis Group

Multiobjective optimization for minimum residual fluoride and specific energy in electrocoagulation process

Richa Sinha[a], Amit Singh[b], Sanjay Mathur[a,*]

[a]*Department of Civil Engineering, Malaviya National Institute of Technology, Jaipur 302017, India, Tel. +917877290494; email: richamnit10@gmail.com (R. Sinha), Tel. +919549654213; email: smathur.ce@mnit.ac.in (S. Mathur)*
[b]*Department of Mechanical Engineering, Malaviya National Institute of Technology, Jaipur 302017, India, Tel. +919549657317; email: asingh.mech@mnit.ac.in*

Received 25 March 2014; Accepted 18 November 2014

ABSTRACT

In the present paper, 2^4 factorial design method was employed for optimization of two responses: residual fluoride and specific energy consumed. The study was based on interaction effect of four factors namely, current, initial fluoride concentration, time, and inter-electrode distance. A regression model equation was developed which was validated by high R^2 values of 98.78 and 99.80% for residual fluoride and specific energy consumed, respectively. Optimization was targeted for residual fluoride concentration less than 1 mg/l and minimum specific energy consumption. The optimized conditions as suggested by the model for initial fluoride concentration 6 mg/l were: applied current—0.27 A, inter-electrode distance—20 mm, treatment time—46.70 min, specific energy—5.85 J/mg, and residual fluoride—0.77 mg/l. These results were used for experimental verification, which was in good agreement with the predicted results.

Keywords: Regression model; Fluoride; Electrocoagulation; Specific energy

1. Introduction

Fluoride contamination in groundwater is a major public health concern of the present time. Excessive exposure to fluoride either from drinking water or from other sources like food, drugs, cosmetics, industrial sources etc. can result into adverse health effects. Health problems associated with high concentrations of fluoride intake are dental fluorosis and skeletal fluorosis [1]. Severity of the fluorosis depends upon the amount of fluoride ingested and the tenure of exposure. In dental fluorosis, excessive fluoride can cause yellowing of teeth, white spots, and pitting or mottling of enamel. The most common symptoms of chronic fluoride exposure are skeletal fluorosis, which can lead to permanent bone and joint deformation [2]. Therefore, fluoride removal has been very important to environmental engineers. The desirable fluoride level in drinking water as set by Indian standards of drinking water is 1 mg/l.

The electrocoagulation (EC) process has been demonstrated as an effective choice for defluoridation by researchers [3,4]. A renaissance has been experienced by EC process. Reduced sludge production, no requirement for chemical handling, and ease of operation are some of the advantages of this process [5]. EC process generates sludge at the

*Corresponding author.

International Journal of Applied Engineering Research.
ISSN 0973-4562, Volume 9, Number 2 (2014) pp. 201-206

http://www.ripublication.com/ijaer.htm

Development of Regression Equation for Defluoridation by Continuous Flow Electrocoagulation

Richa Sinha and Sanjay Mathur

Department of Civil Engineering, MNIT, Jaipur, INDIA.

Abstract

In the present study continuous flow electrocoagulation has been used as a treatment technology for removal of fluoride from water. A laboratory scale continuous flow electrocoagulation system with aluminium electrodes is designed for performing experimental runs. Experimental data is analyzed using factorial design method to study the main effect and interaction effect of three parameters viz flow rate, voltage and time on fluoride removal. A regression equation is developed which is validated by high R^2 value (99.5%) of Analysis of Variance test (ANOVA). Equation reveals that flow rate has a positive effect and voltage and time has negative effect on residual fluoride.

Keywords: Defluoridation, electrocoagulation, factorial method, regression.

1. Introduction

Fluoride contamination in groundwater is a major public health concern of the present time. Health problems associated with high concentrations of fluoride intake are dental fluorosis and skeletal fluorosis (Fawell et al 2006). Generation of large volume of sludge, the hazardous waste categorization of metal hydroxides, and high costs associated with chemical treatments have made the conventional chemical coagulation techniques for defluoridation less acceptable (Emamjomeh et al. 2011). Electrocoagulation (EC) is emerging as a promising process that can be retrofitted to existing methods of defluoridation. EC process has been demonstrated as an effective choice for defluoridation by researchers (Hu et al., 2003; Emamjomeh & Sivakumar, 2009). The removal mechanism has been described by many researchers (Emamjomeh et al. 2011, Hu et al., 2003) in detail and is not described here.

Sinha R, Khazanchi I, Mathur S / International Journal of Engineering Research and Applications (IJERA) ISSN: 2248-9622 www.ijera.com
Vol. 2, Issue 5, September- October 2012, pp.1336-1341

Fluoride Removal By A Continuous Flow Electrocoagulation Reactor From Groundwater Of Shivdaspura.

Sinha R*, Khazanchi I, Mathur S*****

*Department of Civil Engineering, Malaviya National Institute of Technology, Jaipur-302017
** Environment Engineer, Hindustan Zinc Limited, Chittorgarh.
***Department of Civil Engineering, Malaviya National Institute of Technology, Jaipur- 302017

ABSTRACT

The present study focuses on the technique of defluoridation by using the process of electrocoagulation (EC). Efficacy of EC process was investigated for laboratory simulated sample called as control sample and groundwater sample collected from Shivdaspura (Rajasthan) under different operating conditions. Continuous flow experiments were conducted for fluoride removal using aluminium electrodes to study the parameters such as: current density, flow rate, number of stages in treatment, fluoride uptake capacity and residual aluminium. The results obtained showed that double stage treatment system gave higher treatment efficiency than single stage system. Residual Aluminium was measured and found in the range of 0.08-0.1 ppm which shows that EC offers better quality of water when compared with other methods of defluoridation like Activated Alumina (AA) process and Nalgonda technique.

Keywords- defluoridation, electrocoagulation, fluoride uptake capacity, residual aluminium

1. INTRODUCTION

Fluorine, the lightest member of the halogen group is the most electronegative and hence chemically reactive. Fluorine is therefore found as fluorides which together represent about 0.06-0.09% of earth's crust [1]. Prevalence of fluorosis in India is mainly due to hydrogeochemical origin. Groundwater fluoride contents in high levels are present in all the 33 districts and have become a serious health related issue in 23 districts of Rajasthan [2]. Presence of fluoride in traces has beneficial effects on teeth but high and continuous exposure can cause mild dental fluorosis to crippling skeletal fluorosis. Desirable limit of fluoride is less than 1 mg/l [3]. The drawback of defluoridation techniques like Nalgonda and AA process includes large sludge generation and high residual aluminium in the effluent. The present research is directed primarily to address this issue. Hence residual aluminium in the effluent was determined for the process of EC. Also a range of operating parameters such as flow rate, current density, fluoride uptake capacity and multistage treatment were developed to study the efficacy of the process. Lui *et al*,[4] reported that the defluoridation efficiency in the EC system exceeded that of the traditional process due to the electrocondensation effect.

In the process of EC, oxidation reaction occurs which causes dissolution of anode and aqueous Al^{3+} species are formed. The electrode reactions are outlined below [5]:

Anodes: $Al(s) \rightarrow Al^{3+} + 3e^-$ (1)

Cathodes: $2H_2O + 2e^- \rightarrow H_2(g) + 2OH^-$ (2)

The H_2 bubbles float and hence drive the flotation process. The Al^{3+} ions further react to form a solid $Al(OH)_3$ precipitate:

$Al^{3+} + 3H_2O <-> Al(OH)_3(s) + 3H^+$ (3)

The basic principle of the process is adsorption of fluoride at precipitated Al $Al(OH)_3$ as depicted in reaction (4) [5]:

$Al(OH)_3 + x\ F^- <-> Al(OH)_{3-x}F_x + x\ OH^-$ (4)

The EC process is highly dependent on pH of the solution [6, 7]. Studies revealed that pH plays an important role in the formation of $Al(OH)_3$ flocs. The solid $Al(OH)_3$ is most prevalent between pH 6 and 8, and above pH 9, the soluble species $Al(OH)_4^-$ is the predominant species [8]. Mohammad et *al*, [8] found that the defluoridation efficiency decreases from 90 to 75% when the final pH is more than 8. Researches show that more efficiency is obtained when the pH ranges from 6 – 8 [5, 8]. Hence the pH in present study was kept constant at 6 for all runs.

2. MATERIALS AND METHODS

A continuous flow bench scale EC reactor was designed and constructed for fluoride removal as shown in Figure.1. Aluminium electrodes each having surface area of 0.012 m^2 was used with rectangular reactor of dimensions (25 cm X 10 cm X 8 cm, volume 2 litres). The distance between electrodes was kept constant at 1cm for all the runs. Sample to be treated was placed in an influent tank (polycon) which can hold a sample volume of 110 litres. pH of the sample was maintained 6 by using dilute HCl. Conductivity and pH were measured using a calibrated conductivity meter (Lutron CD 4302) and pH meter (Electronics India, deluxe 101) respectively. Sample was continuously fed into EC reactor at desired flow rate which was set using a peristaltic pump (Miclins PP- 20). Before each run electrodes were cleaned by acetone and HCl solution. Electrolysis was performed and samples

Brief Bio-data

Ms. Richa Sinha is a Research scholar in Department of Civil Engineering, Malaviya National Institute of Technology (MNIT), Jaipur. She has received her B.Tech degree in Biotechnology from Amity University, Lucknow. She has received her Master's degree from MNIT, Jaipur in Environmental Engineering. She has joined PhD in 2012 under supervision of Dr. Sanjay Mathur, Department of Civil Engineering, MNIT, Jaipur. Her research interests are mainly in the areas of water treatment. During her research work she has published five research papers in international journals. She has attended various National and International Conferences & workshops.